Supported Metal Catalysts for Water-Gas Shift Conversion

Li-Hsin Tsui

Submitted in partial fulfilment of the requirements for the degree of

Master of Science in Engineering

HySA/Catalysis
Centre for Catalysis Research
Department of Chemical Engineering
University of Cape Town

September 2014

Synopsis

The interests in an alternative, sustainable power generation method has greatly increased in the past decade due to increases in greenhouse gases and its impact on global climate change. The use of fuel cells as a form of energy generation is extremely promising as it converts chemical potential energy directly to electrical energy, bypassing the Carnot cycle limitations. Various types of fuel cells have been developed, with the proton exchange membrane fuel cell (PEMFC) being most promising for mobile and small-scale stationary uses under transient conditions.

The PEMFC uses hydrogen and oxygen to generate electrical energy. While oxygen can be obtained from air, hydrogen does not exist in its elemental form; hence a process train is required to refine fuels (such as fossil fuels and bio-fuels) into pure hydrogen. This has been successfully achieved by large-scale industrial plants.

A typical fuel processing train consists of a steam reforming stage converting the fuel into syngas. This is followed by a water-gas shift (WGS) stage to convert carbon monoxide, which is a poison for the platinum catalysts within fuel cells, into carbon dioxide. If the CO concentration required is extremely low, a methanation or preferential oxidation stage can be used subsequent to the WGS stage. This study focuses on the water-gas shift stage of the fuel processing train.

Industrial base metal WGS catalysts are not suitable for a miniaturized fuel processing train due to the catalysts being developed for continuous operations, as miniaturized fuel processing trains are expected to operate at transient conditions. A slow and controlled reduction process is also required prior to operation, as well as the pyrophoricity of industrial catalysts after reduction. These can pose safety issues with non-technical personnel in household applications (e.g. CHP). PGM-based catalysts have shown high activities for the water-gas shift reaction in literature, are not pyrophoric and do not require lengthy and sensitive reduction processes prior to operation.

The objective of this study was to investigate and compare two base metal catalysts (high temperature (HT) shift Fe_3O_4/Cr_2O_3 and low temperature (LT) shift $CuO/ZnO/Al_2O_3$ catalyst) with a PGM based counterpart, as well as to investigate whether the catalysts are able to achieve a required 1 vol% CO via the water-gas shift reaction. For these investigations a synthetic feedstock was used, based on typical exit concentrations of a steam methane reformer.

The LT catalyst was able achieve the required CO concentration at 190°C and 10,000 h^{-1}, and 200°C and 5,000 h^{-1}, at two different feed conditions. The HT catalyst was unable to reach the

required CO concentration under all conditions tested as it was thermodynamically limited by the water-gas shift equilibrium and kinetically limited at lower temperatures. The PGM-based catalyst had an operating temperature range from 225°C upwards and was able to achieve the required CO concentration at 275°C. However, at 275°C and above, the catalyst stability was poor, and a constant decrease in activity was observed. It was found that the deactivation was not due to coke formation.

Even though the PGM-based WGS catalyst did not outperform the LTS catalyst, the data obtained in this investigation has elucidated an operating range wherein future PGM-based WGS catalysts should be examined.

Acknowledgement

I would like to acknowledge the following individuals and organisations, for without them this research would not have been possible.

Prof. Jack C. Q. Fletcher for the opportunity to conduct this research, overall support, advice, guidance and patience throughout the duration of this project

Mr Stephen Roberts for the continuous advice on various issues during the initial setting up of the rig, as well as supplying endless entertainment

Mr Walter Böhringer for the day-to-day guidance, the deciphering of analytical data, and for just being Walter

Mr Niels Lüchters for the development of the analysis programme, the guidance and advices during day-to-day operation, and the massive amount of help during the overall development of this report

Mr Marc Wüst for providing continuous assistance with all things rig-related and all things electronics-related served with a generous slice of comical relief

Mr Jacobus van der Merwe and the Ikey crew for the construction of the rig for without it, no experiment could be done

Mr Gubevu Maduna and Mr Yi Zhou for the opportunity of working alongside you

University of Cape Town, the Department of Chemical Engineering, HySA/Catalysis, and the Centre for Catalysis Research for providing financial support and the use of their facilities and resources.

And finally, I would like to thank all the office mates for making every day enjoyable.

Declaration

I, the undersigned, hereby certify that the work presented below is my own research. Any information which is not my own has been properly referred to according to the Harvard referencing system.

Signed: _____

Name: _____

Date: _____

Table of Contents

List of Figures

List of Tables

Nomenclature

CHP	**C**ombined **H**eat and **P**ower
Experiment	Defined within this study as a change in conditions
HTS	**H**igh **t**emperature **s**hift
Tammann Temperature	0.3 x $T_{melting}$; at this temperature, surface crystal recrystallization occurs.
LTS	**L**ow **t**emperature **s**hift
MFC	**M**ass **F**low **C**ontroller
PEMFC	**P**olymer **E**lectrolyte **M**embrane **F**uel **C**ell **OR** **P**roton **E**xchange **M**embrane **F**uel **C**ell
PrOX	**Pr**eferential **Ox**idation
Run	Defined within this study as the duration of multiple experiments until the catalyst is changed
sccm	**S**tandard **c**ubic **c**entimetres per **m**inute
TCD	**T**hermal **C**onductivity **D**etector

1. Introduction

The water-gas shift reaction has been used as a key step in hydrogen production since the early 1940s, and modern commercial catalysts are geared for large quantity steady-state operations (Ladebeck and Wagner, 2003). With ever-growing crude oil prices, as well as growing environmental concerns due to increases in greenhouse gases, interests in alternative and sustainable methods for mobile power generation, such as polymer electrolyte membrane (PEM) fuel cells, have grown (Dicks, 1996).

The three major steps seen in current industrial hydrogen production are: reformation of methane, water-gas shift conversion and the further removal of CO via methanation (Ladebeck and Wagner, 2003). Fuel processing for fuel cells produces H_2 through similar steps to current industrial production processes, with the exception of utilizing preferential oxidation for the further removal of CO over methanation (Adachi *et al.*, 2009).

High purity hydrogen, with less than 1% CO, is desired for high temperature fuel cell operation, while low temperature fuel cells require a hydrogen stream with 10 ppm CO maximum. CO is known to poison the Pt catalyst of the fuel cell, hence decreasing overall fuel cell performance (Zhang *et al.*, 2006).

Modern base metal water-gas shift catalysts are unable to be miniaturised directly for fuel cell use as the expected operating conditions differ too much from industrial conditions in terms of space velocity, thus this can cause a rapid decline in the activity of the catalyst. Base metal catalysts are also known to be pyrophoric once reduced, which can be dangerous if not properly handled (Ladebeck and Wagner, 2003).

Fuel processing for fuel cell applications, therefore, requires a catalyst which will be highly active under conditions so that direct hydrogen feed to fuel cell is applicable. Platinum group metal (PGM) catalysts, few only being commercially available, have been shown in research to be highly active under expected fuel cell operating conditions (Ratnasamy and Wagner, 2009).

This project is part of the Hydrogen Catalysis Competence Centre's initial technology development strategy. The main goal of this project is the comparison of available platinum group metal catalysts with their base-metal catalyst counterparts as well as a scoping exercise to determine the ideal conditions at which the various catalysts can operate.

2. Background

2.1. Hydrogen Production and Fuel Cells

Hydrogen is one of the most abundant elements on Earth. It does not, however, occur in pure form (Penner, 2006) and thus a process is needed for hydrogen production to convert non-elemental hydrogen into its elemental form. Hydrogen is used in various industries, with the production of ammonia, the Haber process, being one of the main consumers of industrial hydrogen (Armor, 2005). One of the main sources of hydrogen is from fossil fuels, and with it being a finite resource, the price of fossil fuel will increase with further depletion (Dicks, 1996). Alternative power generations technologies, like fuel cells, are receiving more interest as the hydrogen does not necessarily have to be derived from fossil fuels, thus making it renewable, and it is also more efficient than conventional energy generation via fossil fuel combustion (Penner, 2006).

Fuel cells are "electrochemical devices that convert chemical energy into electrical energy directly" (EG&G Technical Services, 2004, p.1-1). Fuel cell developments started with W.R. Grove & Christian Friedrich Schönbein in 1839 (Penner, 2006; Winter, 2009) and has continued to the present day. Recent developments make fuel cells a plausible alternative power generation method as it avoids direct combustion of the hydrogen, thus allowing the fuel cell to avoid the Carnot cycle limitation seen in combustion engines (Penner, 2006). Combustion engines convert thermal energy into heat, thus a maximum efficiency is dependent on the operating temperature of the engine. Fuel cells also have the ability to produce power with minimal pollutant towards the environment, with the only by-product being water.

Table 2-1 lists all the major fuel cell types, their operating temperature range as well as their best-suited applications. For the purpose of this study, the proton exchange membrane fuel cell (PEMFC) will be focused on.

2.1.1. Industrial Methods for Hydrogen Production

Depending on the availability of raw materials, the two main industrial production methods for hydrogen are either by steam methane reforming, or the gasification of coal (Winter, 2009). Steam methane reforming (Eqn 2.1) reacts methane and water over a nickel catalyst to produce a synthesis gas mixture. Coal gasification (Eqn 2.2), a non-catalytic reaction, also produces a synthesis gas mixture, albeit with a different H:CO ratio (with steam methane reforming able to achieve a theoretical maximum H:CO ratio of 3:1, while coal gasification is only able to achieve a maximum H:CO ratio of 1:1). Steam methane reforming is more endothermic than coal gasification due to the higher enthalpy of reaction.

Table 2-1 – List of Major Types of Fuel Cells and Their Suggested Applications (Dicks and Larminie, 2003)

Fuel cell type	Mobile ion	Operating Temperature Range	Suggested Applications
Alkaline Proton Exchange	OH^-	50-200°C	Space Vehicles
Proton Exchange Membrane	H^+	30-120°C	Vehicles, mobile applications, CHP systems
Direct Methanol	H^+	20-90°C	Portable electronic devices
Phosphoric Acid	H^+	±220°C	CHP, in 200 kW range
Molten Carbonate	CO_3^{2-}	±650°C	medium- to large-scale CHP, MW capacity
Solid Oxide	O^{2-}	500-1000°C	CHP, 2kW to multi-MW capacity

$$CH_4 + H_2O \rightleftharpoons 3H_2 + CO,\ \Delta H^0_{rxn} = 206.2\ kJ/mol \qquad \textbf{Eqn 2.1}$$

$$C + H_2O \rightleftharpoons H_2 + CO,\ \Delta H^0_{rxn} = 175.3\ kJ/mol \qquad \textbf{Eqn 2.2}$$

The water-gas shift (WGS) reaction (Eqn 2.3) is the second step in the industrial production of hydrogen. The catalytic WGS reaction is a two-stage process, with the second step at lower temperature due to the slight exothermic nature of the reaction (Ladebeck and Wagner, 2003).

$$CO + H_2O \rightleftharpoons CO_2 + H_2,\ \Delta H^0_{rxn} = -41.1\ kJ/mol \qquad \textbf{Eqn 2.3}$$

Typical effluent concentration of CO after the second stage of the water-gas shift reaction can vary from 1% - 5% (Ladebeck and Wagner, 2003). If a high H_2 purity is required, a third stage of methanation (Eqn 2.4 and Eqn 2.5) can be applied to further reduce CO and CO_2 concentrations, at the expense of reconverting hydrogen into methane, to less than 5 ppm, which is required for the Haber Process as both CO and CO_2 are considered poisons within that process (Twigg, 1989, p.342).

$$3H_2 + CO \rightleftharpoons CH_4 + H_2O,\ \Delta H^0_{rxn} = -206.2\ kJ/mol \qquad \textbf{Eqn 2.4}$$

$$4H_2 + CO_2 \rightleftharpoons CH_4 + 2H_2O,\ \Delta H^0_{rxn} = -165\ kJ/mol \qquad \textbf{Eqn 2.5}$$

If the minimization of CO concentration is of more importance, while keeping H_2 purity high, such as in the feed streams for a fuel cell, preferential CO oxidation (PrOX) (Eqn 2.6) can be employed to reduce CO concentrations to less than 5 ppm, as selective methanation (selective towards CO, i.e. Eqn 2.4) converts H_2 back into CH_4, which is not desired.

$$CO + \tfrac{1}{2}O_2 \rightleftharpoons CO_2,\ \Delta H^0_{rxn} = -283\ kJ/mol \qquad \textbf{Eqn 2.6}$$

2.1.2. Polymer Electrolyte Membrane Fuel Cell and Operations

As mentioned in Section 2.1, fuel cells are able to convert chemical energy directly into electrical energy, thus bypassing the Carnot limitation due to thermodynamics (Penner, 2006). The main focus for this study will be the generation of a suitable feedstock for the PEMFC, specifically the high temperature PEMFC (operating temperature of 120°C).

The general setup of a simple fuel cell can be seen in Figure 2-1. The setup, referred to as a membrane electrode assembly, or MEA, consists of an anode and a cathode, both of which are platinum dispersed on carbon support, encompassing the electrolyte membrane, which is usually made from Nafion (Du Pont). The design of the MEA allows protons to flow through, but not the electrons, as they are diverted around the electrolyte membrane, thus allowing the generation of electricity (Larminie, 2005).

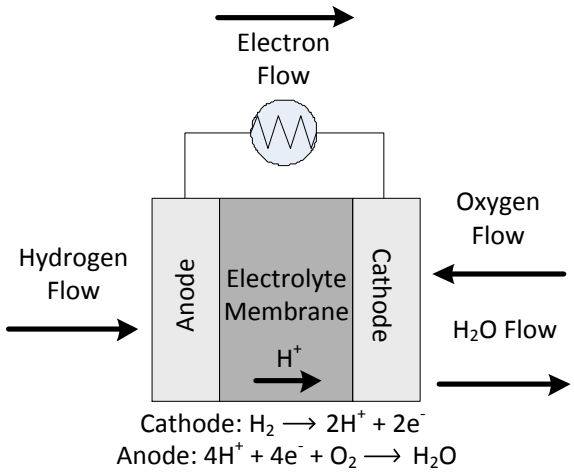

Figure 2-1 – A simplified setup of a PEMFC, showing feed, by-product, electron flow, and cathode and anode reactions (Larminie, 2005)

Water management within the fuel cell is of great importance as the membranes are required to be constantly hydrated to allow proton flow, thus permitting the fuel cell to generate power. If the membranes are under-saturated with water, this results in a reduced proton flow and lowering the efficiency of the fuel cell. When the membranes are over-saturated, thus flooding the cell, this will reduce efficiency (Dicks and Larminie, 2003, p.76). One possible method for water management of a fuel cell is to operate at a temperature where the amount of water produced on the cathode side is enough to keep the cell sufficiently moist. At 60°C, however, it has been shown that the cell will dry out. One possible way to overcome this issue is to humidify the hydrogen feed for the fuel cell (Dicks and Larminie, 2003, p.76).

Another key aspect in the operation of a PEMFC is the CO concentration of the fuel cell feed. As the fuel cell catalyst consists of platinum dispersed on carbon, it is very sensitive to carbon monoxide. The maximum tolerable CO concentration for the low temperature (operating temperature up to 80°C) PEMFC is below 10 ppm (Dicks and Larminie, 2003, p.239). Carbon

monoxide can chemisorb very easily onto platinum at a lower temperatures (Zhang *et al.*, 2006), which will poison the catalyst and reduce the overall efficiency of the fuel cell. Operating the fuel cell at a higher temperature (> 100°C) increases the CO tolerance. Chandan *et al.* (2013) stated that at an operating temperature of 160°C, CO tolerance of a PEMFC is 3% CO.

Smaller PEM fuel cells are able to operate at atmospheric pressures; however larger fuel cells (> 10kW) can be operated at higher pressure. Dicks and Larminie (2003) pointed out that "the advantages and disadvantages of operating at higher pressure are complex", as higher pressures will provide more power generated but power is also required to compress the gases. A balance must be reached between the power generated as well as compressor power consumed.

2.1.3. Miniaturisation of Hydrogen Production for Fuel Cells

Miniaturisation of hydrogen production for fuel cells is an important part of the overall fuel processing train for the fuel cell feed stream. The current base-metal catalysts for water-gas shift are geared for a continuous, steady-state operation, which were not expected for applications in a miniaturised fuel processing train. Base metal catalysts require a slow and controlled reduction process in order for the catalysts to become active. There are also handling issues once these catalysts are reduced. Both the high temperature shift catalyst (Fe_3O_4/Cr_2O_3) and the low temperature shift catalyst ($Cu/ZnO/Al_2O_3$) are pyrophoric in air once reduced, and can lead to safety issues. Cu/Zn will also lose activity when exposed to oxygen after reduction, causing practical complexities when implementing it into a fuel processing unit (Ladebeck and Wagner, 2003; Kolb, 2008, p.68-69).

These limitations tend to hamper the use of industrial catalysts within a portable fuel processing unit. The developments of high activity PGM based catalysts are appropriate as they, although high in price, have higher activity than base metals. PGM catalysts are not known to be pyrophoric and often auto-reduce, making them suitable for portable fuel processors (Ladebeck and Wagner, 2003; Kolb, 2008, p.68-69). Table 2-2 shows some aspects that are important in the miniaturisation of WGS catalysts for fuel cells.

Table 2-2 – Key aspects of miniaturisation of WGS catalysts for fuel cells (Ladebeck and Wagner, 2003)

WGS Catalyst Attributes	Mobile applications	Non-mobile applications
Cost	Critical	Not as critical
Non-pyrophoric	Important	Eliminate purging
Selectivity	Critical	Important
No reduction required	Critical	Important
Oxidation tolerant	Critical	Important
Condensation tolerant	Important	Important

2.2. Water-Gas Shift Reaction

2.2.1. Background of the Water-Gas Shift Reaction

The water-gas shift reaction is an equimolar reaction, with the forward reaction involving reactants H_2O and CO to form CO_2 and H_2.

$$CO + H_2O \rightleftharpoons CO_2 + H_2, \Delta H_{rxn} = -41.1 \text{ kJ/mol} \qquad \textbf{Eqn 2.3}$$

It has been an important part of the overall hydrogen production method since the 1940s (Ladebeck and Wagner, 2003). In 1912, Bosch and Wild discovered that the oxides of iron and chromium can catalytically convert CO to CO_2 at high temperatures, and in 1915, it was incorporated into a coal-fed ammonia plant (Twigg, 1989, p.284). Water-gas shift reaction has since become an integral part of the ammonia process to purify the H_2 stream. Figure 2-2 shows the flow diagram of the overall fuel processing train.

As previously mentioned, the water-gas shift is performed industrially in two stages, with the first stage at higher temperature than the second stage. Water-gas shift utilises two catalysts, a Fe_3O_4/Cr_2O_3 catalyst for the high temperature stage, and a $Cu/ZnO/Al_2O_3$ catalyst for the low temperature stage. Modern water-gas shift reaction occurs over two adiabatic stages, with the water-gas shift feed entering the first stage at 300-360°C and exiting at between 400°C and 500°C with an effluent CO concentration of approximately 5%. The second stage operates at a much lower temperature of 190-230°C. The effluent from the second stage can exit the reactor at up to 280°C due to the adiabatic operation of this stage. This stage is able to reduce the CO concentration to less than 0.5% (Ladebeck and Wagner, 2003).

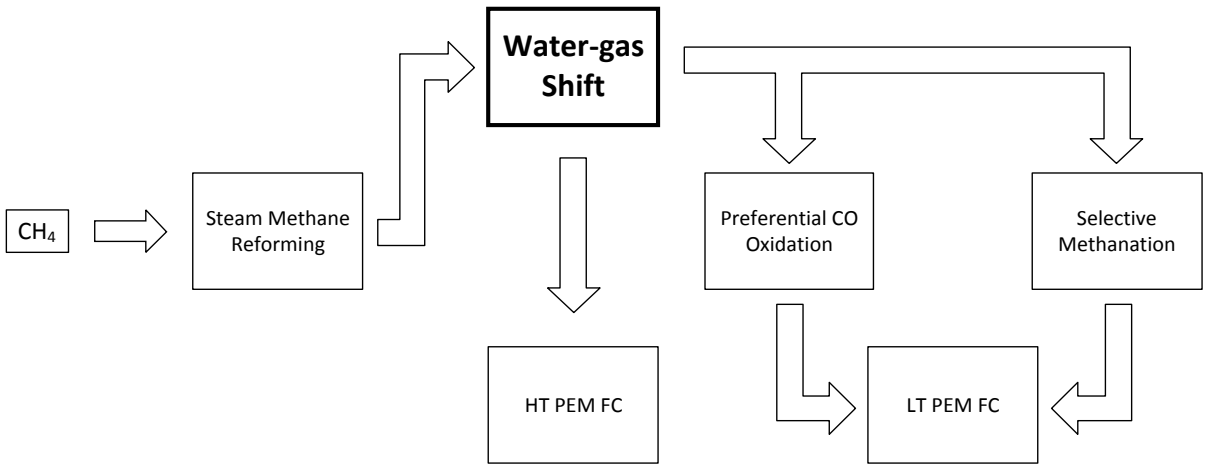

Figure 2-2 – Schematic diagram of the processing train of fuels for fuel cell feed

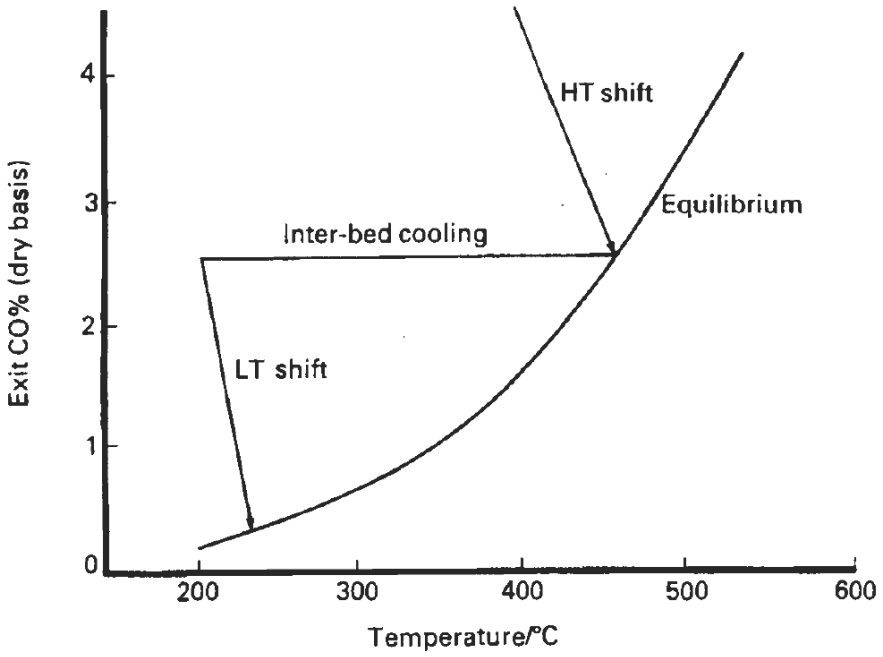

Figure 2-3 – Typical variations of carbon monoxide levels in HT and LT shift catalyst beds (Twigg, 1989, p.278)

The forward reaction is moderately exothermic and high CO equilibrium conversions are expected at lower temperatures. At low temperatures, however, the rate of reaction is much slower than at high temperatures. Thus a two stage shift is implemented for industrial processes. By utilising a high temperature shift to take advantage of the faster rate of reaction, and a low temperature shift to achieve high CO conversion, at the expense of slower rate of reaction, the two-stage process is able to reduce the final effluent stream's CO concentration to below 1% (Ladebeck and Wagner, 2003; Twigg, 1989). Figure 2-3 shows a typical water-gas shift reaction equilibrium curve for industrial conditions. It shows how the two stage process works in reducing the exit CO concentration to below 1%.

2.2.2. Thermodynamics

2.2.2.1. Temperature

As the water-gas shift reaction is an equilibrium reaction, the thermodynamics of the reaction plays an important role. The forward reaction is moderately exothermic (ΔH^0_{rxn} = -41kJ/mol), with the equilibrium constant defined as $K_{eq} = (p_{H_2} \cdot p_{CO_2}) / (p_{CO} \cdot p_{H_2O})$. The equilibrium conversion of CO decreases with increasing temperature.

According to Le Chatlier's Principle, the forward reaction of an exothermic equilibrium reaction will be favoured at lower temperatures. At low temperatures, however, the rate of reaction will be low. A balance must be made between favouring the forward reaction at a slow reaction rate and achieving fast rate at the sacrifice of overall CO conversion. This is achieved by operating a two-stage process where the first stage take advantage of high rate of reaction at high temperature, and the second stage favouring high overall CO conversion.

A simple empirical model developed by Moe (1962), as cited in Smith *et al.* (2010), represents the equilibrium constant as a function of temperature and is given by

$$K_{eq} = \exp\left(\frac{4577.8}{T} - 4.33\right) \qquad \textbf{Eqn 2.7}$$

2.2.2.2. Pressure

According to Le Chatlier's Principle, when pressure is applied to a reaction, the reaction will try to counter the change by favouring the side with the least total moles. For an equimolar reaction (which the water-gas shift reaction is one) the reaction will not favour either forward or reverse as either side will not counter the change in pressure. Literature reports that the system pressure does not affect the equilibrium, but has an impact on kinetically-limited systems as higher pressure can improve systems limited by pore diffusion (Ratnasamy and Wagner, 2009).

2.2.2.3. Steam-to-carbon ratio

An increase of steam to the system, thus an increase to the steam-to-carbon ratio, will favour the forward reaction. If the steam-to-carbon ratio is too low, it can also cause catalyst deactivation due to coke formation. Adversely, if the ratio is too high, it can increase energy consumption due to evaporation of water and negatively affect process economy (Ratnasamy and Wagner, 2009). A typical steam-to-carbon ratio of between 2.5 and 5 is used to both enhance equilibrium conversion, as well as decrease the chance of coke formation.

2.3. Industrial Catalysts for the Water-Gas Shift Reaction

2.3.1. High temperature Shift Catalyst

The commercial Fe/Cr high temperature shift catalyst has been in use for more than 60 years. Ratnasamy and Wagner (2009) report typical Fe/Cr catalyst containing 80-90 wt% Fe_2O_3, 8-10 wt% Cr_2O_3, and the balance being promoters and stabilizers, while Newsome (1980), as quoted in Smith *et al.* (2010), states the composition to be 74.2% Fe_2O_3, 10% Cr_2O_3, 0.2% MgO with the remaining being volatiles. Fe_2O_3, without support, deactivates quickly during operation due to sintering of the iron oxide crystallites. Therefore the addition of Cr_2O_3 and other stabilizers are needed. The ferrochrome catalyst is supplied as Fe_2O_3 and during start-up of a commercial unit the hematite is reduced to its active form of magnetite at typically around 300-450°C (Ratnasamy and Wagner, 2009).

Industrial operations of the high temperature water-gas shift reaction occur in adiabatic reactors with typical operating conditions of 300-360°C at the entrance into the first reactor. The pressure is between 10 and 60 bar and CO concentrations as high as 80 vol% (Newsome (1980) as quoted in Smith *et al.* (2010)). At very high inlet CO concentrations, the exit temperature can often reach in excess of 500-550°C. This, however, is not desired as the catalyst temperature is usually kept at a maximum of 510°C to keep thermal sintering to a minimum.

Commercial operating conditions are set such that the effluent CO concentration is approximately 2-5 vol% (Ratnasamy and Wagner, 2009).

Hydrogen sulphide can sulphide activated iron catalyst, converting Fe_3O_4 into FeS. This reaction, however, is reversible. When the hydrogen sulphide concentration in the feed decreases, FeS will go back to Fe_3O_4.

$$Fe_3O_4 + 3H_2S + H_2 \rightleftharpoons 3FeS + 4H_2O,\ \Delta H_{rxn} = -75.0\ kJ/mol \qquad \textbf{Eqn 2.8}$$

Prior to the development of a dedicated low temperature shift catalyst, a second water-gas shift stage was employed using the same Fe/Cr catalyst, operating at around 330°C (Ladebeck and Wagner, 2003). The success of the second stage water-gas shift in early ammonia generation plants led to the research and development of a dedicated low temperature shift catalyst (Ladebeck and Wagner, 2003).

2.3.2. Low temperature Shift Catalyst

Early implementation of the Fe/Cr catalyst in the lower-temperature second water-gas shift stage resulted in poor performance of the catalyst, which prompted further investigation into other metals. Work done by Bohlbro in 1961 showed the CO_2 in the reacting gas had a retarding effect on the forward reaction rate constant over the iron oxide high temperature catalyst. Larson developed, in as early as 1931, a copper-based catalyst for which CO_2 did not affect the forward rate of the water-gas shift reaction (Ladebeck and Wagner, 2003). Early low temperature catalysts were mainly unsupported Cu or Cu supported on various oxides supports (e.g. SiO_2, Al_2O_3); however these catalysts exhibited low lifetime (6-9 months) and low space velocity (400-1,000 h^{-1}) operation. The addition of ZnO or ZnO/Al_2O_3, as support, drastically increased the lifetime of the catalyst. Modern low temperature shift catalysts' typical lifetime being 2-3 years (Smith *et al.*, 2010), as well as improved turnover numbers in orders of magnitudes.

Typical compositions for the low temperature shift catalyst are 33% CuO, 34% ZnO, and 33% Al_2O_3 (Rhodes *et al.*, 1995), while a copper-zinc supported on chromium oxide consists typically of 68-73% ZnO, 15-20% CuO, 9-14% Cr_2O_3, and 2-5 % Mn, Al and Mg oxides (as stated by Newsome (1980) in Smith *et al.* (2010)). The typical operating temperature of the low temperature shift catalyst is around 200-250°C, with some recent catalysts, however, operating at temperatures of 300°C. Chromia, which was added to the high temperature catalyst to inhibit sintering, was also added to the low temperature catalysts to inhibit sintering. This, however, had little to no effect. ZnO and Al_2O_3 greatly inhibited sintering and allowed for the production of catalysts with high Cu surface area (Twigg, 1989; Ratnasamy and Wagner, 2009).

With typical effluent temperatures from the first high temperature shift reactor reaching as high as 550°C, an inter-bed cooler is needed to reduce the stream temperature to between 190°C

and 230°C, so as not to cause irreversible sintering of the catalyst. Depending on the performance of the high temperature shift stage, typical feed CO concentration for the low temperature shift is between 2-5 vol%. Operating at an exit concentration of less than 0.5%, the exit temperature of the low temperature shift is typically around 280°C.

The reason for sintering of the Cu catalyst is due to its low melting point (1063°C), and surface recrystallization occurring at the Hüttig temperature ($T_{Hüttig}$ = $0.3T_{melting}$; $T_{Hüttig,Cu}$ = 318.9°C). Sulphur poisoning is also a known deactivation mechanism for the copper catalyst. As can be seen from Equation 2.9, activated Cu reacts with hydrogen sulphide and forms copper(I) sulphide. The zinc oxide acts as a trapping mechanism (Eqn 2.10) because hydrogen sulphide will react much more readily with ZnO as compared to Cu. This is because the formation of copper(I) sulphide has a much lower equilibrium constant than the formation of zinc sulphide (Twigg, 1989).

$$2Cu + H_2S \rightleftharpoons Cu_2S + H_2,\ \Delta H_{rxn} = -59.4\ kJ/mol \qquad \textbf{Eqn 2.9}$$

$$ZnO + H_2S \rightleftharpoons ZnS + H_2O,\ \Delta H_{rxn} = -76.6\ kJ/mol \qquad \textbf{Eqn 2.10}$$

Improved activity for Cu/Zn has been seen when promoted with alkali metals, however the inherent problem of pyrophoricity still exists (Faur-Ghenciu, 2002).

2.3.3. Proposed Mechanism for Water-Gas Shift Reaction

Investigations have been carried out since the discovery that water-gas shift can be catalysed over various metallic oxides, to find a universally accepted mechanistic description of the reaction. This, however, has not occurred even though the water-gas shift reaction does not seem to be complex. The sensitivity of both the iron and the copper catalysts to small changes in the feed has complicated studies trying to find a satisfactory description of the mechanism (Rhodes *et al.*, 1995). Koryabkina (2003) said that "[t]he inherent complexity of this reaction is further illustrated by the fact that the same Cu catalyst, under different reaction conditions, is also used to produce methanol.", which can also be an indication as to why no universally accepted mechanistic description has been found.

Rhodes *et al.* (1995) indicated that there are two general mechanisms for the water-gas shift reaction over metallic oxide catalysts. They are (a) the regenerative mechanism, and (b) the associative mechanism. Two more mechanisms were added, by Callaghan (2006), namely (c) the formate mechanism, and the more recently (d) the carbonate mechanism.

First described by Armstrong and Hilditch in 1920 (as stated in Rhodes *et al.* (1995)), the *regenerative mechanism*, also known as the redox mechanism, is the separation of water into its elemental components via reduction and the subsequent oxidation of the catalyst surface (Rhodes *et al.*, 1995). Ovesen *et al.* (1992) described an eight-step elemental reaction (Table 2-3)

for the regenerative mechanism, which appears to be the simplest model that can account for the reactions on a single crystal of Cu.

Table 2-3 – Elementary Reaction Steps for the Regenerative Mechanism

Reaction Steps			Number
$H_2O + *$	⇌	$H_2O.*$	1
$H_2O.* + *$	⇌	$OH.* + H.*$	2
$2OH.*$	⇌	$H_2O.* + O.*$	3
$OH.* + *$	⇌	$O.* + H.*$	4
$2H.*$	⇌	$H_2 + 2*$	5
$CO + *$	⇌	$CO.*$	6
$CO.* + O.*$	⇌	$CO_2.* + *$	7
$CO_2.*$	⇌	$CO_2 + *$	8
$CO + H_2O$	**⇌**	**$CO_2 + H_2$**	**Overall Reaction**

Note: asterisk indicates free surface site

The *associative mechanism*, first described by Armstrong and Hilditch in 1920, was developed on data gathered from a copper chromite catalyst. This mechanism proposes an intermediate of unspecified structure after the adsorption of CO and H_2O onto the catalyst surface which subsequently decomposes into the reaction products (Eqn 2.11) (Rhodes *et al.*, 1995).

$$CO + H_2O \rightleftharpoons (\text{Intermediate}) \rightleftharpoons CO_2 + H_2 \qquad \textbf{Eqn 2.11}$$

Rhodes *et al.* (1995) expanded on the associative mechanism by determining the intermediate formed to most likely be of a formate group, with FTIR confirming the presence of the formate intermediate, arriving at a *formate mechanism* (Table 2-4). The formate intermediate is formed from the adsorbed CO and the hydroxyl group from the dissociation of H_2O. The formate then dissociates into adsorbed CO_2 and atomic H, which further dissociates into the reaction products of CO_2 and H_2.

Table 2-4 – Elementary Reaction Steps for the Formate Mechanism

Reaction Steps			Number
$CO + *$	⇌	$CO.*$	1
$H_2O + 2*$	⇌	$H.* + OH.*$	2
$OH.* + CO.*$	⇌	$HCOO.* + *$	3
$HCOO.* + *$	⇌	$CO_2.* + H.*$	4
$CO_2.*$	⇌	$CO_2 + *$	5
$2H.*$	⇌	$H_2 + 2.*$	6
$CO + H_2O$	**⇌**	**$CO_2 + H_2$**	**Overall Reaction**

Note: asterisk indicates free surface site

It was also proposed that the surface intermediate species is a carbonate group, as Millar *et al.* (in Callaghan (2006)) determined via IR spectroscopy, thus deriving the *carbonate mechanism* (Table 2-5).

Table 2-5 – Elementary Reaction Steps for the Carbonate Mechanism (Callaghan, 2006)

Reaction Steps			Numbers
$CO + 2O.*$	$\rightleftharpoons$	$CO_3.*2$	1
$CO_3.*2$	$\rightleftharpoons$	$CO_3.* + *$	2
$CO_3.*$	$\rightleftharpoons$	$CO_2 + O.*$	3
$H_2O + *$	$\rightleftharpoons$	$H_2O.*$	4
$H_2O.* + O.*$	$\rightleftharpoons$	$2OH.*$	5
$2OH.*$	$\rightleftharpoons$	$2O.* + H_2$	6
$H_2O.* + *$	$\rightleftharpoons$	$OH.* + H.*$	7
$2H.*$	$\rightleftharpoons$	$H_2 + 2*$	8
$CO + H_2O$	$\rightleftharpoons$	**$CO_2 + H_2$**	**Overall Reaction**

Note: asterisk indicates free surface site

2.4. PGM Catalysts for the Water-Gas Shift Reaction

Base-metal catalysts for water-gas shift are designed for industrial applications, requiring lengthy *in-situ* reduction prior to use, as well as the inability to withstand start up-shutdown cycles. These catalysts are also pyrophoric once reduced and thus, require extra care when handling once reduced. The miniaturisation of fuel processing catalysts would require these potential drawbacks to be solved.

Automotive catalysts, mainly based on precious metals supported on monoliths, have been in use for the past 35+ years, show the most promise for possible water-gas shift activity. Although automotive catalysts operate in a oxidative atmosphere, under much higher temperatures (450°C) and lower partial pressures of H_2 and CO_2, they form an interesting base for fuel processing WGS (Ratnasamy and Wagner, 2009; Farrauto *et al.*, 2007). Of the many catalysts that have been studied, platinum-group metals supported on partially reducible oxides (ceria, zirconia, titania) have been the most investigated (Ratnasamy and Wagner, 2009).

PGM catalysts for water-gas shift, specifically Pt/CeO_2, have been studied since 1980s, with Mendelovich and Steinberg (as reported in Faur-Ghenciu (2002)) reporting methanation and water-gas shift activity in 1985. High water-gas shift activity of the PGM catalysts have been known for decades; however the high prices of PGMs have been a barrier to entry for commercial use. The current impetus for more research into this field is due to a renewed interest in alternative power generation methods, specifically in fuel cell power generation (Ratnasamy and Wagner, 2009).

Farrauto *et al.* (2007) indicated that precious metal catalysts are inherently more active than traditional base metals, however Pt-containing catalysts must minimize the production of methane at high temperatures as this undesired side reaction will consume vital H_2. It was also indicated that precious metal catalysts are able to withstand condensation, as well as exposure to air, with no loss to catalyst activity, and no safety issues. Continuous catalyst research has resulted in increased efficiency of precious metals of automotive catalysts, thus a decrease in the usage of metal and the overall cost of the catalyst. Fuel processing catalysts are expected to follow a similar trend.

2.4.1. Metal Type

Various metal types have been investigated for fuel processing for fuel cells. Ratnasamy and Wagner (2009), and Farrauto *et al.* (2007) summarized the various precious metals investigated, including: Ir, Ru, Rh, Pt, Pd, and Au.

2.4.1.1. Non-promoted PGM Catalysts

Flaherty *et al.* (2011) compared the water-gas shift reaction between Cu (1 1 1) and Pt (1 1 1) single crystals under identical conditions (612 K, 26 Torr CO, 10 Torr H_2O) and showed that the observed turnover frequency for Pt was five-times higher than Cu. Pt, however, lacked the long-term stability seen on Cu due to formation of carbonaceous deposits, i.e. coking of the catalyst.

Typical loading of Pt on partially reducible metal oxides, based on various journals, are between 0.5 wt% - 3 wt%. Radhakrishnan *et al.* (2006) studied various precious metal catalysts on a ceria-zirconia in the temperature range of 200°C to 320°C, using 2 simulated feeds (simulating a high temperature shift feed and a low temperature shift feed). A trend of the activity of metals was found to be Pt > Rh > Ru, Pd, > Ir, Au. Optimum Pt loading was determined to be 1-2 wt%. It was also found that both Ru and Rh catalysts, at higher temperatures than base metal LT shift or HT shift, showed methane production.

The trends in the turnover frequency of precious metals on titania is similar to that on ceria-zirconia, where Pt > Rh > Ru > Pd, with Pt being approximately 20 times more active than Pd (Panagiotopoulou, 2004). The optimum Pt loading on TiO_2, according to Panagiotopoulou, however, differed from that reported by Radhakrishnan *et al.*, with increasing metal loading allowing the equilibrium reaction temperature to decrease.

2.4.1.2. Promoted PGM Catalyst

There has also been research into promoted Pt catalysts for the water-gas shift reaction. Choung *et al.* (2005) looked into a Re-promoted Pt catalyst supported on ceria-zirconia. It is reported that as Pt loading increased, CO conversion also increased. The composition of the two ceria-zirconia mixtures used ($Ce_{0.6}Zr_{0.4}O_2$ and $Ce_{0.46}Zr_{0.54}O_2$), however, showed little effect on the overall conversion of CO. It was also shown that 1 wt% Re/ceria-zirconia did not show water-gas

shift activity. Pt-Re/ceria-zirconia (both at 1 wt%), however, outperformed 1 wt% Pt/ceria-zirconia in terms of CO conversion rate. It was noted that with the addition of Re may have stabilized Pt against high temperature sintering, based on TPR data.

Du *et al.* (2008) investigated similar Re promoted $Pt/Ce_{0.8}Zr_{0.2}O_2$ and showed that Re does seem to promote the water-gas shift reaction over a pure supported Pt catalyst, with an optimal Re:Pt weight ratio determined to be 3:1. Azzam *et al.* (2008) looked into Re promoted Pt/TiO_2 and showed that Re exists on the surface of the catalysts partly as ReO_x to provide additional pathways for a redox route, where ReO_x is reduced by CO generating CO_2 and reoxidized by H_2O forming H_2.

Kim *et al.* (2009) used ceria as a promoter for Pt supported on various supports and showed that $Pt\text{-}Ce/TiO_2$ outperformed $Pt\text{-}Ce/CeO_2$ at a Ce:Pt weight ratio of 5:1.

2.4.2. Support Type

Partially reducible oxides have been shown to have the most potential in combination with PGMs for use within a miniaturised fuel processing assembly. During the development of three-way catalysts for the automotive industries, typically Pt-Pd-Rh supported on alumina, ceria was discovered to be the best non-noble metal oxide promoter as it was able to enhance the water-gas shift reaction (Faur-Ghenciu, 2002).

2.4.2.1. Single-component support

A direct comparison of different support materials was done by Panagiotopoulou and Kondarides (2006). They showed that using 0.5 wt% Pt loading on various supports, Pt/TiO_2 was the most active pairing, with measurable CO conversions at temperatures as low as 150°C and achieving equilibrium (feed conditions of 3% CO, 10% H_2O, balance He) at 400°C. Other supports, such as CeO_2, La_2O_3 and yttria-stabilized zirconia, achieve equilibrium CO conversion at approximately 450°C.

Panagiotopoulou (2004) also showed that the activity of Pt/TiO_2 is highly dependent on the morphology of the support, with the rate of reaction per surface Pt atom increasing by two orders of magnitude when the TiO_2 crystal size was halved from 35nm to 16nm.

In a study performed by Hilaire *et al.* (2004), it was shown that Pd/CeO_2 outperformed Pd/SiO_2 as well as pure CeO_2, indicating a possibility of metal support interaction. Hilaire *et al.* (2004) cited experiments performed by Bunluesin *et al.* on ceria using different metals and showed that the rate of reaction was independent of the metal, suggesting that the reaction occurred at the metal-ceria interface so long as the metal is able to adsorb CO, as well as catalyse CO oxidation efficiently. When the rates of Ni/CeO_2 and Pd/CeO_2 were compared by Hilaire *et al.* (2004), it was reported that the rates were indeed similar.

A study by Liu *et al.* (2005) showed possible deactivation of 1 wt% Pt/CeO_2 due to shut-down cycles from formations of carbonates on the support surface thus blocking Pt metal on the surface. The catalyst was unable to regenerate *in-situ*, however, it was able to be regenerated with treatment in air at >400°C (burning off of coke).

2.4.2.2. Mixed support

González *et al.* (2010) made direct comparisons between single component supports (TiO_2, CeO_2) and mixed support ($Ce\text{-}TiO_2$). It was shown that $Pt/Ce\text{-}TiO_2$ outperformed Pt/CeO_2 and Pt/TiO_2 in both CO conversion as well as turnover frequency.

Jeong *et al.* (2013) made similar comparisons between pure and mixed supports, looking at different ratios of CeO_2/ZrO_2. It was, however, determined that Pt/CeO_2 achieved higher CO conversion as well as higher turnover frequency when compared with different ratios of CeO_2/ZrO_2 (80, 60, 40, and 20 mol% CeO_2, balance is ZrO_2) as well as pure ZrO_2. It was concluded that the catalytic performance of $Pt/Ce_{(x)}Zr_{(1-x)}O_2$ is highly dependent on the reducibility of the support.

2.5. Non-PGM Catalysts for the Water-Gas Shift Reaction

There are also various non-PGM supported water-gas shift catalysts that have been investigated for the purpose of fuel processing for fuel cells. The main reason for the investigation into non-PGM catalysts is due to their low cost compared with PGM based catalysts.

High temperature shift alternatives are based on selected metals, including Mg, La, Mn, $Co/MgAl_2O_4$, Mg/ZrO_2, K/ZSM5. These alternatives are typically active above 400°C, with the main benefit over other alternatives, such as Co- or Ni- promoted Mo, V, W oxides, being a lack of methanation at low CO conversions (approximately 25-30% CO conversions). The alternative catalysts have been reported to achieve CO conversion, in a feed containing only CO and H_2O, of approximately 40% at space velocities below 8,000 h^{-1} (Faur-Ghenciu, 2002).

Patt *et al.* (2000), and Moon and Ryu (2004) looked into the suitability of Mo_2C as an alternative to Cu/Zn as a water-gas shift catalyst. It was seen that Mo_2C was able to outperform Cu/Zn under a feed composition of 62.5% H_2, 31.8% H_2O, and 5.7% CO, however, the carburisation temperature, i.e. the temperature at which MoO_2 turns to Mo_2C, plays a key role in whether the catalyst will be comparable with Cu/Zn at those conditions. It was shown by Moon and Ryu that the optimum range for this carburisation of the oxide is between 640°C and 650°C. Moon and Ryu also showed that Mo_2C is more resistant to thermal cycling as compared with Cu/Zn. Another alternative for Cu/Zn was a cobalt-vanadium binary oxide, as reported by Faur-Ghenciu (2002). It was reported that this binary oxide has a higher normalised specific activity than Cu/Zn.

3. Research Aims and Objectives

3.1. Aim

The aim of this investigation is to compare the operating range of commercially available base metal water-gas shift catalysts with that of a range of supported PGM catalysts. This study also aims to determine the operating conditions at which the tested catalysts are able to achieve an effluent CO concentration of 1 vol%, to be used in series with a high temperature PEM fuel cell.

3.2. Hypothesis

It is thus hypothesised, based on literature review, that the supported PGM catalyst will show water-gas shift activity and that there exists a viable combination of temperature and space velocity where the tested catalysts, both base metal catalysts and PGM catalysts, are able to achieve an effluent CO concentration of 1 vol%.

3.3. Objectives

The objectives of this investigation are to investigate the catalysts and to determine if they are able to produce an effluent stream with a CO concentration of 1 vol% or less. This investigation also seeks to screen the catalysts in a temperature range between 180°C – 450°C.

3.4. Key Questions

Some key questions which arise:

- How does the supported PGM catalyst compare, at similar operating conditions, with the commercial catalysts?
- How does the initial steam-to-methane ratio of the upstream steam methane reformer feed affect the effluent stream of the water-gas shift reactor?
- How stable are the catalysts at the chosen operating conditions?
- Which catalyst is most suited in the portable application of fuel processing for fuel cells based on stability and operating conditions?

4. Experimental

4.1. Catalysts Evaluated

The catalysts selected for this investigation were based on readily available base-metal low temperature and high temperature catalysts (both supplied by Süd-Chemie), as well as one currently available PGM-based catalyst. The PGM-based catalyst will henceforth be known as "Catalyst X" due to non-disclosure agreement with the provider as well as for ease of reference.

4.1.1. Catalysts Pre-treatment

The two base-metal catalysts come in tablet form. Tablet dimensions are 5 mm x 3 mm for the low temperature Cu/Zn catalyst, and 6 mm x 6 mm for the high temperature Fe/Cr catalyst. Before use, both catalysts are crushed and sieved such that only catalyst particles of sizes between 350-500μm are used such that it is approximately the same size as the diluent (SiC) used.

The PGM-based Catalyst X comes in powder form with particle sizes of less than 50μm, and was used as is within the reactor.

4.2. Experimental Apparatus

Figure 4-1 shows the flow diagram of the experimental apparatus used for this investigation. The experimental apparatus consists of a feed section, reactors, and a downstream section, which will be discussed in detail. Figure 4-2 indicates the breakdown of these sections on the PFD.

4.2.1.1. Feed Section

The feed section of the experimental apparatus consists of the five gases required in the investigation, with four of the gases, H_2, Ar, CO, and N_2 (Gases supplied by Afrox, 99.99% purity), coming from the internally-provided main laboratory gas network and CO_2 (Afrox, 99.99% purity) connected from external gas cylinders. All gas feeds are controlled via mass flow controllers (Brooks Instruments, SLA 5800 Series) and are fed through a guard catch-pot, used to guard liquid back-flow in case of a blockage within the reactors as this flooding can cause damage to the mass-flow controllers.

Water is fed, independently, via 3 isocratic single-head HPLC pumps (Scientific Systems, Inc., Series-I) into the reactors, as liquid, where it will evaporate in the evaporator section of the reactor.

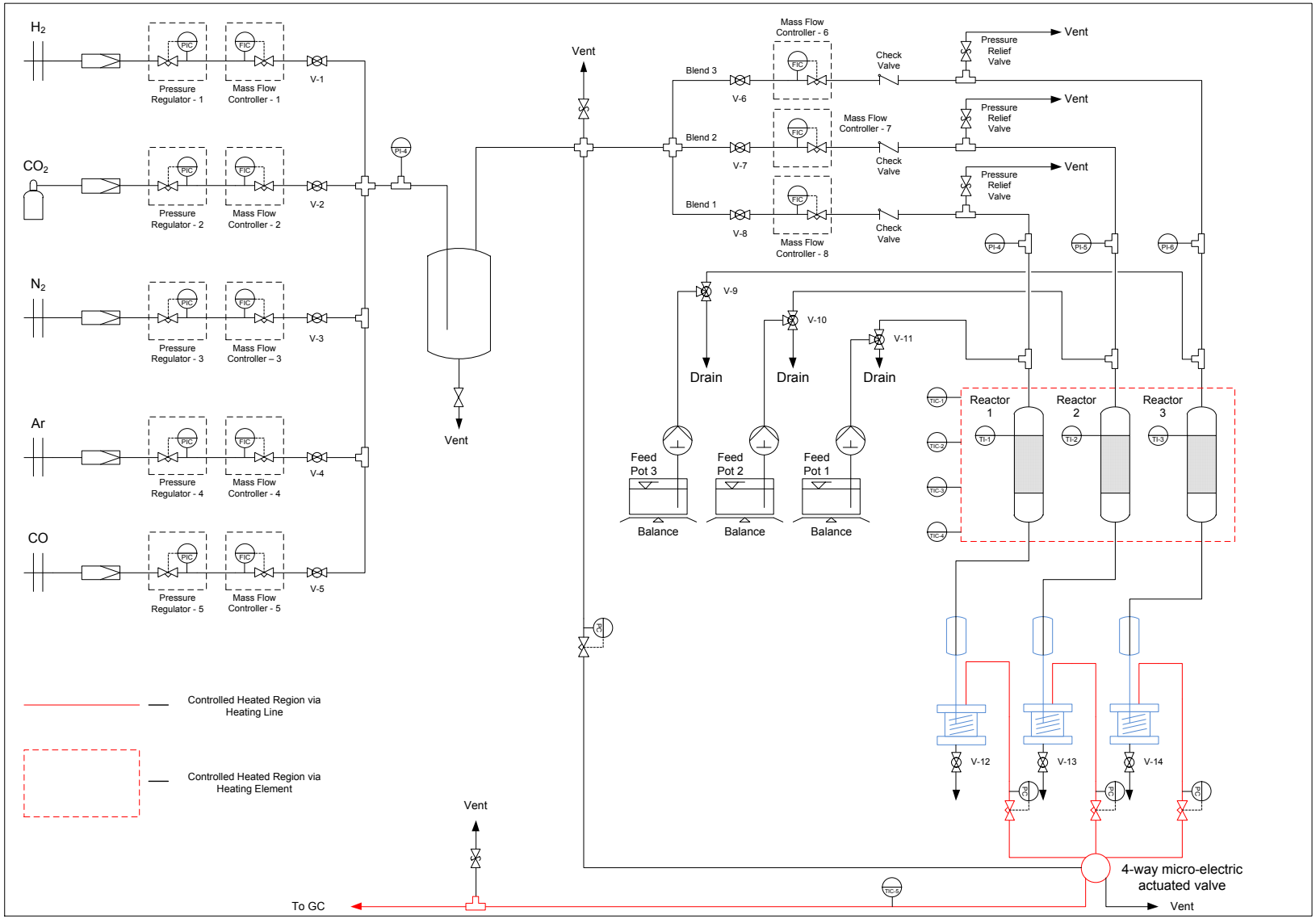

Figure 4-1 – Flow Diagram of Experimental Apparatus

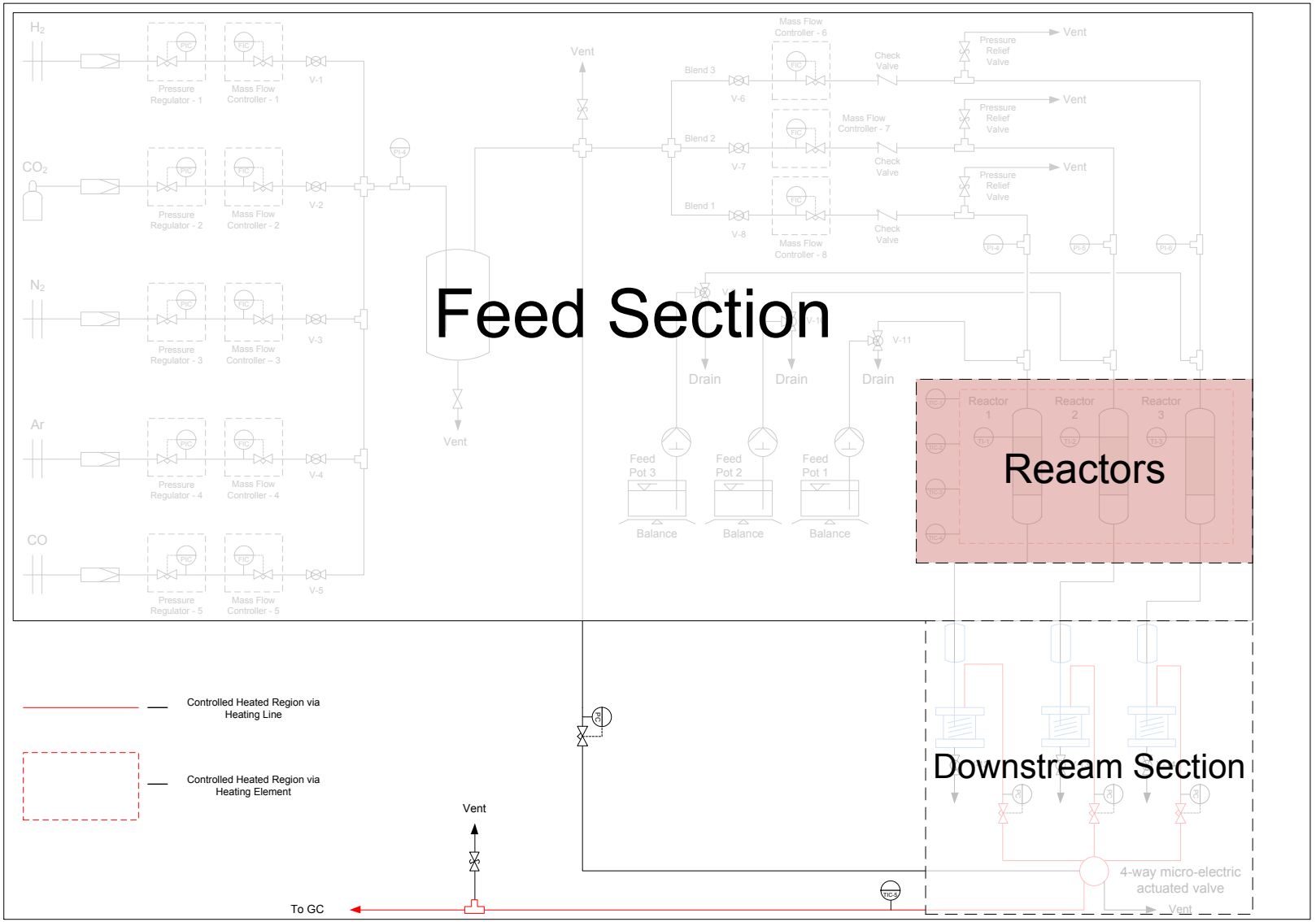

Figure 4-2 – Flow Diagram of Experimental Apparatus Showing Feed, Reactors and Downstream Sections (view in conjunction with Figure 4-1)

4.2.1.2. Reactor

To facilitate the testing of multiple catalysts, the design of the experimental apparatus incorporated 3 vertical parallel tubular fixed-bed reactors. Figure 4-3 shows the schematic drawing of one such reactor. The reactors consist of a 500 mm long stainless steel tube with inner diameter of approximately 15.75 mm. The head of the reactor can be removed to simplify the loading and unloading of catalyst, and is sealed and pressure-tested before any run. Two thermocouple wells are incorporated into the reactor, with one located as part of the head of the reactor to allow the measurement of the liquid feed temperature, and the other acts as the central thermowell to allow the determination of the isothermal zone as well as an overall temperature profile of the reactor.

The reactors sit, vertically, within a brass reactor housing, where four external heating bands, (numbered from the top of reactor, 1 to 4) are located on the outside of the brass housing. Each heating band has its own temperature controller, thus allowing for the creation of an isothermal zone, using temperature controller 2 and 3, where the reactor temperature is at the desired set point, within 1°C of the set point, along the reactor.

The reactor can be divided into three separate zones. The zones are, from the bottom of the reactor: spacer, catalyst bed, and evaporator. The spacer zone consists simply of SiC granulates used to locate the catalyst bed within the isothermal zone. The catalyst bed consists of catalyst particles or powder diluted with SiC such that catalyst bed volume remains constant during different catalyst loadings.

The evaporator zone consists of SiC granulate as used in the spacer zone. The beginning of this zone, i.e. where the temperature is the lowest, must be below the boiling temperature of the liquid being pumped. This is to minimise pulsed flow generated by the pump, as sudden expansion of vaporising liquid can generate poor quality of data.

Figure 4-4 shows the temperature profiles obtained, via the thermocouple through the centre of the reactor, for all three reactors at a set temperature of 200°C. It can be seen that the temperature at the beginning of the evaporator zone is below the boiling point of water at 2 bara (approximately 120°C) as to ensure no occurrence of flash vaporisation. The isothermal zone is between 200 mm and 410 mm from the top of the reactor and the catalyst bed is within this isothermal zone.

4.2.1.3. Downstream Section

The product stream contains water vapour, which can cause flooding within the GC columns when condensation occurs as this section, as well as the GC columns, operates at below the boiling point of water. Flooding will render the GC columns inoperable. Water vapour is thus condensed out of the product stream before being sent into the GC for analysis. The condensers

consist of three cooling vessels, connected in series to each reactor, with coolants set at 2°C, operating counter-current to the gas flow of the reactors. The cooling vessels are connected to the outside of the tubing of the effluent line from the reactor, and this is then connected to Perspex catch-pots such that the liquid water will remain within the catch-pot and the gases can flow from the catch-pot through to the online GC for analysis.

The line extending from the catch-pots, through the back-pressure regulators, are heated to 60°C to ensure the water vapour, which still remains within the gaseous product, does not condense on its way to the GC for analysis. The system is held at pressure via back-pressure regulators (Swagelok) placed after the catch-pots.

4.2.1.4. Gas Analysis

The effluent stream was analysed on-line via an automatically actuated sampling valve. The valve is able to select the effluent streams from one of the three reactors, or the dry feed gas to be analysed by the gas chromatograph.

4.3. General Operating Procedures

The detailed catalyst handling procedures with catalyst shaping, reactor loading, reduction, and removal of catalysts are presented in Section 4.3.1. A step-by-step operating procedure of the experimental apparatus during experiments, start-up, shutdown, and emergency shutdown are provided in Sections 4.3.2 and 4.3.3.

4.3.1. Detailed Catalyst Handling Procedures

4.3.1.1. Reactor Loading

1. Start with clean reactors washed with acetone
2. Secure reactor using vice via adaptor for ease of loading
3. Insert a small plug of silane-treated glass wool, enough to ensure no SiC leaves the outlet port of the reactor. Surround the central thermowell with the glass wool and push down to cover the outlet port of the reactor
4. Weigh the required amount of catalyst, add diluent (SiC) and physically mix the two dry components together, using an empty glass vial large enough to hold both contents, by rotating the vial at an angle such that physical mixing can occur
5. Fill reactor with SiC to the required level such that the catalyst bed will be within the isothermal zone when the catalyst is placed into the reactor. Care must be taken to make sure no SiC escapes the reactor through the outlet port of the reactor. Tap gently to ensure the SiC settles, then add more SiC if required
    a. (**For Catalyst X only**) Insert an extra small plug of silane-treated glass wool into the reactor, making sure it is directly on top of the SiC already in the reactor, to

prevent the powdered catalyst mixture from separating and the possible increase in catalyst bed size

6. Pour the catalyst and diluent mixture into the reactor and tap gently to allow the bed to settle. Do not tap for too long as this can cause the catalyst to separate from the diluent
7. Fill the reactor with SiC until approximately 1 cm from the lip of reactor
8. Make sure liquid feed point in the head of reactor touches the top of the SiC. This will allow excellent mixing conditions for the liquid feed across the cross-section of reactor with the feed gases
9. Insert stainless steel gasket (¾ in.) between reactor head and body. Tighten reactor head onto reactor body to make an air-tight seal

4.3.1.2. Catalyst Reduction

1. Set Reactor MFCs flow rate (MFCs 6-8) to 125 sccm throughput
2. Set gas flow rate of 2% H_2 in N_2 by setting MFC 1 (H_2) to 10 sccm and MFC 3 (N_2) to 490 sccm
3. Set the following setpoints and execute the temperature ramping programs for the temperature controllers as seen in Table 4-1 :

Table 4-1 – Temperature settings and ramping programs required for *in-situ* reduction of catalysts

Temperature Controller	Setpoint			
	LTS/PGM	Corresponding Temperature	HTS	Corresponding Temperature
1	186°C	200°C	372°C	400°C
4	186°C	200°C	372°C	400°C
	Temperature Ramping Program			
	LTS/PGM		HTS	
2	Ramp up to 186°C @ 1°C/min, hold for 16 hours		Ramp up to 372°C @ 1°C/min, hold for 16 hours	
3	Ramp up to 186°C @ 1°C/min, hold for 16 hours		Ramp up to 372°C @ 1°C/min, hold for 16 hours	

4. Once desired temperature has been reached and the set times has passed, set gas to 100% H_2 (500 sccm) for 1 hour by changing MFC 1 to allow reduction to complete
5. Once reduction has been completed, set gas to 100% N_2 (MFC 3) and set temperature to desired temperature required to begin experiment (Refer to Table 4-4 for experimental conditions)

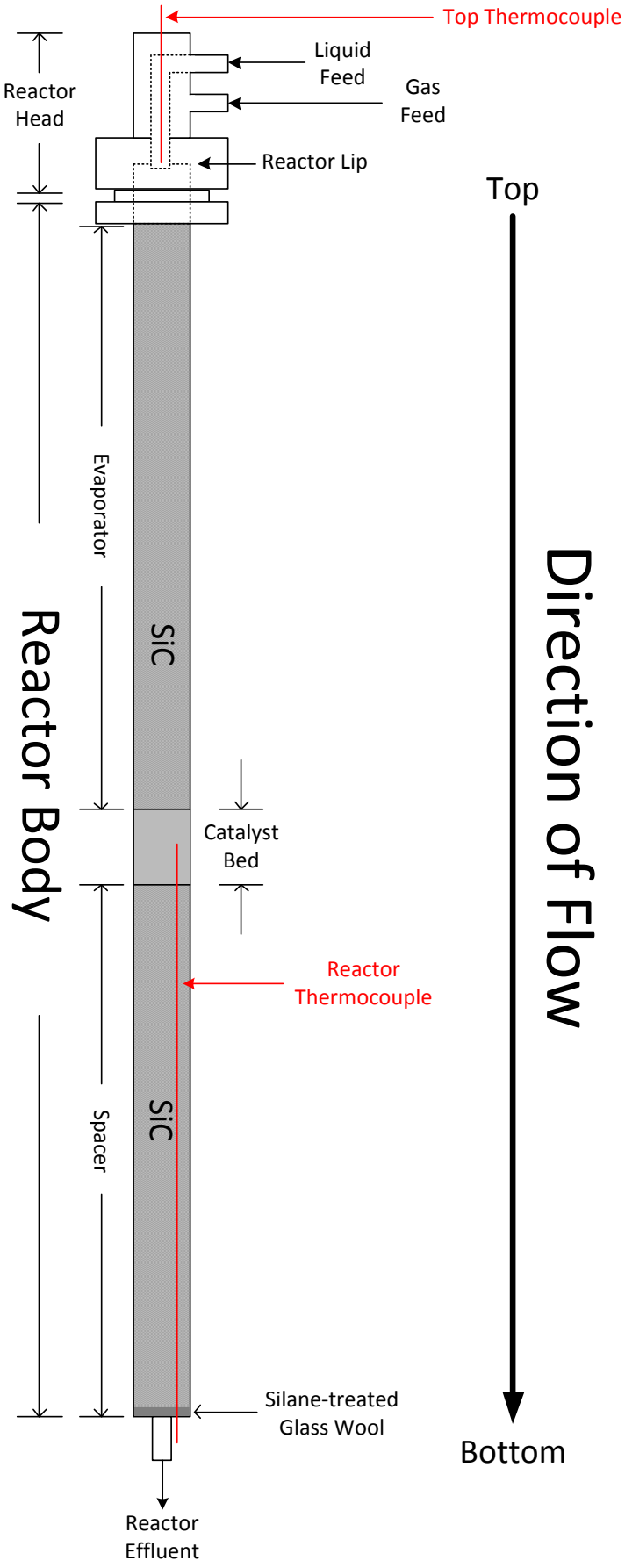

Figure 4-3 – Reactor Schematics

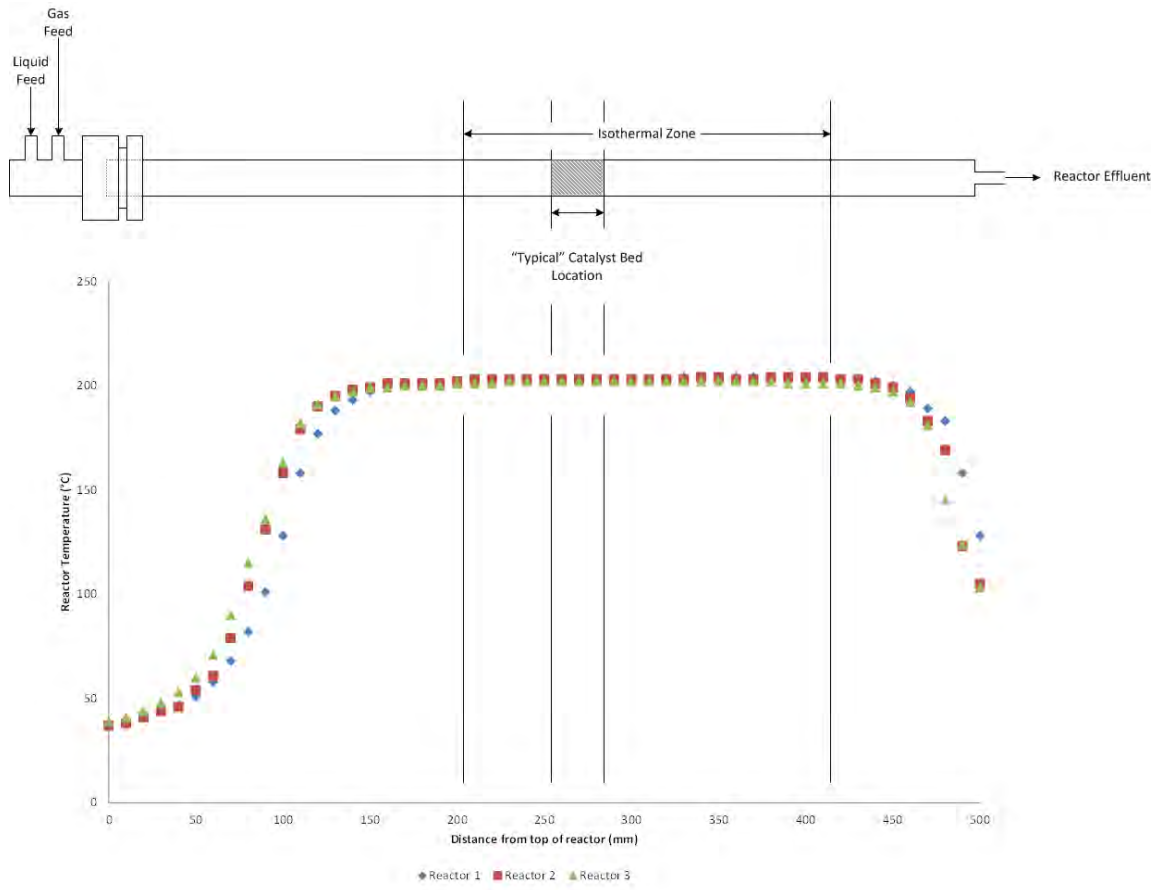

Figure 4-4 – Temperature profile of reactors with graphical representation of a reactor and the indication of isothermal zone and "typical" location of catalyst bed

Note that for Catalyst X, due to the nature of the catalyst, no reduction is required. However, a procedure is used to ease the catalyst into the required temperature. This is done by setting gas flow through the reactor to 100% nitrogen via MFC 3 and setting the temperature ramping program to ramp up to 186°C (this corresponds to 200°C within the reactor) at 1°C/min and holding for 16 hours. The hold-time is used such that it is the same for all three catalysts.

4.3.1.3. Reactor Load Removal

It is assumed that the reactor has been removed from the experimental apparatus as outlined in Section 4.3.3.1.

1. Secure reactor using vice via adapter
2. Remove reactor head using wrench
3. Tip reactor upside down, gently tap the side of reactor and remove SiC and catalyst bed. If needed, use compressed air to blow SiC loose
4. Remove silane-treated glass wool from the bottom of the reactor using adhesive tape secured to the end of a metal rod long enough to reach the end of the reactor
5. Safely dispose the spent catalyst.
6. Rinse reactor in acetone, making sure to clean the threads of reactor

4.3.2. Start-up, Sampling Method, Temperature and Space Velocity Changes

1. Start with all reactors empty and clean
2. Load all three reactors with required amount of catalysts (Refer to Section 4.4.2 for the amount of catalyst required. Section 4.3.1.1 for reactor loading instructions)
3. Following instructions for securing of reactors should be done by securing reactor 3 first, then reactor 2, then reactor 1:
    a. Place reactor into the corresponding position of the brass housing
    b. Connect the gas and the liquid inlet port, ensuring the stainless steel gaskets are in the fittings and are in good condition
    c. Connect the reactor outlet to the effluent line plumbing, ensuring the stainless steel gasket is in the fitting and is in good condition
    d. Insert the appropriate thermocouple into the correct reactor, making sure the tip of the thermocouple is located within the predetermined isothermal zone
4. Ensure all catch-pots, including the guard catch-pot, are empty by opening the drainage valves, allowing any liquid present to drain
5. Open all internal laboratory gas network lines and check the supply pressures for each gas
6. Check all inlet pressure regulators to ensure the feed MFCs (MFCs 1 – 5) are supplied with at least 20 barg of pressure
7. Set N_2 flow rate on MFC 3 to 400 sccm and set MFCs 6 – 8 (reactor MFCs) to 100 sccm to allow the reactors to pressurise to 5 barg
8. Once reactors have been pressurised, perform leak test on the system by checking the MFCs. If the MFCs indicate flow, a leak is present in the system (as once the system is pressurised, no flow should be seen on the MFCs)
9. Switch the cooling bath circulation on, set cooling bath temperature to 2°C
10. Set effluent stream heating line temperature to 60°C
11. Begin reduction of catalyst (Reduction procedures detailed in Section 4.3.1.2)
12. Switch on power for balances and ensure sufficient liquid is in the liquid feed containers
13. Once reduction is complete, switch V-9 – V-11 (liquid feed prime/drain valve) to drain position and prime the pumps for 60 seconds flow or until liquid is seen in the catch-pots
14. Adjust MFCs 1 – 5 to the required feed composition (Refer to Table 4-4 for list of experiments)
15. Adjust MFCs 6 – 8 (Reactor MFCs) to the required flow rate (Refer to Table 4-5 for list of flowrates)
16. Set required pump flowrate and start pump, and record start time of run

17. Using software provided by Varian, instruct the GC to begin automatic sampling as per method described in Section 4.5.1
18. Drain water catch-pot at least once every 24-hours to prevent water build-up in the catch-pots. This will also depressurise the system
19. Once the desired number of data points for the current temperature and space velocity has been obtained, adjust:
    a. MFCs 1 – 5 and pumps 1 – 3 to the new required feed composition
    b. MFCs 6 – 8 to the new required space velocity
20. Once all experiments required to be performed are finished, proceed to shutdown (see Section 4.3.3)

4.3.3. Shutdown Procedures

4.3.3.1. Normal Shutdown

1. Set water pumps flow to 0 sccm
2. Shut off water pumps
3. Switch liquid feed valves to prime position so no liquid will enter reactors
4. Shut off all gas feeds (MFC-1,2,4,5) apart from Nitrogen
5. Close valves V-1, V-2, V-4, V-5 to ensure gases are shut off
6. Set Nitrogen flowrate on MFC-3 to 400 sccm
7. Drain water in water knock-out pot. This will also depressurise the system
8. Shut off heating and power to the experimental apparatus
    a. If reactors are to be reloaded (i.e. a new run is to be started), shut off reactor heating only and leave effluent stream heating line on
    b. If long-term shut down is planned, shut off reactor heating, effluent stream heating line, balances, pumps, cooling bath, and micro GC.
9. Allow system to cool down
10. Shut off nitrogen supply on MFC-3, and shut off reactor MFCs 6 – 8
11. Switch main laboratory gas network nitrogen supply valve and V-3 to off
12. Disconnect inlet and outlet ports of the reactors, starting with reactor 1
13. Remove reactors from brass housing
14. Empty and clean reactors as per Section 4.3.1.3

4.3.3.2. Emergency Shutdown

In case of emergency, the following steps should be followed to allow a safe and quick shutdown of the experimental apparatus.

1. Switch off main illuminated power switch. This will shut off all powered units on the experimental apparatus as well as the MFCs

2. Switch off all main laboratory gas network line supply valves to ensure no gas flows into the experimental apparatus

4.4. Experimental Programmes, Feed Composition, and Catalyst Loading

4.4.1. Feed Composition

Three simulated water-gas shift reaction feed compositions were applied. Their compositions are based on the effluent streams of a steam methane reforming (SMR) reactor operating at equilibrium. The difference between the three feed compositions is the initial steam-to-methane ratio fed into the steam methane reforming reaction which caused differences in the steam-to-carbon monoxide ratio of its effluent stream.

Table 4-2 shows the compositions of Feeds 1, 2, and 3. Unreacted methane from the steam methane reforming has been replaced with argon, to be used as an internal standard of the gas chromatograph. The argon will be used to facilitate the analysis of the gas chromatography results as well as to determine if the water-gas shift reaction, under the proposed operating conditions set out in Section 4.4.2 will give rise to any methane production.

The feed simulates a mock steam methane reformer effluent operating close to thermodynamic equilibrium with differing steam to methane ratio and temperature.

Table 4-2 – Composition of simulated SMR effluent gas (i.e. WGS feed) used

Steam Methane Reforming Conditions	**S/CH_4 Ratio**	2.35	3.02	5.00
	Temperature (°C)	700	800	700
	X_{Eq,CH_4} (%)	94.2	86.6	95
SMR Effluent = WGS Feed Conditions	**Composition (%)**	**Feed 1**	**Feed 2**	**Feed 3**
	H_2	63	49	42
	Ar	1	2	1
	CO_2	9	4	8
	CO	9	10	3
	H_2O	18	35	46
	Total	100	100	100
	S/CO Ratio	2	3.4	14
	S/C Ratio	1	2.5	4.2

4.4.2. Experimental Programmes

The starting conditions, as seen in Table 4-3, are used to determine whether the catalysts have reached pseudo-steady state for commencement of experiments. The conditions are catalyst-dependent as there is a large temperature difference between the LTS catalyst and the

HTS catalyst. Note that there are 2 different SGHSV listed in Table 4-3 are due to the different loadings within the different reactors.

Table 4-3 – Starting Conditions Used

	LTS	HTS	Cat X
Feed	2	2	2
Temperature	200°C	375°C	200°C
Pressure	1 barg	1 barg	1 barg
$SGHSV_{Dry}$ (h^{-1})	10,000/20,000	10,000/20,000	10,000/20,000

Table 4-4 shows the various conditions and feed compositions used in this investigation. A copy of this table is also located in Appendix A to be used for ease of reference in conjunction with Chapter 5 and 6.

Table 4-4 – List of Experimental Programmes

Catalyst Tested	Feed Number	Experiment Number	Experimental Conditions		
			GHSV (hr^{-1})	Pressure (barg)	Temperature (°C)
CuZn	1	1	5000	1	180 - 210
		2	10000	1	180 - 210
CuZn	2	3	5000	1	180 - 210
		4	7500	1	200
		5	10000	1	180 - 210
		6	10000	1	200 - 350
		7	15000	1	200
		8	20000	1	180 - 210
CuZn	3	9	5000	1	180 - 210
		10	10000	1	180 - 210
		11	20000	1	180 - 210
FeCr	2	12	5000	1	350 - 445
		13	10000	1	350 - 445
		14	20000	1	350 - 445
FeCr	3	15	5000	1	375 - 445
		16	10000	1	375 - 445
		17	20000	1	375 - 445
Cat X	2	18	5000	1	200 - 275
		19	10000	1	200 - 350
		20	20000	1	200 - 300

The space velocities are achieved based on the loading within the reactors. The reactors are loaded with either 0.75g or 0.325g of catalysts, in conjunction with the reactor MFCs and pumps to achieve the 3 required space velocities. This is shown in Table 4-5.

Table 4-5 – Catalyst load and feed combination requirements for space velocities

SV Required (h^{-1})		5000	7500	10000	15000	20000
Catalyst Load (g)		-	-	0.75	0.75	0.75
		0.325	0.325	0.325	-	-
Feed Composition	Catalyst Loaded (g)	MFC settings (sccm)				
Feed 1	0.75	-	-	64.1	96.7	128.2
	0.325	64.1	96.7	128.2	-	-
Feed 2	0.75	-	-	62.9	94.4	125.9
	0.325	62.9	94.4	125.9	-	-
Feed 3	0.75	-	-	64.8	97.2	129.6
	0.325	64.8	97.2	129.6	-	-

4.5. Chromatographic Analysis

4.5.1. Sampling Procedure

The sampling of the products and feed streams is achieved through an electric actuated VICI (Valco Instruments Co. Inc.) online 6-port multi-port switching valve. This, in conjunction with the Varian CP-4900 microGC (Varian Inc., now known as Agilent Technologies), allows for the automated sampling of the feed gas as well as all three reactor effluents.

When sampling is required, the 6-port switching valve is automated, through the controls of the GC analysis program (provided by Varian Inc.), to select a stream to sample from. When a stream is selected, a sample time of 60 seconds is necessary to fill the sample loop with the gas to be sampled, as well as to flush away any previous samples left in the sample loop from previous sampling. Sampling occurs continuously throughout the experiment, including re-stabilization after a condition change. An analysis time of 7 minutes was found to be sufficient for the identification of all required peaks.

The GC, a Varian CP-4900 microGC, is fitted with a thermal conductivity detector (TCD). The GC contains 3 columns, hereto referred to as channels: Channel 1 - M5Å Molecular Sieve, 10m; Channel 2 - M5Å Molecular Sieve, 20m; Channel 3 - PoraPLOTQ, 10m (all of the columns provided by Varian Inc.). The GC is connected to a desktop computer for the controlling of the actuated valve as well as data capture via the Varian Galaxie software package supplied by the GC manufacturer. This setup allows for the automation of the sampling process. The GC columns and settings are outlined in Table 4-6.

Table 4-6 – Gas chromatography column type and conditions

	Channel Number		1	2	3
Column	**Type**		M5Å Molecular Sieve	M5Å Molecular Sieve	PoraPLOTQ
	Carrier Gas		Ar	H_2	H_2
	Length	(m)	10	20	10
	Flow	(kPa)	150, Isobaric	150, Isobaric	80, Isobaric
	Oven Temperature	(°C)	50, Isothermal	50, Isothermal	40, Isothermal
Gases analysed			H_2	Ar, CH_4, CO	CO_2
Injector Temperature (°C)			40		
Sampling Line Temperature (°C)			50		

4.5.2. Peak Identification

The peaks were identified initially by analysing a single component of the feed composition. This is achieved by feeding only one component through at a time to the GC to obtain the retention time of said component. Once the gases' retention times have been determined, known compositions of the feed components were fed into the GC to obtain integrated peak areas where these areas are normalized against the peak area of argon, which is present in the feed as the internal standard. The ratios of the areas of the individual components to argon, using linear regression, are used to obtain calibration curves and values, to be used as part of data analysis. Figure 4-5, Figure 4-6, and Figure 4-7 show typical chromatograms from each column, with H_2 in channel 1, argon and CO in channel 2, and permanent gases and CO_2 in channel 3, although the permanent gases integrated area is not evaluated.

4.5.3. Data Analysis

In order to calculate conversion, the integrated areas must be calibrated with the internal standard to obtain actual mass fractions of components. It is achieved by plotting the normalised molar percent $\frac{x_i}{x_{Ar}}$ against normalised area $\frac{Area_i}{Area_{Ar}}$, then using linear regression on the plot to determine the gas response factor, i.e. the gradient of the straight line, R_{f_i} for component *i*. Gas response factor data and calculations are presented in *Appendix B*.

To obtain the actual mole fraction based on the integrated area, equation 4.1 is used.

$$\frac{Area_i}{Area_{Ar}} \times R_{f_i} \times \dot{F}_{Ar_{Feed}} = x_{i_{Product}} \qquad \textbf{Eqn 4.1}$$

where R_{f_i} = gas response factor calculated via linear regression for component i
$\dot{F}_{Ar_{Feed}}$ = molar flowrate of argon in the feed stream

CO conversion is thus defined as:

$$X_{CO} = \frac{\dot{F}_{CO_{Feed}} - \dot{F}_{CO_{Product}}}{\dot{F}_{CO_{Feed}}} \times 100\% \qquad \textbf{Eqn 4.2}$$

A carbon balance, based on CO and CO_2 molar flowrates, was also performed. It was seen that the carbon balance falls in the general range of between 95% and 105%.

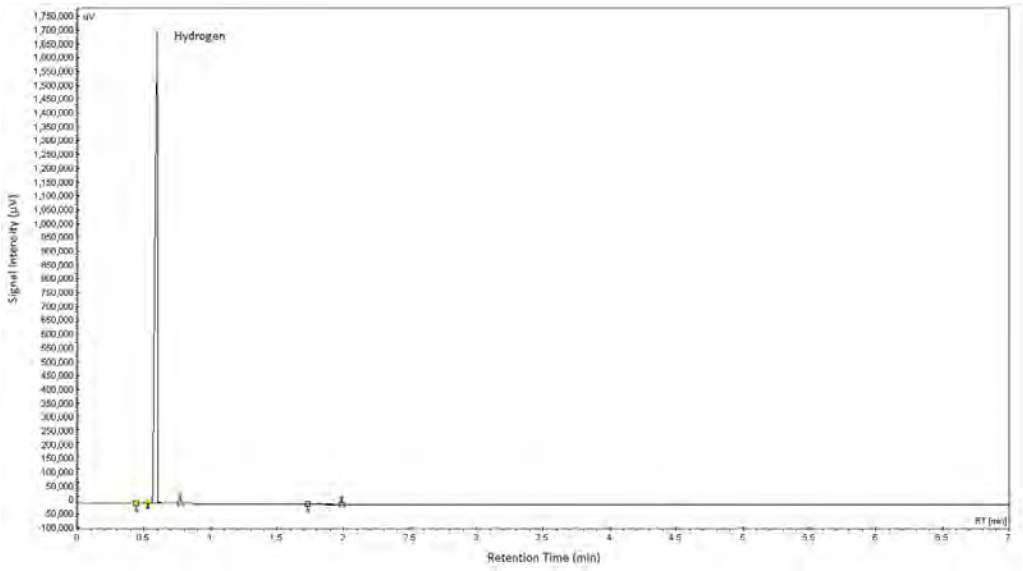

Figure 4-5 – Sample Chromatogram obtained from Channel 1, showing H_2 peak

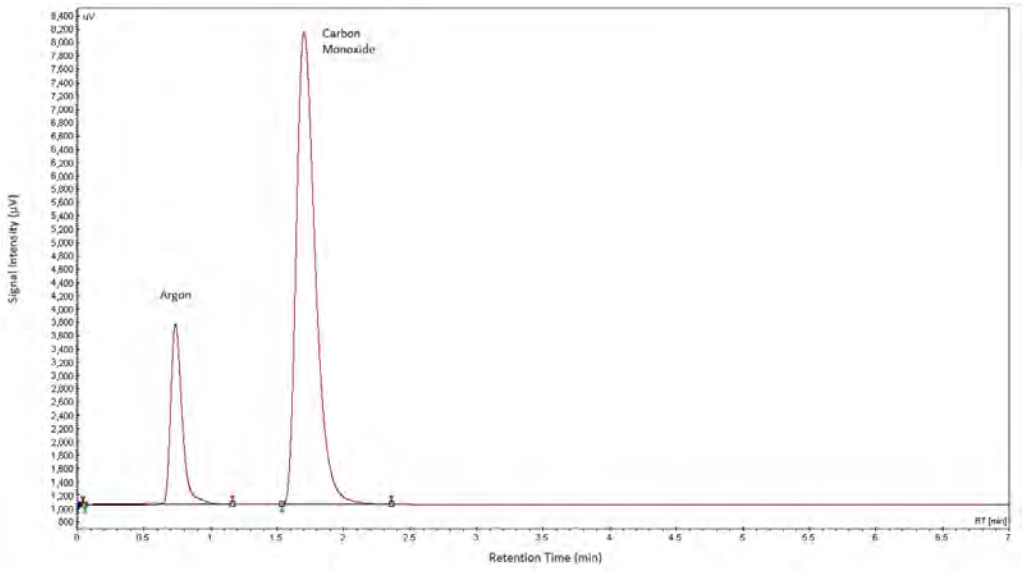

Figure 4-6 – Sample Chromatogram obtained from Channel 2, showing both Ar and CO peaks, with Ar exiting the column first

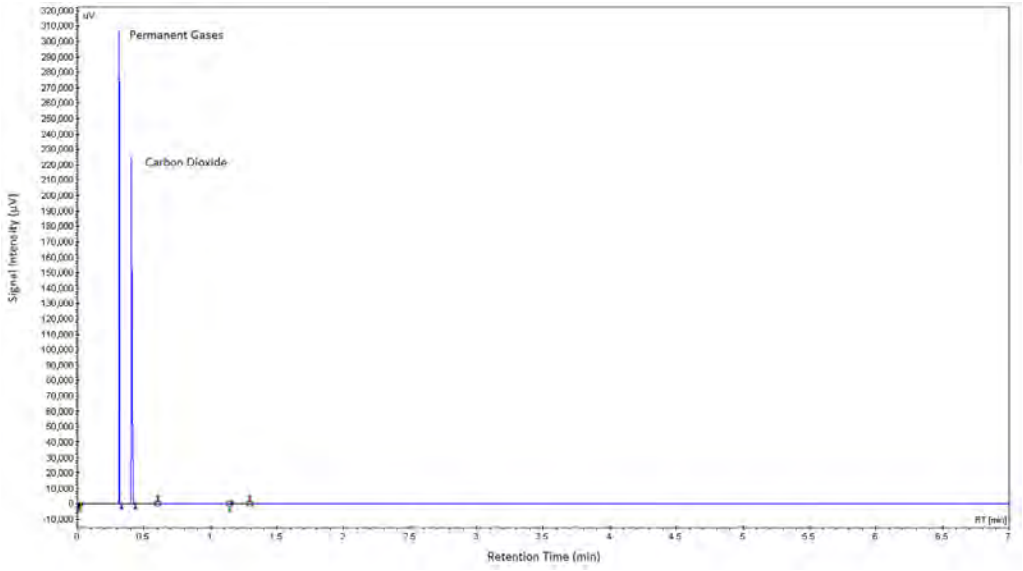

Figure 4-7 – Sample Chromatogram obtained from Channel 3, showing both permanent gases and CO_2, with CO_2 being the latter peak

5. Results

The results from the experiments performed are presented here. *Appendix A* consists of a summary of the experimental programs performed, as well as a copy of the feed compositions table, on a fold-out page. It is suggested that *Appendix A* be used alongside Chapters 5 and 6 for ease of reference. Additionally, the complete tabulated and worked-up data is presented in *Appendix C*.

5.1. Reproducibility of Results

As previously mentioned in Section 4.2.1.2, the experimental apparatus is constructed with a triple-tube parallel reactor setup. Reproducibility test on the reactors was performed prior to the catalyst testing experiments to ensure that all reactors produce comparable results. The reproducibility tests were performed by loading 2 reactors with the same amount (0.75g) of catalyst and 1 with half the amount (0.325g); they are then tested at the same temperature, space velocity, and feed composition. Figure 5-1 and Figure 5-2 show time-on-stream conversion data from the reproducibility experiments. The average conversions achieved are as follows:

Table 5-1 – Conversions achieved during reproducibility tests, all reactors operating at 200°C and using the same feed composition. Standard deviation calculated to determine whether conversions obtained are close to the mean.

Reactors	Space Velocity	Average Conversion	Absolute Error	Relative Error	Standard Deviation
1	10,000 h^{-1}	73.6%	3.8%	5.2%	0.12%
2	10,000 h^{-1}	72.9%	5.1%	7.0%	0.14%
2	20,000 h^{-1}	48.5%	4.3%	8.9%	0.09%
3	20,000 h^{-1}	49.9%	1.8%	3.6%	0.06%

Reactors 1 and 2 are compared with each other at the same condition, and then reactors 2 and 3 are compared with each other at the same condition. Due to the way the reactors are loaded in order to achieve the space velocities required, it was not possible to test all three reactors simultaneously.

Table 5-1 shows that the average conversion for reactors 1 and 2 are very similar. Average conversions from reactors 2 and 3 are also very similar. Standard deviations calculated for all reactors are small, meaning the conversions obtained from the reactors are close to the actual mean conversion. From the above results, it was deemed that all three reactors were operating similar to each other.

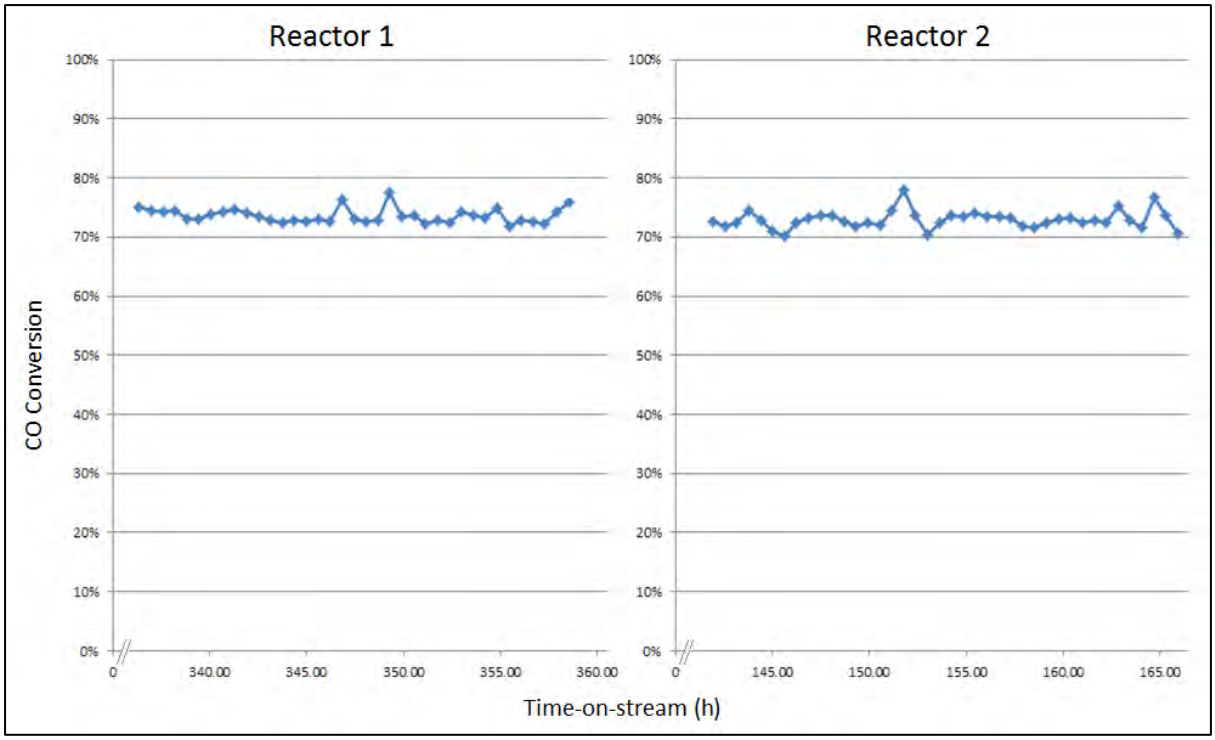

Figure 5-1 – Reproducibility of Reactors 1 and 2. Commercial LTS catalyst, operating at 200°C, 10,000 h^{-1}, 1 barg, Feed composition 2

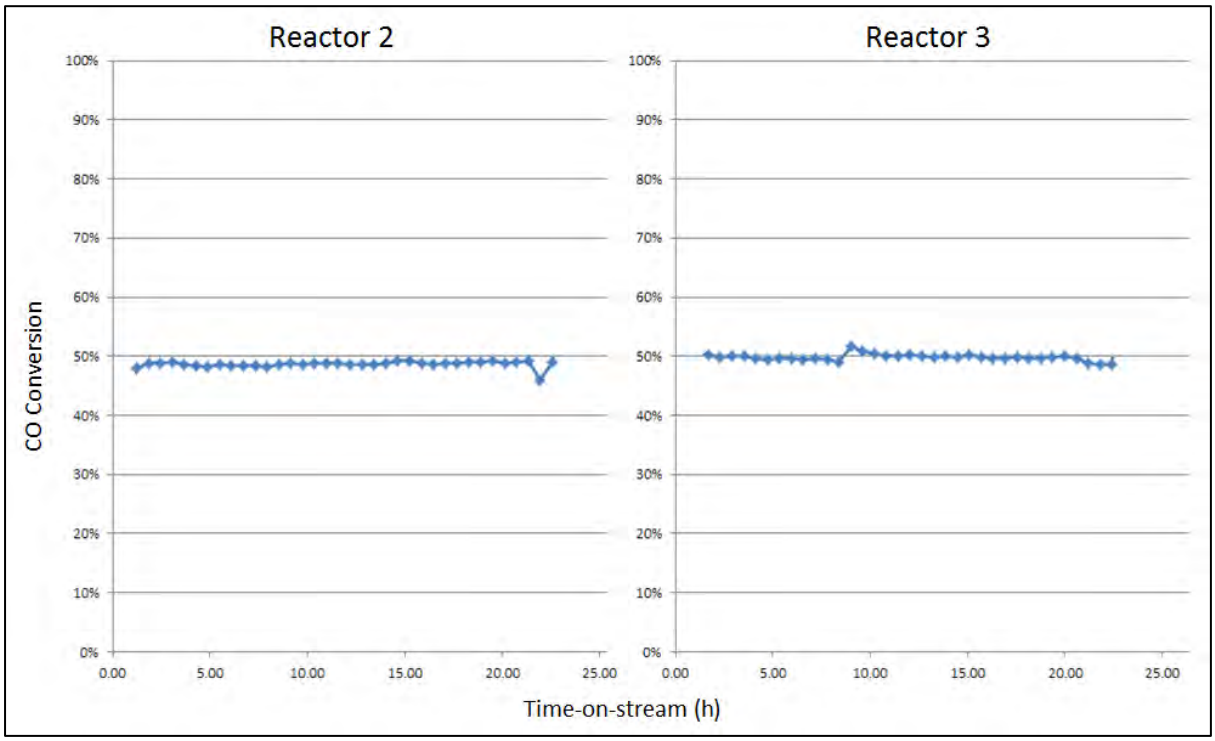

Figure 5-2 – Reproducibility of Reactors 2 and 3. Commercial LTS catalyst, operating at 200°C, 20,000 h^{-1}, 1 barg, Feed composition 2

5.2. Commercial HTS Catalyst

Commercial HTS catalyst (Fe_3O_4/Cr_2O_3) was tested at varying temperatures, space velocities, and feed compositions and the results obtained are presented below. Each data point presented below, apart from time-on-stream data, is an average result of at least 24 hours of time-on-stream data analysed during experiments. The complete experimental data can be seen in Appendix C.

5.2.1. Catalyst Stability

It was seen that the commercial HTS catalyst is able to reach steady state at all temperatures examined. As this catalyst operates at temperature ranges between 400-450°C (Ladebeck and Wagner, 2003), no deactivation of the catalytic activity was seen after exposure to this temperature range. This stability was tested by analysing the previous experimental condition for conversion comparison. This is shown in Figure 5-3 where after exposure to a temperature of 440°C, the conversion at 375°C is comparable to the initial conversion at 375°C.

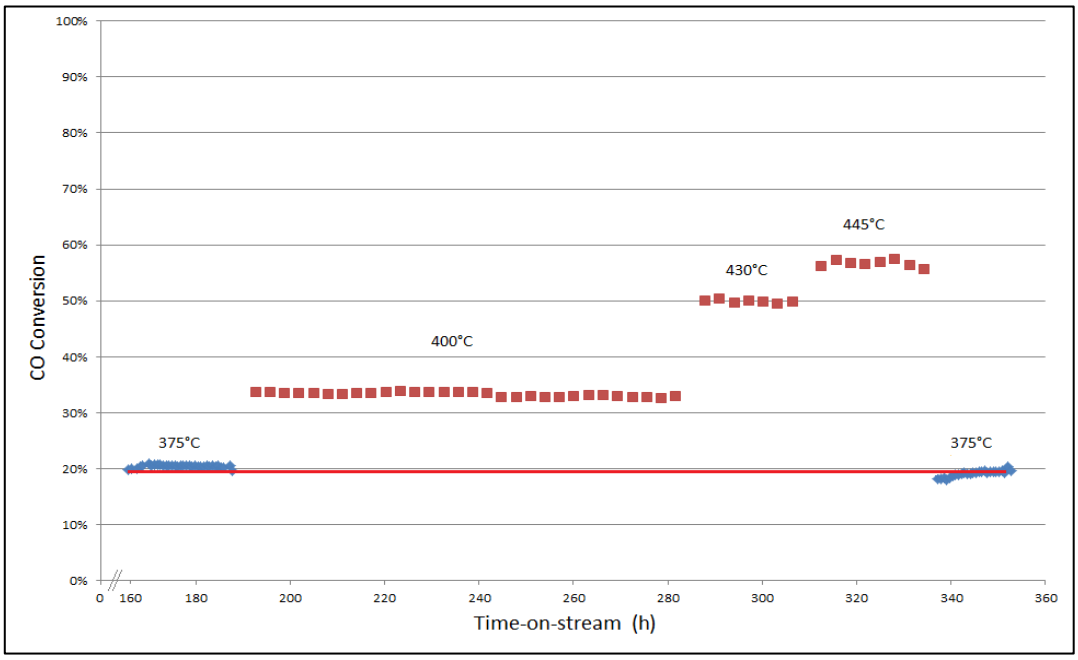

Figure 5-3 – Example of time-on-stream stability of commercial HTS catalyst after exposure to temperatures up to 440°C, operating under Feed composition 2, and a space velocity of 20,000 h^{-1}. Data presented in red squares are 3-hour conversion data averages

Fresh HTS catalyst shows a deactivation in the first few hours after start-up (Figure 5-4). After approximately 10 hours on stream, the catalyst lost approximately 1/3 of its initial activity, after which it remains at a steady activity. Fresh HTS catalyst needs to have a line-in time of at least 10 hours before any commencement to catalytic performance testing.

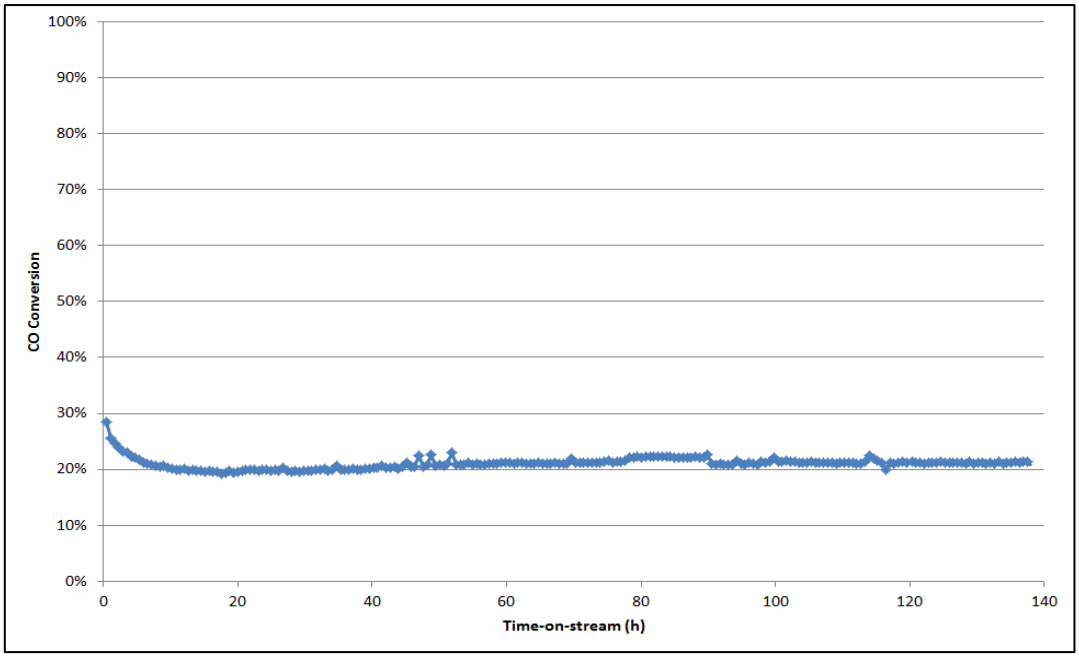

Figure 5-4 – Example of time-on-stream data of commercial HTS catalyst operating at 350°C, 10,000 h^{-1}, and Feed composition 2

5.2.2. Temperature Effects

Figure 5-5 shows the conversion achieved by the commercial HTS catalyst with varying temperature under feed composition 2. The three space velocities are achieved by loading different amount of catalysts into each reactor or varying the feed rates into each reactor. Each space velocity is from a single reactor. The catalyst is active at the temperature range tested and equilibrium conversion of approximately 73% was reached at 430°C at a space velocity of 5,000 h^{-1}, and at 445°C at a space velocity of 10,000 h^{-1} a 70% equilibrium conversion was reached.

Figure 5-6 shows the conversion achieved by the commercial HTS catalyst with varying temperature using a different feed. Feed composition 3 consists of more steam and less CO than feed composition 2, as seen in Figure 5-5. At this feed condition, the catalyst is also able to achieve equilibrium at 430°C at a space velocity of 5,000 h^{-1}, and at 445°C at a space velocity of 10,000 h^{-1}.

Under both feed compositions, the general trend of increasing conversion with increasing temperature was seen until the conversion approaches equilibrium where it is thermodynamically limited by the equilibrium conversion.

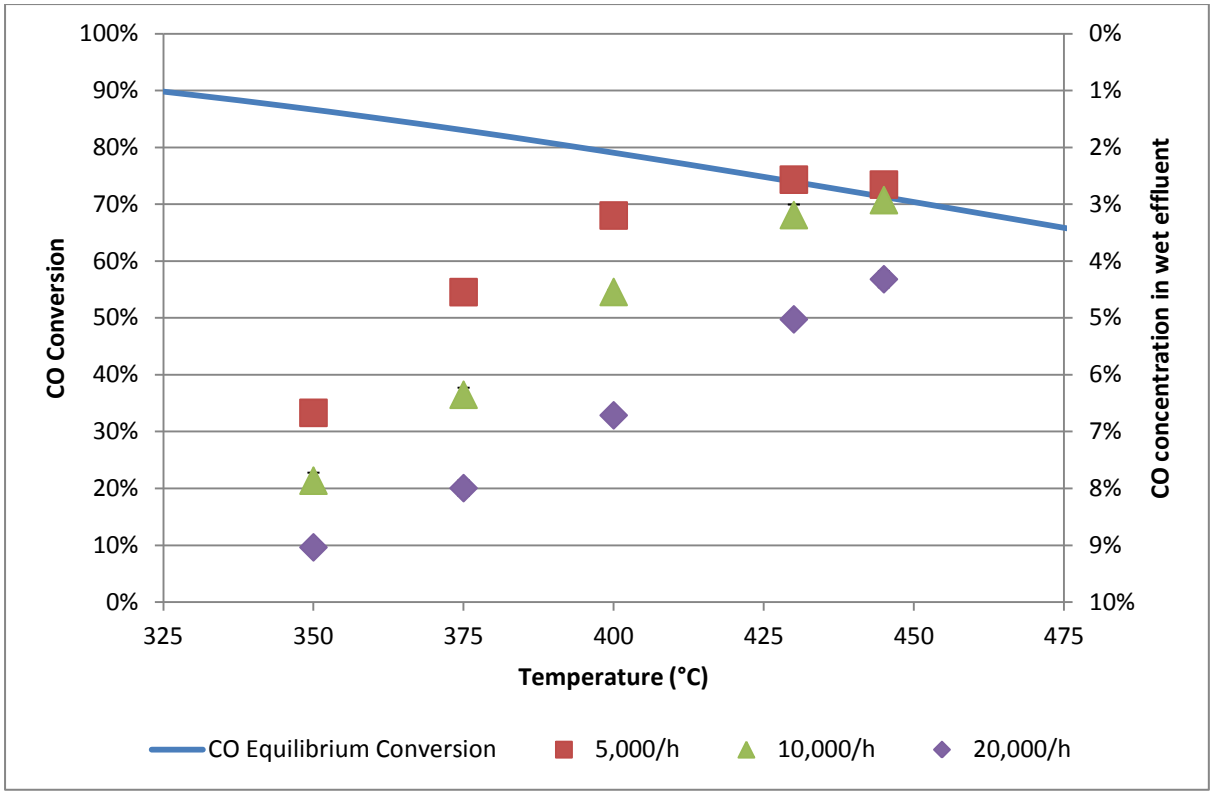

Figure 5-5 – Light-off curves of HTS catalyst (FeCr) with Feed composition 2, SGHSV in dry gas, S:C = 2.5

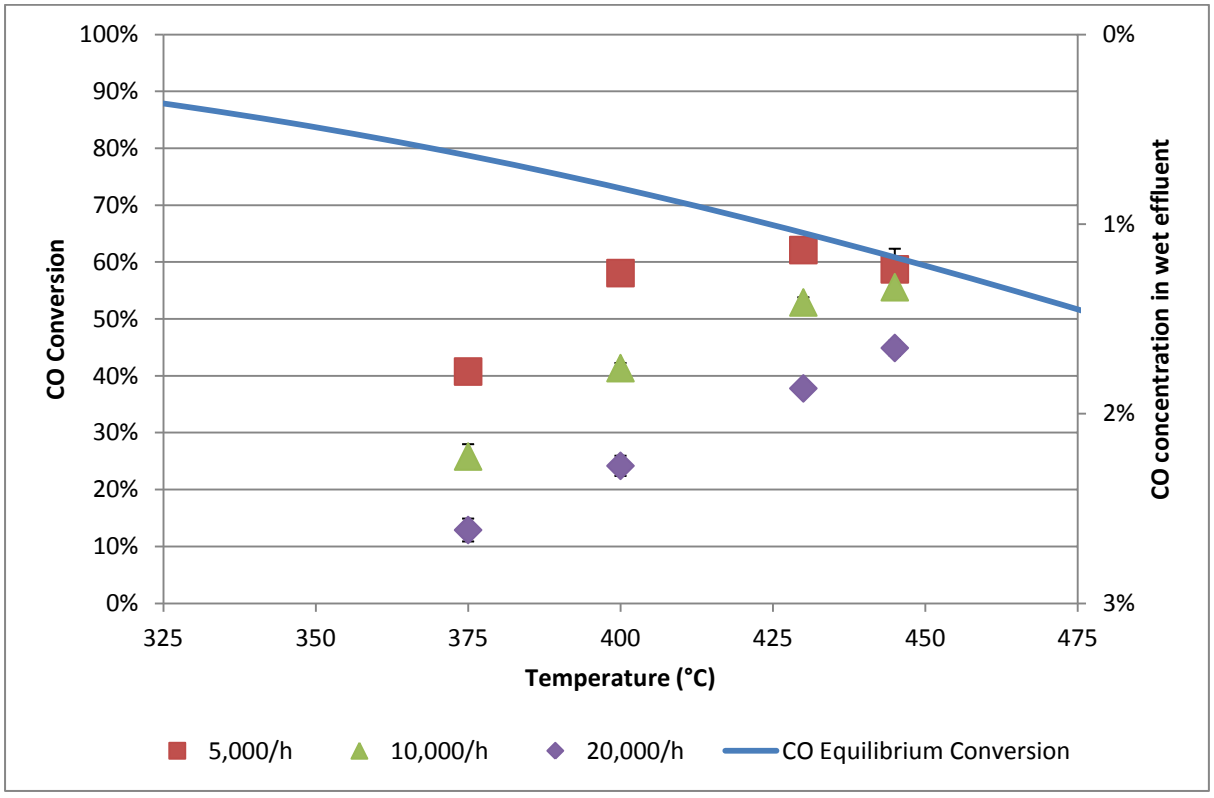

Figure 5-6 – Light-off curves of HTS catalyst (FeCr) using Feed composition 3, SGHSV in dry gas. S:C = 4.1

5.2.3. Space Velocity Effects

Three different dry gas standard gas hourly space velocities were tested, namely 5,000 h^{-1}, 10,000 h^{-1}, and 20,000 h^{-1}. General trends observed are that with increasing space velocity, there is a decrease in conversion. Figure 5-7 and Figure 5-8 shows this trend, with Figure 5-7 using feed composition 2 and Figure 5-8 using feed composition 3. Both figures are at a temperature of 375°C.

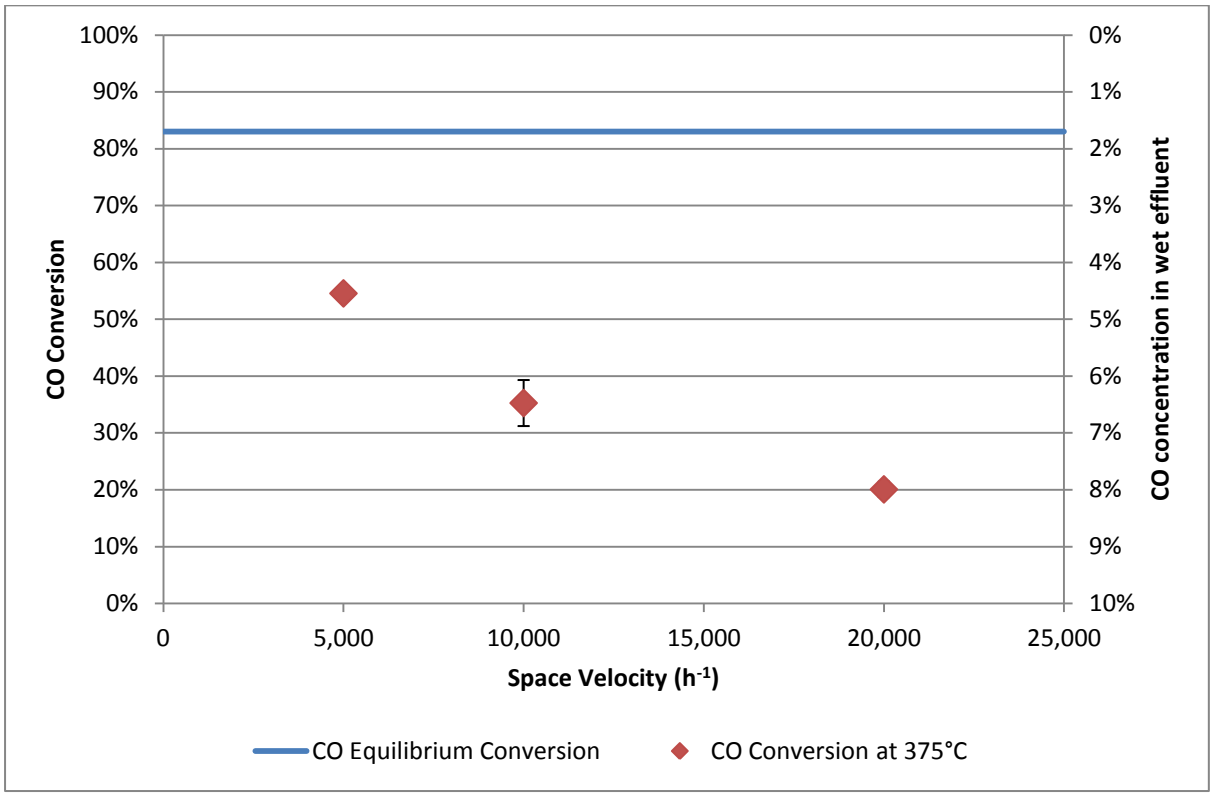

Figure 5-7 – Change in conversion of HTS catalyst with changing space velocity using Feed composition 2

5.3. Commercial LTS Catalyst

Commercial LTS catalyst ($Cu/ZnO/Al_2O_3$) was also tested at varying temperatures, space velocities, and feed compositions, with the results obtained presented below. Each data point presented below, same as in Section 5.2, is an average result of at least 24 hours of time-on-stream data. The 24-hour averaged data does not, however, apply to the time-on-stream figures presented in Section 5.3.1. The complete experimental data is included *Appendix C*.

5.3.1. Catalyst Stability

The commercial LTS catalyst is able to reach pseudo-steady state at all temperatures tested. As the catalyst is able to operate below a temperature of 250°C (Ratnasamy and Wagner, 2009), no deactivation was seen up to the tested temperature of 210°C.

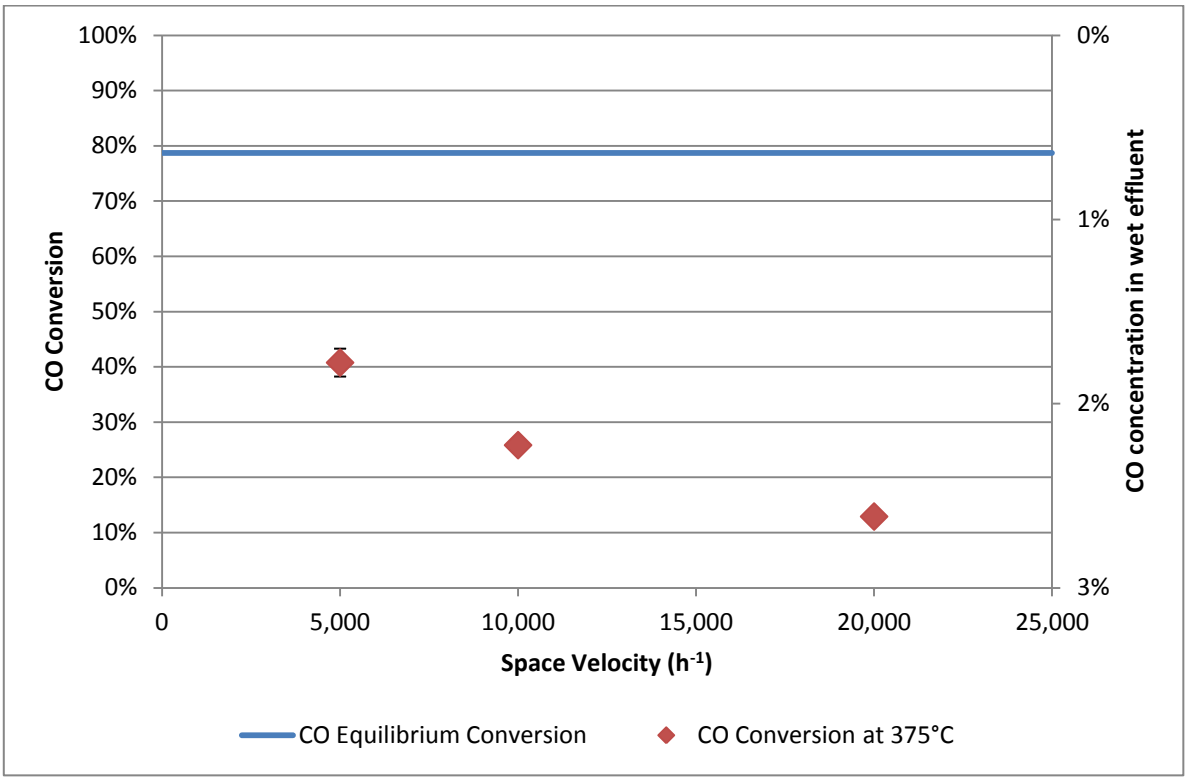

Figure 5-8 – Change in conversion of HTS catalyst with changing space velocity using Feed composition 3

Catalyst deactivation, however, was seen when the catalyst was exposed to temperatures much higher than 210°C. At temperatures of 250°C, 300°C, and 350°C, the catalyst was able to achieve steady state. When comparing catalyst conversion after exposure to high temperatures to previous low temperature results, however, a clear decrease was observed. Figure 5-9 shows that prior to exposure to high temperatures, the catalyst is at steady state at 200°C. After exposure to high temperatures and returning to 200°C, a decrease from approximately 75% down to 68% was observed.

5.3.2. Temperature Effects

Figure 5-10 shows the conversion achieved by the commercial LTS catalyst with varying temperature (from 180°C to 210°C) with feed composition 2. The three space velocities seen in Figure 5-10 are obtained in 3 reactors operating in parallel. It is seen that the catalyst is active in the temperature range examined, and when operated above the normal operating range (above 250°C), the catalyst reaches equilibrium.

The catalyst is able to reach equilibrium conversion of approximately 98%, operating at 210°C and 5,000 h^{-1}. For all space velocities tested, the conversion increases with increase in temperature until the observed conversion reaches equilibrium, and is limited by the equilibrium conversion.

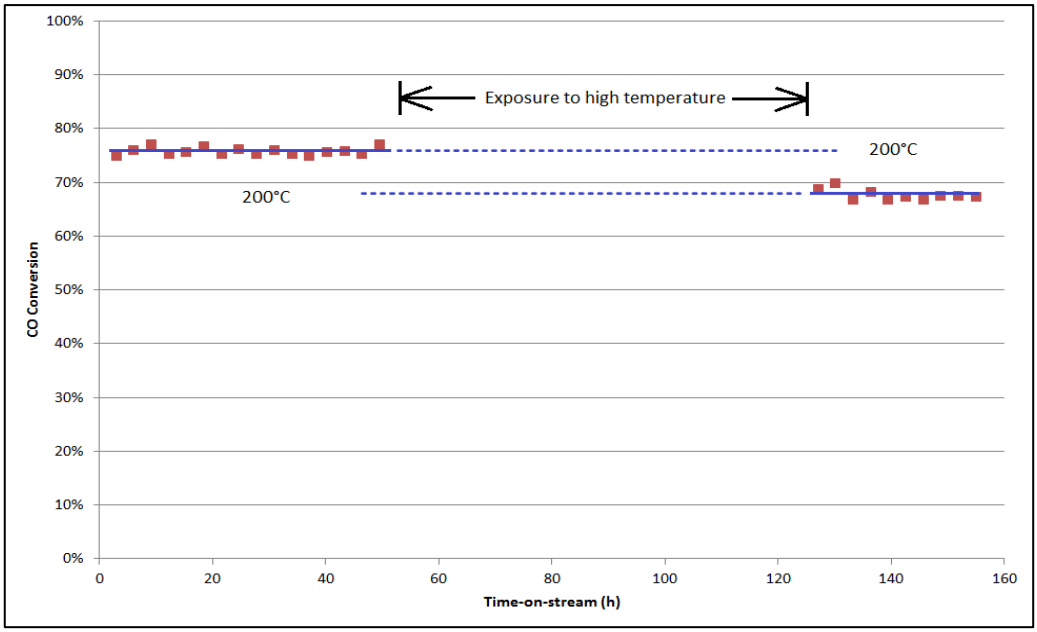

Figure 5-9 – $Cu/ZnO/Al_2O_3$ stability after exposure to high temperature (250°C and 300°C). Space velocity of 10,000 h^{-1}

Similar trend of increasing conversion with increasing reaction temperature was observed with feed composition 3 (Figure 5-11) with the lower CO feed concentration. Equilibrium is reached at a lower temperature, at 200°C instead of 210°C.

Figure 5-12 shows conversion of the commercial LTS catalyst under feed composition 1, with varying temperatures and two space velocities. The conversion of this feed is much lower than that of the previous two feed compositions. This lower conversion is due to a lower steam partial pressure.

5.3.3. Space Velocity Effects

Dry gas standard gas hourly space velocities tested with the commercial LTS catalyst were between 5,000 h^{-1} and 20,000 h^{-1}. AS per the commercial HTS catalyst, a decrease in conversion with increasing space velocity is also observed with the LTS catalyst. Figure 5-13 shows conversion as a function of space velocity at 200°C under feed composition 2 while Figure 5-14 shows conversion as a function of space velocity at 200°C under feed composition 3. Similar trends were observed with other temperatures.

5.3.4. Feed Effects

Figure 5-15 shows the temperature and corresponding space velocity where the 1% CO conversion can be achieved based on the two different feeds. Based on this figure, other operating conditions where 1% CO conversion can be achieved can be estimated. Feed composition 2 (S:C = 2.5) contains a lower S:C ratio than feed 3 (S:C = 4.2), thus achieves the 1% CO concentration at higher temperatures.

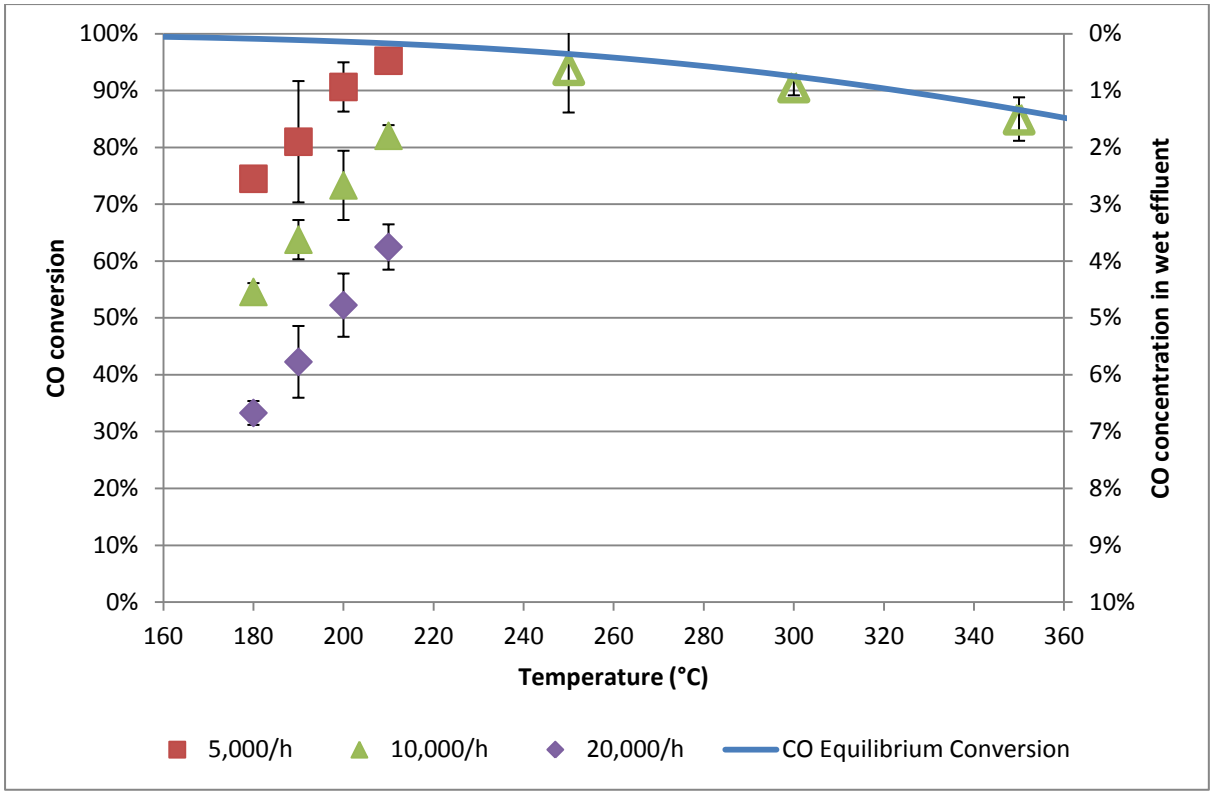

Figure 5-10 – Light-off curves of LTS catalyst ($Cu/ZnO/Al_2O_3$) using Feed composition 2. Open triangle symbol indicates LTS catalyst prior to exposure to temperatures above 250°C

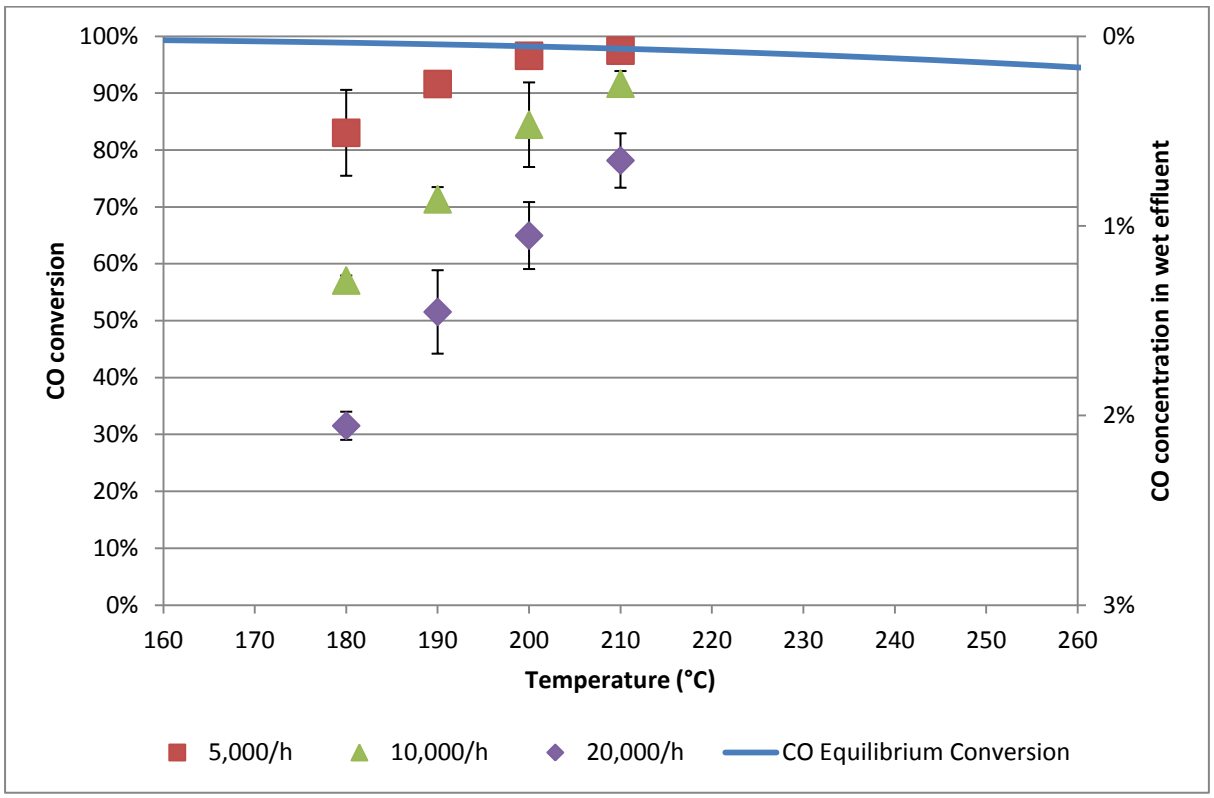

Figure 5-11 – Light-off curves of LTS catalyst ($Cu/ZnO/Al_2O_3$) using Feed composition 3

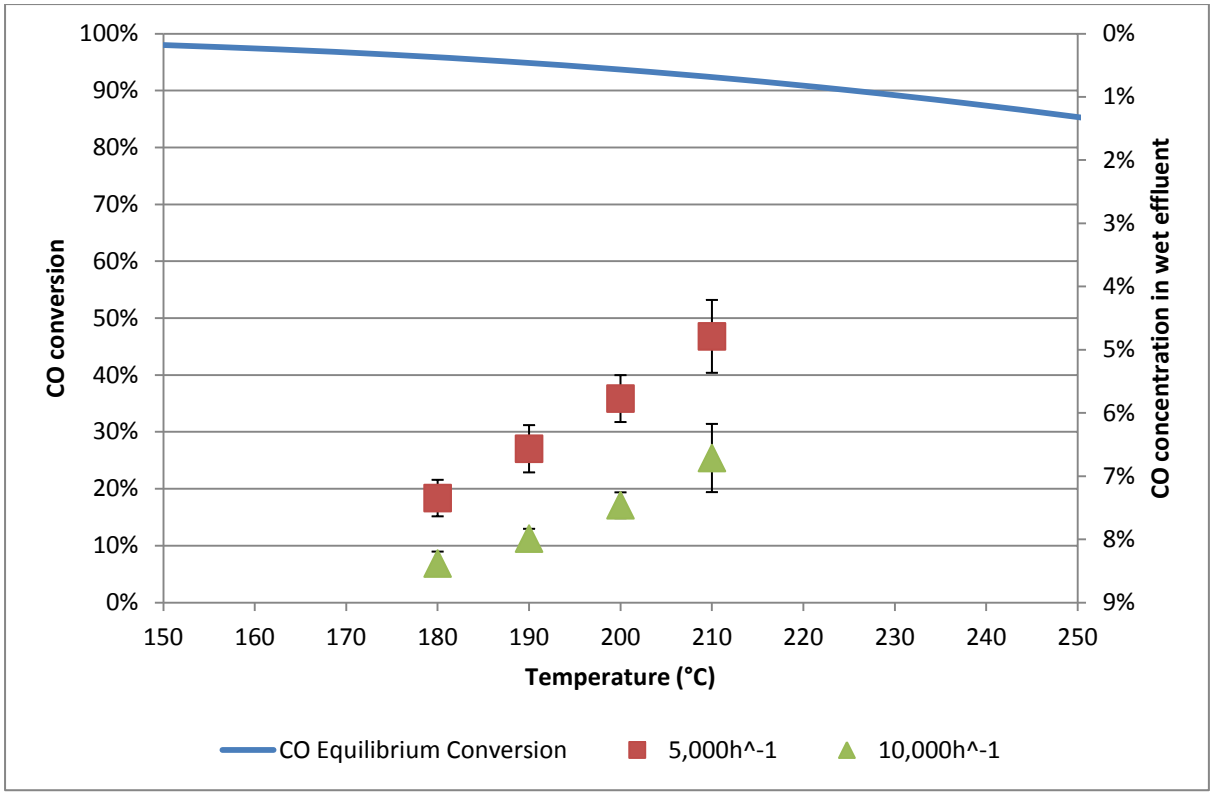

Figure 5-12 – Light-off curves of LTS catalyst ($Cu/ZnO/Al_2O_3$) using Feed composition 1

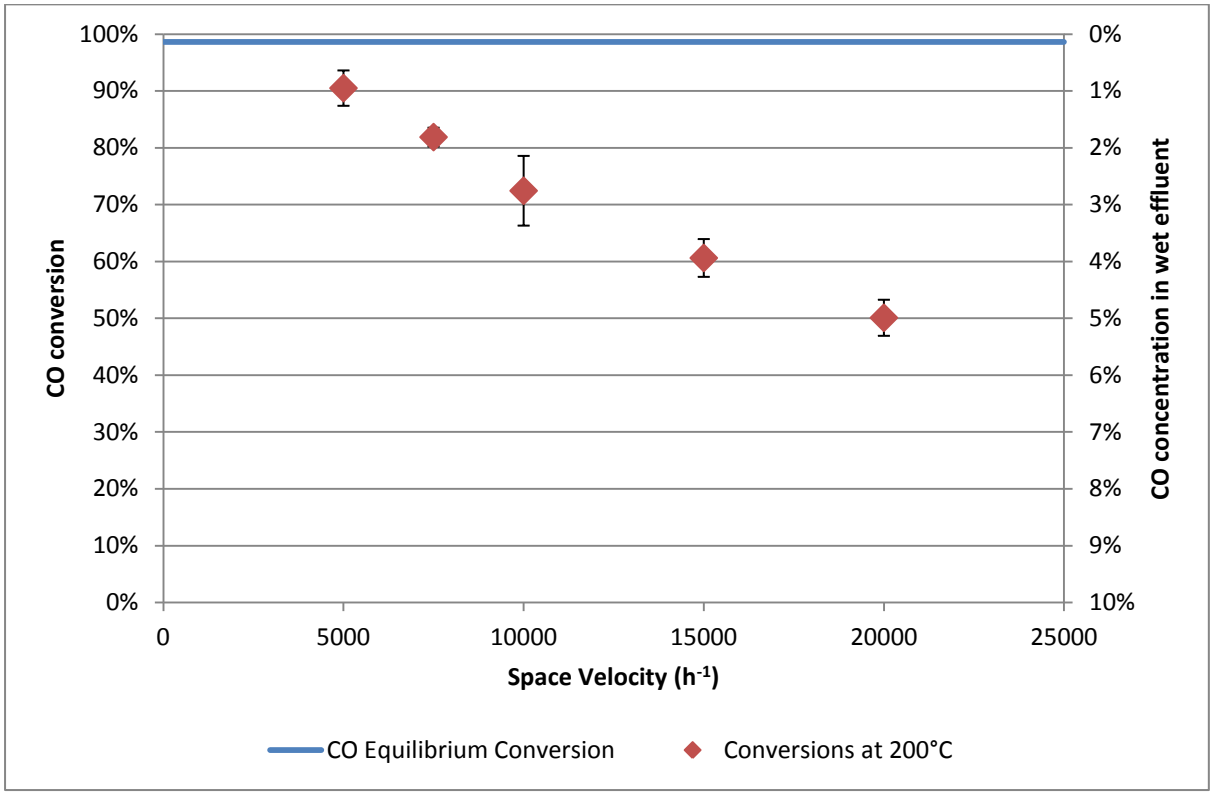

Figure 5-13 – Change in conversion of LTS catalyst with changing space velocity using Feed composition 2

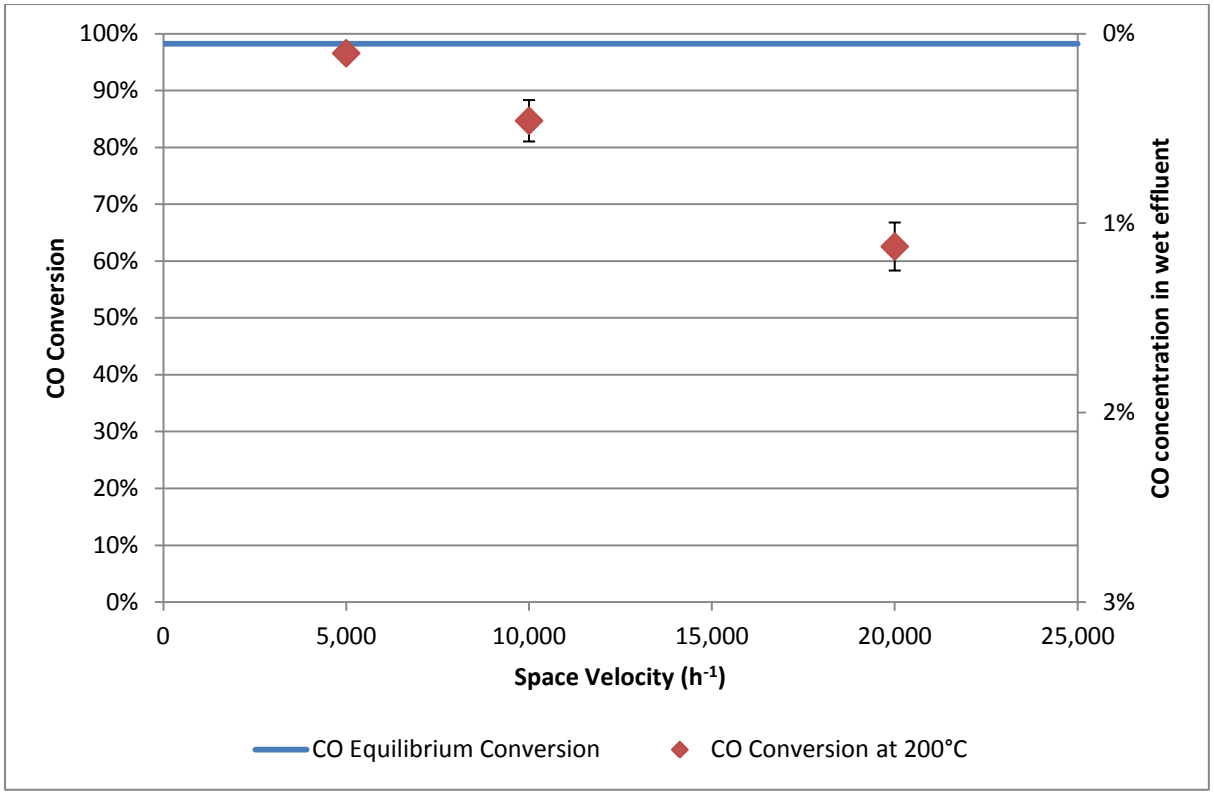

Figure 5-14 – Change in conversion of LTS catalyst with changing space velocity using Feed 3 composition

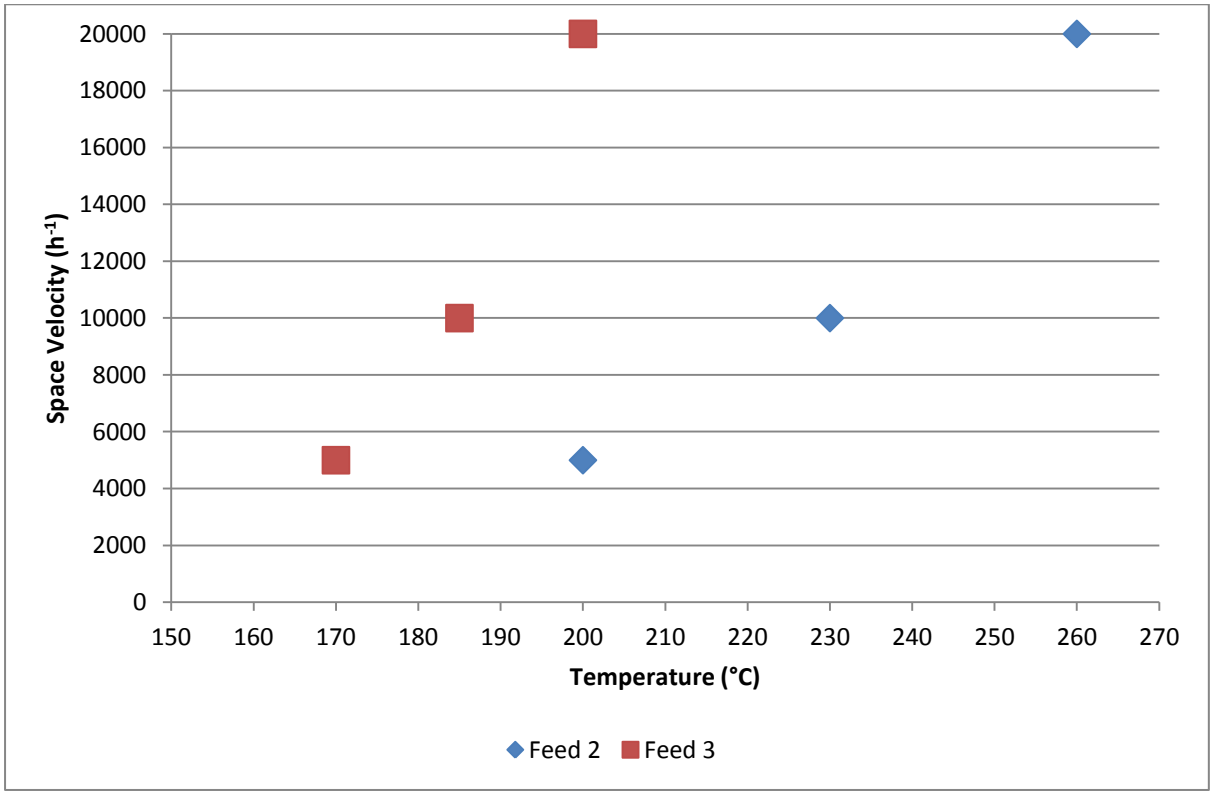

Figure 5-15 – Conditions where 1% CO conversion can be achieved for LTS catalyst

5.4. Catalyst X

Catalyst X was tested at various temperatures and space velocities. Results obtained from the experiments are presented below. Data points presented in temperature-conversion plots and space velocity-conversion plots are averaged results of at least 24 hours of time-on-stream data obtained, unless otherwise mentioned. The complete time-on-stream experimental data is presented in *Appendix C*.

5.4.1. Catalyst Stability

Catalyst X showed stable performance up to 250°C at all space velocities tested. At 275°C and higher, however, the catalyst stability declined. Figure 5-16, Figure 5-17 and Figure 5-18, show Catalyst X operating at space velocities of 20,000 h^{-1}, 10,000 h^{-1}, and 5,000 h^{-1} respectively. The data points presented in these figures are averages of approximately 3 hours of time-on-stream data.

It is observed that at 250°C, Catalyst X is able to maintain steady state conversion at all three space velocities. At 275°C, the catalyst showed a continuous deactivation where in approximately 200 hours, a 20% loss in activity was observed at space velocities of 20,000 h^{-1} and 10,000 h^{-1} while approximately 5% loss was observed at 5,000 h^{-1}. The performance of Catalyst X does not stabilize within the time period where deactivation was observed (approximately 200 hours). Similar loss in activities were also seen at 300°C and 350°C. Therefore, due to the loss of activity at temperatures of 275°C and higher, only the first 40 hours of conversion data is averaged to obtain the conversion used in Section 5.4.2 (marked by open symbols).

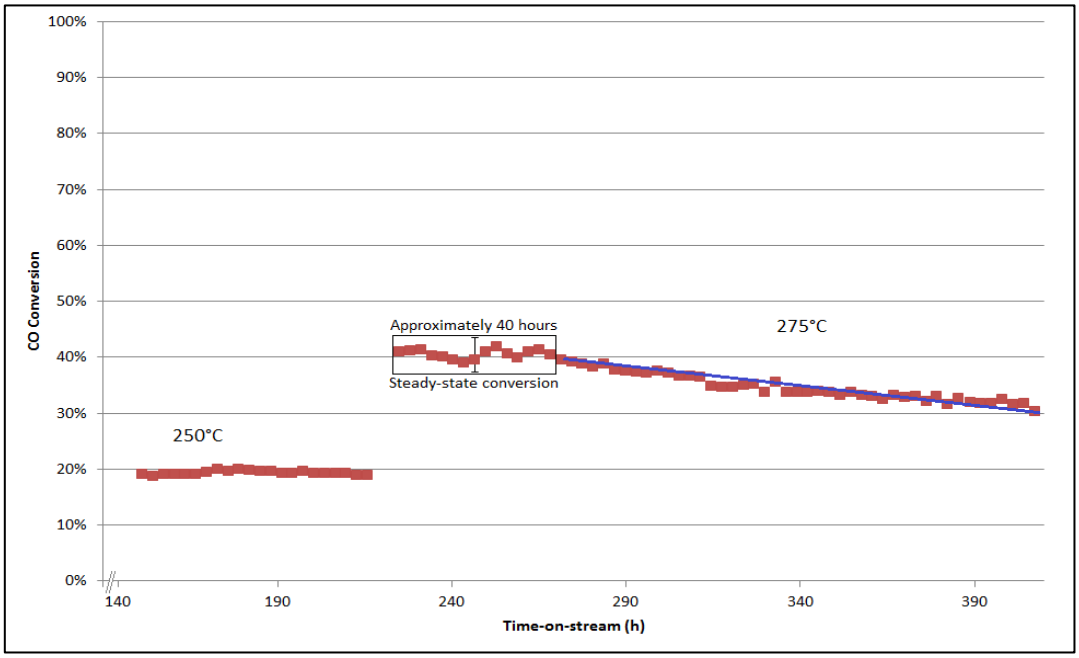

Figure 5-16 – Catalyst X stability at 250°C and 275°C. Operating condition of 20,000 h^{-1} and Feed composition 2

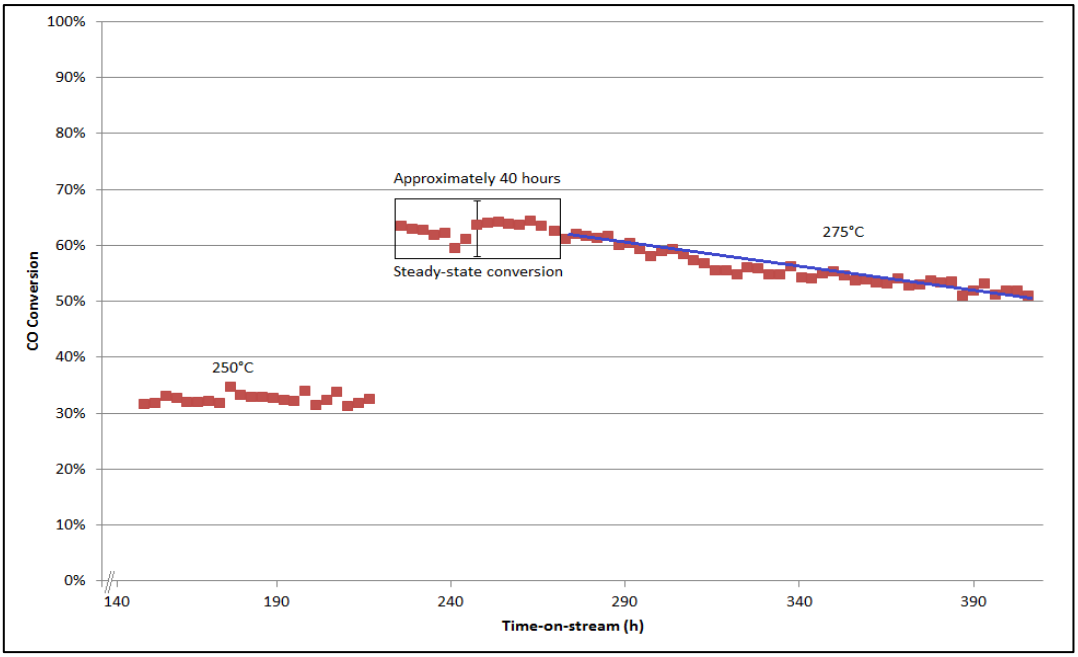

Figure 5-17 – Catalyst X stability at 250°C and 275°C. Operating condition of 10,000 h^{-1} and Feed composition 2

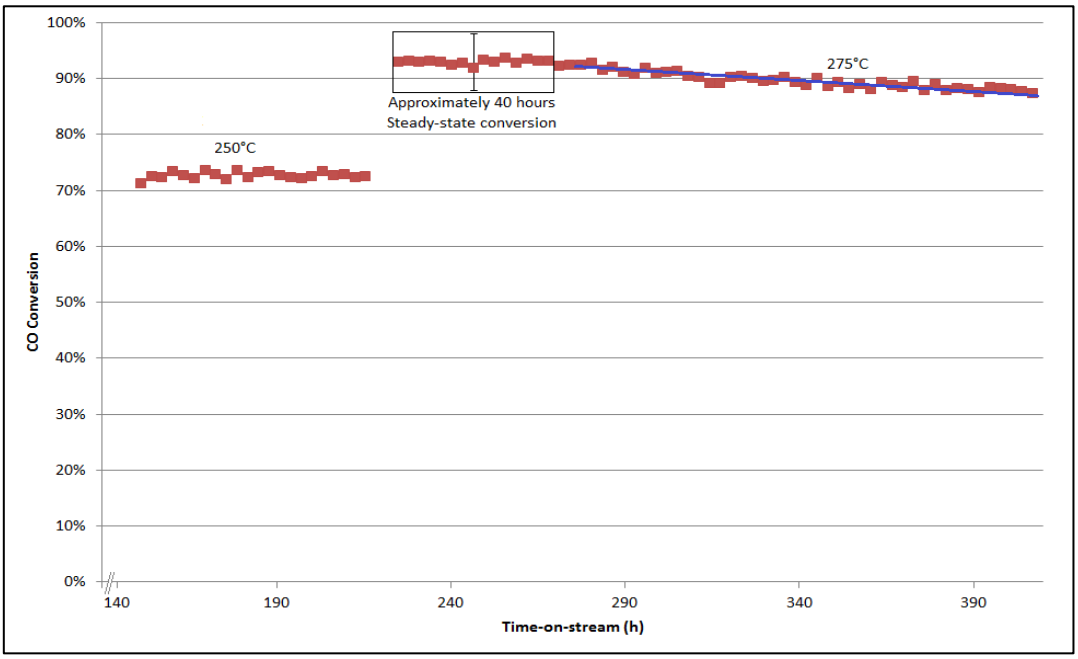

Figure 5-18 – Catalyst X stability at 250°C and 275°C. Operating condition of 5,000 h^{-1} and Feed composition 2

5.4.2. Temperature Effects

Figure 5-19 shows the conversion achieved by Catalyst X with varying temperature at three space velocities with feed composition 2. The open symbols denote the 40-hour average due to deactivation as mentioned in Section 5.4.1.

Increasing conversion with increasing temperature, similar to the LTS and HTS catalysts, is also observed with Catalyst X. The catalyst reaches equilibrium at 275°C and a space velocity of 5,000 h^{-1}. At space velocities of 10,000 h^{-1} and 20,000 h^{-1}, Catalyst X was unable to reach equilibrium, even when the temperature was increased to 300°C.

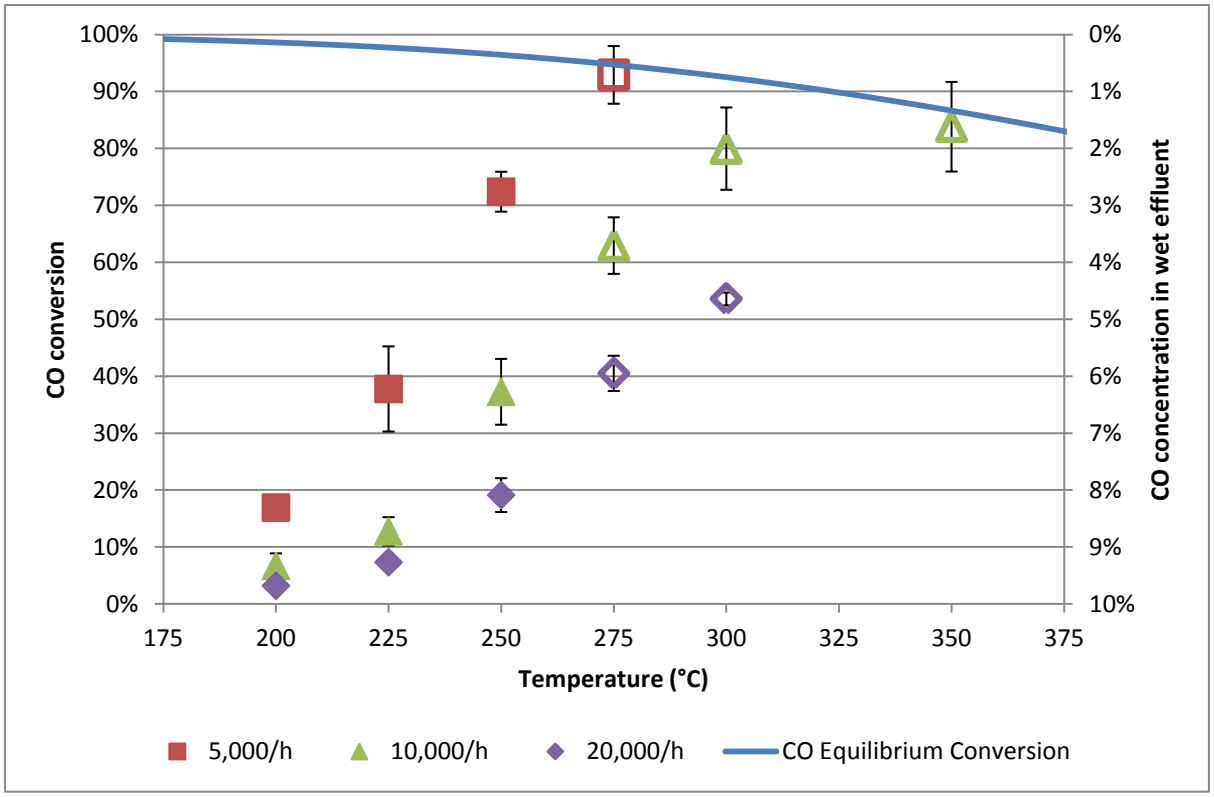

Figure 5-19 – Light-off curves of Catalyst X using Feed composition 2. Open symbols indicate 40-hour average data

5.4.3. Space Velocity Effects

Three dry gas standard hourly space velocities were tested with Catalyst X, namely 5,000 h^{-1}, 10,000 h^{-1}, and 20,000 h^{-1}. As seen with the two previous catalysts, increasing conversion with decreasing space velocity is observed. Figure 5-20 shows conversion as a function of space velocity at 250°C under feed composition 2. Similar trends are observed with other temperatures.

5.4.4. Catalyst Characterisation

Catalyst characterisations were performed on Catalyst X to determine possible mechanisms for the deactivation seen at temperatures of 275°C and higher.

5.4.4.1. Thermo Gravimetric Analysis

Thermo gravimetric analysis was performed on spent Catalyst X in order to determine whether coking occurred on the catalyst, as this is one possible deactivation mechanism. Figure 5-21

shows the TGA samples performed under air. No sudden decrease in the mass of the TGA samples between 600°C and 800°C for both fresh and spent Catalyst X were observed.

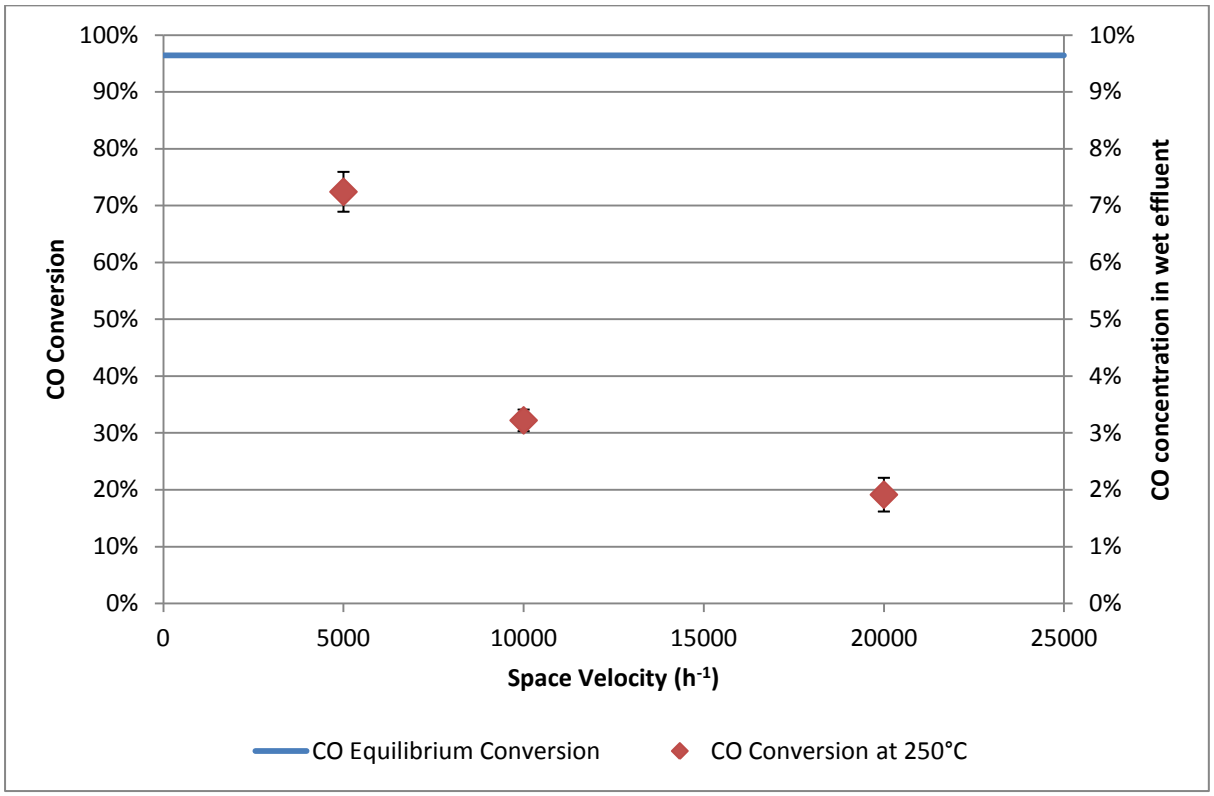

Figure 5-20 – Conversion of Catalyst X as a function of space velocity under Feed composition 2

5.4.4.2. BET Surface Area Analysis

BET surface area analysis was performed on both fresh and spent Catalyst X. From Table 5-2, which shows the BET results, it can be concluded that there is a small decrease between fresh and spent Catalyst X, although there is no trend observed between BET surface area and the space velocity the catalyst was exposed to during experiments.

Table 5-2 – BET surface area obtained on fresh and spent Catalyst X

Sample	BET Surface Area (m^2/g)
Fresh Catalyst X	64 ± 0.2
Spent Catalyst X, 5 000 h^{-1}	58 ± 0.1
Spent Catalyst X, 10 000 h^{-1}	55 ± 0.1
Spent Catalyst X, 20 000 h^{-1}	57 ± 0.1

5.5. Combined Comparison

Figure 5-22 gives an overview on the operating window of the three catalysts tested under feed composition 2. Commercial LTS catalyst (CuZn) was tested between 180°C and 210°C,

commercial HTS catalyst (FeCr) was tested between 350°C and 450°C and Catalyst X was tested in between the two commercial catalysts from 200°C to 350°C. Figure 5-23 gives an overview of only the commercial catalysts tested under feed composition 3 with the same space velocities as Figure 5-22.

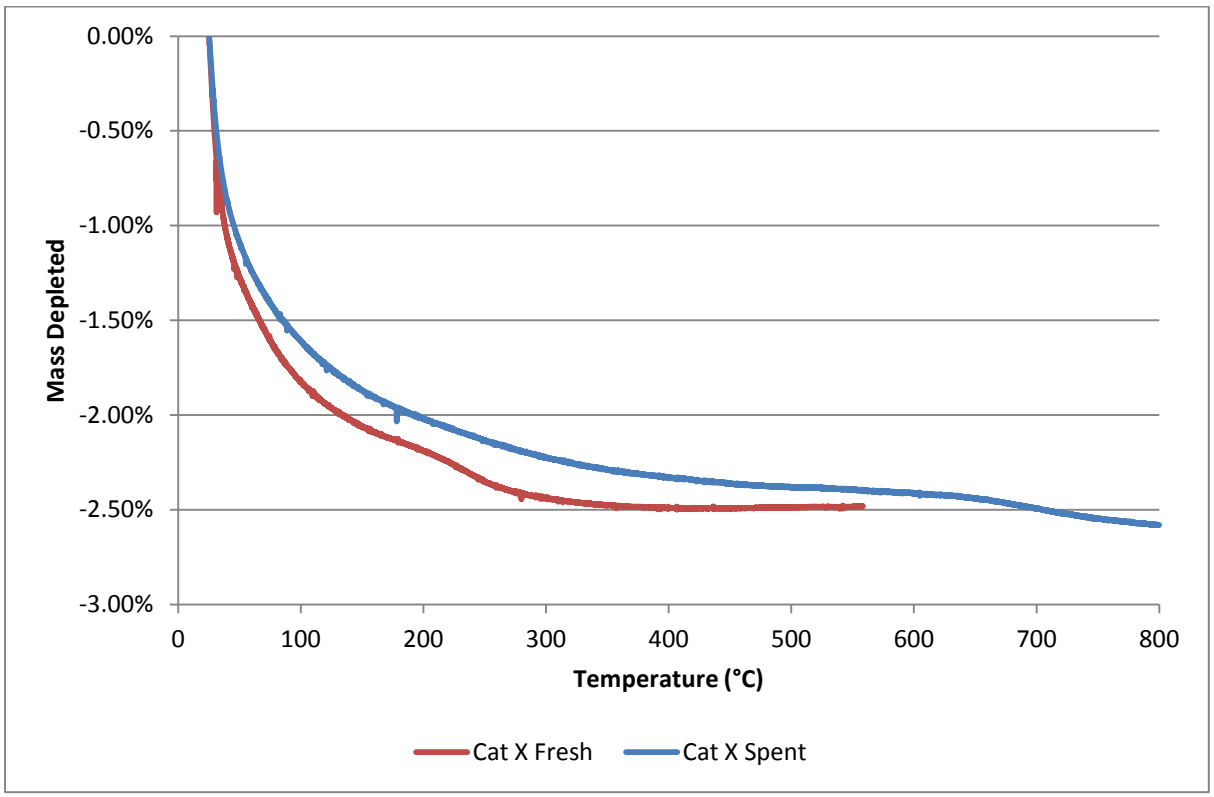

Figure 5-21 – TGA of fresh and spent Catalyst X, 10 sccm Air, 25-800°C @ 1°C/min

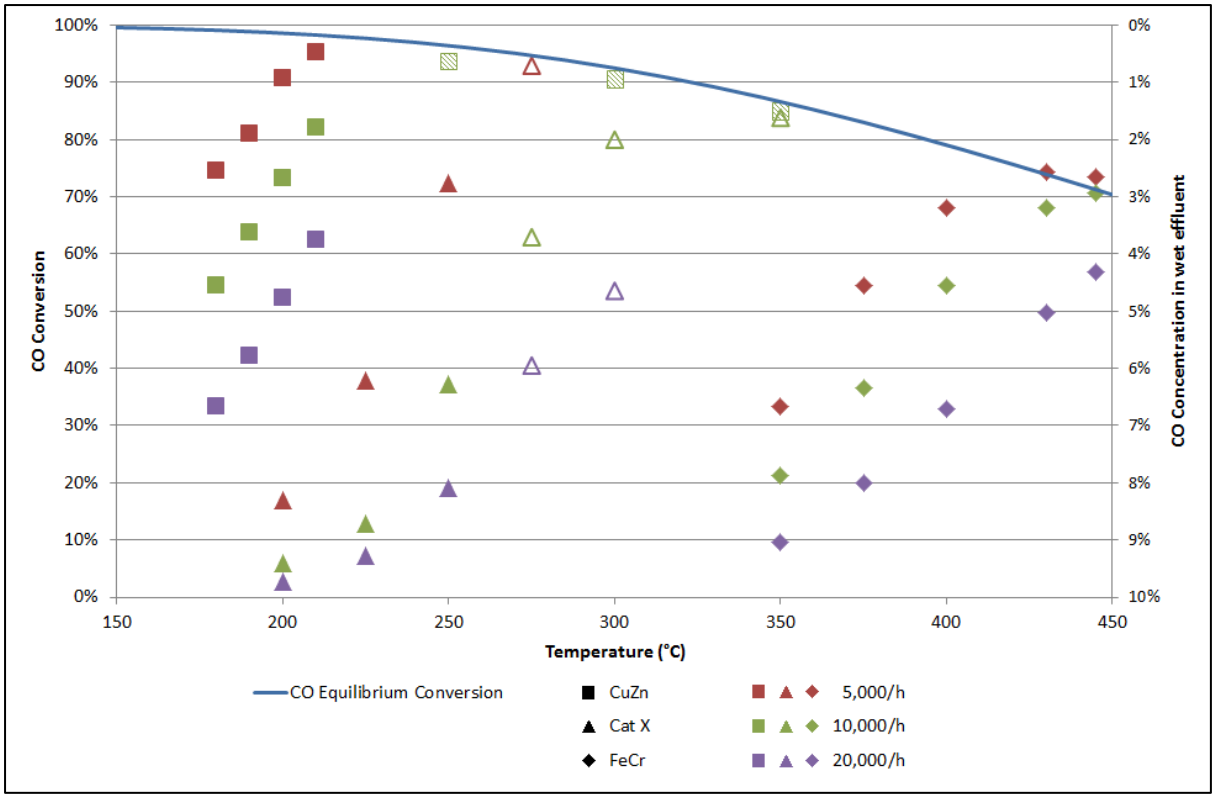

Figure 5-22 – Comparison of conversion across all catalysts tested under Feed composition 2. Open symbols denote the 40-hour average associated with Catalyst X (refer to Section 5.4.1 for more detail). Shaded symbol denote catalysts prior to exposure to high temperatures (250°C, 300°C, and 350°C)

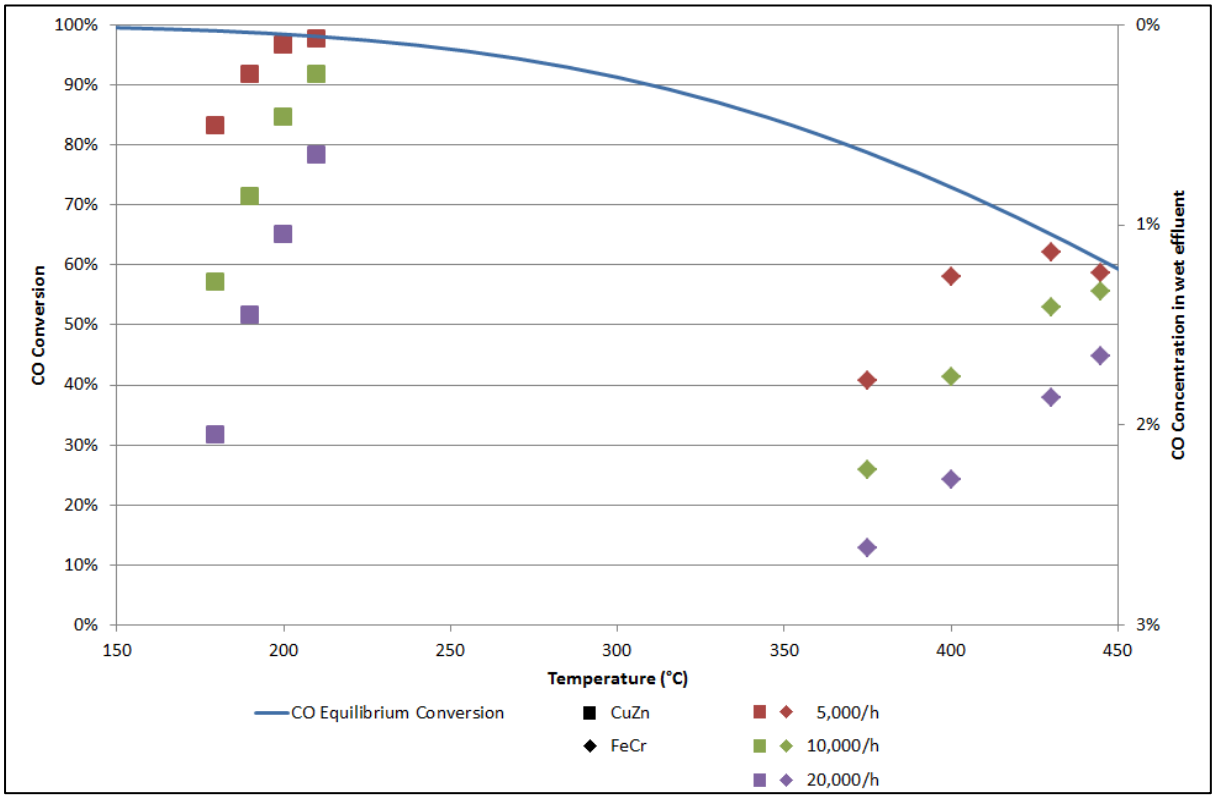

Figure 5-23 – Comparison of conversion across all catalysts tested under Feed conditions 3 (No Catalyst X data due to instability at high temperature)

6. Discussion

As mentioned in Section 2.1.2, maximum tolerable CO concentrations in the hydrogen stream for the operation of a high temperature PEM fuel cell is approximately 1 vol% (wet). To directly feed the hydrogen-rich stream into the fuel cell, without further clean-up by a preferential oxidation stage, the water-gas shift reaction stage should reduce the CO concentration in the reformate to less than 1 vol% CO.

Depending on the temperature and steam/carbon settings of the reformer, different stream compositions will reach the water-gas shift stage (due to equilibrium). Figure 6-1 and Figure 6-2 shows the desired operating zone for the catalysts tested in order to achieve 1 vol% (wet) CO for two reformate compositions. Due to the higher CO concentration with Feed composition 2, Figure 6-1 has a much smaller zone of operation as compared with Feed 3 (Figure 6-2). The maximum possible operating temperature, limited by the equilibrium conversion, with Feed composition 2 is approximately 320°C while with Feed 3 conditions the maximum possible operating temperature is approximately 415°C.

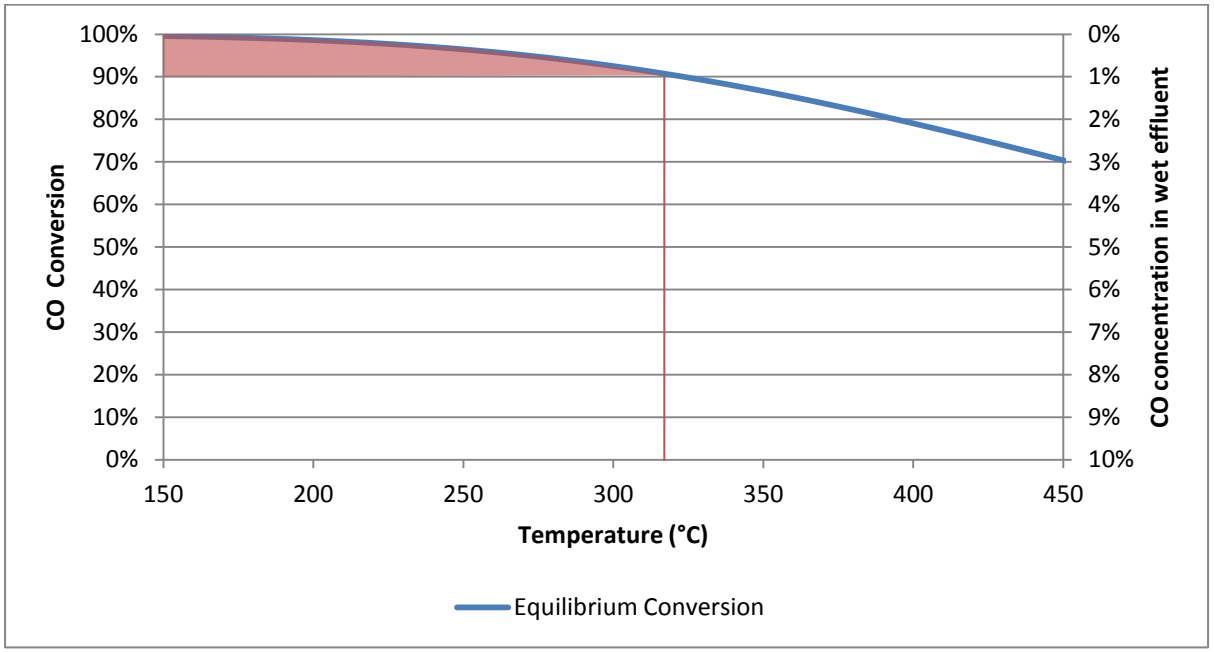

Figure 6-1 – 1 vol% (wet) zone (shaded red) of desired operating condition with Feed composition 2

6.1. Commercial HTS Catalyst

Figure 5-5 and Figure 5-6 show that commercial HTS catalyst was unable to reach the required 1 vol% (wet) of CO in the effluent stream in both feed conditions due to equilibrium limitation by temperature. As the HTS catalyst's operating temperature is already above the maximum temperature for high equilibrium conversions (approximately 320°C and 415°C for Feeds 2 and 3 respectively), this catalyst would not be applicable for a single-stage fuel processing unit. The

FeCr HTS catalyst can only be used as a two-stage process in combination with either a low temperature shift unit or a preferential oxidation unit so that the CO concentration can be further reduced to achieve 1 vol% (wet).

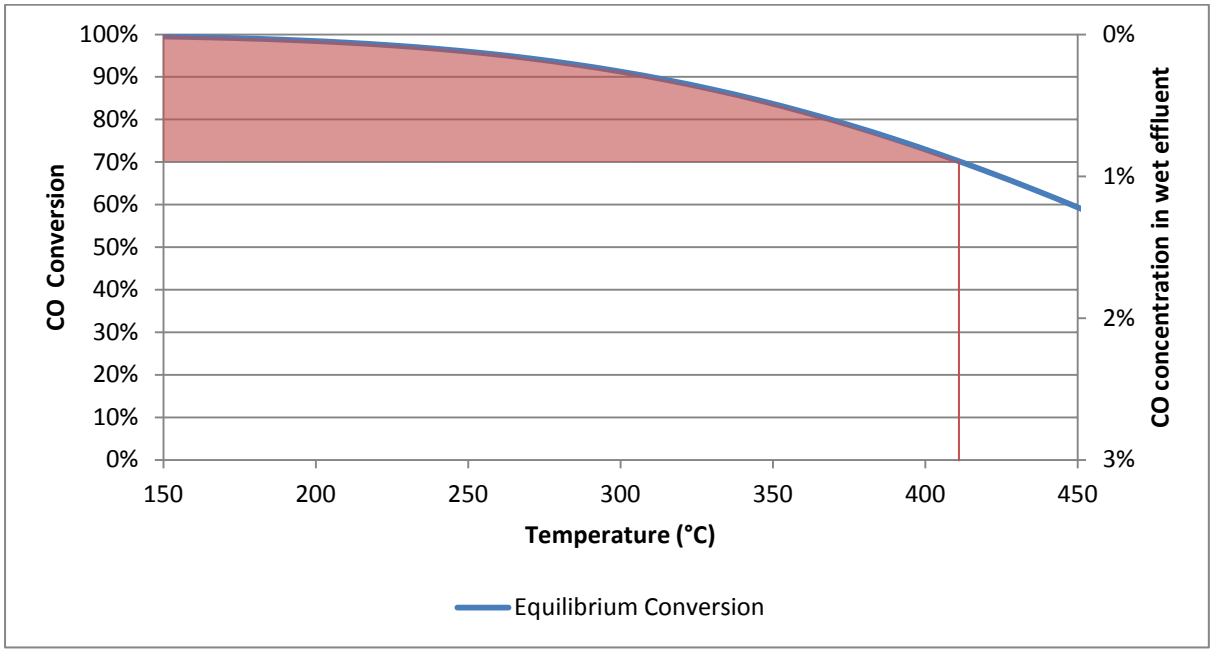

Figure 6-2 – 1 vol% (wet) zone (shaded red) of desired operating condition with Feed composition 3

6.2. Commercial LTS Catalyst

The LTS catalyst is more active at lower temperatures, allowing it to reach higher equilibrium conversions and thus the desired CO concentration for HTPEM fuel cells. The commercial LTS catalyst is able to reach the required 1 vol% (wet) CO in the effluent stream (Figure 5-10 and Figure 5-11) from 200°C (only at 5,000 h^{-1}) with Feed composition 2 and at 210°C and 20,000 h^{-1} with Feed 3 reformate composition. Although, from Figure 5-12 with Feed 1 composition the obtained CO conversion is still below the required CO concentration of 1 vol% (wet). This low activity is resulted from the lower concentration of H_2O in the feed stream.

Figure 5-9 shows that after exposure to high temperatures of 250°C and above, a loss in the activity was seen after the catalyst returned to 200°C. This is caused by sintering of Cu at high temperatures, which has been observed in multiple studies (Twigg, 1989; Ratnasamy and Wagner, 2009).

Considering that in two different feed conditions the catalyst was able to achieve the required CO concentration. It is therefore possible to use the commercial LTS catalyst in a single WGS stage fuel-processing unit to produce hydrogen of sufficiently low CO concentration to be fed directly into a PEMFC.

There are, however, various operating issues associated with the LTS catalyst. It is known that the LTS catalyst is pyrophoric once reduced (Ladebeck and Wagner, 2003), thus will cause the handling of the catalyst a possible hazard. It is also known that the commercial LTS catalyst does not tolerate condensation (Ladebeck and Wagner, 2003; Ratnasamy and Wagner, 2009) on the catalyst surface, which can occur during start-up shutdown cycles if the reactor is not purged with an inert gas to remove liquid water.

6.3. Catalyst X

Based on experiments performed on Catalyst X, it was observed from Figure 5-19 that Catalyst X is only able to achieve the required CO concentration at 275°C and 5,000 h^{-1}, a conversion of approximately 72%. However, Catalyst X is not stable beyond 250°C, as can be seen in Figure 5-16, Figure 5-17, and Figure 5-18. At temperatures 275°C and above, Catalyst X showed a slow decrease in conversion over time, unable to reach steady-state.

Even though at 275°C and 5,000 h^{-1} the catalyst would be able to achieve the required CO concentration, the activity would decrease 10% over approximately 200 hours at 275°C and 300°C. The unstable conversion of the catalyst at a temperature where the desired CO concentration can be reached makes this catalyst unsuitable for single CO clean-up stage within a fuel-processing unit.

In looking into the possible deactivation mechanisms, a TGA analysis was performed on both fresh and spent catalyst to determine whether coke was forming on the surface. From Figure 5-21, it can be observed that after the initial decrease of mass due to the evaporation of water from within the catalyst pores, there was no significant loss of mass between 400-800°C. This indicates no carbon deposition on the surface of the catalyst. The broadness of the curves of the DTA analysis is inconclusive regarding the changes to the crystal structures of the catalyst.

A BET surface area was performed on both fresh and spent Catalyst X. The measured values agree with values in literatures (Kim *et al.*, 2009; Jacobs *et al.*, 2003). The BET surface area showed that there was a decrease of 7 m^2/g, approximately 10%, between fresh and spent catalyst. This is not a clear indication of possible sintering caused by a decrease in catalyst surface area.

Catalyst X, even though it was able to achieve the desired CO concentration of 1 vol% (wet) in the effluent stream, would therefore not be suitable for a single-stage fuel-processing catalyst. The instability seen at the temperature required to achieve the aforementioned concentration limits the catalyst's overall performance.

7. Concluding Remarks

This work has established a working range for the base metal water-gas shift catalysts as well as showed that a platinum group metal catalyst is active for water-gas shift reaction at conditions suitable for fuel cell applications.

It was observed that the high temperature water-gas shift catalyst's region of activity is above 350°C. At this temperature range, however, the HTS catalyst was unable to achieve the required effluent CO concentration of 1 vol% (wet) due to equilibrium limitation.

Nonetheless, it was seen that the low temperature water-gas shift catalyst was active in the region tested (180°C – 210°C). The catalyst is also active above typical industrial operating range of > 250°C, though catalyst deactivation was observed due to the sintering of surface Cu (Ratnasamy and Wagner, 2009). Although the low-temperature shift catalyst was able to achieve the required effluent CO concentration, the LTS catalyst is not applicable for use within a small scale hydrogen production train due to the long reduction time, as well as the pyrophoricity of the catalyst after reduction.

Catalyst X was active for the water-gas shift reaction from temperatures as low as 200°C to as high as 250°. This range is between that of the low-temperature shift and the high-temperature shift, providing a so-called "medium-temperature" shift catalyst for possible commercial use of fuel-processing for fuel cells. Catalyst deactivation, however, was observed at temperatures above 250°C.

Due to the deactivation of Catalyst X, which was observed at temperatures above 250°C, and the low activity up to 250°C, makes this catalyst also not ideal for use within a small scale portable fuel-processing train for fuel cells.

Further benchmarking of other PGM-based water-gas shift catalysts are recommended to determine their suitability as a fuel processing catalyst.

8. References

ADACHI, H., AHMED, S., LEE, S. H. D., PAPADIAS, D., AHLUWALIA, R. K., BENDERT, J. C., KANNER, S. A. & YAMAZAKI, Y. 2009. A natural-gas fuel processor for a residential fuel cell system. *Journal of Power Sources,* 188**,** 244-255.

ARMOR, J. N. 2005. Catalysis and the hydrogen economy. *Catalysis Letters,* 101**,** 131-135.

AZZAM, K. G., BABICH, I. V., SESHAN, K. & LEFFERTS, L. 2008. Role of Re in Pt–Re/TiO2 catalyst for water gas shift reaction: A mechanistic and kinetic study. *Applied Catalysis B: Environmental,* 80**,** 129-140.

CALLAGHAN, C. A. 2006. *Kinetics and Catalysis of the Water-Gas-Shift Reaction: A Microkinetic and Graph Theoretic Approach.* Degree of Doctor of Philosophy in Chemical Engineering, WORCESTER POLYTECHNIC INSTITUTE.

CHANDAN, A., HATTENBERGER, M., EL-KHAROUF, A., DU, S., DHIR, A., SELF, V., POLLET, B. G., INGRAM, A. & BUJALSKI, W. 2013. High temperature (HT) polymer electrolyte membrane fuel cells (PEMFC) – A review. *Journal of Power Sources,* 231**,** 264-278.

CHOUNG, S. Y., FERRANDON, M. & KRAUSE, T. 2005. Pt-Re bimetallic supported on CeO2-ZrO2 mixed oxides as water–gas shift catalysts. *Catalysis Today,* 99**,** 257-262.

DICKS, A. & LARMINIE, J. 2003. *Fuel Cell Systems Explained Second Edition*, John Wiley & Sons, Ltd.

DICKS, A. L. 1996. Hydrogen generation from natural gas for the fuel cell systems of tomorrow. *Journal of Power Sources,* 61**,** 113-124.

DU, X., GAO, D., YUAN, Z., LIU, N., ZHANG, C. & WANG, S. 2008. Monolithic Pt/$Ce_{0.8}Zr_{0.2}O_2$/cordierite catalysts for low temperature water gas shift reaction in the real reformate. *International Journal of Hydrogen Energy,* 33**,** 3710-3718.

EG&G TECHNICAL SERVICES, I. 2004. *Fuel Cell Handbook (Seventh Edition)*.

FARRAUTO, R. J., LIU, Y., RUETTINGER, W., ILINICH, O., SHORE, L. & GIROUX, T. 2007. Precious Metal Catalysts Supported on Ceramic and Metal Monolithic Structures for the Hydrogen Economy. *Catalysis Reviews,* 49**,** 141-196.

FAUR-GHENCIU, A. 2002. Review of fuel processing catalysts for hydrogen production in PEM fuel cell systems. *Current Opinion in Solid State and Materials Science,* 6**,** 389-399.

FLAHERTY, D. W., YU, W.-Y., POZUN, Z. D., HENKELMAN, G. & MULLINS, C. B. 2011. Mechanism for the water–gas shift reaction on monofunctional platinum and cause of catalyst deactivation. *Journal of Catalysis,* 282**,** 278-288.

GONZÁLEZ, I. D., NAVARRO, R. M., WEN, W., MARINKOVIC, N., RODRIGUÉZ, J. A., ROSA, F. & FIERRO, J. L. G. 2010. A comparative study of the water gas shift reaction over platinum catalysts supported on CeO2, TiO2 and Ce-modified TiO2. *Catalysis Today,* 149**,** 372-379.

HILAIRE, S., WANG, X., LUO, T., GORTE, R. J. & WAGNER, J. P. 2004. A comparative study of water-gas-shift reaction over ceria-supported metallic catalysts. *Applied Catalysis A: General,* 258**,** 271-276.

JACOBS, G., WILLIAMS, L., GRAHAM, U., SPARKS, D. & DAVIS, B. H. 2003. Low-Temperature Water-Gas Shift: In-Situ DRIFTS-Reaction Study of a Pt/CeO2 Catalyst for Fuel Cell Reformer Applications. *Journal of Physical Chemistry B,* 107**,** 10398-10404.

JEONG, D.-W., POTDAR, H. S., SHIM, J.-O., JANG, W.-J. & ROH, H.-S. 2013. H2 production from a single stage water–gas shift reaction over Pt/CeO2, Pt/ZrO2, and Pt/Ce(1−x)Zr(x)O2 catalysts. *International Journal of Hydrogen Energy,* 38**,** 4502-4507.

KIM, Y. T., PARK, E. D., LEE, H. C., LEE, D. & LEE, K. H. 2009. Water-gas shift reaction over supported Pt-CeOx catalysts. *Applied Catalysis B: Environmental,* 90**,** 45-54.

KOLB, G. 2008. *Fuel Processing for Fuel Cells,* Federal Republic of Germany, Wiley-VCH.

KORYABKINA, N. 2003. Determination of kinetic parameters for the water–gas shift reaction on copper catalysts under realistic conditions for fuel cell applications. *Journal of Catalysis,* 217**,** 233-239.

LADEBECK, J. R. & WAGNER, J. P. 2003. Catalyst development for water-gas shift. *In:* VEILSTICH, W., LAMM, A. & GASTEIGER, H. A. (eds.) *Handbook of Fuel Cells – Fundamentals, Technology and Applications.* Chichester: John Wiley & Sons, Ltd.

LARMINIE, J. 2005. Fuel Cells. *Kirk-Othmer Encyclopedia of Chemical Technology.* 5 ed.: Wiley-Interscience.

LIU, X., RUETTINGER, W., XU, X. & FARRAUTO, R. 2005. Deactivation of Pt/CeO2 water-gas shift catalysts due to shutdown/startup modes for fuel cell applications. *Applied Catalysis B: Environmental,* 56**,** 69-75.

MOON, D. J. & RYU, J. W. 2004. Molybdenum carbide water–gas shift catalyst for fuel cell-powered vehicles applications. *Catalysis Letters,* 92**,** 17-24.

OVESEN, C. V., STOLTZE, P., NØRSKOV, J. K. & CAMPBELL, C. T. 1992. A Kinetic Model of the Water Gas Shift Reaction. *Journal of Catalysis,* 134**,** 445-468.

PANAGIOTOPOULOU, P. 2004. Effect of morphological characteristics of TiO2-supported noble metal catalysts on their activity for the water-gas shift reaction. *Journal of Catalysis,* 225**,** 327-336.

PANAGIOTOPOULOU, P. & KONDARIDES, D. I. 2006. Effect of the nature of the support on the catalytic performance of noble metal catalysts for the water–gas shift reaction. *Catalysis Today,* 112**,** 49-52.

PATT, J., MOON, D. J., PHILLIPS, C. & THOMPSON, L. 2000. Molybdenum carbide catalysts for water–gas shift. *Catalysis Letters,* 65**,** 193-195.

PENNER, S. S. 2006. Steps toward the hydrogen economy. *Energy,* 31**,** 33-43.

RADHAKRISHNAN, R., WILLIGAN, R. R., DARDAS, Z. & VANDERSPURT, T. H. 2006. Water gas shift activity of noble metals supported on ceria-zirconia oxides. *AIChE Journal,* 52**,** 1888-1894.

RATNASAMY, C. & WAGNER, J. P. 2009. Water Gas Shift Catalysis. *Catalysis Reviews,* 51**,** 325-440.

RHODES, C., HUTCHINGS, G. J. & WARD, A. M. 1995. Water-gas shift reaction: finding the mechanistic boundary. *Catalysis Today,* 23**,** 43-58.

SMITH, B. R. J., LOGANATHAN, M. & SHANTHA, M. S. 2010. A Review of the Water Gas Shift Reaction Kinetics. *International Journal of Chemical Reactor Engineering,* 8**,** 1-32.

TWIGG, M. V. 1989. *Catalyst Handbook*, Wolfe Publishing Ltd.

WINTER, C.-J. 2009. Hydrogen energy — Abundant, efficient, clean: A debate over the energy-system-of-change. *International Journal of Hydrogen Energy,* 34**,** S1-S52.

ZHANG, J., XIE, Z., ZHANG, J., TANG, Y., SONG, C., NAVESSIN, T., SHI, Z., SONG, D., WANG, H., WILKINSON, D. P., LIU, Z.-S. & HOLDCROFT, S. 2006. High temperature PEM fuel cells. *Journal of Power Sources,* 160**,** 872-891.

Appendices

Appendix A - Summary of Experimental Conditions

Feed composition and List of Experimental Programmes are listed below

Table A-1 – Composition of simulated SMR effluent gas (i.e. WGS feed) used

Steam Methane Reforming Conditions	**S/CH_4 Ratio**	2.35	3.02	5.00
	Temperature (°C)	700	800	700
	X_{Eq,CH_4} (%)	94.2	86.6	95
SMR Effluent = WGS Feed Conditions	**Composition (%)**	**Feed 1**	**Feed 2**	**Feed 3**
	H_2	63	49	42
	Ar	1	2	1
	CO_2	9	4	8
	CO	9	10	3
	H_2O	18	35	46
	Total	100	100	100
	S/CO Ratio	2	3.4	14
	S/C Ratio	1	2.5	4.2

Table A-2 – List of Experimental Programmes

Catalyst Tested	Feed Number	Experiment Number	Experimental Conditions		
			GHSV (hr^{-1})	Pressure (barg)	Temperature (°C)
CuZn	1	1	5000	1	180 - 210
		2	10000	1	180 - 210
CuZn	2	3	5000	1	180 - 210
		4	7500	1	200
		5	10000	1	180 - 210
		6	10000	1	200 - 350
		7	15000	1	200
		8	20000	1	180 - 210
CuZn	3	9	5000	1	180 - 210
		10	10000	1	180 - 210
		11	20000	1	180 - 210
FeCr	2	12	5000	1	350 - 445
		13	10000	1	350 - 445
		14	20000	1	350 - 445
FeCr	3	15	5000	1	375 - 445
		16	10000	1	375 - 445
		17	20000	1	375 - 445
Cat X	2	18	5000	1	200 - 275
		19	10000	1	200 - 350
		20	20000	1	200 - 300

Appendix B - Sample Calculations

In order to determine the gas response factors, gas mixtures of known concentrations of the components are analysed in the GC. Gas response factors are thus determined via linear regression of normalized area and normalized composition. Linear regressions trend lines are forced through the origin as at no component *i*, there will be no normalized area and no normalized composition.

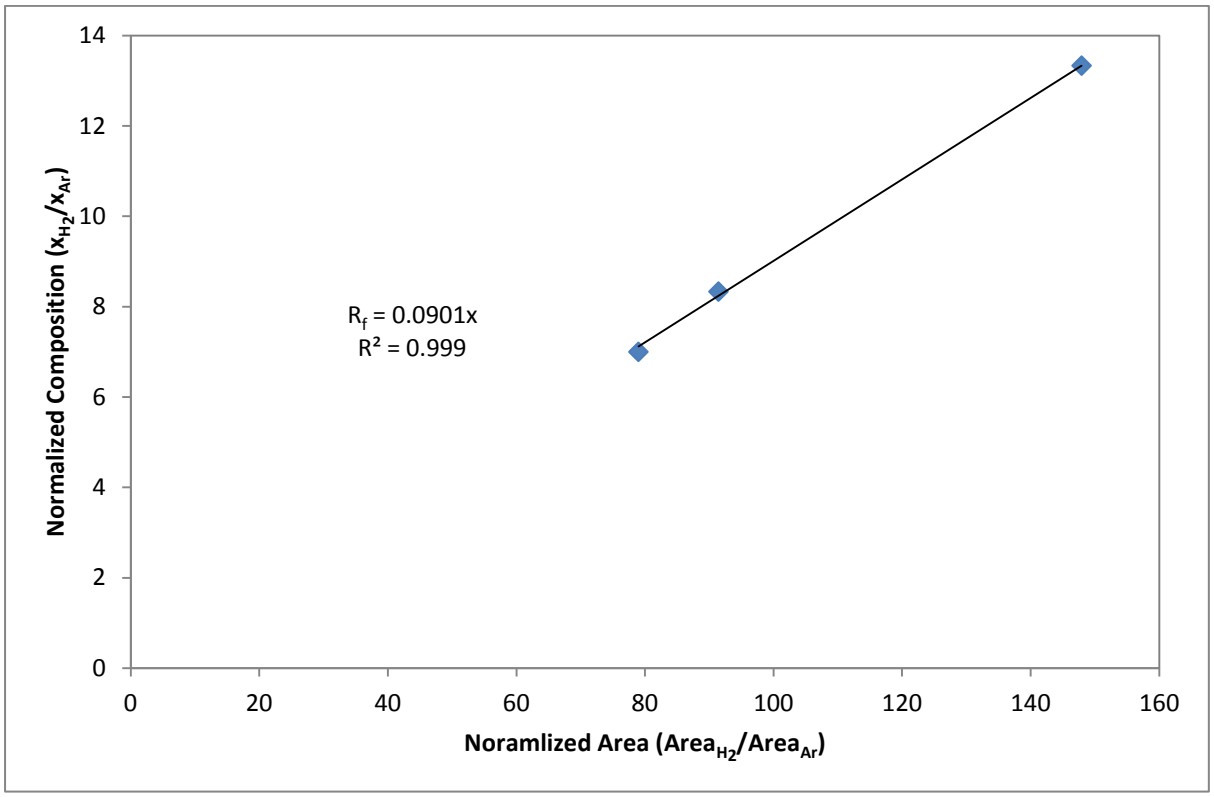

Figure B-1 – Determination of gas response factor for hydrogen. R_{f_H2} = 0.0901

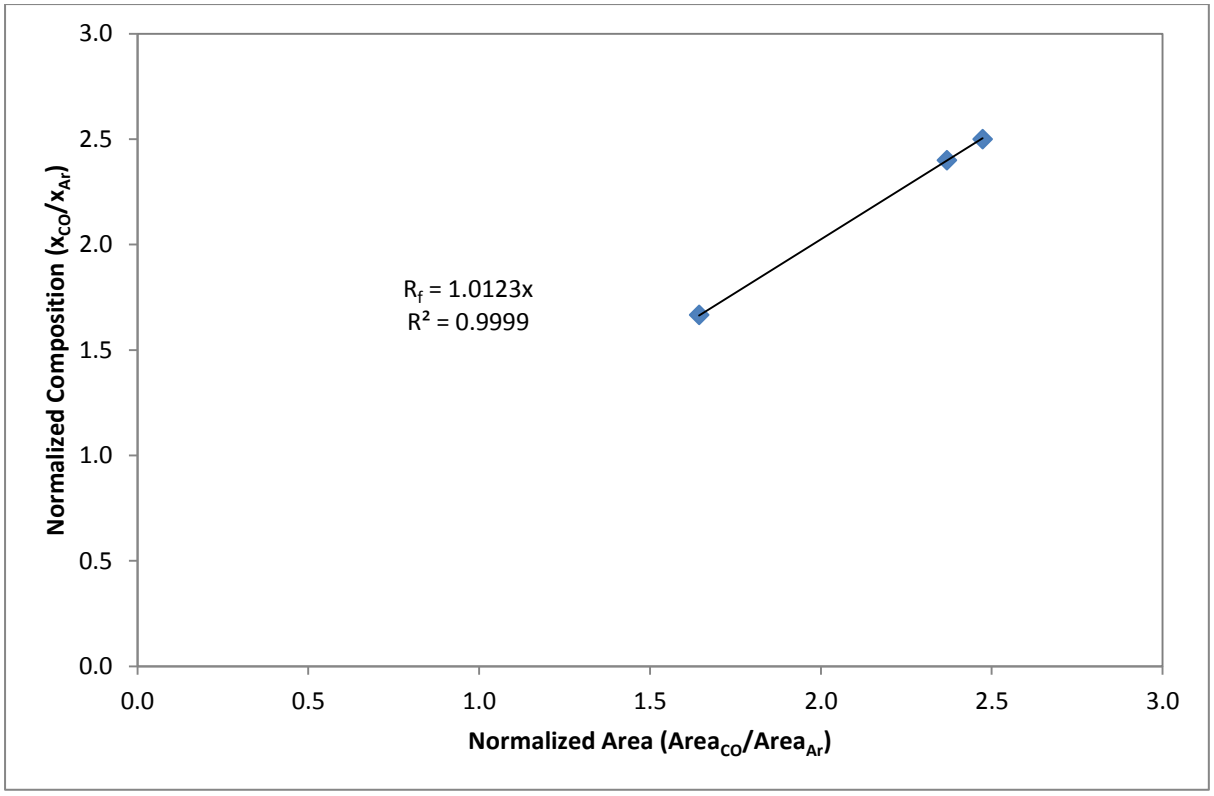

Figure B-2 – Determination of gas response factor for carbon monoxide. R_{f_CO} = 1.0123

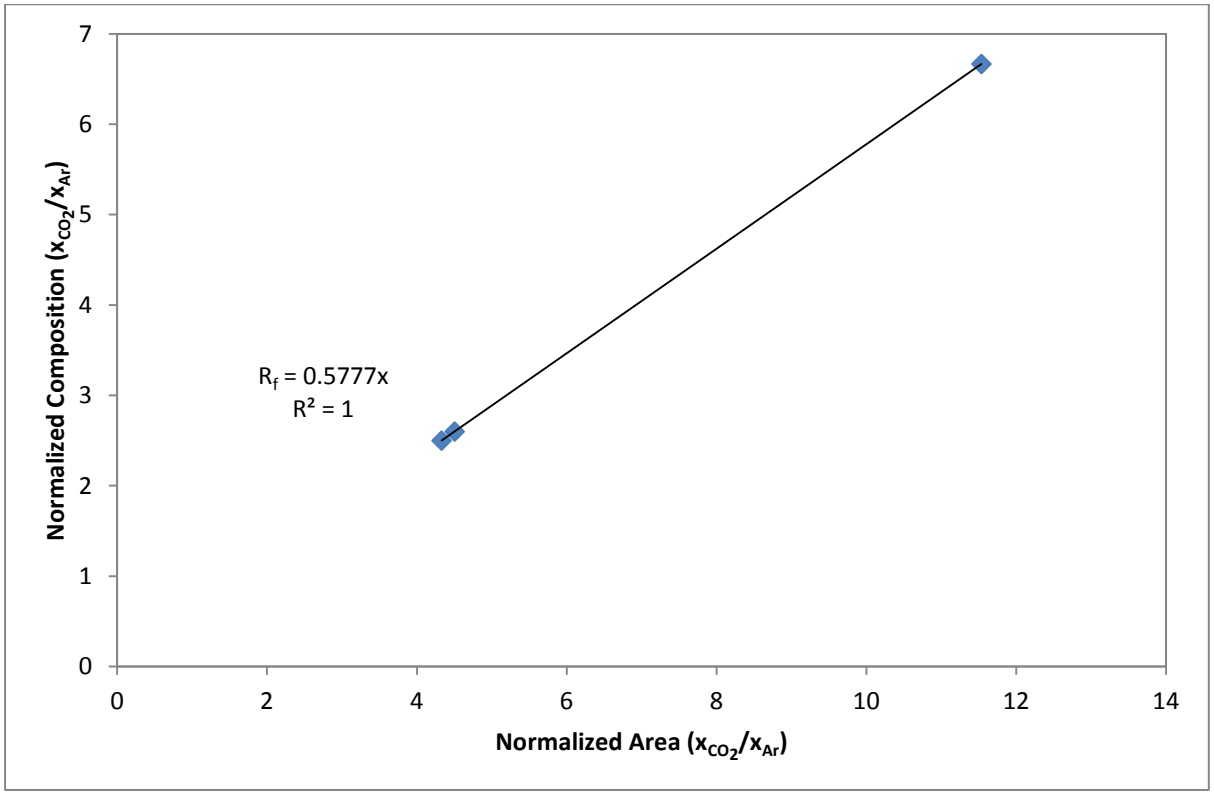

Figure B-3 – Determination of gas response factor for carbon dioxide. R_{f_CO2} = 0.5777

CO conversion is calculated as follows:

(Example based on CuZn, Feed 1, 200°C, 10,000 h^{-1}, TOS:16.62h)

Feed composition 2 @ TOS: 16.62h:

$Area_{CO}.Feed$ = 70253 uV/s; $Area_{CO2}.Feed$ = 52362 uV/s; $AreaAr._{Feed}$ = 15501 uV/s

$Area_{CO}.Product$ = 18715 uV/s; $Area_{CO2}.Product$ = 134147 uV/s; $Area_{Ar}.Product$ = 14134 uV/s

$R_f.CO$ = 1.0123; $R_f.CO_2$ = 0.5777

$x_{CO}.Feed = \frac{Area_{CO}}{Area_{Ar}} \times R_f.CO \times \dot{F}_{Feed_{Ar}} = \frac{70253}{14134} \times 1.0123 \times 3.4\% = 15.6\ mol\%\ CO$

$x_{CO2}.Feed = \frac{Area_{CO_2}}{Area_{Ar}} \times R_f.CO_2 \times \dot{F}_{Feed_{Ar}} = \frac{52362}{14134} \times 0.5777 \times 3.4\% = 6.64\ mol\%\ CO_2$

$x_{CO}.Product = \frac{Area_{CO}}{Area_{Ar}} \times R_f.CO \times \dot{F}_{Feed_{Ar}} = \frac{18715}{14134} \times 1.0123 \times 3.4\% = 4.56\ mol\%\ CO$

$x_{CO2}.Product = \frac{Area_{CO_2}}{Area_{Ar}} \times R_f.CO_2 \times \dot{F}_{Feed_{Ar}} = \frac{134147}{14134} \times 0.5777 \times 3.4\% = 18.64\ mol\%\ CO_2$

$X_{CO} = \frac{\dot{F}CO_{Feed} - \dot{F}CO_{Product}}{\dot{F}CO_{Feed}} = \frac{15.6\% - 4.56\%}{15.6\%} = 70.78\%$

Appendix C - Experimental Data

Experiment 1 & 2 – $Cu/ZnO/Al_2O_3$, Feed 1

Space Velocity – 5,000 h^{-1}

Time-on-stream (h)	T (°C)	X_{CO}	Molar Flow (mmol/min)				$C_{Balance}$
			H_2	CO	CO_2	Ar	
534.4	200	35.3%	1.3	0.2	0.4	0.04	-0.8%
535.0		36.0%	1.3	0.2	0.4	0.04	-0.8%
535.6		36.7%	1.3	0.2	0.4	0.04	-0.6%
536.2		36.0%	1.3	0.2	0.4	0.04	-0.8%
536.8		36.3%	1.3	0.2	0.4	0.04	-0.8%
537.4		35.6%	1.3	0.2	0.4	0.04	-0.8%
538.1		37.1%	1.3	0.2	0.4	0.04	-0.8%
538.7		37.4%	1.3	0.2	0.5	0.04	-0.8%
539.3		37.1%	1.3	0.2	0.4	0.04	-0.8%
539.9		36.8%	1.3	0.2	0.4	0.04	-0.8%
540.5		34.1%	1.3	0.2	0.4	0.04	-0.7%
541.1		33.0%	1.3	0.2	0.4	0.04	-0.7%
541.7		33.0%	1.3	0.2	0.4	0.04	-0.7%
542.3		32.9%	1.3	0.2	0.4	0.04	-0.8%
543.0		33.8%	1.3	0.2	0.4	0.04	-0.7%
543.6		35.0%	1.3	0.2	0.4	0.04	-0.8%
544.2		34.5%	1.3	0.2	0.4	0.04	-0.7%
544.8		35.0%	1.3	0.2	0.4	0.04	-0.7%
545.4		35.6%	1.3	0.2	0.4	0.04	-0.7%
546.0		36.2%	1.3	0.2	0.4	0.04	-0.8%
546.6		36.3%	1.3	0.2	0.4	0.04	-0.8%
547.3		37.2%	1.3	0.2	0.4	0.04	-0.8%
547.9	180	26.8%	1.2	0.2	0.4	0.04	-0.5%
548.5		24.8%	1.2	0.2	0.4	0.04	-0.6%
549.1		21.6%	1.2	0.2	0.4	0.04	-0.3%
549.7		20.5%	1.2	0.2	0.4	0.04	-0.2%
550.3		18.0%	1.2	0.2	0.4	0.04	-0.6%
550.9		17.4%	1.2	0.2	0.4	0.04	-0.6%
551.6		17.3%	1.2	0.2	0.4	0.04	-0.5%
552.2		17.5%	1.2	0.2	0.4	0.04	-0.5%
552.8		17.4%	1.2	0.2	0.4	0.04	-0.6%
553.4		17.4%	1.2	0.2	0.4	0.04	-0.6%
554.0		19.1%	1.2	0.2	0.4	0.04	-0.6%
554.6		18.8%	1.2	0.2	0.4	0.04	-0.6%
555.3		18.7%	1.2	0.2	0.4	0.04	-0.6%
555.9		18.7%	1.2	0.2	0.4	0.04	-0.6%
556.5		17.7%	1.2	0.2	0.4	0.04	-0.6%

Time-on-stream (h)	T (°C)	X_{CO}	Molar Flow (mmol/min)				$C_{Balance}$
			H_2	CO	CO_2	Ar	
557.7	180	17.7%	1.2	0.2	0.4	0.04	-0.6%
558.3		17.6%	1.2	0.2	0.4	0.04	-0.6%
558.9		17.9%	1.2	0.2	0.4	0.04	-0.6%
559.6		17.9%	1.2	0.2	0.4	0.04	-0.6%
560.2		18.0%	1.2	0.2	0.4	0.04	-0.6%
560.8		18.1%	1.2	0.2	0.4	0.04	-0.6%
561.4		18.5%	1.2	0.2	0.4	0.04	-0.6%
562.0		20.5%	1.2	0.2	0.4	0.04	0.0%
562.6		18.4%	1.2	0.2	0.4	0.04	-0.6%
563.3		18.5%	1.2	0.2	0.4	0.04	-0.6%
563.9		18.1%	1.2	0.2	0.4	0.04	-0.6%
564.5		18.1%	1.2	0.2	0.4	0.04	-0.6%
565.1		18.2%	1.2	0.2	0.4	0.04	-0.6%
565.7		18.2%	1.2	0.2	0.4	0.04	-0.6%
566.3		18.2%	1.2	0.2	0.4	0.04	-0.6%
566.9		18.3%	1.2	0.2	0.4	0.04	-0.6%
567.6		18.2%	1.2	0.2	0.4	0.04	-0.6%
568.2		18.2%	1.2	0.2	0.4	0.04	-0.6%
568.8		18.4%	1.2	0.2	0.4	0.04	-0.6%
569.4		18.5%	1.2	0.2	0.4	0.04	-0.5%
570.0		19.1%	1.2	0.2	0.4	0.04	-0.6%
570.6		18.4%	1.2	0.2	0.4	0.04	-0.6%
571.3		21.6%	1.2	0.2	0.4	0.04	-0.1%
571.9		20.3%	1.2	0.2	0.4	0.04	-0.3%
572.5		18.8%	1.2	0.2	0.4	0.04	-0.6%
573.1		18.7%	1.2	0.2	0.4	0.04	-0.6%
573.7	190	21.1%	1.2	0.2	0.4	0.04	-0.6%
574.3		29.3%	1.2	0.2	0.4	0.04	-0.7%
575.0		31.7%	1.3	0.2	0.4	0.04	-0.7%
575.6		29.7%	1.2	0.2	0.4	0.04	-0.6%
576.2		29.0%	1.3	0.2	0.4	0.04	-0.7%
576.8		28.3%	1.3	0.2	0.4	0.04	-0.6%
577.4		28.5%	1.2	0.2	0.4	0.04	-0.6%
578.0		28.6%	1.3	0.2	0.4	0.04	-0.6%
578.7		28.5%	1.2	0.2	0.4	0.04	-0.7%
579.3		28.3%	1.3	0.2	0.4	0.04	-0.6%
579.9		27.9%	1.3	0.2	0.4	0.04	-0.6%
580.5		28.1%	1.2	0.2	0.4	0.04	-0.6%
581.1		28.3%	1.2	0.2	0.4	0.04	-0.6%
581.8		28.4%	1.2	0.2	0.4	0.04	-0.7%
582.4		28.3%	1.2	0.2	0.4	0.04	-0.6%
583.0		28.0%	1.2	0.2	0.4	0.04	-0.6%
583.6		27.9%	1.2	0.2	0.4	0.04	-0.6%

Time-on-stream (h)	T (°C)	X_{CO}	Molar Flow (mmol/min)				$C_{Balance}$
			H_2	CO	CO_2	Ar	
584.8	190	27.9%	1.3	0.2	0.4	0.04	-0.6%
585.5		28.2%	1.3	0.2	0.4	0.04	-0.6%
586.1		28.3%	1.3	0.2	0.4	0.04	-0.6%
586.7		28.2%	1.3	0.2	0.4	0.04	-0.6%
587.3		28.7%	1.3	0.2	0.4	0.04	-0.6%
587.9		28.7%	1.3	0.2	0.4	0.04	-0.6%
588.5		28.4%	1.3	0.2	0.4	0.04	-0.6%
589.2		28.6%	1.3	0.2	0.4	0.04	-0.7%
589.8		28.6%	1.3	0.2	0.4	0.04	-0.6%
590.4		28.2%	1.3	0.2	0.4	0.04	-0.6%
591.0		28.2%	1.3	0.2	0.4	0.04	-0.6%
591.6		28.1%	1.2	0.2	0.4	0.04	-0.6%
592.3		29.1%	1.2	0.2	0.4	0.04	-0.4%
592.9		28.4%	1.2	0.2	0.4	0.04	-0.6%
593.5		29.1%	1.2	0.2	0.4	0.04	-0.4%
594.1		28.5%	1.2	0.2	0.4	0.04	-0.6%
594.7		28.7%	1.2	0.2	0.4	0.04	-0.7%
595.3		29.7%	1.2	0.2	0.4	0.04	-0.4%
596.0		29.6%	1.2	0.2	0.4	0.04	-0.4%
596.6		29.6%	1.2	0.2	0.4	0.04	-0.5%
597.2		28.9%	1.2	0.2	0.4	0.04	-0.7%
597.8		25.6%	1.2	0.2	0.4	0.04	-0.7%
598.4		23.1%	1.2	0.2	0.4	0.04	-0.6%
599.0		22.9%	1.2	0.2	0.4	0.04	-0.6%
599.7		23.1%	1.2	0.2	0.4	0.04	-0.6%
600.3		24.5%	1.2	0.2	0.4	0.04	-0.6%
600.9		23.3%	1.2	0.2	0.4	0.04	-0.6%
601.5		23.1%	1.2	0.2	0.4	0.04	-0.6%
602.2		23.1%	1.2	0.2	0.4	0.04	-0.6%
602.8		25.8%	1.2	0.2	0.4	0.04	-0.6%
603.4		29.1%	1.3	0.2	0.4	0.04	-0.7%
604.0		28.1%	1.3	0.2	0.4	0.04	-0.7%
604.6		24.8%	1.2	0.2	0.4	0.04	-0.6%
605.2		24.7%	1.2	0.2	0.4	0.04	-0.6%
605.9		24.5%	1.2	0.2	0.4	0.04	-0.7%
606.5		24.6%	1.2	0.2	0.4	0.04	-0.7%
607.1		24.9%	1.2	0.2	0.4	0.04	-0.6%
607.7		25.6%	1.2	0.2	0.4	0.04	-0.6%
608.3		26.1%	1.2	0.2	0.4	0.04	-0.6%
608.9		25.8%	1.2	0.2	0.4	0.04	-0.6%
609.6		25.6%	1.2	0.2	0.4	0.04	-0.6%
610.2		25.7%	1.2	0.2	0.4	0.04	-0.6%
610.8		25.7%	1.2	0.2	0.4	0.04	-0.6%
611.4		26.0%	1.2	0.2	0.4	0.04	-0.6%

Time-on-stream (h)	T (°C)	X_{CO}	Molar Flow (mmol/min)				$C_{Balance}$
			H_2	CO	CO_2	Ar	
612.0	190	25.4%	1.2	0.2	0.4	0.04	-0.7%
612.6		26.0%	1.2	0.2	0.4	0.04	-0.7%
613.3		25.7%	1.2	0.2	0.4	0.04	-0.7%
613.9		25.4%	1.2	0.2	0.4	0.04	-0.4%
614.5		25.0%	1.2	0.2	0.4	0.04	-0.6%
615.1		24.8%	1.2	0.2	0.4	0.04	-0.7%
615.7	210	47.1%	1.3	0.2	0.5	0.04	-0.8%
616.4		53.2%	1.3	0.1	0.5	0.04	-1.0%
617.0		46.2%	1.3	0.2	0.5	0.04	-0.9%
617.6		43.6%	1.3	0.2	0.5	0.04	-0.8%
618.2		45.1%	1.3	0.2	0.5	0.04	-0.6%
619.0		47.0%	1.3	0.2	0.5	0.04	-0.6%
619.6		47.7%	1.3	0.1	0.5	0.04	-0.7%
620.2		46.9%	1.3	0.2	0.5	0.04	-0.9%
620.8		49.7%	1.3	0.1	0.5	0.04	-0.8%
621.5		50.5%	1.3	0.1	0.5	0.04	-0.6%
622.1		49.7%	1.3	0.1	0.5	0.04	-0.7%
622.7		48.4%	1.3	0.1	0.5	0.04	-0.8%
623.3		49.5%	1.3	0.1	0.5	0.04	-0.9%
623.9		49.5%	1.3	0.1	0.5	0.04	-0.9%
624.6		42.7%	1.3	0.2	0.5	0.04	-0.7%
625.2		41.2%	1.3	0.2	0.5	0.04	-0.8%
625.8		40.4%	1.3	0.2	0.5	0.04	-0.8%
626.4		42.2%	1.3	0.2	0.5	0.04	-0.6%
627.0		43.1%	1.3	0.2	0.5	0.04	-0.7%
627.7		44.6%	1.2	0.2	0.5	0.04	-0.5%
628.3		46.1%	1.3	0.2	0.5	0.04	-0.6%
628.9		45.7%	1.3	0.2	0.5	0.04	-0.7%
629.5		46.6%	1.3	0.2	0.5	0.04	-0.9%
630.1		46.7%	1.3	0.2	0.5	0.04	-0.7%
630.7		45.9%	1.3	0.2	0.5	0.04	-0.8%
631.4		49.8%	1.3	0.1	0.5	0.04	-0.8%
632.0		49.8%	1.3	0.1	0.5	0.04	-0.6%
632.6		49.1%	1.3	0.1	0.5	0.04	-0.9%
633.2		48.9%	1.3	0.1	0.5	0.04	-1.0%
633.8		48.2%	1.3	0.1	0.5	0.04	-1.0%
634.5		47.1%	1.3	0.2	0.5	0.04	-0.9%
635.1		47.3%	1.3	0.2	0.5	0.04	-0.5%
635.7		47.1%	1.3	0.2	0.5	0.04	-0.7%
636.3		47.8%	1.3	0.1	0.5	0.04	-0.6%
636.9		47.2%	1.3	0.2	0.5	0.04	-0.7%
637.5		46.3%	1.3	0.2	0.5	0.04	-0.9%
638.2		47.5%	1.3	0.2	0.5	0.04	-0.6%
638.8		47.7%	1.3	0.1	0.5	0.04	-0.6%

Time-on-stream (h)	T (°C)	X_{CO}	Molar Flow (mmol/min)				$C_{Balance}$
			H_2	CO	CO_2	Ar	
639.4	210	48.4%	1.2	0.1	0.5	0.04	-0.1%
640.0		46.8%	1.3	0.2	0.5	0.04	-0.9%
644.8		44.5%	1.2	0.2	0.5	0.04	-0.5%
645.5	200	33.3%	1.3	0.2	0.4	0.04	-0.9%
646.1		33.6%	1.3	0.2	0.4	0.04	-0.7%
646.7		34.4%	1.3	0.2	0.4	0.04	-0.7%
647.3		35.7%	1.2	0.2	0.4	0.04	-0.6%
647.9		38.2%	1.3	0.2	0.5	0.04	-0.8%
648.5		38.4%	1.3	0.2	0.5	0.04	-0.8%
649.1		38.8%	1.3	0.2	0.5	0.04	-0.8%
649.8		39.5%	1.2	0.2	0.4	0.04	-0.5%
650.4		38.8%	1.2	0.2	0.4	0.04	-0.1%
651.0		35.0%	1.2	0.2	0.4	0.04	-0.5%
651.6		35.6%	1.2	0.2	0.4	0.04	-0.2%
652.2		35.4%	1.2	0.2	0.4	0.04	-0.4%
652.8		34.7%	1.3	0.2	0.4	0.04	-0.7%
653.4		34.4%	1.3	0.2	0.4	0.04	-0.8%
654.1		36.8%	1.3	0.2	0.5	0.04	-0.9%
654.7		35.5%	1.3	0.2	0.4	0.04	-0.8%
655.3		36.0%	1.2	0.2	0.4	0.04	-0.6%
655.9		35.6%	1.3	0.2	0.4	0.04	-0.7%
656.5		35.7%	1.2	0.2	0.4	0.04	-0.5%
657.1		34.7%	1.3	0.2	0.4	0.04	-0.7%
657.7		35.8%	1.2	0.2	0.4	0.04	-0.6%
658.4		36.5%	1.2	0.2	0.4	0.04	-0.5%
659.0		36.8%	1.2	0.2	0.4	0.04	-0.4%
659.6		36.4%	1.2	0.2	0.4	0.04	-0.5%
660.2		36.8%	1.2	0.2	0.4	0.04	-0.5%
660.8		36.6%	1.2	0.2	0.4	0.04	-0.5%
661.4		36.5%	1.2	0.2	0.4	0.04	-0.4%
662.1		36.0%	1.2	0.2	0.4	0.04	-0.5%
662.7		37.0%	1.2	0.2	0.4	0.04	-0.4%
663.3		36.3%	1.3	0.2	0.4	0.04	-0.8%
663.9		35.5%	1.3	0.2	0.4	0.04	-0.8%
664.5		37.2%	1.2	0.2	0.4	0.04	-0.2%
665.1		35.6%	1.3	0.2	0.4	0.04	-0.7%
665.7		37.8%	1.2	0.2	0.4	0.04	-0.3%
669.2		58.8%	0.5	0.1	0.1	0.09	12.5%
669.8		38.1%	1.2	0.2	0.4	0.04	-0.3%
670.4		37.8%	1.2	0.2	0.4	0.04	-0.4%

Space Velocity – 10,000 h^{-1}

Time-on-stream (h)	T (°C)	X_{CO}	Molar Flow (mmol/min)				$C_{Balance}$
			H_2	CO	CO_2	Ar	
533.0	200	29.0%	2.5	0.4	0.8	0.09	-0.5%
533.6		21.9%	2.5	0.4	0.8	0.09	-0.7%
534.2		18.0%	2.5	0.5	0.8	0.09	-0.6%
534.8		17.0%	2.5	0.5	0.8	0.09	-0.7%
535.4		17.2%	2.5	0.5	0.8	0.09	-0.6%
536.1		17.1%	2.5	0.5	0.8	0.09	-0.6%
536.7		17.0%	2.5	0.5	0.8	0.09	-0.6%
537.3		16.9%	2.5	0.5	0.8	0.09	-0.6%
537.9		16.8%	2.5	0.5	0.8	0.09	-0.6%
538.5		16.8%	2.5	0.5	0.8	0.09	-0.6%
539.1		16.8%	2.5	0.5	0.8	0.09	-0.6%
539.7		16.6%	2.5	0.5	0.8	0.09	-0.6%
540.4		16.7%	2.5	0.5	0.8	0.09	-0.6%
541.0		16.1%	2.5	0.5	0.8	0.09	-0.6%
541.6		15.7%	2.5	0.5	0.8	0.09	-0.6%
542.2		15.6%	2.5	0.5	0.8	0.09	-0.6%
542.8		15.8%	2.5	0.5	0.8	0.09	-0.6%
543.4		16.8%	2.5	0.5	0.8	0.09	-0.6%
544.0		16.0%	2.5	0.5	0.8	0.09	-0.5%
544.6		17.3%	2.4	0.5	0.8	0.09	-0.3%
545.3		16.6%	2.5	0.5	0.8	0.09	-0.6%
545.9		17.8%	2.5	0.5	0.8	0.09	-0.5%
546.5		18.0%	2.5	0.5	0.8	0.09	-0.6%
547.1		18.1%	2.5	0.5	0.8	0.09	-0.6%
547.7		19.8%	2.5	0.5	0.8	0.09	-0.6%
548.3	180	6.9%	2.4	0.5	0.7	0.09	-0.4%
548.9		7.3%	2.4	0.5	0.7	0.09	-0.4%
549.6		7.8%	2.4	0.5	0.7	0.09	-0.4%
550.2		6.4%	2.4	0.5	0.7	0.09	-0.5%
550.8		6.4%	2.4	0.5	0.7	0.09	-0.5%
551.4		7.8%	2.4	0.5	0.0	0.09	12.2%
552.0		8.2%	2.4	0.5	0.7	0.09	-0.2%
552.6		6.8%	2.4	0.5	0.7	0.09	-0.5%
553.3		6.6%	2.4	0.5	0.7	0.09	-0.5%
553.9		8.2%	2.4	0.5	0.7	0.09	-0.1%
554.5		6.4%	2.4	0.5	0.7	0.09	-0.5%
555.1		8.6%	2.4	0.5	0.7	0.09	0.0%
555.7		6.5%	2.4	0.5	0.7	0.09	-0.5%
556.3		6.4%	2.4	0.5	0.7	0.09	-0.5%
556.9		6.3%	2.4	0.5	0.7	0.09	-0.5%
557.6		6.2%	2.4	0.5	0.7	0.09	-0.5%
558.2		6.2%	2.4	0.5	0.7	0.09	-0.5%

Time-on-stream (h)	T (°C)	X_{CO}	Molar Flow (mmol/min)				$C_{Balance}$
			H_2	CO	CO_2	Ar	
558.8	180	6.1%	2.4	0.5	0.7	0.09	-0.5%
559.4		6.5%	2.4	0.5	0.7	0.09	-0.5%
560.0		6.6%	2.4	0.5	0.7	0.09	-0.5%
560.6		6.6%	2.5	0.5	0.7	0.09	-0.5%
561.3		6.7%	2.4	0.5	0.7	0.09	-0.5%
561.9		6.7%	2.4	0.5	0.7	0.09	-0.5%
562.5		6.6%	2.4	0.5	0.7	0.09	-0.5%
563.1		6.6%	2.4	0.5	0.7	0.09	-0.5%
563.7		6.6%	2.4	0.5	0.7	0.09	-0.5%
564.3		6.5%	2.4	0.5	0.7	0.09	-0.5%
564.9		6.6%	2.4	0.5	0.7	0.09	-0.5%
565.6		6.5%	2.4	0.5	0.7	0.09	-0.5%
566.2		6.6%	2.4	0.5	0.7	0.09	-0.4%
566.8		6.6%	2.4	0.5	0.7	0.09	-0.5%
567.4		6.6%	2.4	0.5	0.7	0.09	-0.5%
568.0		9.0%	2.4	0.5	0.7	0.09	0.1%
568.6		6.6%	2.4	0.5	0.7	0.09	-0.5%
569.3		6.9%	2.4	0.5	0.7	0.09	-0.4%
569.9		6.8%	2.4	0.5	0.7	0.09	-0.5%
570.5		6.9%	2.5	0.5	0.7	0.09	-0.6%
571.1		6.7%	2.4	0.5	0.7	0.09	-0.4%
571.7		6.7%	2.4	0.5	0.7	0.09	-0.4%
572.3		7.8%	2.4	0.5	0.7	0.09	-0.3%
573.0		6.7%	2.4	0.5	0.7	0.09	-0.5%
573.6	190	24.5%	2.0	0.4	0.6	0.10	3.1%
574.2		14.1%	2.4	0.5	0.8	0.09	-0.5%
574.8		14.9%	2.5	0.5	0.8	0.09	-0.5%
575.4		14.1%	2.5	0.5	0.8	0.09	-0.5%
576.0		10.4%	2.4	0.5	0.7	0.09	-0.4%
576.7		10.6%	2.4	0.5	0.7	0.09	-0.5%
577.3		11.1%	2.5	0.5	0.7	0.09	-0.5%
577.9		11.7%	2.5	0.5	0.7	0.09	-0.4%
578.5		12.1%	2.5	0.5	0.7	0.09	-0.4%
579.1		12.5%	2.5	0.5	0.7	0.09	-0.5%
579.7		12.5%	2.5	0.5	0.7	0.09	-0.5%
580.4		12.8%	2.5	0.5	0.7	0.09	-0.5%
581.0		12.6%	2.5	0.5	0.7	0.09	-0.4%
581.6		12.8%	2.5	0.5	0.7	0.09	-0.5%
582.2		12.7%	2.5	0.5	0.7	0.09	-0.5%
582.8		12.3%	2.5	0.5	0.7	0.09	-0.5%
583.5		12.1%	2.5	0.5	0.7	0.09	-0.5%
584.1		12.3%	2.5	0.5	0.7	0.09	-0.4%
584.7		12.3%	2.5	0.5	0.7	0.09	-0.4%

Time-on-stream (h)	T (°C)	X_{CO}	Molar Flow (mmol/min)				$C_{Balance}$
			H_2	CO	CO_2	Ar	
585.3	190	12.2%	2.5	0.5	0.7	0.09	-0.4%
585.9		12.4%	2.5	0.5	0.7	0.09	-0.4%
586.5		12.4%	2.5	0.5	0.7	0.09	-0.5%
587.2		12.4%	2.5	0.5	0.7	0.09	-0.4%
587.8		12.3%	2.5	0.5	0.7	0.09	-0.4%
588.4		12.0%	2.5	0.5	0.7	0.09	-0.4%
589.0		12.0%	2.5	0.5	0.7	0.09	-0.5%
589.6		11.9%	2.5	0.5	0.7	0.09	-0.5%
590.2		11.8%	2.5	0.5	0.7	0.09	-0.5%
590.9		11.6%	2.5	0.5	0.7	0.09	-0.5%
591.5		11.4%	2.5	0.5	0.7	0.09	-0.5%
592.1		11.6%	2.5	0.5	0.7	0.09	-0.4%
592.7		11.7%	2.5	0.5	0.7	0.09	-0.4%
593.3		11.6%	2.4	0.5	0.7	0.09	-0.5%
594.0		12.1%	2.4	0.5	0.7	0.09	-0.4%
594.6		12.4%	2.4	0.5	0.7	0.09	-0.4%
595.2		12.4%	2.4	0.5	0.7	0.09	-0.5%
595.8		12.6%	2.4	0.5	0.7	0.09	-0.4%
596.4		12.6%	2.4	0.5	0.7	0.09	-0.5%
597.0		12.8%	2.4	0.5	0.7	0.09	-0.5%
597.7		11.0%	2.5	0.5	0.7	0.09	-0.5%
598.3		9.8%	2.4	0.5	0.7	0.09	-0.5%
598.9		9.6%	2.4	0.5	0.7	0.09	-0.5%
599.5		9.5%	2.5	0.5	0.7	0.09	-0.5%
600.1		10.1%	2.5	0.5	0.7	0.09	-0.5%
600.8		10.4%	2.5	0.5	0.7	0.09	-0.5%
601.4		10.2%	2.5	0.5	0.7	0.09	-0.5%
602.0		10.3%	2.4	0.5	0.7	0.09	-0.5%
602.6		10.2%	2.4	0.5	0.7	0.09	-0.5%
603.2		10.2%	2.5	0.5	0.7	0.09	-0.5%
603.8		10.2%	2.4	0.5	0.7	0.09	-0.5%
604.5		10.3%	2.4	0.5	0.7	0.09	-0.5%
605.1		10.4%	2.5	0.5	0.7	0.09	-0.5%
605.7		9.9%	2.5	0.5	0.7	0.09	-0.5%
606.3		10.2%	2.4	0.5	0.7	0.09	-0.5%
606.9		10.1%	2.5	0.5	0.7	0.09	-0.5%
607.6		10.2%	2.4	0.5	0.7	0.09	-0.5%
608.2		11.9%	2.4	0.5	0.7	0.09	0.0%
608.8		10.3%	2.4	0.5	0.7	0.09	-0.5%
609.4		10.2%	2.4	0.5	0.7	0.09	-0.5%
610.0		10.2%	2.4	0.5	0.7	0.09	-0.5%
610.6		10.3%	2.4	0.5	0.7	0.09	-0.5%
611.3		10.1%	2.4	0.5	0.7	0.09	-0.5%
611.9		10.2%	2.4	0.5	0.7	0.09	-0.5%

Time-on-stream (h)	T (°C)	X_{CO}	Molar Flow (mmol/min)				$C_{Balance}$
			H_2	CO	CO_2	Ar	
612.5	190	10.4%	2.4	0.5	0.7	0.09	-0.5%
613.1		10.2%	2.4	0.5	0.7	0.09	-0.5%
613.7		10.2%	2.4	0.5	0.7	0.09	-0.5%
614.3		10.1%	2.4	0.5	0.7	0.09	-0.5%
615.0		10.1%	2.4	0.5	0.7	0.09	-0.5%
615.6	210	19.3%	2.5	0.5	0.8	0.09	-0.5%
616.2		31.5%	2.5	0.4	0.9	0.09	-0.7%
616.8		27.7%	2.5	0.4	0.8	0.09	-0.8%
617.4		26.5%	2.5	0.4	0.8	0.09	-0.6%
618.1		25.9%	2.5	0.4	0.8	0.09	-0.7%
618.8		25.8%	2.5	0.4	0.8	0.09	-0.8%
619.5		26.7%	2.5	0.4	0.8	0.09	-0.5%
620.1		26.3%	2.5	0.4	0.8	0.09	-0.4%
620.7		25.2%	2.5	0.4	0.8	0.09	-0.6%
621.3		25.6%	2.5	0.4	0.8	0.09	-0.7%
621.9		25.3%	2.5	0.4	0.8	0.09	-0.6%
622.6		23.3%	2.5	0.4	0.8	0.09	-0.6%
623.2		25.7%	2.5	0.4	0.8	0.09	-0.6%
623.8		24.9%	2.5	0.4	0.8	0.09	-0.7%
624.4		25.1%	2.5	0.4	0.8	0.09	-0.6%
625.0		24.8%	2.5	0.4	0.8	0.09	-0.6%
625.6		24.9%	2.5	0.4	0.8	0.09	-0.6%
626.3		25.2%	2.5	0.4	0.8	0.09	-0.7%
626.9		25.4%	2.5	0.4	0.8	0.09	-0.7%
627.5		24.9%	2.5	0.4	0.8	0.09	-0.7%
628.1		24.9%	2.5	0.4	0.8	0.09	-0.7%
628.7		24.9%	2.5	0.4	0.8	0.09	-0.7%
629.4		26.3%	2.5	0.4	0.8	0.09	-0.3%
630.0		25.1%	2.5	0.4	0.8	0.09	-0.7%
630.6		24.6%	2.5	0.4	0.8	0.09	-0.7%
631.2		24.3%	2.5	0.4	0.8	0.09	-0.6%
631.8		24.5%	2.5	0.4	0.8	0.09	-0.6%
632.4		24.5%	2.5	0.4	0.8	0.09	-0.7%
633.1		24.2%	2.5	0.4	0.8	0.09	-0.7%
633.7		23.7%	2.5	0.4	0.8	0.09	-0.7%
634.3		31.4%	2.5	0.4	0.9	0.09	-0.5%
634.9		29.8%	2.5	0.4	0.9	0.09	-0.7%
635.5		23.4%	2.5	0.4	0.8	0.09	-0.7%
636.2		23.6%	2.5	0.4	0.8	0.09	-0.7%
636.8		23.8%	2.5	0.4	0.8	0.09	-0.7%
637.4		25.0%	2.5	0.4	0.8	0.09	-0.7%
638.0		25.3%	2.5	0.4	0.8	0.09	-0.7%
638.6		25.1%	2.5	0.4	0.8	0.09	-0.7%
639.2		25.9%	2.5	0.4	0.8	0.09	-0.4%

Time-on-stream (h)	T (°C)	X_{CO}	Molar Flow (mmol/min)				$C_{Balance}$
			H_2	CO	CO_2	Ar	
639.9	210	26.2%	2.5	0.4	0.8	0.09	-0.5%
644.7		25.3%	2.5	0.4	0.8	0.09	-0.7%
645.3	200	17.4%	2.5	0.5	0.8	0.09	-0.6%
645.9		17.7%	2.4	0.5	0.8	0.09	-0.3%
646.5		18.0%	2.4	0.5	0.8	0.09	-0.3%
647.1		16.3%	2.5	0.5	0.8	0.09	-0.6%
647.8		17.3%	2.4	0.5	0.8	0.09	-0.4%
648.4		17.0%	2.5	0.5	0.8	0.09	-0.5%
649.0		16.9%	2.5	0.5	0.8	0.09	-0.6%
649.6		18.5%	2.4	0.5	0.8	0.09	-0.1%
650.2		17.4%	2.4	0.5	0.8	0.09	-0.4%
650.8		17.0%	2.4	0.5	0.8	0.09	-0.4%
651.4		16.5%	2.5	0.5	0.8	0.09	-0.6%
652.1		16.2%	2.5	0.5	0.8	0.09	-0.6%
652.7		17.6%	2.4	0.5	0.8	0.09	-0.3%
653.3		16.7%	2.4	0.5	0.8	0.09	-0.4%
653.9		18.0%	2.4	0.5	0.8	0.09	-0.2%
654.5		17.7%	2.4	0.5	0.8	0.09	-0.2%
655.1		18.9%	2.4	0.5	0.8	0.09	0.0%
655.8		17.3%	2.5	0.5	0.8	0.09	-0.6%
656.4		19.3%	2.4	0.5	0.8	0.09	0.0%
657.0		17.7%	2.4	0.5	0.8	0.09	-0.4%
657.6		17.8%	2.4	0.5	0.8	0.09	-0.3%
658.2		17.3%	2.5	0.5	0.8	0.09	-0.5%
658.8		16.5%	2.5	0.5	0.8	0.09	-0.7%
659.4		17.9%	2.4	0.5	0.8	0.09	-0.3%
660.1		17.5%	2.4	0.5	0.8	0.09	-0.4%
660.7		17.2%	2.4	0.5	0.8	0.09	-0.5%
661.3		17.7%	2.4	0.5	0.8	0.09	-0.2%
661.9		16.9%	2.5	0.5	0.8	0.09	-0.5%
662.5		17.8%	2.4	0.5	0.8	0.09	-0.3%
663.1		17.9%	2.4	0.5	0.8	0.09	-0.3%
663.7		16.2%	2.5	0.5	0.8	0.09	-0.6%
664.4		17.4%	2.4	0.5	0.8	0.09	-0.4%
665.0		16.4%	2.5	0.5	0.8	0.09	-0.6%
665.6		17.1%	2.4	0.5	0.8	0.09	-0.4%
666.2		20.4%	2.4	0.5	0.8	0.09	-0.3%
669.6		15.5%	2.4	0.5	0.7	0.09	-0.3%
670.2		15.7%	2.4	0.5	0.7	0.09	-0.3%

Experiment 3-8 – $Cu/ZnO/Al_2O_3$, Feed 2

Space Velocity – 5,000 h^{-1}

Time-on-stream (h)	T (°C)	X_{CO}	Molar Flow (mmol/min)				$C_{Balance}$
			H_2	CO	CO_2	Ar	
359.1	200	93.6%	1.3	0.0	0.6	0.10	-0.5%
359.8		91.0%	1.3	0.0	0.6	0.10	-0.5%
360.4		88.1%	1.3	0.1	0.6	0.10	-0.4%
361.0		89.4%	1.3	0.0	0.6	0.10	-0.4%
361.6		92.1%	1.3	0.0	0.6	0.10	-0.4%
362.2		91.0%	1.3	0.0	0.6	0.10	-0.4%
362.8		90.2%	1.3	0.0	0.6	0.10	-0.4%
363.4		91.3%	1.3	0.0	0.6	0.10	-0.4%
364.1		90.9%	1.3	0.0	0.6	0.10	-0.4%
364.7		90.9%	1.3	0.0	0.6	0.10	-0.4%
365.3		90.9%	1.3	0.0	0.6	0.10	-0.4%
365.9		91.9%	1.3	0.0	0.6	0.10	-0.4%
366.5		91.6%	1.3	0.0	0.6	0.10	-0.5%
367.1		91.4%	1.3	0.0	0.6	0.10	-0.5%
367.7		90.5%	1.3	0.0	0.6	0.10	-0.4%
368.4		90.6%	1.3	0.0	0.6	0.10	-0.5%
369.0		90.2%	1.3	0.0	0.6	0.10	-0.5%
369.6		90.1%	1.3	0.0	0.6	0.10	-0.5%
370.2		90.3%	1.3	0.0	0.6	0.10	-0.5%
370.8		90.7%	1.3	0.0	0.6	0.10	-0.5%
371.4		90.5%	1.3	0.0	0.6	0.10	-0.5%
372.1		90.9%	1.3	0.0	0.6	0.10	-0.5%
372.7		90.4%	1.3	0.0	0.6	0.10	-0.5%
373.3		90.4%	1.3	0.0	0.6	0.10	-0.5%
373.9		91.0%	1.3	0.0	0.6	0.10	-0.5%
374.5		91.1%	1.3	0.0	0.6	0.10	-0.5%
375.1		91.1%	1.3	0.0	0.6	0.10	-0.4%
375.8		91.3%	1.3	0.0	0.6	0.10	-0.5%
376.4		91.3%	1.3	0.0	0.6	0.10	-0.2%
377.0		88.4%	1.3	0.1	0.6	0.10	-0.5%
377.6		89.5%	1.3	0.0	0.6	0.10	-0.4%
378.2		89.1%	1.3	0.0	0.6	0.10	-0.4%
378.8		89.2%	1.3	0.0	0.6	0.10	-0.1%
379.4		89.3%	1.3	0.0	0.6	0.10	-0.5%
380.1		89.7%	1.3	0.0	0.6	0.10	-0.8%
380.7		90.7%	1.3	0.0	0.6	0.10	-0.3%
381.3		90.2%	1.3	0.0	0.6	0.10	-0.5%
381.9		92.7%	1.3	0.0	0.6	0.10	-0.6%
382.5		90.3%	1.3	0.0	0.6	0.10	-0.2%

Time-on-stream (h)	T (°C)	X_{CO}	Molar Flow (mmol/min)				$C_{Balance}$
			H_2	CO	CO_2	Ar	
383.1		0.0%	1.3	0.1	0.6	0.10	-0.3%
383.8		0.0%	1.2	0.1	0.5	0.11	0.4%
384.4		0.0%	1.2	0.1	0.5	0.11	0.3%
385.0		0.0%	1.3	0.1	0.5	0.10	-0.2%
385.6		0.0%	1.2	0.1	0.5	0.11	0.4%
386.2		0.0%	1.3	0.1	0.5	0.11	0.4%
386.9		0.0%	1.2	0.2	0.4	0.11	0.6%
387.5		0.0%	1.2	0.2	0.4	0.11	0.6%
388.1		0.0%	1.2	0.1	0.5	0.11	0.4%
388.7		0.0%	1.3	0.1	0.6	0.10	0.3%
389.3		0.0%	1.3	0.1	0.6	0.11	0.3%
389.9		0.0%	1.2	0.1	0.5	0.11	0.5%
390.7		0.0%	1.2	0.1	0.5	0.11	0.6%
391.3		0.0%	1.2	0.1	0.5	0.11	0.4%
391.9	180	0.0%	1.3	0.1	0.5	0.11	0.4%
392.5		0.0%	1.2	0.1	0.5	0.11	0.5%
393.1		0.0%	1.2	0.1	0.5	0.11	0.5%
393.8		0.0%	1.2	0.2	0.4	0.11	0.7%
394.4		0.0%	1.3	0.1	0.6	0.11	0.3%
395.0		75.0%	1.2	0.1	0.5	0.11	0.5%
395.6		72.7%	1.2	0.1	0.5	0.11	0.5%
396.2		74.5%	1.2	0.1	0.5	0.11	0.5%
396.8		74.1%	1.2	0.1	0.5	0.11	0.5%
397.4		73.9%	1.2	0.1	0.5	0.11	0.5%
398.1		73.7%	1.2	0.1	0.5	0.11	0.4%
398.7		74.5%	1.2	0.1	0.5	0.11	0.4%
399.3		74.6%	1.2	0.1	0.5	0.11	0.4%
399.9		75.1%	1.2	0.1	0.5	0.11	0.5%
400.5		74.9%	1.2	0.1	0.5	0.11	0.4%
401.1		75.9%	1.2	0.1	0.5	0.11	0.5%
401.8		74.7%	1.2	0.1	0.5	0.11	0.5%
402.5		83.2%	1.2	0.1	0.6	0.11	0.4%
403.2		77.1%	1.2	0.1	0.5	0.11	0.4%
403.8		78.1%	1.2	0.1	0.5	0.11	0.4%
404.4		90.6%	1.3	0.0	0.6	0.10	0.2%
405.0	190	76.7%	1.2	0.1	0.5	0.11	0.4%
405.6		77.4%	1.2	0.1	0.5	0.11	0.4%
406.2		89.9%	1.3	0.0	0.6	0.10	0.2%
406.8		89.5%	1.3	0.0	0.6	0.10	0.2%
407.4		77.0%	1.2	0.1	0.5	0.11	0.4%
408.1		77.1%	1.2	0.1	0.5	0.11	0.3%

Time-on-stream (h)	T (°C)	X_{CO}	Molar Flow (mmol/min)				$C_{Balance}$
			H_2	CO	CO_2	Ar	
408.7	190	90.2%	1.3	0.0	0.6	0.10	0.3%
409.3		88.3%	1.3	0.1	0.6	0.10	0.2%
409.9		76.9%	1.2	0.1	0.5	0.11	0.4%
410.5		77.3%	1.2	0.1	0.5	0.11	0.4%
411.1		90.0%	1.3	0.0	0.6	0.10	0.2%
411.7		82.9%	1.3	0.1	0.6	0.11	0.2%
412.4		76.8%	1.3	0.1	0.5	0.11	0.3%
413.0		78.0%	1.3	0.1	0.5	0.11	0.3%
413.6		89.5%	1.3	0.0	0.6	0.10	0.0%
414.2		76.4%	1.3	0.1	0.5	0.11	0.3%
414.8		76.9%	1.3	0.1	0.5	0.11	0.3%
415.4		84.0%	1.3	0.1	0.6	0.11	0.2%
416.0		89.7%	1.3	0.0	0.6	0.10	0.2%
416.6		79.4%	1.3	0.1	0.5	0.11	0.2%
417.3		76.7%	1.3	0.1	0.5	0.11	0.3%
417.9		76.5%	1.2	0.1	0.5	0.11	0.4%
418.5		76.2%	1.3	0.1	0.5	0.11	0.2%
419.1		83.6%	1.3	0.1	0.6	0.10	0.2%
419.7		77.0%	1.3	0.1	0.5	0.11	0.3%
420.3		76.3%	1.3	0.1	0.5	0.11	0.3%
420.9		76.9%	1.3	0.1	0.5	0.11	0.3%
421.5		76.7%	1.3	0.1	0.5	0.11	0.2%
422.2		77.0%	1.3	0.1	0.5	0.11	0.3%
422.8		76.6%	1.3	0.1	0.5	0.11	0.3%
423.4		76.9%	1.3	0.1	0.5	0.11	0.3%
424.0		76.8%	1.3	0.1	0.5	0.11	0.3%
424.6		76.9%	1.3	0.1	0.5	0.11	0.3%
425.2		90.1%	1.3	0.0	0.6	0.10	0.1%
425.8		91.7%	1.3	0.0	0.6	0.10	0.1%
426.5		88.1%	1.3	0.1	0.6	0.10	0.1%
427.1		76.7%	1.3	0.1	0.5	0.11	0.3%
427.7		76.6%	1.3	0.1	0.5	0.11	0.3%
428.3	210	80.6%	1.3	0.1	0.5	0.11	0.3%
428.9		94.9%	1.3	0.0	0.6	0.10	0.0%
429.5		96.5%	1.3	0.0	0.6	0.10	-0.1%
430.1		93.7%	1.3	0.0	0.6	0.10	0.0%
430.7		94.3%	1.3	0.0	0.6	0.10	-0.1%
431.4		95.2%	1.3	0.0	0.6	0.10	-0.1%
432.0		95.4%	1.3	0.0	0.6	0.10	-0.1%
432.6		95.4%	1.3	0.0	0.6	0.10	-0.1%
433.2		95.5%	1.3	0.0	0.6	0.10	-0.1%
433.8		95.5%	1.3	0.0	0.6	0.10	-0.1%
434.4		95.6%	1.3	0.0	0.6	0.10	0.0%

Time-on-stream (h)	T (°C)	X_{CO}	Molar Flow (mmol/min)				$C_{Balance}$
			H_2	CO	CO_2	Ar	
435.1	210	95.6%	1.3	0.0	0.6	0.10	-0.1%
435.7		95.5%	1.3	0.0	0.6	0.10	0.0%
436.3		95.5%	1.3	0.0	0.6	0.10	-0.1%
436.9		95.5%	1.3	0.0	0.6	0.10	-0.1%
437.5		95.5%	1.3	0.0	0.6	0.10	0.0%
438.1		95.4%	1.3	0.0	0.6	0.10	-0.2%
438.8		95.4%	1.3	0.0	0.6	0.10	-0.1%
439.4		95.2%	1.3	0.0	0.6	0.10	-0.1%
440.0		95.3%	1.3	0.0	0.6	0.10	-0.1%
440.6		95.2%	1.3	0.0	0.6	0.10	-0.1%
441.2		95.3%	1.3	0.0	0.6	0.10	-0.1%
441.8		95.4%	1.3	0.0	0.6	0.10	-0.1%
442.4		95.1%	1.3	0.0	0.6	0.10	-0.1%
443.1		95.2%	1.3	0.0	0.6	0.10	0.0%
443.7		95.1%	1.3	0.0	0.6	0.10	0.0%
444.3		95.2%	1.3	0.0	0.6	0.10	-0.1%
444.9		95.0%	1.3	0.0	0.6	0.10	-0.1%
445.5		95.2%	1.3	0.0	0.6	0.10	-0.1%
446.1		95.2%	1.3	0.0	0.6	0.10	-0.1%
446.7		95.3%	1.3	0.0	0.6	0.10	-0.1%
447.4		95.4%	1.3	0.0	0.6	0.10	0.0%
448.0		95.2%	1.3	0.0	0.6	0.10	-0.1%
448.6		95.4%	1.3	0.0	0.6	0.10	-0.1%
449.2		94.2%	1.3	0.0	0.6	0.10	0.1%
449.8		95.2%	1.3	0.0	0.6	0.10	0.0%
450.4	200	93.2%	1.3	0.0	0.6	0.10	-0.1%
451.1		91.6%	1.3	0.0	0.6	0.10	0.1%
451.7		87.6%	1.3	0.1	0.6	0.10	0.1%
452.3		87.1%	1.3	0.1	0.6	0.10	0.2%
452.9		92.6%	1.3	0.0	0.6	0.10	0.0%
453.5		88.1%	1.3	0.1	0.6	0.10	0.1%
454.1		89.3%	1.3	0.0	0.6	0.10	0.0%
454.8		91.0%	1.3	0.0	0.6	0.10	0.0%
455.4		90.3%	1.3	0.0	0.6	0.10	0.0%
456.0		89.8%	1.3	0.0	0.6	0.10	0.0%
456.6		91.5%	1.3	0.0	0.6	0.10	-0.1%
457.2		91.2%	1.3	0.0	0.6	0.10	0.0%
457.8		91.6%	1.3	0.0	0.6	0.10	0.0%
458.5		92.2%	1.3	0.0	0.6	0.10	-0.8%
459.1		91.6%	1.3	0.0	0.6	0.10	-0.1%
459.7		92.0%	1.3	0.0	0.6	0.10	-0.1%
460.3		92.0%	1.3	0.0	0.6	0.10	-0.1%
460.9		92.1%	1.3	0.0	0.6	0.10	-0.1%

Time-on-stream (h)	T (°C)	X_{CO}	Molar Flow (mmol/min)				$C_{Balance}$
			H_2	CO	CO_2	Ar	
461.5	200	92.0%	1.3	0.0	0.6	0.10	-0.2%
462.1		91.2%	1.3	0.0	0.6	0.10	-0.2%
462.8		90.8%	1.3	0.0	0.6	0.10	-0.1%
463.4		91.0%	1.3	0.0	0.6	0.10	-0.2%
464.0		90.9%	1.3	0.0	0.6	0.10	-0.2%
464.6		90.9%	1.3	0.0	0.6	0.10	-0.2%
465.2		91.4%	1.3	0.0	0.6	0.10	-0.7%
465.8		91.2%	1.3	0.0	0.6	0.10	-0.2%
466.5		91.0%	1.3	0.0	0.6	0.10	-0.2%
467.1		90.8%	1.3	0.0	0.6	0.10	-0.2%
467.7		90.2%	1.3	0.0	0.6	0.10	-0.2%
468.3		90.7%	1.3	0.0	0.6	0.10	-0.4%

Space Velocity – 7,500 h^{-1}

Time-on-stream (h)	T (°C)	X_{CO}	Molar Flow (mmol/min)				$C_{Balance}$
			H_2	CO	CO_2	Ar	
93.3	200	85.1%	2.1	0.1	0.9	0.15	-1.5%
93.9		81.5%	2.0	0.1	0.9	0.15	-1.4%
94.5		81.6%	2.0	0.1	0.9	0.15	-1.4%
95.1		81.5%	2.1	0.1	0.9	0.15	-1.4%
95.8		81.3%	2.1	0.1	0.9	0.15	-1.4%
96.4		80.9%	2.1	0.1	0.9	0.15	-1.6%
97.0		81.2%	2.0	0.1	0.9	0.15	-1.4%
97.6		81.5%	2.1	0.1	0.9	0.15	-1.3%
98.2		81.5%	2.0	0.1	0.9	0.15	-1.4%
98.8		81.8%	2.1	0.1	0.9	0.15	-1.4%
99.4		81.7%	2.1	0.1	0.9	0.15	-1.6%
100.1		81.5%	2.1	0.1	0.9	0.15	-1.4%
100.7		83.4%	2.1	0.1	0.9	0.15	-1.4%
101.3		83.5%	2.1	0.1	0.9	0.15	-1.4%
101.9		81.8%	2.1	0.1	0.9	0.15	-1.4%
102.5		81.4%	2.1	0.1	0.9	0.15	-1.4%
103.1		80.6%	2.0	0.1	0.9	0.15	-1.4%
103.7		80.8%	2.1	0.1	0.9	0.15	-1.4%
104.4		81.4%	2.1	0.1	0.9	0.15	-1.4%
105.0		81.7%	2.1	0.1	0.9	0.15	-1.4%
105.6		81.6%	2.0	0.1	0.9	0.15	-1.4%
106.2		81.6%	2.1	0.1	0.9	0.15	-1.5%
106.8		81.5%	2.0	0.1	0.9	0.15	-1.4%
107.4		81.5%	2.1	0.1	0.9	0.14	-1.7%
108.1		81.8%	2.1	0.1	0.9	0.15	-1.4%
108.7		81.4%	2.0	0.1	0.9	0.15	-1.4%
109.3		81.2%	2.1	0.1	0.9	0.15	-1.4%
109.9		82.7%	2.1	0.1	0.9	0.15	-1.4%

Time-on-stream (h)	T (°C)	X_{CO}	Molar Flow (mmol/min)				$C_{Balance}$
			H_2	CO	CO_2	Ar	
110.5	200	83.1%	2.1	0.1	0.9	0.15	-1.5%
111.1		83.1%	2.1	0.1	0.9	0.15	-1.4%
111.7		82.9%	2.1	0.1	0.9	0.15	-1.5%
112.4		82.9%	2.1	0.1	0.9	0.15	-1.5%
113.0		83.5%	2.1	0.1	0.9	0.15	-1.4%

Space Velocity – 10,000 h^{-1}, Experiment 1

Time-on-stream (h)	T (°C)	X_{CO}	Molar Flow (mmol/min)				$C_{Balance}$
			H_2	CO	CO_2	Ar	
359.0	200	76.7%	2.5	0.2	1.1	0.21	0.1%
359.6		72.8%	2.6	0.2	1.0	0.21	-0.1%
360.2		71.2%	2.6	0.3	1.0	0.21	-0.4%
360.8		72.3%	2.6	0.2	1.0	0.21	-0.1%
361.4		71.8%	2.6	0.3	1.0	0.21	-0.1%
362.1		72.2%	2.6	0.3	1.0	0.21	-0.1%
362.7		71.5%	2.6	0.3	1.0	0.21	-0.1%
363.3		71.8%	2.6	0.3	1.0	0.21	-0.1%
363.9		72.0%	2.6	0.3	1.0	0.21	-0.1%
364.5		72.8%	2.6	0.2	1.0	0.21	-0.1%
365.1		73.7%	2.5	0.2	1.0	0.21	0.4%
365.8		72.7%	2.5	0.2	1.0	0.21	0.3%
366.4		73.9%	2.6	0.2	1.1	0.21	-0.2%
367.0		74.4%	2.6	0.2	1.1	0.21	-0.2%
367.6		73.9%	2.6	0.2	1.1	0.21	-0.1%
368.2		73.4%	2.6	0.2	1.1	0.21	-0.2%
368.8		73.6%	2.6	0.2	1.1	0.21	-0.2%
369.4		73.1%	2.6	0.2	1.1	0.21	-0.2%
370.1		72.4%	2.6	0.2	1.1	0.21	-0.2%
370.7		71.9%	2.6	0.3	1.0	0.21	-0.2%
371.3		72.4%	2.5	0.2	1.0	0.21	0.3%
371.9		73.0%	2.6	0.2	1.1	0.21	-0.3%
372.5		73.7%	2.5	0.2	1.0	0.21	0.2%
373.1		74.3%	2.5	0.2	1.0	0.21	0.2%
373.8		73.4%	2.5	0.2	1.0	0.21	0.2%
374.4		73.5%	2.6	0.2	1.1	0.21	-0.3%
375.0		74.1%	2.6	0.2	1.1	0.21	-0.3%
375.6		74.7%	2.5	0.2	1.0	0.21	0.3%
376.2		74.9%	2.6	0.2	1.1	0.21	-0.4%
376.8		72.4%	2.5	0.2	1.0	0.21	0.3%
377.4		70.7%	2.6	0.3	1.1	0.20	-0.5%
378.1		70.9%	2.6	0.3	1.0	0.21	-0.2%
378.7		71.2%	2.5	0.3	1.0	0.21	0.3%
379.3		71.9%	2.5	0.3	1.0	0.21	0.0%

Time-on-stream (h)	T (°C)	X_{CO}	Molar Flow (mmol/min)				$C_{Balance}$
			H_2	CO	CO_2	Ar	
379.9	200	72.6%	2.5	0.2	1.0	0.21	0.2%
380.5		74.6%	2.5	0.2	1.0	0.21	0.4%
381.1		72.8%	2.5	0.2	1.0	0.21	0.2%
381.8		77.1%	2.5	0.2	1.1	0.21	0.1%
382.4		75.1%	2.5	0.2	1.1	0.21	0.1%
383.0	180	53.0%	2.5	0.4	0.8	0.21	0.3%
383.6		52.3%	2.4	0.4	0.8	0.22	0.6%
384.2		51.5%	2.4	0.4	0.8	0.22	0.6%
384.8		51.9%	2.4	0.4	0.8	0.22	0.7%
385.5		56.1%	2.4	0.4	0.9	0.22	0.6%
386.1		55.8%	2.4	0.4	0.9	0.22	0.6%
386.7		55.4%	2.4	0.4	0.8	0.22	0.6%
387.3		55.7%	2.4	0.4	0.9	0.22	0.6%
387.9		54.9%	2.4	0.4	0.8	0.22	0.6%
388.5		54.5%	2.4	0.4	0.8	0.22	0.7%
389.2		54.5%	2.4	0.4	0.8	0.22	0.6%
389.8		54.0%	2.4	0.4	0.8	0.22	0.7%
390.5		54.2%	2.4	0.4	0.8	0.22	0.7%
391.1		53.6%	2.4	0.4	0.8	0.22	0.7%
391.8		53.8%	2.4	0.4	0.8	0.22	0.7%
392.4		54.8%	2.4	0.4	0.8	0.22	0.7%
393.0		54.2%	2.4	0.4	0.8	0.22	0.8%
393.6		53.6%	2.4	0.4	0.8	0.22	0.7%
394.2		54.6%	2.4	0.4	0.8	0.22	0.7%
394.8		54.2%	2.4	0.4	0.8	0.22	0.7%
395.5		54.2%	2.4	0.4	0.8	0.22	0.7%
396.1		54.3%	2.4	0.4	0.8	0.22	0.7%
396.7		54.3%	2.4	0.4	0.8	0.22	0.7%
397.3		53.9%	2.4	0.4	0.8	0.22	0.7%
397.9		54.1%	2.4	0.4	0.8	0.22	0.7%
398.5		54.5%	2.4	0.4	0.8	0.22	0.7%
399.1		54.6%	2.4	0.4	0.8	0.22	0.7%
399.8		54.9%	2.4	0.4	0.8	0.22	0.7%
400.4		54.6%	2.4	0.4	0.8	0.22	0.7%
401.0		55.2%	2.4	0.4	0.8	0.22	0.7%
401.6		55.1%	2.4	0.4	0.8	0.22	0.7%
402.2		54.6%	2.4	0.4	0.8	0.22	0.9%
402.4	190	60.7%	2.4	0.4	0.9	0.22	0.7%
403.0		61.6%	2.4	0.3	0.9	0.22	0.6%
403.6		63.5%	2.4	0.3	0.9	0.22	0.7%
404.2		62.3%	2.4	0.3	0.9	0.22	0.6%
404.8		60.3%	2.4	0.4	0.9	0.22	0.7%
405.5		60.8%	2.4	0.4	0.9	0.22	0.7%

Time-on-stream (h)	T (°C)	X_{CO}	Molar Flow (mmol/min)				$C_{Balance}$
			H_2	CO	CO_2	Ar	
406.1	190	62.0%	2.4	0.3	0.9	0.22	0.7%
406.7		63.2%	2.4	0.3	0.9	0.22	0.6%
407.3		64.0%	2.4	0.3	0.9	0.22	0.6%
407.9		63.5%	2.4	0.3	0.9	0.22	0.6%
408.5		64.2%	2.4	0.3	0.9	0.22	0.5%
409.1		64.2%	2.4	0.3	0.9	0.22	0.6%
409.7		64.3%	2.4	0.3	0.9	0.22	0.5%
410.4		64.4%	2.4	0.3	0.9	0.22	0.6%
411.0		64.0%	2.4	0.3	0.9	0.22	0.6%
411.6		64.5%	2.4	0.3	0.9	0.22	0.6%
412.2		64.0%	2.5	0.3	0.9	0.22	0.5%
412.8		64.3%	2.4	0.3	0.9	0.22	0.5%
413.4		64.1%	2.4	0.3	0.9	0.22	0.5%
414.0		63.8%	2.4	0.3	0.9	0.22	0.5%
414.7		63.8%	2.5	0.3	0.9	0.22	0.5%
415.3		64.0%	2.5	0.3	0.9	0.22	0.5%
415.9		64.0%	2.5	0.3	0.9	0.22	0.5%
416.5		63.9%	2.5	0.3	0.9	0.22	0.5%
417.1		64.5%	2.5	0.3	0.9	0.22	0.5%
417.7		64.4%	2.5	0.3	0.9	0.22	0.5%
418.3		64.8%	2.4	0.3	0.9	0.22	0.5%
418.9		64.6%	2.5	0.3	0.9	0.22	0.5%
419.6		64.4%	2.5	0.3	0.9	0.22	0.5%
420.2		64.3%	2.5	0.3	0.9	0.22	0.5%
420.8		64.1%	2.5	0.3	0.9	0.22	0.5%
421.4		64.1%	2.5	0.3	0.9	0.22	0.5%
422.0		64.1%	2.5	0.3	0.9	0.22	0.4%
422.6		64.1%	2.5	0.3	0.9	0.22	0.5%
423.2		64.1%	2.5	0.3	0.9	0.22	0.5%
423.8		64.0%	2.5	0.3	0.9	0.22	0.4%
424.5		64.2%	2.5	0.3	0.9	0.22	0.5%
425.1		63.8%	2.5	0.3	0.9	0.22	0.4%
425.7		64.7%	2.5	0.3	0.9	0.21	0.4%
426.3		64.2%	2.5	0.3	0.9	0.22	0.4%
426.9		63.3%	2.4	0.3	0.9	0.22	0.5%
427.5		62.6%	2.4	0.3	0.9	0.22	0.5%
428.1		62.7%	2.4	0.3	0.9	0.22	0.5%
428.8	210	78.4%	2.5	0.2	1.1	0.21	0.2%
429.4		84.1%	2.6	0.1	1.1	0.21	0.1%
430.0		80.2%	2.5	0.2	1.1	0.21	0.2%
430.6		81.3%	2.5	0.2	1.1	0.21	0.1%
431.2		82.3%	2.6	0.2	1.1	0.21	0.0%
431.8		83.5%	2.6	0.1	1.1	0.21	0.0%

Time-on-stream (h)	T (°C)	X_{CO}	Molar Flow (mmol/min)				$C_{Balance}$
			H_2	CO	CO_2	Ar	
432.4	210	83.0%	2.6	0.2	1.2	0.20	-0.7%
433.1		83.7%	2.6	0.1	1.1	0.21	0.0%
433.7		81.0%	2.5	0.2	1.1	0.21	0.1%
434.3		80.7%	2.5	0.2	1.1	0.21	0.2%
434.9		80.6%	2.6	0.2	1.1	0.21	0.0%
435.5		81.2%	2.6	0.2	1.1	0.21	0.0%
436.1		80.7%	2.5	0.2	1.1	0.21	0.2%
436.8		81.6%	2.6	0.2	1.1	0.21	0.1%
437.4		83.3%	2.6	0.2	1.1	0.21	0.0%
438.0		83.0%	2.6	0.2	1.1	0.21	0.0%
438.6		82.9%	2.6	0.2	1.1	0.21	0.0%
439.2		82.6%	2.6	0.2	1.1	0.21	0.0%
439.8		82.8%	2.6	0.2	1.1	0.21	0.0%
440.4		82.8%	2.6	0.2	1.1	0.21	0.0%
441.1		82.7%	2.6	0.2	1.1	0.21	0.1%
441.7		83.1%	2.6	0.2	1.1	0.21	0.0%
442.3		82.6%	2.6	0.2	1.1	0.21	0.1%
442.9		82.8%	2.6	0.2	1.1	0.21	0.1%
443.5		82.6%	2.5	0.2	1.1	0.21	0.1%
444.1		82.6%	2.5	0.2	1.1	0.21	0.1%
444.8		82.1%	2.5	0.2	1.1	0.21	0.2%
445.4		82.7%	2.6	0.2	1.1	0.21	0.1%
446.0		80.3%	2.5	0.2	1.1	0.21	0.2%
446.6		81.0%	2.5	0.2	1.1	0.21	0.1%
447.2		81.4%	2.5	0.2	1.1	0.21	0.2%
447.8		82.0%	2.5	0.2	1.1	0.21	0.1%
448.4		82.4%	2.5	0.2	1.1	0.21	0.1%
449.1		81.5%	2.5	0.2	1.1	0.21	0.1%
449.7		80.5%	2.5	0.2	1.1	0.21	0.1%
450.3		73.3%	2.5	0.2	1.1	0.21	-0.4%
450.9	200	68.2%	2.5	0.3	1.0	0.21	0.4%
451.5		72.9%	2.5	0.2	1.0	0.21	0.3%
452.1		75.8%	2.5	0.2	1.1	0.21	0.3%
452.8		77.4%	2.5	0.2	1.1	0.21	0.1%
453.4		70.9%	2.5	0.3	1.0	0.21	0.4%
454.0		69.3%	2.5	0.3	1.0	0.21	0.3%
454.6		77.4%	2.5	0.2	1.1	0.21	0.4%
455.2		74.1%	2.5	0.2	1.0	0.21	0.3%
455.8		73.6%	2.5	0.2	1.0	0.21	0.2%
456.5		73.3%	2.5	0.2	1.0	0.21	0.2%
457.1		73.8%	2.5	0.2	1.0	0.21	0.2%
457.7		73.8%	2.5	0.2	1.0	0.21	0.2%

Time-on-stream (h)	T (°C)	X_{CO}	Molar Flow (mmol/min)				$C_{Balance}$
			H_2	CO	CO_2	Ar	
458.3	200	75.5%	2.5	0.2	1.1	0.21	0.2%
458.9		74.0%	2.5	0.2	1.0	0.21	0.1%
459.5		73.9%	2.5	0.2	1.0	0.21	0.1%
460.1		73.3%	2.5	0.2	1.0	0.21	0.1%
460.8		72.8%	2.5	0.2	1.0	0.21	0.2%
461.4		72.8%	2.5	0.2	1.0	0.21	0.1%
462.0		72.3%	2.5	0.2	1.0	0.21	0.2%
462.6		71.9%	2.5	0.3	1.0	0.21	0.2%
463.2		72.3%	2.5	0.2	1.0	0.21	0.2%
463.8		72.8%	2.5	0.2	1.0	0.21	0.1%
464.5		73.3%	2.5	0.2	1.0	0.21	0.1%
465.1		73.4%	2.5	0.2	1.0	0.21	0.1%
465.7		73.7%	2.5	0.2	1.0	0.21	0.1%
466.3		73.7%	2.5	0.2	1.0	0.21	0.1%
466.9		74.1%	2.5	0.2	1.0	0.21	0.1%
467.5		73.5%	2.5	0.2	1.0	0.21	0.0%
468.2		73.6%	2.5	0.2	1.0	0.21	0.0%

Space Velocity – 10,000 h^{-1}, Experiment 2

Time-on-stream (h)	T (°C)	X_{CO}	Molar Flow (mmol/min)				$C_{Balance}$
			H_2	CO	CO_2	Ar	
0.7	200	71.5%	4.2	0.3	1.0	0.21	-0.8%
1.3		73.9%	4.2	0.2	1.1	0.21	-1.0%
2.0		73.1%	4.2	0.2	1.1	0.21	-1.1%
2.6		77.6%	4.2	0.2	1.1	0.21	-1.1%
3.2		78.1%	4.2	0.2	1.1	0.21	-1.2%
3.8		77.0%	4.3	0.2	1.1	0.20	-1.6%
4.4		78.4%	4.2	0.2	1.1	0.21	-1.1%
5.0		72.5%	4.2	0.2	1.1	0.21	-1.0%
5.6		75.1%	4.2	0.2	1.1	0.21	-1.0%
6.2		76.3%	4.2	0.2	1.1	0.21	-1.0%
6.8		77.1%	4.2	0.2	1.1	0.21	-1.2%
7.4		76.7%	4.2	0.2	1.1	0.21	-1.1%
8.0		76.3%	4.3	0.2	1.1	0.21	-1.1%
8.6		75.9%	4.3	0.2	1.1	0.21	-1.1%
9.2		78.6%	4.3	0.2	1.1	0.21	-1.1%
9.8		73.2%	4.2	0.2	1.1	0.21	-1.2%
10.4		73.5%	4.3	0.2	1.1	0.21	-1.1%
11.0		74.6%	4.3	0.2	1.1	0.21	-1.1%
11.7		77.3%	4.3	0.2	1.1	0.20	-1.2%
12.3		77.0%	4.3	0.2	1.1	0.21	-1.1%
12.9		77.0%	4.3	0.2	1.1	0.21	-1.1%
13.5		77.1%	4.3	0.2	1.1	0.21	-1.1%

Time-on-stream (h)	T (°C)	X_{CO}	Molar Flow (mmol/min)				$C_{Balance}$
			H_2	CO	CO_2	Ar	
14.1		74.0%	4.3	0.2	1.1	0.21	-1.0%
14.7		74.4%	4.3	0.2	1.1	0.21	-1.1%
15.3		75.2%	4.3	0.2	1.1	0.21	-1.1%
15.9		76.4%	4.3	0.2	1.1	0.20	-1.2%
16.6		76.4%	4.3	0.2	1.1	0.20	-1.3%
17.2		76.5%	4.3	0.2	1.1	0.20	-1.3%
17.8		76.6%	4.3	0.2	1.1	0.20	-1.3%
18.4		76.6%	4.3	0.2	1.1	0.21	-1.1%
19.0		74.1%	4.2	0.2	1.1	0.21	-1.0%
19.6		74.6%	4.3	0.2	1.1	0.21	-1.1%
20.2		75.2%	4.3	0.2	1.1	0.21	-1.1%
20.8		75.5%	4.3	0.2	1.1	0.21	-1.1%
21.5		76.0%	4.3	0.2	1.1	0.21	-1.1%
22.1		76.1%	4.3	0.2	1.1	0.21	-1.1%
22.7		76.0%	4.3	0.2	1.1	0.21	-1.1%
23.3		76.2%	4.3	0.2	1.1	0.21	-1.1%
23.9		76.3%	4.3	0.2	1.1	0.21	-1.1%
24.5		75.4%	4.3	0.2	1.1	0.21	-1.1%
25.1		75.2%	4.3	0.2	1.1	0.21	-1.1%
25.7		74.7%	4.2	0.2	1.1	0.21	-1.0%
26.4		74.2%	4.3	0.2	1.1	0.21	-1.2%
27.0	200	79.4%	4.3	0.2	1.1	0.20	-1.2%
27.6		72.8%	4.2	0.2	1.1	0.21	-1.1%
28.2		78.8%	4.3	0.2	1.1	0.21	-1.2%
28.8		74.5%	4.3	0.2	1.1	0.21	-1.2%
29.4		75.3%	4.2	0.2	1.1	0.21	-1.1%
30.0		75.2%	4.2	0.2	1.1	0.21	-1.1%
30.6		75.2%	4.2	0.2	1.1	0.21	-1.1%
31.3		74.8%	4.3	0.2	1.1	0.21	-1.1%
31.9		75.3%	4.3	0.2	1.1	0.21	-1.0%
32.5		75.2%	4.3	0.2	1.1	0.21	-1.1%
33.1		75.2%	4.3	0.2	1.1	0.21	-1.1%
33.7		75.3%	4.3	0.2	1.1	0.21	-1.1%
34.3		75.5%	4.3	0.2	1.1	0.21	-1.1%
34.9		73.6%	4.2	0.2	1.1	0.21	-1.0%
35.5		74.4%	4.3	0.2	1.1	0.21	-1.1%
36.1		75.0%	4.3	0.2	1.1	0.21	-1.1%
36.7		75.1%	4.2	0.2	1.1	0.21	-1.1%
37.4		75.8%	4.3	0.2	1.1	0.21	-1.1%
38.0		75.8%	4.3	0.2	1.1	0.21	-1.1%
38.6		76.4%	4.3	0.2	1.1	0.21	-1.1%
39.2		76.4%	4.3	0.2	1.1	0.21	-1.2%
39.8		73.3%	4.3	0.2	1.1	0.21	-1.1%
40.4		74.0%	4.3	0.2	1.1	0.21	-1.1%
41.0		74.6%	4.3	0.2	1.1	0.21	-1.1%

Time-on-stream (h)	T (°C)	X_{CO}	Molar Flow (mmol/min)				$C_{Balance}$
			H_2	CO	CO_2	Ar	
41.6	200	76.5%	4.3	0.2	1.1	0.21	-1.1%
42.2		76.6%	4.3	0.2	1.1	0.21	-1.1%
42.8		76.7%	4.3	0.2	1.1	0.21	-1.1%
43.5		76.0%	4.3	0.2	1.1	0.21	-1.1%
44.1		74.9%	4.3	0.2	1.1	0.21	-1.1%
44.7		74.8%	4.2	0.2	1.1	0.21	-1.1%
45.3		75.0%	4.3	0.2	1.1	0.21	-1.1%
45.9		75.2%	4.2	0.2	1.1	0.21	-1.0%
46.5		75.0%	4.2	0.2	1.1	0.21	-1.1%
47.1		75.1%	4.2	0.2	1.1	0.21	-1.0%
47.7		70.4%	4.2	0.3	1.0	0.21	-1.0%
48.3		86.2%	4.3	0.1	1.2	0.20	-1.2%
49.0		78.0%	0.1	0.2	1.1	0.21	-1.0%
49.6		75.4%	4.3	0.2	1.1	0.21	-1.1%
50.2		75.8%	4.2	0.2	1.1	0.21	-1.1%
50.8	250	92.9%	4.4	0.1	1.3	0.20	-1.4%
51.4		93.5%	4.4	0.1	1.3	0.20	-1.4%
52.0		93.7%	4.4	0.1	1.3	0.20	-1.4%
53.0		97.0%	4.4	0.0	1.3	0.20	-1.3%
53.6		93.7%	4.4	0.1	1.3	0.20	-1.3%
54.2		93.0%	4.4	0.1	1.3	0.20	-1.4%
54.8		93.2%	4.4	0.1	1.3	0.20	-1.4%
55.4		93.2%	4.4	0.1	1.3	0.20	-1.4%
56.0		93.1%	4.4	0.1	1.3	0.20	-1.4%
56.6		93.1%	4.4	0.1	1.3	0.20	-1.5%
57.3		93.4%	4.4	0.1	1.3	0.20	-1.4%
57.9		93.4%	4.4	0.1	1.3	0.20	-1.4%
58.5		93.2%	4.4	0.1	1.3	0.20	-1.4%
59.1		93.1%	4.4	0.1	1.3	0.20	-1.4%
59.7		93.2%	4.4	0.1	1.3	0.20	-1.4%
60.3		93.3%	4.4	0.1	1.3	0.20	-1.5%
60.9		93.2%	4.4	0.1	1.3	0.20	-1.4%
61.5		93.1%	4.4	0.1	1.3	0.20	-1.4%
62.1		93.2%	4.4	0.1	1.3	0.20	-1.4%
62.7		93.2%	4.4	0.1	1.3	0.20	-1.4%
63.4		93.2%	4.4	0.1	1.3	0.20	-1.4%
64.0		93.2%	4.4	0.1	1.3	0.20	-1.4%
64.6		93.2%	4.4	0.1	1.3	0.20	-1.5%
65.2		93.2%	4.4	0.1	1.3	0.20	-1.4%
65.8		93.3%	4.5	0.1	1.3	0.20	-1.9%
66.4		93.3%	4.4	0.1	1.3	0.20	-1.5%
67.0		93.4%	4.4	0.1	1.3	0.20	-1.5%
67.6		93.0%	4.4	0.1	1.3	0.20	-1.5%

Time-on-stream (h)	T (°C)	X_{CO}	Molar Flow (mmol/min)				$C_{Balance}$
			H_2	CO	CO_2	Ar	
68.3	250	93.3%	4.4	0.1	1.3	0.20	-1.5%
68.9		93.4%	4.4	0.1	1.3	0.20	-1.4%
69.5		93.4%	4.4	0.1	1.3	0.20	-1.5%
70.1		93.2%	4.5	0.1	1.3	0.19	-2.0%
70.7		93.1%	4.4	0.1	1.3	0.20	-1.3%
71.3		94.1%	4.4	0.1	1.3	0.20	-1.4%
71.9		93.5%	4.4	0.1	1.3	0.20	-1.4%
72.5		93.1%	4.4	0.1	1.3	0.20	-1.3%
73.1		93.0%	4.4	0.1	1.3	0.20	-1.4%
73.8		92.9%	4.4	0.1	1.3	0.20	-1.5%
74.4		92.8%	4.4	0.1	1.3	0.20	-1.4%
75.0		92.7%	4.3	0.1	1.3	0.20	-1.3%
75.6		92.2%	4.4	0.1	1.3	0.20	-1.4%
76.2		92.5%	4.4	0.1	1.3	0.20	-1.4%
76.8		94.0%	4.4	0.1	1.3	0.20	-1.4%
77.4	300	91.7%	4.4	0.1	1.3	0.20	-1.3%
78.0		91.0%	4.4	0.1	1.2	0.20	-1.4%
78.6		90.6%	4.4	0.1	1.2	0.20	-1.4%
79.3		89.8%	4.4	0.1	1.2	0.20	-1.3%
79.9		90.0%	4.4	0.1	1.2	0.20	-1.3%
80.5		90.1%	4.4	0.1	1.2	0.20	-1.3%
81.1		90.9%	4.4	0.1	1.2	0.20	-1.4%
81.7		90.7%	4.4	0.1	1.2	0.20	-1.3%
82.3		90.6%	4.4	0.1	1.2	0.20	-1.3%
82.9		90.8%	4.4	0.1	1.2	0.20	-1.3%
83.6		90.6%	4.4	0.1	1.2	0.20	-1.3%
84.2		90.5%	4.4	0.1	1.2	0.20	-1.3%
84.8		90.4%	4.4	0.1	1.2	0.20	-1.3%
85.4		90.3%	4.4	0.1	1.2	0.20	-1.3%
86.0		90.5%	4.4	0.1	1.2	0.20	-1.3%
86.6		90.5%	4.4	0.1	1.2	0.20	-1.4%
87.2		90.5%	4.4	0.1	1.2	0.20	-1.3%
87.9		90.5%	4.4	0.1	1.2	0.20	-1.4%
88.5		90.5%	4.4	0.1	1.2	0.20	-1.4%
89.1		90.4%	4.4	0.1	1.2	0.20	-1.4%
89.7		90.6%	4.5	0.1	1.3	0.20	-1.8%
90.3		90.5%	4.4	0.1	1.2	0.20	-1.4%
90.9		90.4%	4.4	0.1	1.2	0.20	-1.4%
91.5		90.4%	4.4	0.1	1.3	0.20	-1.7%
92.2		90.5%	4.4	0.1	1.2	0.20	-1.4%
92.8		90.5%	4.4	0.1	1.2	0.20	-1.4%
93.4		90.6%	4.4	0.1	1.2	0.20	-1.4%
94.0		90.5%	4.4	0.1	1.2	0.20	-1.4%

Time-on-stream (h)	T (°C)	X_{CO}	Molar Flow (mmol/min)				$C_{Balance}$
			H_2	CO	CO_2	Ar	
94.6	300	90.7%	4.4	0.1	1.3	0.20	-1.4%
95.2		90.9%	4.4	0.1	1.3	0.20	-1.4%
96.2		91.9%	4.4	0.1	1.3	0.20	-1.4%
96.8		91.7%	4.4	0.1	1.3	0.20	-1.4%
97.4	350	87.0%	4.3	0.1	1.2	0.20	-1.3%
98.0		84.7%	4.3	0.1	1.2	0.20	-1.2%
98.6		84.6%	4.3	0.1	1.2	0.20	-1.4%
101.8		84.8%	4.3	0.1	1.2	0.20	-1.3%
102.4		84.1%	4.3	0.1	1.2	0.20	-1.2%
103.1		84.5%	4.3	0.1	1.2	0.20	-1.3%
103.7		84.5%	4.3	0.1	1.2	0.20	-1.4%
119.2		84.1%	4.3	0.1	1.2	0.20	-1.3%
119.8		83.9%	4.3	0.1	1.2	0.20	-1.2%

Space Velocity – 15,000 h^{-1}

Time-on-stream (h)	T (°C)	X_{CO}	Molar Flow (mmol/min)				$C_{Balance}$
			H_2	CO	CO_2	Ar	
93.1	200	69.4%	2.0	0.2	0.8	0.15	-1.4%
93.8		60.6%	2.0	0.3	0.7	0.15	-1.0%
94.4		59.4%	2.0	0.3	0.7	0.15	-1.0%
95.0		60.2%	2.0	0.3	0.7	0.15	-1.0%
95.6		60.3%	2.0	0.3	0.7	0.15	-1.0%
96.2		60.4%	2.0	0.3	0.7	0.15	-0.9%
96.8		60.3%	2.0	0.3	0.7	0.15	-1.0%
97.4		60.4%	2.0	0.3	0.7	0.15	-1.1%
98.1		60.5%	2.0	0.3	0.7	0.15	-1.0%
98.7		60.6%	2.0	0.3	0.7	0.15	-1.0%
99.3		60.5%	2.0	0.3	0.7	0.15	-1.0%
99.9		60.7%	2.0	0.3	0.7	0.15	-1.0%
100.5		60.3%	2.0	0.3	0.7	0.15	-1.2%
101.1		60.8%	2.0	0.3	0.7	0.15	-1.0%
101.7		60.8%	2.0	0.3	0.7	0.15	-1.0%
102.4		60.4%	2.0	0.3	0.7	0.15	-1.1%
103.0		60.4%	2.0	0.3	0.7	0.15	-1.1%
103.6		60.5%	2.0	0.3	0.7	0.15	-1.0%
104.2		60.7%	2.0	0.3	0.7	0.15	-1.0%
104.8		60.5%	2.0	0.3	0.7	0.15	-1.1%
105.4		60.6%	2.0	0.3	0.7	0.15	-1.0%
106.1		60.7%	2.0	0.3	0.7	0.15	-1.1%
106.7		60.3%	2.0	0.3	0.8	0.15	-1.3%
107.3		60.6%	2.0	0.3	0.7	0.15	-1.0%
107.9		60.7%	2.0	0.3	0.7	0.15	-1.0%
108.5		60.4%	2.0	0.3	0.7	0.15	-1.1%
109.1		60.7%	2.0	0.3	0.7	0.15	-1.0%

Time-on-stream (h)	T (°C)	X_{CO}	Molar Flow (mmol/min)				$C_{Balance}$
			H_2	CO	CO_2	Ar	
109.7	200	60.7%	2.0	0.3	0.7	0.15	-1.0%
110.4		62.8%	2.0	0.3	0.8	0.15	-1.1%
111.0		63.9%	2.0	0.2	0.8	0.15	-1.1%
111.6		63.5%	2.0	0.2	0.8	0.15	-1.1%
112.2		63.0%	2.0	0.3	0.8	0.15	-1.1%
112.8		62.8%	2.0	0.3	0.8	0.15	-1.2%
113.4		61.8%	2.0	0.3	0.8	0.15	-1.0%
114.1		63.0%	2.0	0.3	0.8	0.15	-1.2%

Time-on-stream (h)	T (°C)	X_{CO}	Molar Flow (mmol/min)				$C_{Balance}$
			H_2	CO	CO_2	Ar	
93.6	200	59.7%	2.0	0.3	0.7	0.15	-1.0%
94.2		59.2%	2.0	0.3	0.7	0.15	-1.0%
94.8		63.3%	2.0	0.2	0.8	0.15	-1.0%
95.4		59.5%	2.0	0.3	0.7	0.15	-0.9%
96.1		59.8%	2.0	0.3	0.7	0.15	-1.0%
96.7		60.7%	2.0	0.3	0.7	0.15	-1.0%
97.3		60.4%	2.0	0.3	0.8	0.15	-1.3%
97.9		59.9%	2.0	0.3	0.7	0.15	-1.0%
98.5		59.8%	2.0	0.3	0.7	0.15	-1.0%
99.1		59.6%	2.0	0.3	0.7	0.15	-1.0%
99.8		59.9%	2.0	0.3	0.7	0.15	-1.0%
100.4		62.7%	2.0	0.3	0.8	0.15	-1.0%
101.0		59.4%	2.0	0.3	0.7	0.15	-1.0%
101.6		60.1%	2.0	0.3	0.7	0.15	-1.0%
102.2		59.8%	2.0	0.3	0.7	0.15	-1.0%
102.8		59.3%	2.0	0.3	0.7	0.15	-1.0%
103.4		59.0%	2.0	0.3	0.7	0.15	-1.0%
104.1		61.3%	2.0	0.3	0.7	0.15	-1.0%
104.7		61.0%	2.0	0.3	0.7	0.15	-1.0%
105.3		60.6%	2.0	0.3	0.7	0.15	-1.0%
105.9		60.5%	2.0	0.3	0.7	0.15	-1.0%
106.5		60.1%	2.0	0.3	0.7	0.15	-1.0%
107.1		60.7%	2.0	0.3	0.7	0.15	-1.0%
107.7		60.5%	2.0	0.3	0.7	0.15	-1.0%
108.4		60.4%	2.0	0.3	0.7	0.15	-1.0%
109.0		57.8%	2.0	0.3	0.7	0.15	-1.1%
109.6		58.2%	2.0	0.3	0.7	0.15	-1.0%
110.2		59.2%	2.0	0.3	0.7	0.15	-1.0%
110.8		62.0%	2.0	0.3	0.8	0.15	-1.4%
111.4		61.0%	2.0	0.3	0.7	0.15	-1.1%
112.1		61.1%	2.0	0.3	0.7	0.15	-1.0%
112.7		61.4%	2.0	0.3	0.7	0.15	-1.1%

Space Velocity – 20,000 h^{-1}

Time-on-stream (h)	T (°C)	X_{CO}	Molar Flow (mmol/min)				$C_{Balance}$
			H_2	CO	CO_2	Ar	
359.4	200	52.4%	2.5	0.4	0.8	0.21	0.2%
360.1		53.7%	2.5	0.4	0.9	0.21	0.1%
360.7		54.2%	2.5	0.4	0.9	0.21	0.1%
361.3		52.5%	2.5	0.4	0.8	0.21	0.1%
361.9		51.9%	2.5	0.4	0.8	0.21	0.2%
362.5		51.2%	2.5	0.4	0.8	0.21	0.2%
363.1		51.3%	2.5	0.4	0.8	0.21	0.2%
363.8		51.1%	2.5	0.4	0.8	0.21	0.2%
364.4		51.0%	2.5	0.4	0.8	0.21	0.2%
365.0		53.0%	2.4	0.4	0.8	0.22	1.0%
365.6		66.5%	2.5	0.3	1.0	0.21	0.5%
366.2		52.8%	2.5	0.4	0.9	0.21	0.1%
366.8		50.9%	2.5	0.4	0.8	0.21	0.2%
367.4		51.7%	2.4	0.4	0.8	0.22	0.5%
368.1		51.3%	2.5	0.4	0.8	0.21	0.1%
368.7		52.1%	2.5	0.4	0.8	0.21	0.1%
369.3		53.1%	2.4	0.4	0.8	0.22	0.6%
369.9		52.5%	2.5	0.4	0.8	0.21	0.1%
370.5		53.5%	2.4	0.4	0.8	0.22	0.6%
371.1		53.8%	2.4	0.4	0.8	0.22	0.6%
371.7		59.1%	2.4	0.4	0.9	0.22	0.5%
372.4		51.8%	2.5	0.4	0.8	0.21	0.1%
373.0		52.8%	2.4	0.4	0.8	0.22	0.6%
373.6		53.0%	2.4	0.4	0.8	0.22	0.5%
374.2		52.7%	2.4	0.4	0.8	0.22	0.6%
374.8		53.5%	2.4	0.4	0.8	0.22	0.5%
375.4		53.3%	2.4	0.4	0.8	0.22	0.6%
376.1		52.2%	2.5	0.4	0.8	0.21	0.2%
376.7		53.1%	2.5	0.4	0.9	0.21	0.1%
377.3		52.1%	2.5	0.4	0.9	0.21	0.1%
377.9		52.7%	2.4	0.4	0.8	0.22	0.6%
378.5		52.8%	2.4	0.4	0.8	0.22	0.5%
379.1		52.1%	2.5	0.4	0.8	0.21	0.1%
379.8		53.5%	2.4	0.4	0.8	0.22	0.5%
380.4		50.8%	2.4	0.4	0.8	0.22	0.5%
381.0		51.9%	2.4	0.4	0.8	0.22	0.4%
381.6		52.8%	2.4	0.4	0.8	0.22	0.8%
382.2		58.5%	2.4	0.4	0.9	0.22	0.7%
382.8	180	42.4%	2.3	0.5	0.7	0.22	1.1%
383.5		41.4%	2.4	0.5	0.7	0.22	0.7%
384.1		32.2%	2.3	0.6	0.6	0.22	0.9%

Time-on-stream (h)	T (°C)	X_{CO}	Molar Flow (mmol/min)				$C_{Balance}$
			H_2	CO	CO_2	Ar	
384.7	180	31.8%	2.3	0.6	0.6	0.22	1.0%
385.3		32.9%	2.3	0.6	0.6	0.22	1.0%
385.9		31.6%	2.3	0.6	0.6	0.22	0.9%
386.5		40.3%	2.3	0.5	0.7	0.22	0.9%
387.2		32.6%	2.3	0.6	0.6	0.23	1.2%
387.8		31.8%	2.3	0.6	0.6	0.22	1.0%
388.4		36.5%	2.3	0.6	0.7	0.22	0.9%
389.0		31.9%	2.3	0.6	0.6	0.22	1.0%
389.6		34.2%	2.3	0.6	0.6	0.22	0.9%
390.4		34.1%	2.3	0.6	0.6	0.22	0.9%
391.0		31.8%	2.3	0.6	0.6	0.22	1.0%
391.6		35.4%	2.3	0.6	0.6	0.22	0.9%
392.2		31.5%	2.3	0.6	0.6	0.22	1.0%
392.8		31.9%	2.3	0.6	0.6	0.22	1.0%
393.5		34.1%	2.3	0.6	0.6	0.22	1.0%
394.1		34.1%	2.3	0.6	0.6	0.22	1.0%
394.7		34.1%	2.3	0.6	0.6	0.22	1.0%
395.3		34.1%	2.3	0.6	0.6	0.22	1.0%
395.9		33.6%	2.3	0.6	0.6	0.22	1.0%
396.5		33.8%	2.3	0.6	0.6	0.22	1.0%
397.1		33.4%	2.3	0.6	0.6	0.22	1.0%
397.8		33.3%	2.3	0.6	0.6	0.22	1.0%
398.4		33.3%	2.3	0.6	0.6	0.22	1.0%
399.0		34.8%	2.3	0.6	0.6	0.22	1.0%
399.6		35.2%	2.3	0.6	0.6	0.22	1.0%
400.2		31.8%	2.3	0.6	0.6	0.23	1.1%
400.8		33.7%	2.3	0.6	0.6	0.22	1.0%
401.4		33.6%	2.3	0.6	0.6	0.22	1.0%
402.1		35.1%	2.3	0.6	0.6	0.22	1.0%
404.7		41.5%	2.3	0.5	0.7	0.22	0.9%
405.3		41.7%	2.3	0.5	0.7	0.22	1.0%
405.9		41.6%	2.3	0.5	0.7	0.22	1.0%
406.5		42.7%	2.3	0.5	0.7	0.22	0.9%
407.1		42.6%	2.3	0.5	0.7	0.22	0.9%
407.8		42.7%	2.3	0.5	0.7	0.22	0.9%
408.4		42.6%	2.3	0.5	0.7	0.22	0.9%
409.0		41.3%	2.3	0.5	0.7	0.22	0.9%
409.6		41.5%	2.3	0.5	0.7	0.22	0.9%
410.2		46.3%	2.3	0.5	0.8	0.22	0.8%
410.8		40.6%	2.3	0.5	0.7	0.22	0.9%
411.4		41.0%	2.3	0.5	0.7	0.22	0.8%
412.0		59.1%	2.4	0.4	0.9	0.22	0.7%
412.7		41.9%	2.4	0.5	0.7	0.22	0.8%
413.3		42.3%	2.4	0.5	0.7	0.22	0.8%

Time-on-stream (h)	T (°C)	X_{CO}	Molar Flow (mmol/min)				$C_{Balance}$
			H_2	CO	CO_2	Ar	
413.9	180	42.3%	2.4	0.5	0.7	0.22	0.8%
414.5		42.5%	2.4	0.5	0.7	0.22	0.9%
415.1		40.9%	2.3	0.5	0.7	0.22	0.9%
415.7		41.1%	2.3	0.5	0.7	0.22	0.9%
416.3		55.5%	2.4	0.4	0.9	0.22	0.5%
417.0		43.4%	2.4	0.5	0.7	0.22	0.8%
417.6		41.9%	2.3	0.5	0.7	0.22	0.8%
418.2		42.1%	2.4	0.5	0.7	0.22	0.8%
418.8		40.4%	2.3	0.5	0.7	0.22	0.8%
419.4		53.5%	2.4	0.4	0.8	0.22	0.6%
420.0		42.2%	2.4	0.5	0.7	0.22	0.8%
420.6		39.0%	2.3	0.5	0.7	0.22	0.8%
421.2		42.2%	2.4	0.5	0.7	0.22	0.8%
421.9		40.6%	2.3	0.5	0.7	0.22	0.8%
422.5		41.3%	2.4	0.5	0.7	0.22	0.8%
423.1		46.0%	2.4	0.5	0.8	0.22	0.7%
423.7		41.7%	2.4	0.5	0.7	0.22	0.8%
424.3		42.2%	2.4	0.5	0.7	0.22	0.8%
424.9		44.3%	2.4	0.5	0.7	0.22	0.7%
425.5		48.6%	2.4	0.5	0.8	0.22	0.7%
426.1		41.2%	2.3	0.5	0.7	0.22	0.8%
426.8		42.4%	2.4	0.5	0.7	0.22	0.8%
427.4		42.4%	2.4	0.5	0.7	0.22	0.8%
428.0		42.6%	2.4	0.5	0.7	0.22	0.8%
428.6	210	56.4%	2.4	0.4	0.9	0.22	0.5%
429.2		61.4%	2.5	0.3	0.9	0.21	0.4%
429.8		62.7%	2.5	0.3	0.9	0.21	0.4%
430.4		62.8%	2.5	0.3	0.9	0.22	0.5%
431.1		58.5%	2.4	0.4	0.9	0.22	0.5%
431.7		64.6%	2.5	0.3	0.9	0.21	0.3%
432.3		64.6%	2.5	0.3	1.0	0.21	0.3%
432.9		63.4%	2.5	0.3	0.9	0.21	0.4%
433.5		59.1%	2.4	0.4	0.9	0.22	0.5%
434.1		62.9%	2.5	0.3	0.9	0.21	0.3%
434.8		62.7%	2.5	0.3	0.9	0.21	0.3%
435.4		62.6%	2.5	0.3	0.9	0.21	0.4%
436.0		63.0%	2.5	0.3	0.9	0.21	0.4%
436.6		62.8%	2.5	0.3	0.9	0.21	0.3%
437.2		63.1%	2.5	0.3	0.9	0.21	0.4%
437.8		62.7%	2.5	0.3	0.9	0.21	0.3%
438.4		62.6%	2.5	0.3	0.9	0.21	0.3%
439.1		62.5%	2.5	0.3	0.9	0.21	0.3%
439.7		62.5%	2.5	0.3	0.9	0.21	0.3%

Time-on-stream (h)	T (°C)	X_{CO}	Molar Flow (mmol/min)				$C_{Balance}$
			H_2	CO	CO_2	Ar	
440.3	210	62.5%	2.5	0.3	0.9	0.21	0.3%
440.9		62.7%	2.5	0.3	0.9	0.21	0.4%
441.5		62.7%	2.5	0.3	0.9	0.21	0.3%
442.1		62.5%	2.5	0.3	0.9	0.21	0.4%
442.7		62.5%	2.5	0.3	0.9	0.21	0.4%
443.4		62.4%	2.5	0.3	0.9	0.21	0.3%
444.0		62.9%	2.5	0.3	0.9	0.21	0.4%
444.6		62.3%	2.4	0.3	0.9	0.22	0.5%
445.2		62.6%	2.5	0.3	0.9	0.21	0.4%
445.8		62.5%	2.5	0.3	0.9	0.22	0.4%
446.4		59.7%	2.4	0.4	0.9	0.22	0.5%
447.1		62.6%	2.5	0.3	0.9	0.22	0.5%
447.7		63.0%	2.5	0.3	0.9	0.21	0.5%
448.3		63.9%	2.4	0.3	0.9	0.22	0.6%
448.9		61.8%	2.5	0.3	0.9	0.21	0.3%
449.5		61.6%	2.5	0.3	0.9	0.22	0.5%
450.1		62.6%	2.5	0.3	0.9	0.21	0.5%
450.8	200	52.5%	2.4	0.4	0.8	0.22	0.8%
451.4		51.8%	2.4	0.4	0.8	0.22	0.7%
452.0		51.1%	2.4	0.4	0.8	0.22	0.6%
452.6		54.6%	2.4	0.4	0.8	0.22	0.8%
453.2		50.5%	2.4	0.4	0.8	0.22	0.5%
453.8		51.0%	2.4	0.4	0.8	0.22	0.5%
454.5		52.1%	2.4	0.4	0.8	0.22	0.7%
455.1		52.7%	2.4	0.4	0.8	0.22	0.6%
455.7		47.9%	2.4	0.5	0.8	0.22	0.6%
456.3		52.1%	2.4	0.4	0.8	0.22	0.6%
456.9		52.9%	2.4	0.4	0.8	0.22	0.6%
457.5		52.0%	2.4	0.4	0.8	0.22	0.5%
458.1		51.7%	2.4	0.4	0.8	0.22	0.6%
458.8		71.3%	2.5	0.3	1.0	0.21	0.1%
459.4		51.3%	2.4	0.4	0.8	0.22	0.5%
460.0		51.5%	2.4	0.4	0.8	0.22	0.5%
460.6		51.6%	2.4	0.4	0.8	0.22	0.5%
461.2		51.8%	2.4	0.4	0.8	0.22	0.5%
461.8		52.4%	2.4	0.4	0.8	0.22	0.4%
462.5		54.0%	2.4	0.4	0.8	0.22	0.4%
463.1		53.4%	2.4	0.4	0.8	0.22	0.4%
463.7		51.6%	2.4	0.4	0.8	0.22	0.5%
464.3		51.5%	2.4	0.4	0.8	0.22	0.4%
464.9		53.6%	2.4	0.4	0.8	0.21	0.3%
465.5		53.5%	2.4	0.4	0.8	0.22	0.4%
466.2		51.7%	2.4	0.4	0.8	0.22	0.4%

Time-on-stream (h)	T (°C)	X_{CO}	Molar Flow (mmol/min)				$C_{Balance}$
			H_2	CO	CO_2	Ar	
466.8	200	51.5%	2.4	0.4	0.8	0.22	0.4%
467.4		53.7%	2.4	0.4	0.8	0.21	0.3%
468.0		53.6%	2.4	0.4	0.8	0.21	0.3%
468.6		54.0%	2.4	0.4	0.8	0.21	0.4%

Experiment 9-11 – $Cu/ZnO/Al_2O_3$, Feed 3

Space Velocity – 5,000 h^{-1}

Time-on-stream (h)	T (°C)	X_{CO}	Molar Flow (mmol/min)				$C_{Balance}$
			H_2	CO	CO_2	Ar	
236.3	200	91.0%	1.2	0.0	0.6	0.04	-0.9%
236.9		95.9%	1.3	0.0	0.6	0.03	-1.5%
237.5		96.1%	1.2	0.0	0.6	0.04	-0.9%
238.1		96.1%	1.2	0.0	0.6	0.04	-0.9%
238.7		96.7%	1.2	0.0	0.6	0.04	-0.9%
239.3		96.7%	1.2	0.0	0.6	0.04	-1.0%
240.0		97.1%	1.3	0.0	0.6	0.03	-1.6%
240.6		96.3%	1.2	0.0	0.6	0.04	-0.8%
241.2		96.0%	1.3	0.0	0.6	0.03	-1.5%
241.8		96.9%	1.2	0.0	0.6	0.04	-0.7%
242.4		97.0%	1.2	0.0	0.6	0.04	-0.9%
243.0		96.2%	1.2	0.0	0.6	0.04	-0.9%
243.7		96.7%	1.2	0.0	0.6	0.04	-0.9%
244.3		96.8%	1.2	0.0	0.6	0.04	-0.9%
244.9		96.1%	1.2	0.0	0.6	0.04	-0.8%
245.5		96.6%	1.2	0.0	0.6	0.04	-0.9%
246.1		96.6%	1.2	0.0	0.6	0.04	-0.8%
246.7		96.5%	1.2	0.0	0.6	0.04	-0.9%
247.3		96.5%	1.2	0.0	0.6	0.04	-0.9%
248.0		97.1%	1.2	0.0	0.6	0.04	-0.9%
248.6		97.2%	1.2	0.0	0.6	0.04	-0.9%
249.2		96.1%	1.2	0.0	0.6	0.04	-0.9%
249.8		96.6%	1.2	0.0	0.6	0.04	-0.9%
250.4		96.5%	1.2	0.0	0.6	0.04	-0.8%
251.0		96.4%	1.2	0.0	0.6	0.04	-1.0%
251.7		96.4%	1.2	0.0	0.6	0.04	-0.9%
252.3		96.5%	1.2	0.0	0.6	0.04	-0.9%
252.9		96.9%	1.4	0.0	0.7	0.03	-3.2%
253.5		96.6%	1.2	0.0	0.6	0.04	-0.8%
254.1		95.9%	1.2	0.0	0.6	0.04	-0.9%
254.7		96.9%	1.4	0.0	0.7	0.03	-3.2%
255.3		95.5%	1.4	0.0	0.7	0.03	-3.2%

Time-on-stream (h)	T (°C)	X_{CO}	Molar Flow (mmol/min)				$C_{Balance}$
			H_2	CO	CO_2	Ar	
256.0	200	96.4%	1.4	0.0	0.7	0.03	-3.2%
256.6		96.5%	1.4	0.0	0.7	0.03	-3.2%
257.2		96.5%	1.4	0.0	0.7	0.03	-3.2%
257.8		95.9%	1.3	0.0	0.6	0.03	-1.6%
258.6	180	94.8%	1.4	0.0	0.7	0.03	-2.9%
259.2		85.0%	1.4	0.0	0.6	0.03	-2.8%
259.8		80.5%	1.3	0.0	0.6	0.03	-2.8%
260.4		83.8%	1.4	0.0	0.6	0.03	-2.9%
261.0		82.9%	1.4	0.0	0.6	0.03	-2.9%
261.6		82.9%	1.3	0.0	0.6	0.03	-2.9%
262.3		82.2%	1.3	0.0	0.7	0.03	-3.1%
262.9		82.8%	1.3	0.0	0.7	0.03	-3.1%
263.5		86.0%	1.3	0.0	0.7	0.03	-3.2%
264.1		84.9%	1.4	0.0	0.7	0.03	-3.2%
264.7		75.5%	1.3	0.0	0.6	0.03	-3.1%
265.3		84.3%	1.3	0.0	0.7	0.03	-3.2%
265.9		85.4%	1.4	0.0	0.7	0.03	-3.2%
266.6		84.5%	1.4	0.0	0.7	0.03	-3.2%
267.2		75.5%	1.3	0.0	0.6	0.03	-3.1%
267.8		85.7%	1.4	0.0	0.7	0.03	-3.2%
268.4		84.5%	1.4	0.0	0.7	0.03	-3.2%
269.0		83.9%	1.4	0.0	0.7	0.03	-3.2%
269.6		84.8%	1.4	0.0	0.7	0.03	-3.3%
270.3		84.3%	1.4	0.0	0.7	0.03	-3.3%
273.2		92.3%	1.4	0.0	0.7	0.03	-3.3%
273.8		92.6%	1.4	0.0	0.7	0.03	-3.4%
274.4		81.7%	1.4	0.0	0.7	0.03	-3.3%
275.0		90.4%	1.4	0.0	0.7	0.03	-3.4%
275.6		92.3%	1.4	0.0	0.7	0.03	-3.3%
276.2		90.8%	1.4	0.0	0.7	0.03	-3.4%
276.9		92.3%	1.4	0.0	0.7	0.03	-3.4%
277.5		92.3%	1.4	0.0	0.7	0.03	-3.4%
278.1		90.1%	1.4	0.0	0.7	0.03	-3.3%
278.7		91.1%	1.4	0.0	0.7	0.03	-3.4%
279.3		92.4%	1.4	0.0	0.7	0.03	-3.4%
279.9		92.6%	1.4	0.0	0.7	0.03	-3.4%
280.5		91.0%	1.4	0.0	0.7	0.03	-3.5%
281.1		91.3%	1.4	0.0	0.7	0.03	-3.4%
281.7		90.8%	1.4	0.0	0.7	0.03	-3.6%
282.4		91.3%	1.4	0.0	0.7	0.03	-3.6%
283.0		91.1%	1.4	0.0	0.7	0.03	-3.6%
283.6		91.4%	1.4	0.0	0.7	0.03	-3.7%
284.2		91.3%	1.4	0.0	0.7	0.03	-3.9%

Time-on-stream (h)	T (°C)	X_{CO}	Molar Flow (mmol/min)				$C_{Balance}$
			H_2	CO	CO_2	Ar	
284.8	180	79.6%	1.4	0.0	0.7	0.03	-3.7%
285.4		98.0%	1.4	0.0	0.7	0.03	-3.7%
286.0		97.7%	1.4	0.0	0.7	0.03	-3.9%
286.7		96.4%	1.4	0.0	0.7	0.03	-4.0%
287.3		97.4%	1.4	0.0	0.7	0.03	-3.9%
287.9		97.3%	1.4	0.0	0.7	0.03	-4.0%
288.5		97.4%	1.4	0.0	0.7	0.03	-4.1%
289.1		97.1%	1.4	0.0	0.7	0.03	-4.1%
289.7		97.1%	1.4	0.0	0.7	0.03	-4.1%
290.3		97.2%	1.4	0.0	0.7	0.03	-4.1%
290.9		97.2%	1.4	0.0	0.7	0.03	-4.1%
291.6		97.7%	1.4	0.0	0.7	0.03	-4.1%
292.2		96.7%	1.4	0.0	0.7	0.03	-4.1%
292.8		96.2%	1.4	0.0	0.7	0.03	-3.8%
293.4		97.8%	1.4	0.0	0.7	0.03	-3.8%
294.0		98.0%	1.1	0.0	0.5	0.04	1.4%
294.6		98.0%	1.1	0.0	0.6	0.04	1.2%
295.2		97.9%	1.1	0.0	0.5	0.04	1.4%
295.9		97.8%	1.1	0.0	0.6	0.04	1.2%
296.5	210	97.9%	1.1	0.0	0.5	0.04	1.4%
297.1		97.8%	1.1	0.0	0.5	0.04	1.3%
297.7		97.8%	1.1	0.0	0.5	0.04	1.4%
298.3		97.7%	1.1	0.0	0.5	0.04	1.2%
298.9		98.2%	1.1	0.0	0.5	0.04	1.4%
299.5		97.8%	1.1	0.0	0.6	0.04	1.2%
300.1		97.8%	1.1	0.0	0.5	0.04	1.5%
300.8		98.2%	1.1	0.0	0.5	0.04	1.4%
301.4		98.0%	1.1	0.0	0.5	0.04	1.5%
302.0		97.9%	1.1	0.0	0.5	0.04	1.4%
302.6		97.9%	1.1	0.0	0.5	0.04	1.4%
303.2		97.8%	1.1	0.0	0.5	0.04	1.4%
303.8		97.9%	1.1	0.0	0.5	0.04	1.7%
304.4		96.9%	1.1	0.0	0.5	0.04	1.6%
305.1		97.9%	1.1	0.0	0.5	0.04	1.5%
305.7		96.5%	1.1	0.0	0.5	0.04	1.3%
306.3		96.5%	1.1	0.0	0.5	0.04	1.5%
306.9		97.4%	1.1	0.0	0.5	0.04	1.5%
307.5		96.5%	1.1	0.0	0.5	0.04	1.4%
308.1		97.2%	1.1	0.0	0.5	0.04	1.4%
308.7		95.1%	1.1	0.0	0.5	0.04	1.4%
309.3	200	96.4%	1.0	0.0	0.5	0.04	2.5%
310.0		96.5%	1.1	0.0	0.5	0.04	1.5%
310.6		96.2%	1.1	0.0	0.5	0.04	1.7%

Space Velocity – 10,000 h^{-1}

Time-on-stream (h)	T (°C)	X_{CO}	Molar Flow (mmol/min)				$C_{Balance}$
			H_2	CO	CO_2	Ar	
236.1		30.5%	2.3	0.2	1.0	0.07	-0.4%
236.7		79.6%	2.4	0.1	1.2	0.07	-0.8%
237.3		84.0%	2.4	0.0	1.2	0.07	-0.8%
238.0		83.6%	2.5	0.1	1.2	0.07	-1.5%
238.6		84.2%	2.4	0.0	1.2	0.07	-0.8%
239.2		84.6%	2.4	0.0	1.2	0.07	-0.7%
239.8		84.3%	2.4	0.0	1.2	0.07	-0.9%
240.4		83.9%	2.5	0.1	1.2	0.07	-1.5%
241.0		84.3%	2.4	0.0	1.2	0.07	-0.9%
241.6		84.4%	2.4	0.0	1.2	0.07	-0.6%
242.3		84.1%	2.4	0.0	1.2	0.07	-0.8%
242.9		83.8%	2.5	0.1	1.2	0.07	-1.4%
243.5		84.2%	2.4	0.0	1.2	0.07	-0.8%
244.1		87.0%	2.4	0.0	1.2	0.07	-0.9%
244.7		84.4%	2.4	0.0	1.2	0.07	-0.8%
245.3		84.0%	2.4	0.0	1.2	0.07	-0.8%
246.0		84.1%	2.4	0.0	1.2	0.07	-0.8%
246.6	200	82.5%	2.7	0.1	1.3	0.07	-2.9%
247.2		84.0%	2.4	0.0	1.2	0.07	-0.8%
247.8		83.1%	2.7	0.1	1.3	0.07	-2.9%
248.4		84.3%	2.4	0.0	1.2	0.07	-0.8%
249.0		84.2%	2.4	0.0	1.2	0.07	-0.8%
249.6		84.3%	2.4	0.0	1.2	0.07	-0.7%
250.3		82.7%	2.7	0.1	1.3	0.07	-3.0%
250.9		82.4%	2.7	0.1	1.3	0.07	-3.0%
251.5		82.8%	2.7	0.1	1.3	0.07	-3.0%
252.1		82.9%	2.7	0.1	1.3	0.07	-2.9%
252.7		82.5%	2.7	0.1	1.3	0.07	-2.9%
253.3		84.4%	2.4	0.0	1.2	0.07	-0.8%
254.0		84.2%	2.4	0.0	1.2	0.07	-0.8%
254.6		83.0%	2.7	0.1	1.3	0.07	-3.0%
255.2		82.9%	2.7	0.1	1.3	0.07	-3.0%
255.8		82.5%	2.7	0.1	1.3	0.07	-3.0%
256.4		82.9%	2.7	0.1	1.3	0.07	-3.0%
257.0		83.0%	2.7	0.1	1.3	0.07	-3.0%
257.6		83.0%	2.7	0.1	1.3	0.07	-3.0%
258.4		81.9%	2.7	0.1	1.3	0.06	-2.8%
259.0		54.5%	2.7	0.1	1.2	0.06	-2.6%
259.7	180	63.3%	2.6	0.1	1.2	0.06	-2.7%
260.3		57.8%	2.6	0.1	1.2	0.06	-2.7%
260.9		57.7%	2.6	0.1	1.2	0.06	-2.8%
261.5		56.2%	2.7	0.1	1.2	0.06	-2.8%

Time-on-stream (h)	T (°C)	X_{CO}	Molar Flow (mmol/min)				$C_{Balance}$
			H_2	CO	CO_2	Ar	
262.1	180	56.7%	2.7	0.1	1.2	0.06	-2.8%
262.7		57.1%	2.7	0.1	1.2	0.07	-2.9%
263.3		57.4%	2.6	0.1	1.2	0.07	-2.9%
263.9		57.4%	2.6	0.1	1.2	0.07	-2.9%
264.6		57.3%	2.6	0.1	1.2	0.07	-2.9%
265.2		57.5%	2.6	0.1	1.2	0.07	-2.9%
265.8		56.7%	2.7	0.1	1.2	0.07	-2.9%
266.4		56.6%	2.7	0.1	1.2	0.07	-3.0%
267.0		56.7%	2.6	0.1	1.2	0.07	-2.9%
267.6		56.8%	2.6	0.1	1.2	0.07	-2.8%
268.3		56.8%	2.6	0.1	1.2	0.07	-2.9%
268.9		57.3%	2.6	0.1	1.2	0.07	-2.9%
269.5		57.1%	2.6	0.1	1.2	0.07	-2.9%
270.1		56.7%	2.7	0.1	1.2	0.07	-3.0%
270.6	190	49.7%	2.7	0.2	1.2	0.07	-2.8%
271.2		64.2%	2.7	0.1	1.2	0.07	-3.1%
271.8		73.1%	2.7	0.1	1.3	0.07	-3.1%
272.4		73.5%	2.7	0.1	1.3	0.07	-3.1%
273.0		72.9%	2.7	0.1	1.3	0.07	-3.0%
273.6		71.8%	2.7	0.1	1.3	0.07	-2.8%
274.3		76.0%	2.3	0.1	1.1	0.08	0.8%
274.9		71.3%	2.7	0.1	1.3	0.07	-2.9%
275.5		70.8%	2.7	0.1	1.3	0.07	-2.9%
276.1		71.1%	2.7	0.1	1.3	0.07	-2.9%
276.7		70.5%	2.7	0.1	1.3	0.07	-3.1%
277.3		70.8%	2.7	0.1	1.3	0.07	-3.1%
277.9		70.6%	2.7	0.1	1.3	0.07	-3.2%
278.5		76.6%	2.2	0.1	1.0	0.08	1.3%
279.1		71.1%	2.7	0.1	1.3	0.07	-2.9%
279.8		76.4%	2.2	0.1	1.0	0.08	1.2%
280.4		76.3%	2.2	0.1	1.0	0.08	1.3%
281.0		76.2%	2.2	0.1	1.0	0.08	1.1%
281.6		77.4%	2.1	0.1	1.0	0.08	1.7%
282.2		70.1%	2.7	0.1	1.3	0.06	-3.5%
282.8		70.9%	2.7	0.1	1.3	0.06	-3.5%
283.4		70.8%	2.7	0.1	1.3	0.06	-3.5%
284.1		71.0%	2.7	0.1	1.3	0.06	-3.6%
284.7		70.9%	2.7	0.1	1.3	0.06	-3.5%
285.3	210	83.1%	2.8	0.1	1.3	0.06	-3.6%
285.9		90.8%	2.8	0.0	1.4	0.06	-3.7%
286.5		90.8%	2.8	0.0	1.4	0.06	-3.8%
287.1		89.5%	2.8	0.0	1.4	0.06	-3.8%
287.7		89.9%	2.8	0.0	1.4	0.06	-3.8%

Time-on-stream (h)	T (°C)	X_{CO}	Molar Flow (mmol/min)				$C_{Balance}$
			H_2	CO	CO_2	Ar	
288.3		89.7%	2.8	0.0	1.4	0.06	-3.8%
289.0		89.8%	2.8	0.0	1.4	0.06	-4.0%
289.6		90.3%	2.8	0.0	1.4	0.06	-3.7%
290.2		92.1%	2.2	0.0	1.1	0.08	1.3%
290.8		92.5%	2.2	0.0	1.1	0.08	1.2%
291.4		92.4%	2.2	0.0	1.1	0.08	1.2%
292.0		92.5%	2.2	0.0	1.1	0.08	1.5%
292.6		92.5%	2.2	0.0	1.1	0.08	1.4%
293.2		92.4%	2.2	0.0	1.1	0.08	1.2%
293.9		92.3%	2.2	0.0	1.1	0.08	1.0%
294.5		92.1%	2.2	0.0	1.1	0.08	1.3%
295.1		92.1%	2.2	0.0	1.1	0.08	1.2%
295.7		91.9%	2.2	0.0	1.1	0.08	1.2%
296.3		92.2%	2.2	0.0	1.1	0.08	1.2%
296.9		91.7%	2.2	0.0	1.1	0.08	1.2%
297.5	210	92.0%	2.2	0.0	1.1	0.08	1.2%
298.2		92.2%	2.2	0.0	1.1	0.08	1.2%
298.8		92.0%	2.2	0.0	1.1	0.08	1.3%
299.4		92.0%	2.2	0.0	1.1	0.08	1.2%
300.0		92.1%	2.2	0.0	1.1	0.08	1.1%
300.6		92.4%	2.2	0.0	1.1	0.08	1.2%
301.2		92.3%	2.2	0.0	1.1	0.08	1.2%
301.8		92.3%	2.2	0.0	1.1	0.08	1.3%
302.4		92.4%	2.2	0.0	1.1	0.08	1.2%
303.1		91.9%	2.2	0.0	1.1	0.08	1.3%
303.7		92.4%	2.1	0.0	1.0	0.09	2.6%
304.3		92.1%	2.2	0.0	1.1	0.08	1.3%
304.9		92.3%	2.2	0.0	1.1	0.08	1.1%
305.5		89.8%	2.8	0.0	1.4	0.06	-3.6%
306.1		89.4%	2.2	0.0	1.1	0.08	1.3%
306.7		91.6%	2.2	0.0	1.1	0.08	1.6%
307.4		92.2%	2.2	0.0	1.1	0.08	1.5%
308.0		92.3%	2.2	0.0	1.1	0.08	1.3%
308.6		92.2%	2.2	0.0	1.1	0.08	1.2%
309.2		82.5%	2.0	0.1	1.0	0.09	2.6%
309.8		85.9%	2.2	0.0	1.0	0.08	1.5%
310.4		85.9%	2.2	0.0	1.1	0.08	1.3%
311.0	200	85.8%	2.2	0.0	1.1	0.08	1.3%
311.7		85.7%	2.2	0.0	1.0	0.08	1.5%
312.3		87.5%	2.2	0.0	1.1	0.08	1.2%
312.9		86.4%	2.2	0.0	1.1	0.08	1.3%
313.5		84.4%	2.2	0.0	1.1	0.08	1.3%
314.1		84.1%	2.2	0.0	1.1	0.08	1.2%

Time-on-stream (h)	T (°C)	X_{CO}	Molar Flow (mmol/min)				$C_{Balance}$
			H_2	CO	CO_2	Ar	
314.7	200	85.3%	2.2	0.0	1.1	0.08	1.2%
315.3		85.7%	2.2	0.0	1.1	0.08	1.1%
316.0		85.3%	2.2	0.0	1.1	0.08	1.1%
316.6		86.6%	2.2	0.0	1.1	0.08	1.2%
317.2		86.5%	2.2	0.0	1.1	0.08	1.1%
317.8		86.3%	2.2	0.0	1.1	0.08	1.1%
318.4		84.5%	2.2	0.0	1.1	0.08	1.2%
319.0		85.0%	2.2	0.0	1.1	0.08	1.2%
319.7		84.8%	2.2	0.0	1.1	0.08	1.2%
320.3		84.9%	2.2	0.0	1.0	0.08	1.6%
320.9		84.4%	2.2	0.0	1.1	0.08	1.1%
321.5		84.9%	2.2	0.0	1.1	0.08	1.2%
322.1		85.1%	2.2	0.0	1.1	0.08	1.3%
322.7		85.6%	2.2	0.0	1.1	0.08	1.2%
323.3		85.2%	2.2	0.0	1.1	0.08	1.1%
324.0		85.9%	2.2	0.0	1.1	0.08	1.4%
324.6		86.0%	2.2	0.0	1.1	0.08	1.0%
325.2		86.1%	2.2	0.0	1.1	0.08	1.0%
325.8		85.8%	2.2	0.0	1.1	0.08	1.1%
326.4		84.9%	2.2	0.0	1.1	0.08	1.1%
327.0		84.3%	2.2	0.0	1.1	0.08	1.1%
327.6		84.9%	2.2	0.0	1.1	0.08	1.1%
328.2		84.9%	2.1	0.0	1.0	0.08	1.9%
328.9		84.9%	2.2	0.0	1.1	0.08	1.0%
329.5		86.4%	2.2	0.0	1.1	0.08	1.1%
330.1		85.7%	2.2	0.0	1.1	0.08	1.1%
330.7		85.5%	2.2	0.0	1.1	0.08	1.1%
331.3		86.9%	2.3	0.0	1.1	0.07	0.8%
331.9		85.9%	2.2	0.0	1.1	0.08	1.1%
332.5		78.5%	2.2	0.1	1.0	0.08	1.1%
333.1		81.3%	2.3	0.1	1.1	0.08	0.9%
333.8		87.2%	2.2	0.0	1.1	0.08	1.1%
334.4		87.8%	2.2	0.0	1.1	0.08	1.2%
335.0		87.8%	2.2	0.0	1.1	0.08	1.2%

Space Velocity – 20,000 h^{-1}

Time-on-stream (h)	T (°C)	X_{CO}	Molar Flow (mmol/min)				$C_{Balance}$
			H_2	CO	CO_2	Ar	
236.6	200	68.1%	2.4	0.1	1.1	0.07	-0.6%
237.2		63.2%	2.4	0.1	1.1	0.07	-0.6%
237.8		64.7%	2.4	0.1	1.1	0.07	-0.7%
238.4		63.8%	2.4	0.1	1.1	0.07	-0.7%
239.0		65.3%	2.4	0.1	1.1	0.07	-0.7%
239.6		64.4%	2.4	0.1	1.1	0.07	-0.6%

Time-on-stream (h)	T (°C)	X_{CO}	Molar Flow (mmol/min)				$C_{Balance}$
			H_2	CO	CO_2	Ar	
240.3	200	63.6%	2.4	0.1	1.1	0.07	-0.6%
240.9		63.2%	2.5	0.1	1.1	0.07	-1.3%
241.5		64.7%	2.4	0.1	1.1	0.07	-0.7%
242.1		61.6%	2.6	0.1	1.2	0.07	-2.7%
242.7		64.1%	2.5	0.1	1.1	0.07	-1.4%
243.3		64.9%	2.4	0.1	1.1	0.07	-0.7%
244.0		64.4%	2.4	0.1	1.1	0.07	-0.7%
244.6		64.5%	2.4	0.1	1.1	0.07	-0.6%
245.2		64.5%	2.4	0.1	1.1	0.07	-0.7%
245.8		63.6%	2.4	0.1	1.1	0.07	-0.7%
246.4		64.0%	2.4	0.1	1.1	0.07	-0.7%
247.0		61.3%	2.7	0.1	1.2	0.07	-2.8%
247.6		65.3%	2.4	0.1	1.1	0.07	-0.6%
248.3		65.4%	2.4	0.1	1.1	0.07	-0.7%
248.9		64.9%	2.4	0.1	1.1	0.07	-0.8%
249.5		61.3%	2.7	0.1	1.2	0.07	-2.9%
250.1		61.5%	2.6	0.1	1.2	0.07	-2.9%
250.7		60.7%	2.6	0.1	1.2	0.07	-2.8%
251.3		61.0%	2.7	0.1	1.2	0.07	-2.9%
252.0		64.3%	2.4	0.1	1.1	0.07	-0.7%
252.6		60.8%	2.7	0.1	1.2	0.07	-2.9%
253.2		61.4%	2.7	0.1	1.2	0.07	-2.7%
253.8		60.9%	2.7	0.1	1.2	0.07	-2.9%
254.4		60.8%	2.7	0.1	1.2	0.07	-2.8%
255.0		61.0%	2.6	0.1	1.2	0.07	-2.9%
255.6		60.8%	2.7	0.1	1.2	0.07	-2.9%
256.3		61.0%	2.6	0.1	1.2	0.07	-2.8%
256.9		62.2%	2.7	0.1	1.2	0.06	-2.8%
257.5		56.1%	2.6	0.1	1.2	0.06	-2.9%
258.3		67.5%	2.3	0.1	1.0	0.08	0.8%
258.9	180	48.6%	2.2	0.2	1.0	0.08	1.1%
259.5		40.2%	2.2	0.2	0.9	0.08	1.1%
260.1		38.7%	2.6	0.2	1.1	0.06	-2.5%
260.7		29.0%	2.6	0.2	1.1	0.06	-2.5%
261.3		30.4%	2.6	0.2	1.1	0.06	-2.6%
261.9		32.2%	2.6	0.2	1.1	0.06	-2.6%
262.6		31.6%	2.6	0.2	1.1	0.06	-2.7%
263.2		32.3%	2.6	0.2	1.1	0.07	-2.8%
263.8		32.4%	2.6	0.2	1.1	0.07	-2.7%
264.4		32.6%	2.6	0.2	1.1	0.07	-2.8%
265.0		30.4%	2.6	0.2	1.1	0.07	-2.7%
265.6		30.2%	2.6	0.2	1.1	0.07	-2.8%
266.3		32.4%	2.6	0.2	1.1	0.07	-2.8%

Time-on-stream (h)	T (°C)	X_{CO}	Molar Flow (mmol/min)				$C_{Balance}$
			H_2	CO	CO_2	Ar	
266.9	180	31.7%	2.6	0.2	1.1	0.07	-2.8%
267.5		31.6%	2.6	0.2	1.1	0.07	-2.7%
268.1		32.3%	2.6	0.2	1.1	0.07	-2.7%
268.7		31.6%	2.6	0.2	1.1	0.07	-2.7%
269.3		32.3%	2.6	0.2	1.1	0.07	-2.7%
269.9	190	31.9%	2.6	0.2	1.1	0.07	-2.7%
271.0		44.4%	2.6	0.2	1.2	0.07	-2.9%
271.7		47.8%	2.6	0.2	1.2	0.07	-2.9%
272.3		46.0%	2.7	0.2	1.2	0.07	-2.9%
272.9		46.8%	2.6	0.2	1.2	0.07	-2.8%
273.5		46.8%	2.6	0.2	1.2	0.07	-2.9%
274.1		47.3%	2.6	0.2	1.2	0.07	-2.7%
274.7		55.9%	2.2	0.1	1.0	0.08	1.1%
275.3		55.8%	2.2	0.1	1.0	0.08	1.2%
275.9		55.8%	2.2	0.1	1.0	0.08	1.1%
276.5		53.4%	2.3	0.1	1.0	0.08	0.1%
277.2		55.7%	2.2	0.1	1.0	0.08	1.2%
277.8		55.1%	2.2	0.1	1.0	0.08	0.9%
278.4		53.7%	2.3	0.1	1.0	0.08	0.3%
279.0		57.1%	2.1	0.1	0.9	0.08	1.9%
279.6		53.6%	2.2	0.1	1.0	0.08	1.2%
280.2		56.3%	2.2	0.1	1.0	0.08	1.3%
280.8		54.7%	2.2	0.1	1.0	0.08	1.0%
281.4		54.5%	2.2	0.1	1.0	0.08	1.2%
282.1		61.7%	1.9	0.1	0.9	0.09	3.6%
282.7		46.4%	2.7	0.2	1.2	0.06	-3.3%
283.3		44.2%	2.7	0.2	1.2	0.06	-3.4%
283.9		41.5%	2.7	0.2	1.2	0.06	-3.4%
284.5		50.9%	2.7	0.2	1.2	0.06	-3.4%
285.1	210	59.7%	2.7	0.1	1.2	0.06	-3.4%
285.7		74.8%	2.7	0.1	1.3	0.06	-3.6%
286.4		69.1%	2.7	0.1	1.3	0.06	-3.6%
287.0		73.7%	2.8	0.1	1.3	0.06	-3.7%
287.6		73.6%	2.8	0.1	1.3	0.06	-3.7%
288.2		76.7%	2.8	0.1	1.3	0.06	-3.8%
288.8		73.4%	2.8	0.1	1.3	0.06	-3.8%
289.4		78.7%	2.3	0.1	1.1	0.08	0.6%
290.0		78.9%	2.1	0.1	1.0	0.08	1.7%
290.6		79.1%	2.2	0.1	1.0	0.08	1.2%
291.3		79.3%	2.2	0.1	1.0	0.08	1.2%
291.9		79.5%	2.2	0.1	1.0	0.08	1.4%
292.5		79.4%	2.2	0.1	1.0	0.08	1.2%
293.1		79.1%	2.2	0.1	1.0	0.08	1.3%

Time-on-stream (h)	T (°C)	X_{CO}	Molar Flow (mmol/min)				$C_{Balance}$
			H_2	CO	CO_2	Ar	
293.7	210	79.1%	2.2	0.1	1.0	0.08	1.4%
294.3		79.0%	2.2	0.1	1.0	0.08	1.2%
294.9		78.3%	2.2	0.1	1.0	0.08	1.4%
295.5		78.1%	2.2	0.1	1.0	0.08	1.3%
296.2		78.8%	2.2	0.1	1.0	0.08	1.2%
296.8		78.8%	2.2	0.1	1.0	0.08	1.2%
297.4		78.6%	2.2	0.1	1.0	0.08	1.2%
298.0		77.7%	2.2	0.1	1.0	0.08	1.1%
298.6		78.0%	2.2	0.1	1.0	0.08	1.4%
299.2		82.0%	2.2	0.1	1.1	0.08	1.2%
299.8		76.3%	2.2	0.1	1.0	0.08	1.2%
300.5		77.3%	2.2	0.1	1.0	0.08	1.2%
301.1		80.3%	2.2	0.1	1.0	0.08	1.2%
301.7		79.8%	2.2	0.1	1.0	0.08	1.3%
302.3		77.2%	2.2	0.1	1.0	0.08	1.1%
302.9		77.7%	2.2	0.1	1.0	0.08	1.2%
303.5		81.6%	2.2	0.1	1.0	0.08	1.4%
304.1		77.9%	2.2	0.1	1.0	0.08	1.2%
304.8		77.8%	2.2	0.1	1.0	0.08	1.2%
305.4		77.8%	2.2	0.1	1.0	0.08	1.2%
306.0		77.9%	2.2	0.1	1.0	0.08	1.3%
306.6		78.5%	2.2	0.1	1.0	0.08	1.4%
307.2		76.6%	2.2	0.1	1.0	0.08	1.3%
307.8		78.0%	2.2	0.1	1.0	0.08	1.2%
308.4		79.0%	2.0	0.1	0.9	0.09	3.0%
309.0	200	71.5%	2.2	0.1	1.0	0.08	1.1%
309.7		66.9%	2.1	0.1	1.0	0.08	1.6%
310.3		67.1%	2.2	0.1	1.0	0.08	1.4%
310.9		67.4%	2.2	0.1	1.0	0.08	1.4%
311.5		67.2%	2.2	0.1	1.0	0.08	1.5%
312.1		65.3%	2.2	0.1	1.0	0.08	1.4%
312.7		65.6%	2.2	0.1	1.0	0.08	1.3%
313.3		65.3%	2.2	0.1	1.0	0.08	1.0%
314.0		83.6%	2.2	0.1	1.1	0.08	1.2%
314.6		66.0%	2.1	0.1	1.0	0.08	1.5%
315.2		65.2%	2.2	0.1	1.0	0.08	1.3%
315.8		65.6%	2.2	0.1	1.0	0.08	1.3%
316.4		66.8%	2.2	0.1	1.0	0.08	1.1%
317.0		65.3%	2.2	0.1	1.0	0.08	1.2%
317.7		66.3%	2.2	0.1	1.0	0.08	1.4%
318.3		66.1%	2.2	0.1	1.0	0.08	1.1%
318.9		67.2%	2.2	0.1	1.0	0.08	1.3%
319.5		70.7%	2.2	0.1	1.0	0.08	1.2%

Time-on-stream (h)	T (°C)	X_{CO}	Molar Flow (mmol/min)				$C_{Balance}$
			H_2	CO	CO_2	Ar	
320.1	200	65.2%	2.2	0.1	1.0	0.08	1.2%
320.7		66.6%	2.2	0.1	1.0	0.08	1.2%
321.3		66.4%	2.2	0.1	1.0	0.08	1.2%
322.0		67.2%	2.2	0.1	1.0	0.08	1.1%
322.6		66.5%	2.2	0.1	1.0	0.08	1.2%
323.2		66.4%	2.2	0.1	1.0	0.08	1.0%
323.8		66.9%	2.2	0.1	1.0	0.08	1.1%
324.4		67.6%	2.2	0.1	1.0	0.08	1.2%
325.0		67.0%	2.2	0.1	1.0	0.08	1.1%
325.6		64.7%	2.2	0.1	1.0	0.08	1.0%
326.3		68.5%	2.2	0.1	1.0	0.08	1.1%
326.9		66.6%	2.2	0.1	1.0	0.08	1.0%
327.5		66.1%	2.2	0.1	1.0	0.08	1.2%
328.1		67.1%	2.2	0.1	1.0	0.08	1.2%
328.7		68.7%	2.2	0.1	1.0	0.08	1.1%
329.3		66.8%	2.1	0.1	1.0	0.08	1.8%
329.9		66.8%	2.2	0.1	1.0	0.08	1.2%
330.5		67.8%	2.2	0.1	1.0	0.08	0.9%
331.2		70.0%	2.1	0.1	1.0	0.08	2.1%
331.8		67.3%	2.3	0.1	1.0	0.07	0.7%
332.4		16.9%	2.0	0.3	0.8	0.08	2.8%
333.0		66.6%	2.3	0.1	1.0	0.07	0.6%
333.6		68.0%	2.2	0.1	1.0	0.08	1.0%
334.2		68.9%	2.2	0.1	1.0	0.08	1.5%
334.8		69.9%	2.2	0.1	1.0	0.08	1.3%

Experiment 12-14 – Fe_3O_4/Cr_2O_3, Feed 2

Space Velocity – 5,000 h^{-1}

Time-on-stream (h)	T (°C)	X_{CO}	Molar Flow (mmol/min)				$C_{Balance}$
			H_2	CO	CO_2	Ar	
120.1	350	33.7%	1.3	0.3	0.4	0.10	-0.3%
120.7		33.6%	1.3	0.3	0.4	0.10	-0.3%
121.4		33.5%	1.3	0.3	0.4	0.10	-0.3%
122.0		33.3%	1.3	0.3	0.4	0.10	-0.4%
122.6		33.3%	1.3	0.3	0.4	0.10	-0.3%
123.2		33.4%	1.3	0.3	0.4	0.10	-0.3%
123.8		33.4%	1.3	0.3	0.4	0.10	-0.3%
124.4		33.5%	1.3	0.3	0.4	0.10	-0.3%
125.1		33.5%	1.3	0.3	0.4	0.10	-0.4%
125.7		33.3%	1.3	0.3	0.4	0.10	-0.4%
126.3		33.4%	1.3	0.3	0.4	0.10	-0.3%
126.9		33.5%	1.3	0.3	0.4	0.10	-0.4%
127.5		33.4%	1.3	0.3	0.4	0.10	-0.3%

Time-on-stream (h)	T (°C)	X_{CO}	Molar Flow (mmol/min)				$C_{Balance}$
			H_2	CO	CO_2	Ar	
128.1	350	33.4%	1.3	0.3	0.4	0.10	-0.3%
128.7		33.3%	1.3	0.3	0.4	0.10	-0.3%
129.4		33.3%	1.3	0.3	0.4	0.10	-0.3%
130.0		33.2%	1.3	0.3	0.4	0.10	-0.3%
130.6		33.2%	1.3	0.3	0.4	0.10	-0.3%
131.2		33.2%	1.3	0.3	0.4	0.10	-0.3%
131.8		33.0%	1.3	0.3	0.4	0.10	-0.3%
132.4		33.0%	1.3	0.3	0.4	0.10	-0.3%
133.1		33.0%	1.3	0.3	0.4	0.10	-0.4%
133.7		33.2%	1.3	0.3	0.4	0.10	-0.3%
134.3		33.3%	1.3	0.3	0.4	0.10	-0.3%
134.9		33.1%	1.3	0.3	0.4	0.10	-0.3%
135.5		33.2%	1.3	0.3	0.4	0.10	-0.3%
136.1		33.3%	1.3	0.3	0.4	0.10	-0.3%
136.8		33.2%	1.3	0.3	0.4	0.10	-0.3%
137.4		33.1%	1.3	0.3	0.4	0.10	-0.3%
138.0		33.1%	1.3	0.3	0.4	0.10	-0.3%
172.2	375	55.4%	1.3	0.3	0.3	0.10	-0.8%
172.8		55.8%	1.3	0.3	0.4	0.10	-0.4%
173.4		55.2%	1.3	0.2	0.4	0.10	-0.7%
174.0		55.2%	1.3	0.2	0.4	0.10	-0.7%
174.7		55.3%	1.3	0.2	0.4	0.10	-0.7%
175.3		55.1%	1.4	0.2	0.4	0.10	-0.7%
175.9		55.2%	1.3	0.2	0.4	0.10	-0.7%
176.5		54.8%	1.3	0.2	0.4	0.10	-0.7%
177.1		54.8%	1.4	0.2	0.4	0.10	-0.7%
177.7		54.9%	1.4	0.2	0.4	0.10	-0.7%
178.3		54.9%	1.3	0.2	0.4	0.10	-0.7%
178.9		54.9%	1.3	0.2	0.4	0.10	-0.7%
179.6		54.8%	1.3	0.2	0.4	0.10	-0.8%
180.2		54.8%	1.3	0.2	0.4	0.10	-0.7%
180.8		55.0%	1.3	0.2	0.4	0.10	-0.8%
181.4		54.7%	1.3	0.2	0.4	0.10	-0.8%
182.0		54.8%	1.3	0.2	0.4	0.10	-0.7%
182.6		55.0%	1.3	0.2	0.4	0.10	-0.7%
183.2		54.8%	1.3	0.2	0.4	0.10	-0.7%
183.9		55.3%	1.3	0.2	0.4	0.10	-0.5%
184.5		54.5%	1.3	0.2	0.4	0.10	-0.8%
185.1		54.3%	1.3	0.2	0.4	0.10	-0.7%
185.7		54.4%	1.3	0.2	0.4	0.10	-0.7%
186.3		54.4%	1.3	0.2	0.4	0.10	-0.8%
258.7	400	67.7%	1.3	0.2	0.4	0.10	-1.0%
259.3		69.3%	1.3	0.2	0.4	0.10	-1.0%

Time-on-stream (h)	T (°C)	X_{CO}	Molar Flow (mmol/min)				$C_{Balance}$
			H_2	CO	CO_2	Ar	
259.9	400	68.1%	1.3	0.2	0.4	0.10	-1.0%
260.6		68.0%	1.3	0.2	0.4	0.10	-1.0%
261.2		67.7%	1.3	0.2	0.4	0.10	-1.0%
261.8		67.7%	1.3	0.2	0.4	0.10	-1.0%
262.4		67.9%	1.3	0.2	0.4	0.10	-1.0%
263.0		68.0%	1.3	0.2	0.4	0.10	-1.0%
263.6		68.1%	1.3	0.2	0.4	0.10	-1.0%
264.3		67.7%	1.3	0.2	0.4	0.10	-1.0%
293.2	430	74.2%	1.3	0.2	0.4	0.10	-1.2%
293.8		74.8%	1.3	0.2	0.4	0.10	-1.1%
294.5		74.7%	1.4	0.2	0.5	0.10	-1.1%
295.1		74.7%	1.4	0.2	0.5	0.10	-1.2%
295.7		74.5%	1.4	0.2	0.5	0.10	-1.2%
296.3		74.9%	1.4	0.2	0.5	0.10	-1.2%
296.9		75.0%	1.4	0.2	0.5	0.10	-1.1%
297.5		75.3%	1.3	0.2	0.4	0.10	-1.1%
298.2		73.7%	1.4	0.2	0.5	0.10	-1.1%
298.8		73.5%	1.4	0.2	0.5	0.10	-1.2%
299.4		73.5%	1.3	0.2	0.5	0.10	-1.2%
300.0		73.5%	1.3	0.2	0.5	0.10	-1.2%
300.6		73.2%	1.3	0.2	0.5	0.10	-1.1%
301.2		73.9%	1.4	0.2	0.5	0.10	-1.1%
301.9		74.9%	1.3	0.2	0.5	0.10	-1.2%
302.5		74.5%	1.4	0.2	0.5	0.10	-1.1%
303.1		74.2%	1.3	0.2	0.5	0.10	-1.1%
303.7		75.8%	1.3	0.2	0.5	0.10	-1.1%
304.3		74.0%	1.3	0.2	0.5	0.10	-1.1%
304.9		73.9%	1.4	0.2	0.5	0.10	-1.1%
305.6		0.0%	1.4	0.2	0.5	0.10	-1.0%
306.2		74.0%	1.3	0.2	0.5	0.10	-1.1%
306.8	445	74.6%	1.4	0.2	0.5	0.10	-1.0%
307.4		72.4%	1.4	0.2	0.5	0.10	-1.0%
308.0		0.0%	1.4	0.2	0.5	0.10	-1.0%
308.6		73.5%	1.4	0.2	0.5	0.10	-1.0%
309.3		73.0%	1.4	0.2	0.5	0.10	-1.0%
309.9		0.0%	1.4	0.2	0.5	0.10	-1.1%
310.5		74.8%	1.4	0.2	0.5	0.10	-1.1%
311.1		0.0%	1.4	0.2	0.5	0.10	-1.0%
311.7		72.8%	1.4	0.2	0.5	0.10	-1.0%
312.4		74.1%	1.4	0.2	0.5	0.10	-1.1%
313.0		72.0%	1.4	0.2	0.5	0.10	-1.1%
313.6		73.3%	1.4	0.2	0.5	0.10	-1.1%
314.2		74.6%	1.4	0.2	0.5	0.10	-1.1%

Time-on-stream (h)	T (°C)	X_{CO}	Molar Flow (mmol/min)				$C_{Balance}$
			H_2	CO	CO_2	Ar	
314.8	445	73.0%	1.4	0.2	0.5	0.10	-1.0%
315.4		72.9%	1.4	0.2	0.5	0.10	-1.1%
316.1		71.3%	1.4	0.2	0.5	0.10	-1.1%
316.7		72.1%	1.4	0.2	0.5	0.10	-1.0%
317.3		0.0%	1.3	0.2	0.5	0.10	-1.1%
317.9		0.0%	1.4	0.2	0.5	0.10	-1.1%
318.5		73.2%	1.4	0.2	0.5	0.10	-1.1%
319.2		73.1%	1.4	0.2	0.5	0.10	-1.1%
319.8		73.9%	1.4	0.2	0.5	0.10	-1.1%
320.4		73.8%	1.3	0.2	0.4	0.10	-1.1%
321.0		74.1%	1.4	0.2	0.5	0.10	-1.1%
321.6		74.1%	0.4	0.1	0.1	0.24	-1.1%
322.3		74.2%	1.4	0.2	0.5	0.10	-1.1%
322.9		0.0%	1.4	0.1	0.5	0.10	-1.1%
323.5		0.0%	1.4	0.1	0.5	0.10	-1.1%
324.1		73.3%	1.4	0.1	0.5	0.10	-1.1%
324.7		73.2%	1.4	0.1	0.5	0.10	-1.1%
325.3		73.1%	1.4	0.1	0.5	0.10	-1.1%
326.0		73.3%	1.4	0.1	0.5	0.10	-1.1%
326.6		73.1%	1.4	0.1	0.5	0.10	-1.1%
327.2		73.9%	1.4	0.1	0.5	0.10	-1.1%
327.8		74.1%	1.4	0.1	0.5	0.10	-1.1%
328.4		74.0%	1.4	0.1	0.5	0.10	-1.1%
329.1		74.2%	1.4	0.1	0.5	0.10	-1.2%
329.7		0.0%	1.4	0.1	0.5	0.10	-1.0%
330.3		74.1%	1.4	0.1	0.5	0.10	-1.1%
393.0	350	54.1%	1.4	0.1	0.5	0.10	-0.7%
393.6		54.0%	1.4	0.1	0.5	0.10	-0.7%
394.2		54.3%	1.4	0.1	0.5	0.10	-0.8%
394.9		53.9%	1.4	0.1	0.5	0.10	-0.7%
395.5		53.9%	1.4	0.1	0.5	0.10	-0.8%
396.1		54.0%	1.4	0.1	0.5	0.10	-0.8%
396.7		54.1%	1.4	0.1	0.5	0.10	-0.7%
397.3		53.8%	1.4	0.1	0.5	0.10	-0.8%
397.9		53.8%	1.4	0.1	0.5	0.10	-0.8%
398.6		53.9%	1.4	0.1	0.5	0.10	-0.8%
399.2		53.6%	1.4	0.1	0.5	0.10	-0.8%
399.8		53.7%	1.4	0.1	0.5	0.10	-0.8%
400.4		53.8%	1.4	0.1	0.5	0.10	-0.8%
401.0		53.8%	1.4	0.1	0.5	0.10	-0.7%
401.6		53.6%	1.4	0.1	0.5	0.10	-0.7%

Space Velocity – 10,000 h^{-1}

Time-on-stream (h)	T (°C)	X_{CO}	Molar Flow (mmol/min)				$C_{Balance}$
			H_2	CO	CO_2	Ar	
58.0	350	21.1%	2.6	0.4	0.2	0.72	-0.1%
58.6		21.1%	2.6	0.4	0.2	0.72	-0.2%
59.2		21.1%	2.6	0.4	0.2	0.72	-0.1%
59.8		21.3%	2.6	0.4	0.2	0.72	-0.1%
60.4		21.2%	2.6	0.4	0.2	0.72	-0.1%
61.1		21.1%	2.6	0.4	0.2	0.72	-0.2%
61.7		21.1%	2.6	0.4	0.2	0.72	-0.2%
62.3		21.3%	2.6	0.4	0.2	0.72	-0.1%
62.9		21.1%	2.6	0.4	0.2	0.72	-0.2%
63.5		21.1%	2.6	0.4	0.2	0.72	-0.2%
64.1		21.1%	2.6	0.4	0.2	0.72	-0.2%
64.7		21.2%	2.6	0.4	0.2	0.72	-0.2%
65.3		21.1%	2.6	0.4	0.2	0.72	-0.1%
66.0		21.1%	2.6	0.4	0.2	0.72	-0.2%
66.6		21.1%	2.6	0.4	0.2	0.72	-0.2%
67.2		21.2%	2.6	0.4	0.2	0.72	-0.2%
67.8		21.0%	2.6	0.4	0.2	0.72	-0.2%
68.4		21.1%	2.6	0.4	0.2	0.72	-0.1%
69.0		21.1%	2.6	0.4	0.2	0.72	-0.2%
69.6		21.9%	2.5	0.4	0.2	0.71	0.1%
70.3		21.1%	2.6	0.4	0.2	0.72	-0.2%
70.9		21.1%	2.6	0.4	0.2	0.72	-0.2%
71.5		21.1%	2.6	0.4	0.2	0.72	-0.2%
72.1		21.2%	2.6	0.4	0.2	0.72	-0.2%
72.7		21.2%	2.6	0.4	0.2	0.72	-0.2%
73.3		21.2%	2.6	0.4	0.2	0.72	-0.1%
73.9		21.3%	2.5	0.4	0.2	0.72	-0.2%
74.6		21.3%	2.6	0.4	0.2	0.72	-0.2%
75.2		21.5%	2.6	0.4	0.2	0.72	-0.2%
75.8		21.3%	2.6	0.4	0.2	0.72	-0.2%
76.4		21.3%	2.5	0.4	0.2	0.72	-0.1%
77.0		21.3%	2.6	0.4	0.2	0.72	-0.2%
77.6		21.5%	2.6	0.4	0.2	0.72	-0.1%
78.2		22.1%	2.6	0.4	0.2	0.71	-0.1%
78.9		22.2%	2.6	0.4	0.2	0.71	-0.1%
79.5		22.3%	2.6	0.4	0.2	0.71	-0.1%
80.1		22.2%	2.6	0.4	0.2	0.71	-0.1%
80.7		22.2%	2.6	0.4	0.2	0.71	-0.1%
81.3		22.3%	2.6	0.4	0.2	0.71	-0.1%
81.9		22.3%	2.6	0.4	0.2	0.71	-0.1%
82.5		22.3%	2.6	0.4	0.2	0.71	-0.1%

Time-on-stream (h)	T (°C)	X_{CO}	Molar Flow (mmol/min)				$C_{Balance}$
			H_2	CO	CO_2	Ar	
83.2		22.3%	2.6	0.4	0.2	0.71	-0.1%
83.8		22.3%	2.6	0.4	0.2	0.71	-0.1%
84.4		22.4%	2.6	0.4	0.2	0.71	-0.1%
85.0		22.2%	2.6	0.4	0.2	0.71	-0.1%
85.6		22.2%	2.6	0.4	0.2	0.71	-0.1%
86.2		22.1%	2.6	0.4	0.2	0.71	-0.1%
86.8		22.1%	2.6	0.4	0.2	0.71	-0.1%
87.4		22.1%	2.6	0.4	0.2	0.71	-0.1%
88.1		22.2%	2.6	0.4	0.2	0.71	-0.1%
88.7		22.0%	2.6	0.4	0.2	0.71	-0.2%
89.3		22.1%	2.6	0.4	0.2	0.71	-0.2%
89.9		22.6%	2.5	0.4	0.2	0.71	0.2%
90.5		21.0%	2.6	0.4	0.2	0.72	-0.1%
91.1		20.9%	2.6	0.4	0.2	0.72	-0.2%
91.8		21.0%	2.6	0.4	0.2	0.72	-0.1%
92.4		20.8%	2.6	0.4	0.2	0.72	-0.2%
93.0		20.9%	2.6	0.4	0.2	0.72	-0.2%
93.6		20.9%	2.5	0.4	0.2	0.72	-0.2%
94.2		21.6%	2.5	0.4	0.2	0.72	0.0%
94.8		21.0%	2.6	0.4	0.2	0.72	-0.1%
95.5	350	20.9%	2.6	0.4	0.2	0.72	-0.2%
96.1		21.2%	2.5	0.4	0.2	0.72	-0.1%
96.7		21.1%	2.6	0.4	0.2	0.72	-0.2%
97.3		20.9%	2.6	0.4	0.2	0.72	-0.2%
97.9		21.4%	2.5	0.4	0.2	0.72	-0.1%
98.5		21.2%	2.6	0.4	0.2	0.72	-0.2%
99.2		21.4%	2.6	0.4	0.2	0.72	-0.2%
99.8		22.2%	2.5	0.4	0.2	0.71	0.1%
100.4		21.4%	2.6	0.4	0.2	0.72	-0.2%
101.0		21.4%	2.6	0.4	0.2	0.72	-0.2%
101.6		21.5%	2.6	0.4	0.2	0.72	-0.2%
102.2		21.4%	2.6	0.4	0.2	0.72	-0.1%
102.9		21.3%	2.6	0.4	0.2	0.72	-0.2%
103.5		21.3%	2.6	0.4	0.2	0.72	-0.1%
104.1		21.2%	2.6	0.4	0.2	0.72	-0.2%
104.7		21.2%	2.6	0.4	0.2	0.72	-0.2%
105.3		21.3%	2.6	0.4	0.2	0.72	-0.1%
105.9		21.2%	2.6	0.4	0.2	0.72	-0.2%
106.6		21.3%	2.6	0.4	0.2	0.72	-0.1%
107.2		21.3%	2.6	0.4	0.2	0.72	-0.2%
107.8		21.2%	2.6	0.4	0.2	0.72	-0.2%
108.4		21.2%	2.6	0.4	0.2	0.72	-0.2%
109.0		21.0%	2.6	0.4	0.2	0.72	-0.2%

Time-on-stream (h)	T (°C)	X_{CO}	Molar Flow (mmol/min)				$C_{Balance}$
			H_2	CO	CO_2	Ar	
109.6	350	21.1%	2.6	0.4	0.2	0.72	-0.2%
110.3		21.3%	2.5	0.4	0.2	0.72	-0.2%
110.9		21.2%	2.5	0.4	0.2	0.72	-0.1%
111.5		21.1%	2.5	0.4	0.2	0.72	-0.1%
112.1		21.1%	2.6	0.4	0.2	0.72	-0.2%
112.7		21.0%	2.6	0.4	0.2	0.72	-0.2%
113.3		21.3%	2.6	0.4	0.2	0.72	-0.1%
114.0		22.5%	2.5	0.4	0.2	0.71	0.2%
114.6		21.8%	2.5	0.4	0.2	0.71	-0.1%
115.2		21.6%	2.6	0.4	0.2	0.72	-0.1%
115.8		21.2%	2.5	0.4	0.2	0.72	-0.1%
116.4		20.0%	2.5	0.4	0.2	0.73	-0.1%
117.0		21.3%	2.6	0.4	0.2	0.72	-0.2%
117.7		21.1%	2.6	0.4	0.2	0.72	-0.2%
118.3		21.3%	2.5	0.4	0.2	0.72	-0.1%
118.9		21.3%	2.5	0.4	0.2	0.72	-0.1%
119.5		21.3%	2.5	0.4	0.2	0.72	-0.1%
120.3		21.4%	2.5	0.4	0.2	0.72	-0.1%
120.9		21.2%	2.6	0.4	0.2	0.72	-0.1%
121.5		21.2%	2.5	0.4	0.2	0.72	-0.1%
122.1		21.0%	2.5	0.4	0.2	0.72	-0.2%
122.7		21.2%	2.5	0.4	0.2	0.72	-0.1%
123.4		21.2%	2.5	0.4	0.2	0.72	-0.1%
124.0		21.2%	2.5	0.4	0.2	0.72	-0.2%
124.6		21.3%	2.5	0.4	0.2	0.72	-0.2%
125.2		21.2%	2.5	0.4	0.2	0.72	-0.2%
125.8		21.1%	2.5	0.4	0.2	0.72	-0.1%
126.4		21.3%	2.5	0.4	0.2	0.72	-0.1%
127.1		21.3%	2.5	0.4	0.2	0.72	-0.2%
127.7		21.2%	2.5	0.4	0.2	0.72	-0.2%
128.3		21.0%	2.5	0.4	0.2	0.72	-0.2%
128.9		21.4%	2.5	0.4	0.2	0.72	-0.1%
129.5		21.0%	2.5	0.4	0.2	0.72	-0.2%
130.1		21.2%	2.5	0.4	0.2	0.72	-0.1%
130.8		21.2%	2.5	0.4	0.2	0.72	-0.1%
131.4		21.1%	2.5	0.4	0.2	0.72	-0.1%
132.0		21.2%	2.5	0.4	0.2	0.72	-0.1%
132.6		21.1%	2.5	0.4	0.2	0.72	-0.1%
133.2		21.3%	2.5	0.4	0.2	0.72	-0.1%
133.8		21.1%	2.5	0.4	0.2	0.72	-0.1%
134.4		21.2%	2.5	0.4	0.2	0.72	-0.1%
135.1		21.2%	2.5	0.4	0.2	0.72	-0.1%
135.7		21.3%	2.5	0.4	0.2	0.72	-0.1%
136.3		21.2%	2.5	0.4	0.2	0.72	-0.2%

Time-on-stream (h)	T (°C)	X_{CO}	Molar Flow (mmol/min)				$C_{Balance}$
			H_2	CO	CO_2	Ar	
136.9	350	21.3%	2.5	0.4	0.2	0.72	-0.1%
137.5		21.3%	2.5	0.4	0.2	0.72	-0.1%
170.5	375	40.3%	2.5	0.4	0.2	0.73	-0.2%
171.1		39.7%	2.5	0.4	0.2	0.74	-0.5%
171.7		39.8%	2.6	0.4	0.2	0.70	-0.5%
172.4		39.7%	2.6	0.4	0.2	0.62	-0.4%
173.0		40.0%	2.6	0.3	0.2	0.61	-0.3%
173.6		39.4%	2.6	0.3	0.2	0.61	-0.5%
174.2		39.4%	2.6	0.3	0.2	0.60	-0.5%
174.8		39.6%	2.6	0.3	0.2	0.60	-0.5%
175.4		39.4%	2.6	0.3	0.2	0.60	-0.5%
176.0		39.3%	2.6	0.3	0.2	0.60	-0.4%
176.6		39.1%	2.6	0.3	0.2	0.59	-0.5%
177.3		39.3%	2.6	0.3	0.2	0.60	-0.5%
177.9		39.2%	2.6	0.3	0.2	0.60	-0.5%
178.5		39.1%	2.6	0.3	0.2	0.60	-0.5%
179.1		39.2%	2.6	0.3	0.2	0.60	-0.4%
179.7		39.2%	2.6	0.3	0.2	0.59	-0.5%
180.3		39.2%	2.6	0.3	0.2	0.60	-0.5%
180.9		39.3%	2.6	0.3	0.2	0.60	-0.5%
181.6		39.1%	2.6	0.3	0.2	0.60	-0.5%
182.2		39.2%	2.6	0.3	0.2	0.60	-0.5%
182.8		39.4%	2.6	0.3	0.2	0.60	-0.5%
183.4		39.1%	2.5	0.3	0.2	0.58	-0.4%
184.0		39.0%	2.6	0.3	0.2	0.60	-0.5%
184.6		39.0%	2.6	0.3	0.2	0.60	-0.5%
185.2		38.7%	2.6	0.3	0.2	0.60	-0.5%
185.9		38.6%	2.6	0.3	0.2	0.60	-0.5%
186.5		38.6%	2.6	0.3	0.2	0.60	-0.5%
258.3	400	54.4%	2.6	0.3	0.2	0.60	-0.8%
258.9		54.4%	2.6	0.3	0.2	0.60	-0.8%
259.5		54.9%	2.6	0.3	0.2	0.60	-0.8%
260.1		54.7%	2.6	0.3	0.2	0.60	-0.8%
260.7		54.4%	2.5	0.3	0.2	0.59	-0.8%
261.3		54.4%	2.6	0.3	0.2	0.60	-0.8%
262.0		54.7%	2.6	0.3	0.2	0.60	-0.8%
262.6		54.4%	2.6	0.3	0.2	0.60	-0.8%
263.2		54.8%	2.6	0.3	0.2	0.61	-0.8%
263.8		54.4%	2.6	0.3	0.2	0.61	-0.8%
294.6	430	68.7%	2.6	0.3	0.2	0.58	-1.0%
295.2		68.8%	2.6	0.3	0.2	0.60	-1.1%
295.8		68.5%	2.6	0.3	0.2	0.57	-1.1%
296.5		68.5%	2.6	0.3	0.2	0.57	-1.1%

Time-on-stream (h)	T (°C)	X_{CO}	Molar Flow (mmol/min)				$C_{Balance}$
			H_2	CO	CO_2	Ar	
297.1	430	68.5%	2.6	0.3	0.2	0.57	-1.0%
297.7		67.9%	2.6	0.3	0.2	0.57	-1.0%
298.3		67.6%	2.6	0.3	0.2	0.57	-1.0%
298.9		67.5%	2.6	0.3	0.2	0.56	-1.0%
299.5		67.6%	2.6	0.3	0.2	0.56	-1.1%
300.2		67.6%	2.6	0.3	0.2	0.56	-1.0%
300.8		67.7%	2.6	0.3	0.2	0.57	-1.0%
301.4		67.6%	2.6	0.3	0.2	0.56	-1.1%
302.0		68.1%	2.6	0.3	0.2	0.55	-1.1%
302.6		0.0%	2.6	0.3	0.2	0.55	0.0%
303.3		68.4%	2.6	0.3	0.2	0.55	-1.0%
303.9		67.6%	2.6	0.3	0.2	0.55	-1.0%
304.5		67.5%	2.6	0.3	0.2	0.55	-1.0%
305.1		67.9%	2.6	0.3	0.2	0.55	-0.9%
305.7		67.4%	2.6	0.3	0.2	0.55	-0.7%
306.3		70.0%	2.6	0.3	0.2	0.55	-0.9%
311.3	445	71.4%	2.6	0.3	0.2	0.55	-1.0%
311.9		70.5%	2.6	0.3	0.2	0.55	-1.1%
312.5		70.6%	2.6	0.3	0.2	0.55	-1.1%
313.1		70.2%	2.6	0.3	0.2	0.55	-0.9%
313.7		71.0%	2.6	0.3	0.2	0.56	-1.0%
314.4		70.4%	2.6	0.3	0.2	0.56	-1.0%
315.0		71.6%	2.6	0.3	0.2	0.55	-1.0%
315.6		71.0%	2.6	0.3	0.2	0.56	-1.1%
316.2		71.0%	2.6	0.3	0.2	0.56	-1.0%
316.8		69.9%	2.6	0.3	0.2	0.56	-1.1%
317.5		71.1%	2.6	0.3	0.2	0.56	-1.0%
318.1		70.3%	2.6	0.3	0.2	0.56	-1.1%
318.7		70.4%	2.6	0.3	0.2	0.56	-1.1%
319.3		70.0%	2.6	0.3	0.2	0.56	-1.1%
319.9		70.8%	2.6	0.3	0.2	0.56	-1.1%
320.5		70.9%	2.6	0.3	0.2	0.55	-1.1%
321.2		70.6%	2.6	0.3	0.2	0.56	-1.0%
321.8		70.3%	2.6	0.3	0.2	0.56	-1.1%
322.4		71.1%	2.6	0.3	0.2	0.56	-1.1%
323.0		71.2%	2.6	0.3	0.2	0.56	-1.1%
323.6		71.1%	2.6	0.3	0.2	0.56	-1.1%
324.3		71.1%	2.6	0.3	0.2	0.56	-1.1%
324.9		70.8%	2.6	0.3	0.2	0.58	-1.1%
325.5		71.2%	2.6	0.3	0.2	0.57	-1.1%
326.1		71.6%	2.6	0.3	0.2	0.54	-1.1%
326.7		71.4%	2.7	0.3	0.2	0.46	-1.1%
327.4		71.3%	2.7	0.2	0.2	0.41	-1.1%

Time-on-stream (h)	T (°C)	X_{CO}	Molar Flow (mmol/min)				$C_{Balance}$
			H_2	CO	CO_2	Ar	
328.0	445	69.3%	2.7	0.2	0.2	0.41	-1.1%
328.6		69.6%	2.7	0.2	0.2	0.41	-1.1%
329.2		69.0%	2.7	0.2	0.2	0.40	-1.1%
329.8		71.6%	2.7	0.2	0.2	0.40	-1.1%
364.2	350	33.4%	2.7	0.2	0.2	0.40	-0.4%
364.8		33.4%	2.7	0.2	0.2	0.40	-0.4%
365.4		33.3%	2.7	0.2	0.2	0.40	-0.5%
366.0		33.3%	2.7	0.2	0.2	0.39	-0.4%
366.7		33.0%	2.7	0.2	0.2	0.40	-0.4%
367.3		33.1%	2.7	0.2	0.2	0.40	-0.4%
367.9		33.2%	2.7	0.2	0.2	0.40	-0.4%
368.5		33.2%	2.7	0.2	0.2	0.41	-0.4%
369.1		33.3%	2.7	0.2	0.2	0.41	-0.5%
369.7		33.3%	2.7	0.2	0.2	0.41	-0.4%
370.4		33.3%	2.7	0.2	0.2	0.40	-0.4%
371.0		33.2%	2.7	0.2	0.2	0.40	-0.4%
371.6		33.3%	2.7	0.2	0.2	0.40	-0.4%
372.2		33.4%	2.7	0.2	0.2	0.40	-0.4%
372.8		33.4%	2.7	0.2	0.2	0.40	-0.4%
373.4		33.4%	2.7	0.2	0.2	0.40	-0.4%
374.1		33.2%	2.7	0.2	0.2	0.40	-0.4%
374.7		33.2%	2.7	0.2	0.2	0.40	-0.4%
375.3		33.4%	2.7	0.2	0.2	0.41	-0.4%
375.9		33.2%	2.7	0.2	0.2	0.40	-0.4%
376.5		33.3%	2.7	0.2	0.2	0.40	-0.4%
377.1		33.2%	2.7	0.2	0.2	0.41	-0.4%
377.8		33.3%	2.7	0.2	0.2	0.41	-0.4%
378.4		33.2%	2.7	0.2	0.2	0.41	-0.4%
379.0		33.3%	2.7	0.2	0.2	0.41	-0.4%
379.6		33.3%	2.7	0.2	0.2	0.41	-0.4%
380.2		33.4%	2.7	0.2	0.2	0.41	-0.4%
380.8		33.1%	2.7	0.2	0.2	0.40	-0.4%
381.5		33.1%	2.7	0.2	0.2	0.41	-0.4%
382.1		33.3%	2.7	0.2	0.2	0.41	-0.4%
382.7		33.5%	2.5	0.4	0.2	0.77	-0.4%
383.3		33.5%	2.7	0.2	0.2	0.41	-0.4%
383.9		33.7%	2.7	0.2	0.2	0.41	-0.4%
384.5		33.6%	2.7	0.2	0.2	0.40	-0.4%
385.2		33.5%	2.7	0.2	0.2	0.41	-0.4%
385.8		33.8%	2.7	0.2	0.2	0.41	-0.4%
386.4		33.8%	2.7	0.2	0.2	0.41	-0.4%
387.0		33.8%	2.7	0.2	0.2	0.41	-0.4%
387.6		33.9%	2.7	0.2	0.2	0.41	-0.4%

Time-on-stream (h)	T (°C)	X_{CO}	Molar Flow (mmol/min)				$C_{Balance}$
			H_2	CO	CO_2	Ar	
388.2	350	33.7%	2.7	0.2	0.2	0.41	-0.4%
388.8		33.7%	2.7	0.2	0.2	0.41	-0.4%
389.5		33.9%	2.7	0.2	0.2	0.41	-0.4%
390.1		33.9%	2.7	0.2	0.2	0.41	-0.4%
390.7		33.9%	2.7	0.2	0.2	0.41	-0.4%
391.3		33.8%	2.7	0.2	0.2	0.41	-0.4%
391.9		33.9%	2.7	0.2	0.2	0.41	-0.4%
392.5		33.9%	2.7	0.2	0.2	0.41	-0.4%
393.2		34.0%	2.7	0.2	0.2	0.41	-0.4%
393.8		33.9%	2.7	0.2	0.2	0.41	-0.4%
394.4		34.0%	2.7	0.2	0.2	0.41	-0.4%
395.0		33.9%	2.7	0.2	0.2	0.41	-0.4%
395.6		33.9%	2.7	0.2	0.2	0.41	-0.5%
396.2		33.9%	2.7	0.2	0.2	0.41	-0.4%
396.9		33.9%	2.7	0.2	0.2	0.41	-0.4%
397.5		33.7%	2.7	0.2	0.2	0.41	-0.4%
398.1		33.8%	2.7	0.2	0.2	0.41	-0.4%
398.7		33.6%	2.7	0.2	0.2	0.41	-0.4%
399.3		33.5%	2.7	0.2	0.2	0.41	-0.4%
399.9		33.6%	2.7	0.2	0.2	0.41	-0.4%
400.5		33.6%	2.7	0.2	0.2	0.41	-0.4%
401.2		33.6%	2.7	0.2	0.2	0.41	-0.4%
401.8		33.5%	2.7	0.2	0.2	0.41	-0.4%
402.4		33.6%	2.7	0.2	0.2	0.41	-0.4%
403.0		33.7%	2.7	0.2	0.2	0.41	-0.4%
403.6		33.7%	2.7	0.2	0.2	0.41	-0.5%
404.2		33.6%	2.7	0.2	0.2	0.41	-0.4%
404.9		33.7%	2.7	0.2	0.2	0.41	-0.4%
405.5		33.6%	2.7	0.2	0.2	0.41	-0.4%
406.1		33.4%	2.7	0.2	0.2	0.41	-0.5%
406.7		33.4%	2.7	0.2	0.2	0.41	-0.4%
407.3		33.6%	2.7	0.2	0.2	0.41	-0.4%
408.6		33.4%	2.7	0.2	0.2	0.41	-0.4%
409.2		34.0%	2.7	0.2	0.2	0.41	-0.4%
409.8		34.1%	2.7	0.2	0.2	0.41	-0.4%
410.4		34.1%	2.7	0.2	0.2	0.41	-0.4%
411.0		34.2%	2.7	0.2	0.2	0.41	-0.4%
411.6		33.6%	2.7	0.2	0.2	0.41	-0.5%
412.3		33.9%	2.5	0.4	0.2	0.76	-0.4%
412.9		33.9%	2.7	0.2	0.2	0.42	-0.4%
413.5		33.9%	2.7	0.2	0.2	0.41	-0.4%
414.1		33.9%	2.7	0.2	0.2	0.42	-0.4%
414.7		33.9%	2.7	0.2	0.2	0.42	-0.4%
415.3		34.2%	2.7	0.2	0.2	0.42	-0.4%

Time-on-stream (h)	T (°C)	X_{CO}	Molar Flow (mmol/min)				$C_{Balance}$
			H_2	CO	CO_2	Ar	
416.0	350	34.0%	2.7	0.2	0.2	0.42	-0.4%
416.6		33.9%	2.7	0.2	0.2	0.42	-0.4%
417.2		34.0%	2.7	0.2	0.2	0.41	-0.4%
417.8		34.0%	2.7	0.2	0.2	0.42	-0.4%
418.4		34.3%	2.7	0.2	0.2	0.42	-0.3%
419.0		33.9%	2.7	0.2	0.2	0.42	-0.4%
419.6		34.1%	2.7	0.2	0.2	0.42	-0.3%
420.3		34.1%	2.7	0.2	0.2	0.41	-0.4%
420.9		34.0%	2.7	0.2	0.2	0.42	-0.4%
421.5		34.0%	2.7	0.2	0.2	0.41	-0.4%
422.1		34.2%	2.7	0.2	0.2	0.41	-0.4%
422.7		34.0%	2.7	0.2	0.2	0.42	-0.4%
423.3		33.9%	2.7	0.2	0.2	0.42	-0.4%
424.0		34.0%	2.7	0.2	0.2	0.42	-0.4%
424.6		34.2%	2.7	0.2	0.2	0.42	-0.3%
425.2		34.0%	2.7	0.2	0.2	0.42	-0.4%
425.8		34.2%	2.7	0.2	0.2	0.42	-0.4%
426.4		34.3%	2.7	0.2	0.2	0.42	-0.3%

Space Velocity – 20,000 h^{-1}

Time-on-stream (h)	T (°C)	X_{CO}	Molar Flow (mmol/min)				$C_{Balance}$
			H_2	CO	CO_2	Ar	
119.7	350	9.5%	2.5	0.5	0.2	0.83	0.0%
120.4		9.6%	2.5	0.5	0.2	0.83	0.0%
121.1		9.5%	2.5	0.5	0.2	0.83	0.0%
121.7		9.5%	2.5	0.5	0.2	0.83	0.0%
122.3		9.3%	2.5	0.5	0.2	0.83	0.0%
122.9		9.3%	2.5	0.5	0.2	0.83	0.0%
123.5		9.6%	2.5	0.5	0.2	0.83	0.0%
124.1		9.7%	2.5	0.5	0.2	0.83	0.0%
124.7		9.7%	2.5	0.5	0.2	0.83	0.0%
125.4		9.5%	2.5	0.5	0.2	0.83	0.0%
126.0		9.6%	2.5	0.5	0.2	0.83	0.0%
126.6		9.6%	2.5	0.5	0.2	0.83	0.0%
127.2		9.6%	2.5	0.5	0.2	0.83	0.0%
127.8		9.5%	2.5	0.5	0.2	0.83	0.0%
128.4		9.4%	2.5	0.5	0.2	0.83	0.0%
129.1		9.4%	2.5	0.5	0.2	0.83	0.0%
129.7		9.6%	2.5	0.5	0.2	0.83	0.0%
130.3		9.7%	2.5	0.5	0.2	0.83	0.0%
130.9		9.8%	2.5	0.5	0.2	0.82	0.0%
131.5		9.7%	2.5	0.5	0.2	0.83	0.0%
132.1		9.7%	2.5	0.5	0.2	0.83	0.0%

Time-on-stream (h)	T (°C)	X_{CO}	Molar Flow (mmol/min)				$C_{Balance}$
			H_2	CO	CO_2	Ar	
132.8	350	9.9%	2.5	0.5	0.2	0.82	0.1%
133.4		9.8%	2.5	0.5	0.2	0.82	0.0%
134.0		9.6%	2.5	0.5	0.2	0.83	0.0%
134.6		9.9%	2.5	0.5	0.2	0.82	0.1%
135.2		9.9%	2.5	0.5	0.2	0.82	0.1%
135.8		9.9%	2.5	0.5	0.2	0.82	0.0%
136.5		9.8%	2.5	0.5	0.2	0.82	0.0%
137.1		9.7%	2.5	0.5	0.2	0.83	0.0%
137.7		9.9%	2.5	0.5	0.2	0.82	0.0%
138.3		9.5%	2.5	0.5	0.2	0.83	0.0%
170.1	375	20.9%	2.5	0.5	0.2	0.82	-0.1%
170.7		20.6%	2.5	0.5	0.2	0.84	-0.2%
171.3		20.8%	2.5	0.4	0.2	0.79	-0.2%
171.9		20.7%	2.5	0.4	0.2	0.76	-0.2%
172.5		20.7%	2.5	0.4	0.2	0.76	-0.2%
173.1		20.5%	2.5	0.4	0.2	0.76	-0.2%
173.7		20.6%	2.5	0.4	0.2	0.76	-0.1%
174.3		20.5%	2.5	0.4	0.2	0.76	-0.2%
175.0		20.5%	2.5	0.4	0.2	0.75	-0.2%
175.6		20.5%	2.5	0.4	0.2	0.76	-0.2%
176.2		20.4%	2.5	0.4	0.2	0.76	-0.2%
176.8		20.5%	2.5	0.4	0.2	0.76	-0.1%
177.4		20.5%	2.5	0.4	0.2	0.76	-0.2%
178.0		20.5%	2.5	0.4	0.2	0.76	-0.2%
178.6		20.5%	2.5	0.4	0.2	0.76	-0.2%
179.3		20.4%	2.5	0.4	0.2	0.76	-0.2%
179.9		20.5%	2.5	0.4	0.2	0.76	-0.2%
180.5		20.4%	2.5	0.4	0.2	0.76	-0.2%
181.1		20.4%	2.5	0.4	0.2	0.76	-0.2%
181.7		20.3%	2.5	0.4	0.2	0.76	-0.2%
182.3		20.6%	2.5	0.4	0.2	0.76	-0.2%
182.9		20.4%	2.5	0.4	0.2	0.76	-0.2%
183.6		20.5%	2.5	0.4	0.2	0.76	-0.2%
184.2		20.5%	2.5	0.4	0.2	0.76	-0.2%
184.8		20.5%	2.5	0.4	0.2	0.76	-0.1%
185.4		20.2%	2.5	0.4	0.2	0.76	-0.2%
186.0		20.2%	2.5	0.4	0.2	0.76	-0.1%
257.8	400	33.1%	2.5	0.4	0.2	0.76	-0.4%
258.4		32.3%	2.5	0.4	0.2	0.76	-0.5%
259.0		33.0%	2.5	0.4	0.2	0.76	-0.4%
259.6		33.0%	2.5	0.4	0.2	0.76	-0.4%
260.3		33.2%	2.5	0.4	0.2	0.76	-0.4%
260.9		33.1%	2.5	0.4	0.2	0.76	-0.4%

Time-on-stream (h)	T (°C)	X_{CO}	Molar Flow (mmol/min)				$C_{Balance}$
			H_2	CO	CO_2	Ar	
261.5	400	33.4%	2.5	0.4	0.2	0.76	-0.4%
262.1		33.0%	2.5	0.4	0.2	0.76	-0.4%
262.7		33.1%	2.5	0.4	0.2	0.76	-0.5%
263.3		33.2%	2.5	0.4	0.2	0.75	-0.4%
263.9		32.8%	2.5	0.4	0.2	0.74	-0.4%
264.6		33.2%	2.5	0.4	0.2	0.74	-0.4%
265.2		33.3%	2.5	0.4	0.2	0.74	-0.5%
265.8		33.5%	2.5	0.4	0.2	0.74	-0.4%
266.4		32.9%	2.5	0.4	0.2	0.74	-0.5%
267.0		33.1%	2.5	0.4	0.2	0.74	-0.5%
267.6		32.8%	2.5	0.4	0.2	0.74	-0.4%
268.3		32.8%	2.5	0.4	0.2	0.73	-0.4%
268.9		32.9%	2.5	0.4	0.2	0.73	-0.4%
269.5		32.8%	2.5	0.4	0.2	0.72	-0.5%
270.1		32.8%	2.5	0.4	0.2	0.73	-0.4%
270.7		32.8%	2.5	0.4	0.2	0.73	-0.5%
271.3		32.8%	2.5	0.4	0.2	0.73	-0.5%
272.0		32.8%	2.5	0.4	0.2	0.71	-0.5%
272.6		32.7%	2.5	0.4	0.2	0.72	-0.5%
273.2		32.7%	2.5	0.4	0.2	0.73	-0.4%
273.8		33.1%	2.5	0.4	0.2	0.72	-0.5%
274.4		32.5%	2.5	0.4	0.2	0.73	-0.5%
275.0		32.4%	2.5	0.4	0.2	0.73	-0.5%
275.6		32.5%	2.6	0.4	0.2	0.73	-0.5%
276.3		32.5%	2.5	0.4	0.2	0.73	-0.5%
276.9		32.6%	2.5	0.4	0.2	0.73	-0.5%
277.5		32.6%	2.6	0.4	0.2	0.73	-0.4%
278.1		32.5%	2.6	0.4	0.2	0.73	-0.5%
278.7		32.5%	2.6	0.4	0.2	0.73	-0.5%
279.3		32.4%	2.6	0.4	0.2	0.73	-0.5%
280.0		32.6%	2.6	0.4	0.2	0.73	-0.5%
280.6		32.7%	2.6	0.4	0.2	0.73	-0.4%
281.2		33.2%	2.5	0.4	0.2	0.73	-0.4%
281.8		33.4%	2.6	0.4	0.2	0.73	-0.6%
296.6	430	50.1%	2.5	0.4	0.2	0.73	-0.7%
297.2		50.4%	2.6	0.4	0.2	0.73	-0.6%
297.8		50.3%	2.5	0.4	0.2	0.73	-0.7%
298.5		49.7%	2.6	0.4	0.2	0.73	-0.8%
299.1		49.7%	2.6	0.4	0.2	0.73	-0.8%
299.7		49.8%	2.5	0.4	0.2	0.73	-0.7%
300.3		49.6%	2.6	0.4	0.2	0.73	-0.8%
300.9		49.5%	2.5	0.4	0.2	0.73	-0.7%

Time-on-stream (h)	T (°C)	X_{CO}	Molar Flow (mmol/min)				$C_{Balance}$
			H_2	CO	CO_2	Ar	
301.6	430	49.1%	2.5	0.4	0.2	0.73	-0.8%
302.2		49.0%	2.6	0.4	0.2	0.73	-0.8%
302.8		50.2%	2.5	0.4	0.2	0.73	-0.1%
303.4		49.5%	2.4	0.5	0.2	0.86	-0.9%
304.0		50.3%	2.5	0.4	0.2	0.73	-0.8%
304.6		49.1%	2.5	0.4	0.2	0.73	-0.7%
305.3		50.2%	2.6	0.4	0.2	0.70	-0.7%
305.9		49.4%	2.6	0.4	0.2	0.63	-0.7%
310.8	445	56.2%	2.6	0.3	0.2	0.61	-0.8%
311.4		55.7%	2.6	0.3	0.2	0.61	-0.7%
312.0		57.1%	2.6	0.3	0.2	0.61	-0.9%
312.7		56.1%	2.6	0.3	0.2	0.61	-0.8%
313.3		56.3%	2.6	0.3	0.2	0.60	-0.8%
313.9		57.2%	2.6	0.3	0.2	0.60	-0.8%
314.5		57.6%	2.6	0.3	0.2	0.61	-0.8%
315.1		57.8%	2.6	0.3	0.2	0.60	-0.8%
315.8		57.2%	2.6	0.3	0.2	0.61	-0.8%
316.4		56.8%	2.6	0.3	0.2	0.61	-0.8%
317.0		56.0%	2.6	0.3	0.2	0.61	-0.8%
317.6		57.4%	2.6	0.3	0.2	0.61	-0.8%
318.2		56.7%	2.6	0.3	0.2	0.61	-0.9%
318.8		56.8%	2.6	0.3	0.2	0.61	-0.9%
319.5		56.5%	2.6	0.3	0.2	0.61	-0.9%
320.1		56.4%	2.6	0.3	0.2	0.61	-0.8%
320.7		56.4%	2.6	0.3	0.2	0.61	-0.8%
321.3		56.7%	2.6	0.3	0.2	0.61	-0.8%
321.9		56.5%	2.6	0.3	0.2	0.61	-0.9%
322.6		56.8%	2.6	0.3	0.2	0.61	-0.9%
323.2		56.7%	2.6	0.3	0.2	0.61	-0.9%
323.8		56.9%	2.6	0.3	0.2	0.61	-0.9%
324.4		57.0%	2.6	0.3	0.2	0.61	-0.9%
325.0		57.1%	2.6	0.3	0.2	0.61	-0.8%
325.7		57.6%	2.6	0.3	0.2	0.61	-0.9%
326.3		57.9%	2.6	0.3	0.2	0.61	-0.9%
326.9		57.8%	2.6	0.3	0.2	0.61	-0.9%
327.5		57.5%	2.6	0.3	0.2	0.61	-0.8%
328.1		56.3%	2.6	0.3	0.2	0.61	-0.8%
328.7		55.4%	2.6	0.3	0.2	0.61	-0.7%
329.4		56.8%	2.6	0.3	0.2	0.61	-0.9%
330.0		56.4%	2.6	0.3	0.2	0.61	-0.9%
383.5	350	18.2%	2.6	0.3	0.2	0.61	-0.2%
384.1		18.3%	2.6	0.3	0.2	0.61	-0.2%

Time-on-stream (h)	T (°C)	X_{CO}	Molar Flow (mmol/min)				$C_{Balance}$
			H_2	CO	CO_2	Ar	
384.7		18.3%	2.6	0.3	0.2	0.61	-0.2%
385.3		18.3%	2.6	0.3	0.2	0.61	-0.1%
385.9		18.2%	2.6	0.3	0.2	0.61	-0.2%
386.5		18.4%	2.6	0.3	0.2	0.61	-0.2%
387.2		18.5%	2.6	0.3	0.2	0.61	-0.2%
387.8		18.5%	2.6	0.3	0.2	0.61	-0.2%
388.4		18.4%	2.6	0.3	0.2	0.61	-0.2%
389.0		18.4%	2.6	0.3	0.2	0.61	-0.2%
389.6		18.5%	2.6	0.3	0.2	0.61	-0.2%
390.2		18.5%	2.6	0.3	0.2	0.61	-0.1%
390.9		18.5%	2.6	0.3	0.2	0.61	-0.2%
391.5		18.4%	2.6	0.3	0.2	0.61	-0.2%
392.1		18.5%	2.6	0.3	0.2	0.61	-0.2%
392.7		18.5%	2.6	0.3	0.2	0.61	-0.2%
393.3		18.5%	2.6	0.3	0.2	0.61	-0.1%
393.9		18.5%	2.6	0.3	0.2	0.61	-0.1%
394.5		18.6%	2.6	0.3	0.2	0.61	-0.2%
395.2		18.6%	2.6	0.3	0.2	0.61	-0.2%
395.8		18.6%	2.6	0.3	0.2	0.61	-0.2%
396.4		18.6%	2.6	0.3	0.2	0.61	9.7%
397.0	350	18.5%	2.6	0.3	0.2	0.61	-0.1%
397.6		18.6%	2.6	0.3	0.2	0.61	-0.1%
398.2		18.6%	2.6	0.3	0.2	0.61	-0.1%
398.9		18.2%	2.6	0.3	0.2	0.61	-0.2%
399.5		18.4%	2.6	0.3	0.2	0.61	-0.2%
400.1		18.4%	2.6	0.3	0.2	0.61	-0.2%
400.7		18.4%	2.6	0.3	0.2	0.61	-0.2%
401.3		18.3%	2.6	0.3	0.2	0.61	-0.2%
401.9		18.4%	2.6	0.3	0.2	0.61	-0.2%
402.6		18.6%	2.6	0.3	0.2	0.61	-0.2%
403.2		18.5%	2.6	0.3	0.2	0.61	-0.2%
403.8		18.6%	2.6	0.3	0.2	0.61	-0.2%
404.4		18.2%	2.6	0.3	0.2	0.61	-0.2%
405.0		18.5%	2.6	0.3	0.2	0.61	-0.2%
405.6		18.5%	2.6	0.3	0.2	0.61	-0.2%
406.3		18.6%	2.6	0.3	0.2	0.61	-0.2%
406.9		18.5%	2.6	0.3	0.2	0.61	-0.2%
407.5		18.6%	2.6	0.3	0.2	0.61	-0.2%
408.1		19.7%	2.6	0.3	0.2	0.61	0.0%
408.7		0.0%	2.6	0.3	0.2	0.60	-1.1%
409.3		19.0%	2.6	0.3	0.2	0.61	-0.2%
410.0		19.1%	2.6	0.3	0.2	0.60	-0.2%
410.6		19.2%	2.6	0.3	0.2	0.61	-0.2%

Time-on-stream (h)	T (°C)	X_{CO}	Molar Flow (mmol/min)				$C_{Balance}$
			H_2	CO	CO_2	Ar	
411.2	350	19.2%	2.6	0.3	0.2	0.61	-0.1%
411.8		19.1%	2.6	0.3	0.2	0.61	-0.2%
412.4		19.0%	2.6	0.3	0.2	0.61	-0.1%
413.0		19.0%	2.6	0.3	0.2	0.61	-0.2%
413.6		19.0%	2.6	0.3	0.2	0.61	-0.2%
414.3		19.0%	2.6	0.3	0.2	0.61	-0.1%
414.9		19.0%	2.6	0.3	0.2	0.61	-0.2%
415.5		18.8%	2.6	0.3	0.2	0.61	-0.2%
416.1		18.9%	2.6	0.3	0.2	0.61	-0.2%
416.7		19.1%	2.6	0.3	0.2	0.62	-0.1%
417.3		19.0%	2.6	0.3	0.2	0.62	-0.2%
417.9		19.0%	2.6	0.3	0.2	0.62	-0.2%
418.6		19.0%	2.6	0.3	0.2	0.62	-0.2%
419.2		18.9%	2.6	0.3	0.2	0.62	-0.2%
419.8		19.0%	2.6	0.3	0.2	0.61	-0.1%
420.4		19.1%	2.6	0.3	0.2	0.61	-0.2%
421.0		19.1%	2.6	0.3	0.2	0.61	-0.2%
421.6		19.0%	2.6	0.3	0.2	0.62	-0.2%
422.3		19.1%	2.6	0.3	0.2	0.62	-0.2%
422.9		19.1%	2.6	0.3	0.2	0.61	-0.2%
423.5		18.9%	2.6	0.3	0.2	0.61	-0.2%
424.1		19.1%	2.6	0.3	0.2	0.61	-0.2%
424.7		18.8%	2.6	0.3	0.2	0.61	-0.2%
425.3		19.1%	2.6	0.3	0.2	0.61	-0.1%
426.0		19.0%	2.6	0.3	0.2	0.61	-0.2%
426.6		18.4%	2.6	0.3	0.2	0.61	-0.3%

Experiment 15-17 – Fe_3O_4/Cr_2O_3, Feed 3

Space Velocity – 5,000 h^{-1}

Time-on-stream (h)	T (°C)	X_{CO}	Molar Flow (mmol/min)				$C_{Balance}$
			H_2	CO	CO_2	Ar	
436.8	375	43.4%	1.3	0.0	0.0	0.1	-0.1%
437.4		43.4%	1.3	0.0	0.0	0.1	0.0%
438.0		43.5%	1.2	0.0	0.0	0.1	0.1%
438.6		42.0%	1.2	0.0	0.0	0.1	-0.1%
439.2		43.6%	1.2	0.0	0.0	0.1	0.2%
439.9		42.8%	1.3	0.0	0.0	0.1	-0.2%
440.5		42.5%	1.3	0.1	0.0	0.1	-0.2%
441.1		43.2%	1.3	0.0	0.0	0.1	-0.1%
441.7		43.3%	1.2	0.0	0.0	0.1	0.0%
442.3		43.5%	1.3	0.0	0.0	0.1	0.0%
442.9		43.3%	1.3	0.0	0.0	0.1	-0.1%
443.6		43.4%	1.2	0.0	0.0	0.1	0.0%

Time-on-stream (h)	T (°C)	X_{CO}	Molar Flow (mmol/min)				$C_{Balance}$
			H_2	CO	CO_2	Ar	
444.2	375	43.5%	1.3	0.0	0.0	0.1	-0.1%
444.8		43.3%	1.3	0.0	0.0	0.1	-0.1%
445.4		43.0%	1.3	0.0	0.0	0.1	-0.1%
446.0		43.7%	1.2	0.0	0.0	0.1	0.1%
446.7		43.3%	1.3	0.0	0.0	0.1	0.0%
447.3		42.9%	1.3	0.0	0.0	0.1	-0.1%
447.9		43.1%	1.3	0.0	0.0	0.1	-0.1%
448.5		42.7%	1.3	0.0	0.0	0.1	-0.2%
449.1		43.6%	1.3	0.0	0.0	0.1	0.0%
449.7		43.8%	1.2	0.0	0.0	0.1	0.3%
450.4		42.8%	1.3	0.0	0.0	0.1	-0.1%
451.0		44.5%	1.2	0.0	0.0	0.1	0.1%
451.6		42.8%	1.3	0.0	0.0	0.1	-0.2%
452.2		43.0%	1.3	0.0	0.0	0.1	-0.2%
452.8		44.3%	1.2	0.0	0.0	0.1	0.2%
456.6	400	57.6%	1.3	0.0	0.0	0.1	-0.1%
457.2		58.4%	1.3	0.0	0.0	0.1	-0.2%
457.8		60.0%	1.3	0.0	0.0	0.1	0.2%
458.4		59.4%	1.3	0.0	0.0	0.1	-0.1%
459.0		56.8%	1.3	0.0	0.0	0.1	-0.1%
459.7		57.2%	1.3	0.0	0.0	0.1	-0.1%
460.3		58.6%	1.3	0.0	0.0	0.1	-0.1%
460.9		59.6%	1.3	0.0	0.0	0.1	-0.1%
461.5		58.7%	1.3	0.0	0.0	0.1	-0.1%
462.1		58.5%	1.3	0.0	0.0	0.1	-0.1%
462.7		58.0%	1.3	0.0	0.0	0.1	-0.1%
463.4		56.7%	1.3	0.0	0.0	0.1	-0.2%
464.0		57.2%	1.3	0.0	0.0	0.1	-0.2%
464.6		58.1%	1.3	0.0	0.0	0.1	0.0%
465.2		57.7%	1.3	0.0	0.0	0.1	-0.1%
465.8		59.3%	1.3	0.0	0.0	0.1	-0.1%
466.4		58.9%	1.3	0.0	0.0	0.1	-0.1%
467.0		57.8%	1.3	0.0	0.0	0.1	-0.1%
467.7		58.0%	1.3	0.0	0.0	0.1	-0.1%
468.3		58.1%	1.3	0.0	0.0	0.1	-0.1%
468.9		58.1%	1.3	0.0	0.0	0.1	-0.1%
469.5		57.2%	1.3	0.0	0.0	0.1	-0.2%
470.1		56.2%	1.3	0.0	0.0	0.1	-0.1%
470.7		56.1%	1.3	0.0	0.0	0.1	-0.2%
471.3		58.4%	1.3	0.0	0.0	0.1	-0.1%
472.0		58.0%	1.3	0.0	0.0	0.1	-0.2%
472.6		58.5%	1.3	0.0	0.0	0.1	-0.1%

Time-on-stream (h)	T (°C)	X_{CO}	Molar Flow (mmol/min)				$C_{Balance}$
			H_2	CO	CO_2	Ar	
480.6	430	62.1%	1.3	0.0	0.0	0.1	-0.1%
481.2		61.2%	1.3	0.0	0.0	0.1	0.0%
481.8		62.6%	1.3	0.0	0.0	0.1	-0.2%
482.4		63.2%	1.3	0.0	0.0	0.1	-0.1%
483.0		63.1%	1.3	0.0	0.0	0.1	-0.1%
483.6		63.2%	1.3	0.0	0.0	0.1	-0.2%
484.2		62.8%	1.3	0.0	0.0	0.1	0.0%
484.9		62.7%	1.3	0.0	0.0	0.1	-0.2%
485.5		62.8%	1.3	0.0	0.0	0.1	-0.2%
486.1		0.0%	1.3	0.0	0.0	0.1	0.1%
486.7		0.0%	1.3	0.0	0.0	0.1	-0.1%
487.3		0.0%	1.3	0.0	0.0	0.1	-0.1%
487.9		0.0%	1.3	0.0	0.0	0.1	-0.2%
488.6		61.4%	1.3	0.0	0.0	0.1	-0.1%
489.2		61.3%	1.3	0.0	0.0	0.1	-0.2%
489.8		61.5%	1.3	0.0	0.0	0.1	-0.2%
490.4		61.4%	1.3	0.0	0.0	0.1	-0.1%
491.0		61.1%	1.3	0.0	0.0	0.1	-0.1%
491.6		61.0%	1.3	0.0	0.0	0.1	-0.1%
492.2		62.9%	1.3	0.0	0.0	0.1	-0.1%
492.9		0.0%	1.3	0.0	0.0	0.1	-0.1%
493.5		0.0%	1.3	0.0	0.0	0.1	-0.1%
494.1		0.0%	1.3	0.0	0.0	0.1	-0.2%
494.7		0.0%	1.3	0.0	0.0	0.1	-0.1%
495.3		62.3%	1.3	0.0	0.0	0.1	-0.2%
495.9		62.3%	1.3	0.0	0.0	0.1	-0.2%
496.6		62.4%	1.3	0.0	0.0	0.1	-0.1%
497.2		0.0%	1.3	0.0	0.0	0.1	-0.1%
497.8		60.5%	1.3	0.0	0.0	0.1	-0.1%
511.3	445	56.3%	1.3	0.0	0.0	0.1	-0.1%
511.9		59.9%	1.3	0.0	0.0	0.1	-0.1%
512.5		62.3%	1.3	0.0	0.0	0.1	-0.1%
513.2		58.2%	1.3	0.0	0.0	0.1	-0.1%
513.8		58.3%	1.3	0.0	0.0	0.1	-0.1%
514.4		58.5%	1.3	0.0	0.0	0.1	0.0%
515.0		58.3%	1.3	0.0	0.0	0.1	-0.1%
515.6		58.6%	1.3	0.0	0.0	0.1	-0.1%
516.2		58.7%	1.3	0.0	0.0	0.1	-0.1%
516.8		58.2%	1.3	0.0	0.0	0.1	-0.1%
517.5		56.4%	1.3	0.0	0.0	0.1	-0.1%
518.1		60.6%	1.3	0.0	0.0	0.1	-0.1%
518.7		60.6%	1.3	0.0	0.0	0.1	-0.1%
519.3		58.3%	1.3	0.0	0.0	0.1	-0.1%

Time-on-stream (h)	T (°C)	X_{CO}	Molar Flow (mmol/min)				$C_{Balance}$
			H_2	CO	CO_2	Ar	
519.9	445	59.7%	1.3	0.0	0.0	0.1	-0.1%
520.5		57.3%	1.3	0.0	0.0	0.1	-0.1%
521.1		60.0%	1.3	0.0	0.0	0.1	0.0%
521.8		58.3%	1.3	0.0	0.0	0.1	0.1%
529.8	375	37.2%	1.2	0.1	0.0	0.1	0.1%
530.4		37.1%	1.2	0.1	0.0	0.1	0.0%
531.0		37.3%	1.2	0.1	0.0	0.1	0.0%
531.6		37.6%	1.2	0.1	0.0	0.1	0.0%
532.2		37.9%	1.2	0.1	0.0	0.1	0.0%
532.8		37.6%	1.2	0.1	0.0	0.1	0.0%
533.5		37.9%	1.2	0.1	0.0	0.1	0.0%
534.1		37.8%	1.2	0.1	0.0	0.1	0.0%
534.7		37.8%	1.2	0.1	0.0	0.1	0.0%
535.3		37.9%	1.2	0.1	0.0	0.1	0.0%
535.9		37.9%	1.2	0.1	0.0	0.1	0.0%
536.5		38.2%	1.2	0.1	0.0	0.1	0.0%
537.2		38.0%	1.2	0.1	0.0	0.1	0.0%
537.8		38.2%	1.2	0.1	0.0	0.1	0.1%
538.4		38.2%	1.2	0.1	0.0	0.1	0.0%
539.0		38.1%	1.2	0.1	0.0	0.1	0.0%
539.6		38.1%	1.2	0.1	0.0	0.1	0.0%
540.2		38.3%	1.2	0.1	0.0	0.1	0.0%
540.9		38.2%	1.2	0.1	0.0	0.1	0.0%
541.5		38.2%	1.2	0.1	0.0	0.1	0.0%
542.1		38.3%	1.2	0.1	0.0	0.1	0.0%
542.7		38.0%	1.2	0.1	0.0	0.1	0.0%
543.3		38.0%	1.2	0.1	0.0	0.1	0.0%
543.9		37.9%	1.2	0.1	0.0	0.1	0.0%
544.6		39.8%	1.2	0.1	0.0	0.1	0.6%
545.2		39.0%	1.2	0.1	0.0	0.1	0.2%
545.8		0.0%	1.0	0.0	0.0	0.1	4.6%
546.4		39.3%	1.2	0.1	0.0	0.1	0.2%
547.0		39.8%	1.2	0.1	0.0	0.1	0.3%
547.6		39.2%	1.2	0.1	0.0	0.1	0.2%
548.3		39.2%	1.2	0.1	0.0	0.1	0.3%
548.9		39.2%	1.2	0.1	0.0	0.1	0.3%
549.5		37.6%	1.2	0.1	0.0	0.1	0.0%

Space Velocity – 10,000 h^{-1}

Time-on-stream (h)	T (°C)	X_{CO}	Molar Flow (mmol/min)				$C_{Balance}$
			H_2	CO	CO_2	Ar	
438.2	375	26.9%	2.5	0.1	0.1	0.2	0.2%
438.8		26.3%	2.5	0.1	0.1	0.2	0.1%
439.4		27.0%	2.5	0.1	0.1	0.2	0.2%

Time-on-stream (h)	T (°C)	X_{CO}	Molar Flow (mmol/min)				$C_{Balance}$
			H_2	CO	CO_2	Ar	
440.0	375	26.7%	2.5	0.1	0.1	0.2	0.2%
440.6		26.0%	2.4	0.1	0.1	0.2	0.2%
441.2		26.5%	2.5	0.1	0.1	0.2	0.2%
441.9		26.6%	2.5	0.1	0.1	0.2	0.2%
442.5		26.6%	2.5	0.1	0.1	0.2	0.0%
443.1		26.5%	2.5	0.1	0.1	0.2	0.0%
443.7		26.4%	2.5	0.1	0.1	0.2	0.0%
444.3		26.7%	2.5	0.1	0.1	0.2	0.1%
445.0		26.8%	2.5	0.1	0.1	0.2	0.1%
445.6		26.0%	2.5	0.1	0.1	0.2	0.0%
446.2		26.3%	2.5	0.1	0.1	0.2	0.0%
446.8		28.2%	2.4	0.1	0.1	0.2	0.6%
447.4		26.8%	2.5	0.1	0.1	0.2	0.2%
448.0		26.3%	2.5	0.1	0.1	0.2	0.0%
448.7		27.2%	2.4	0.1	0.1	0.2	0.3%
449.3		26.5%	2.5	0.1	0.1	0.2	0.1%
449.9		26.5%	2.5	0.1	0.1	0.2	0.0%
450.5		27.2%	2.4	0.1	0.1	0.2	0.3%
451.1		25.6%	2.5	0.1	0.1	0.2	0.0%
451.7		25.7%	2.5	0.1	0.1	0.2	0.0%
452.4		26.3%	2.5	0.1	0.1	0.2	0.0%
458.6	400	41.6%	2.5	0.1	0.1	0.2	0.0%
459.2		41.6%	2.5	0.1	0.1	0.2	0.0%
459.8		41.1%	2.5	0.1	0.1	0.2	0.0%
460.4		41.3%	2.5	0.1	0.1	0.2	0.0%
461.0		41.4%	2.5	0.1	0.1	0.2	0.0%
461.7		41.4%	2.5	0.1	0.1	0.2	0.0%
462.3		41.7%	2.5	0.1	0.1	0.2	0.0%
462.9		41.7%	2.5	0.1	0.1	0.2	0.0%
463.5		41.1%	2.5	0.1	0.1	0.2	0.0%
464.1		41.7%	2.5	0.1	0.1	0.2	0.2%
464.7		41.3%	2.5	0.1	0.1	0.2	-0.1%
465.3		41.2%	2.5	0.1	0.1	0.2	0.0%
466.0		41.4%	2.5	0.1	0.1	0.2	0.0%
466.6		41.3%	2.5	0.1	0.1	0.2	0.0%
467.2		41.2%	2.5	0.1	0.1	0.2	-0.1%
467.8		41.5%	2.5	0.1	0.1	0.2	0.0%
468.4		40.8%	2.5	0.1	0.1	0.2	0.0%
469.0		40.9%	2.5	0.1	0.1	0.2	0.0%
469.7		41.2%	2.5	0.1	0.1	0.2	0.0%
470.3		41.5%	2.5	0.1	0.1	0.2	0.0%
470.9		41.2%	2.5	0.1	0.1	0.2	-0.1%

Time-on-stream (h)	T (°C)	X_{CO}	Molar Flow (mmol/min)				$C_{Balance}$
			H_2	CO	CO_2	Ar	
471.5	400	41.1%	2.5	0.1	0.1	0.2	0.0%
472.1		40.8%	2.5	0.1	0.1	0.2	0.0%
472.7		42.2%	2.5	0.1	0.1	0.2	0.2%
482.6	430	53.3%	2.5	0.1	0.1	0.2	-0.1%
483.2		52.7%	2.5	0.1	0.1	0.2	0.1%
483.8		52.8%	2.5	0.1	0.1	0.2	-0.1%
484.4		53.4%	2.5	0.1	0.1	0.2	-0.1%
485.0		53.4%	2.5	0.1	0.1	0.2	-0.1%
485.6		53.2%	2.5	0.1	0.1	0.2	0.0%
486.2		53.3%	2.5	0.1	0.1	0.2	-0.1%
486.9		53.5%	2.5	0.1	0.1	0.2	-0.1%
487.5		53.7%	2.5	0.1	0.1	0.2	-0.1%
488.1		53.3%	2.5	0.1	0.1	0.2	-0.1%
488.7		53.4%	2.5	0.1	0.1	0.2	-0.1%
489.3		53.1%	2.5	0.1	0.1	0.2	-0.1%
489.9		52.4%	2.5	0.1	0.1	0.2	-0.1%
490.6		52.5%	2.5	0.1	0.1	0.2	-0.1%
491.2		52.2%	2.5	0.1	0.1	0.2	-0.1%
491.8		52.9%	2.5	0.1	0.1	0.2	-0.1%
492.4		52.7%	2.5	0.1	0.1	0.2	-0.1%
493.0		53.8%	2.5	0.1	0.1	0.2	-0.1%
493.6		53.2%	2.5	0.1	0.1	0.2	-0.1%
494.3		52.4%	2.5	0.1	0.1	0.2	-0.1%
494.9		52.4%	2.5	0.1	0.1	0.2	-0.1%
495.5		52.4%	2.5	0.1	0.1	0.2	-0.1%
496.1		52.4%	2.5	0.1	0.1	0.2	-0.1%
496.7		52.4%	2.5	0.1	0.1	0.2	-0.1%
497.3		52.1%	2.5	0.1	0.1	0.2	-0.1%
497.9		52.2%	2.5	0.1	0.1	0.2	0.0%
510.2	445	55.6%	2.5	0.1	0.1	0.1	-0.1%
510.9		55.6%	2.5	0.1	0.1	0.1	-0.1%
511.5		56.2%	2.5	0.1	0.1	0.1	-0.1%
512.1		55.8%	2.5	0.1	0.1	0.1	-0.1%
512.7		55.7%	2.5	0.1	0.1	0.1	0.0%
513.3		55.1%	2.5	0.1	0.1	0.1	-0.1%
513.9		55.1%	2.5	0.1	0.1	0.1	-0.1%
514.5		54.8%	2.5	0.1	0.1	0.1	-0.1%
515.2		54.6%	2.5	0.1	0.1	0.1	-0.1%
515.8		55.3%	2.5	0.1	0.1	0.1	-0.1%
516.4		56.3%	2.5	0.1	0.1	0.1	-0.1%
517.0		56.4%	2.5	0.1	0.1	0.1	-0.1%
517.6		56.0%	2.5	0.1	0.1	0.1	-0.1%
518.2		56.2%	2.5	0.1	0.1	0.1	-0.1%

Time-on-stream (h)	T (°C)	X_{CO}	Molar Flow (mmol/min)				$C_{Balance}$
			H_2	CO	CO_2	Ar	
518.8	445	55.7%	2.5	0.1	0.1	0.1	-0.1%
519.5		55.9%	2.5	0.1	0.1	0.1	-0.1%
520.1		55.7%	2.5	0.1	0.1	0.1	-0.2%
520.7		55.6%	2.5	0.1	0.1	0.1	-0.1%
521.9		54.1%	2.5	0.1	0.1	0.1	0.3%
528.1	375	24.6%	2.5	0.1	0.1	0.2	0.1%
528.7		24.3%	2.5	0.1	0.1	0.2	0.1%
529.3		24.2%	2.5	0.1	0.1	0.2	0.1%
529.9		23.6%	2.5	0.1	0.1	0.2	0.1%
530.5		24.6%	2.5	0.1	0.1	0.2	0.1%
531.2		24.7%	2.5	0.1	0.1	0.2	0.1%
531.8		24.4%	2.5	0.1	0.1	0.2	0.1%
532.4		24.7%	2.5	0.1	0.1	0.2	0.1%
533.0		25.0%	2.5	0.1	0.1	0.2	0.1%
533.6		25.0%	2.5	0.1	0.1	0.2	0.1%
534.2		25.0%	2.5	0.1	0.1	0.2	0.1%
534.8		24.9%	2.5	0.1	0.1	0.2	0.1%
535.5		25.0%	2.5	0.1	0.1	0.2	0.1%
536.1		24.9%	2.5	0.1	0.1	0.2	0.1%
536.7		25.1%	2.5	0.1	0.1	0.2	0.1%
537.3		25.0%	2.5	0.1	0.1	0.2	0.1%
537.9		25.2%	2.5	0.1	0.1	0.2	0.1%
538.5		25.0%	2.5	0.1	0.1	0.2	0.1%
539.2		25.1%	2.5	0.1	0.1	0.2	0.1%
539.8		24.9%	2.5	0.1	0.1	0.2	0.1%
540.4		25.1%	2.5	0.1	0.1	0.2	0.1%
541.0		25.0%	2.5	0.1	0.1	0.2	0.1%
541.6		25.0%	2.5	0.1	0.1	0.2	0.1%
542.2		24.9%	2.5	0.1	0.1	0.2	0.1%
542.9		25.0%	2.5	0.1	0.1	0.2	0.1%
543.5		25.0%	2.5	0.1	0.1	0.2	0.1%
544.7		26.2%	2.4	0.1	0.1	0.2	0.4%
545.3		25.3%	2.5	0.1	0.1	0.2	0.2%
546.6		25.8%	2.4	0.1	0.1	0.2	0.3%
547.2		26.2%	2.4	0.1	0.1	0.2	0.4%
547.8		26.1%	2.4	0.1	0.1	0.2	0.3%
548.4		26.0%	2.4	0.1	0.1	0.2	0.3%
549.0		25.5%	2.4	0.1	0.1	0.2	0.3%
599.8		24.3%	2.4	0.1	0.1	0.2	0.8%

Space Velocity – 20,000 h^{-1}

Time-on-stream (h)	T (°C)	X_{CO}	Molar Flow (mmol/min)				$C_{Balance}$
			H_2	CO	CO_2	Ar	
437.1	375	13.8%	2.4	0.3	0.9	0.1	0.2%
437.7		13.1%	2.5	0.3	1.0	0.1	0.1%
438.3		13.6%	2.5	0.3	1.0	0.1	0.1%
438.9		13.1%	2.5	0.3	1.0	0.1	0.1%
439.5		13.5%	2.5	0.3	1.0	0.1	0.1%
440.2		13.1%	2.5	0.3	1.0	0.1	0.1%
440.8		12.1%	2.4	0.3	0.9	0.1	0.2%
441.4		13.5%	2.5	0.3	1.0	0.1	0.1%
442.0		13.3%	2.5	0.3	1.0	0.1	0.1%
442.6		13.1%	2.5	0.3	1.0	0.1	0.0%
443.3		12.4%	2.5	0.3	1.0	0.1	-0.1%
443.9		13.6%	2.5	0.3	1.0	0.1	0.1%
444.5		14.0%	2.4	0.3	0.9	0.1	0.3%
445.1		13.7%	2.5	0.3	1.0	0.1	0.1%
445.7		13.4%	2.5	0.3	1.0	0.1	0.1%
446.3		13.3%	2.5	0.3	1.0	0.1	0.1%
447.0		14.2%	2.4	0.3	0.9	0.1	0.4%
447.6		12.9%	2.5	0.3	1.0	0.1	0.0%
448.2		13.3%	2.5	0.3	1.0	0.1	0.0%
448.8		13.0%	2.5	0.3	1.0	0.1	0.0%
449.4		13.2%	2.5	0.3	1.0	0.1	0.1%
450.1		13.2%	2.5	0.3	1.0	0.1	0.0%
450.7		12.8%	2.5	0.3	1.0	0.1	0.0%
451.3		13.4%	2.5	0.3	1.0	0.1	0.1%
452.5		13.6%	2.4	0.3	0.9	0.1	0.2%
456.3	400	24.3%	2.5	0.2	1.0	0.1	-0.1%
456.9		24.4%	2.5	0.2	1.0	0.1	0.0%
457.5		22.4%	2.5	0.3	1.0	0.1	0.1%
458.1		24.6%	2.5	0.2	1.0	0.1	0.1%
458.7		24.1%	2.5	0.2	1.0	0.1	0.0%
459.4		24.3%	2.5	0.2	1.0	0.1	0.0%
460.0		24.2%	2.5	0.2	1.0	0.1	0.0%
460.6		24.1%	2.5	0.2	1.0	0.1	0.1%
461.2		24.1%	2.5	0.2	1.0	0.1	0.0%
461.8		24.4%	2.5	0.2	1.0	0.1	0.1%
462.4		24.1%	2.5	0.2	1.0	0.1	0.0%
463.0		24.2%	2.5	0.2	1.0	0.1	0.0%
464.3		24.2%	2.5	0.2	1.0	0.1	-0.1%
464.9		24.0%	2.5	0.2	1.0	0.1	0.0%
465.5		24.3%	2.5	0.2	1.0	0.1	0.0%
466.1		24.3%	2.5	0.2	1.0	0.1	0.0%

Time-on-stream (h)	T (°C)	X_{CO}	Molar Flow (mmol/min)				$C_{Balance}$
			H_2	CO	CO_2	Ar	
466.7	400	24.2%	2.5	0.2	1.0	0.1	0.0%
467.3		24.2%	2.5	0.2	1.0	0.1	0.0%
468.0		24.2%	2.5	0.2	1.0	0.1	0.0%
468.6		24.2%	2.5	0.2	1.0	0.1	0.1%
469.2		24.4%	2.5	0.2	1.0	0.1	0.1%
469.8		24.5%	2.5	0.2	1.0	0.1	0.0%
470.4		24.2%	2.5	0.2	1.0	0.1	0.0%
471.0		24.3%	2.5	0.2	1.0	0.1	0.0%
471.7		23.6%	2.5	0.2	1.0	0.1	0.0%
472.3		24.4%	2.5	0.2	1.0	0.1	0.0%
472.9		24.4%	2.5	0.2	1.0	0.1	0.0%
482.7	430	38.2%	2.5	0.2	1.0	0.1	-0.1%
483.3		37.8%	2.5	0.2	1.0	0.1	-0.1%
483.9		38.1%	2.5	0.2	1.0	0.1	-0.1%
484.6		38.0%	2.5	0.2	1.0	0.1	-0.1%
485.2		38.1%	2.5	0.2	1.0	0.1	-0.1%
485.8		37.7%	2.5	0.2	1.0	0.1	0.0%
486.4		38.2%	2.5	0.2	1.0	0.1	0.2%
487.0		37.9%	2.5	0.2	1.0	0.1	-0.1%
487.6		38.8%	2.5	0.2	1.0	0.1	0.1%
488.2		37.9%	2.5	0.2	1.0	0.1	0.0%
488.9		38.0%	2.5	0.2	1.0	0.1	-0.1%
489.5		38.0%	2.5	0.2	1.0	0.1	0.0%
490.1		38.0%	2.5	0.2	1.0	0.1	-0.1%
490.7		37.1%	2.5	0.2	1.0	0.1	0.0%
491.3		37.3%	2.5	0.2	1.0	0.1	-0.1%
491.9		37.8%	2.5	0.2	1.0	0.1	-0.1%
492.6		38.6%	2.5	0.2	1.0	0.1	-0.1%
493.2		37.5%	2.5	0.2	1.0	0.1	-0.1%
493.8		37.6%	2.5	0.2	1.0	0.1	-0.1%
494.4		37.6%	2.5	0.2	1.0	0.1	-0.1%
495.0		37.6%	2.5	0.2	1.0	0.1	-0.1%
495.6		37.5%	2.5	0.2	1.0	0.1	-0.1%
496.3		37.6%	2.5	0.2	1.0	0.1	-0.1%
496.9		37.3%	2.5	0.2	1.0	0.1	-0.1%
497.5		37.5%	2.5	0.2	1.0	0.1	0.1%
498.1		36.6%	2.5	0.2	1.0	0.1	0.3%
510.4	445	44.7%	2.5	0.2	0.0	0.1	18.5%
511.0		45.4%	2.5	0.2	1.1	0.1	-0.1%
511.6		45.3%	2.5	0.2	1.1	0.1	-0.1%
512.2		45.2%	2.5	0.2	1.1	0.1	0.0%
512.9		45.4%	2.5	0.2	1.1	0.1	-0.1%

Time-on-stream (h)	T (°C)	X_{CO}	Molar Flow (mmol/min)				$C_{Balance}$
			H_2	CO	CO_2	Ar	
513.5	445	45.3%	2.5	0.2	1.1	0.1	-0.1%
514.1		44.6%	2.5	0.2	1.1	0.1	-0.1%
514.7		44.6%	2.5	0.2	1.1	0.1	-0.1%
515.3		44.8%	2.5	0.2	1.1	0.1	0.0%
515.9		44.8%	2.5	0.2	1.1	0.1	-0.1%
516.5		44.6%	2.5	0.2	1.1	0.1	0.0%
517.2		44.2%	2.5	0.2	1.1	0.1	0.0%
517.8		44.6%	2.5	0.2	1.1	0.1	-0.1%
518.4		44.4%	2.5	0.2	1.1	0.1	-0.1%
519.0		43.5%	2.5	0.2	1.1	0.1	-0.1%
519.6		44.7%	2.5	0.2	1.1	0.1	-0.1%
520.2		45.3%	2.5	0.2	1.1	0.1	-0.1%
520.8		45.6%	2.5	0.2	1.1	0.1	0.2%
521.5		45.1%	2.5	0.2	1.1	0.1	0.2%
522.1		45.6%	2.5	0.2	1.1	0.1	0.2%
527.0	375	12.1%	2.5	0.3	1.0	0.1	0.1%
527.6		12.2%	2.5	0.3	0.9	0.1	0.1%
528.2		12.2%	2.4	0.3	0.9	0.1	0.2%
528.8		12.2%	2.5	0.3	0.9	0.1	0.2%
529.5		12.2%	2.5	0.3	0.9	0.1	0.2%
530.1		12.0%	2.4	0.3	0.9	0.1	0.1%
530.7		12.4%	2.5	0.3	0.9	0.1	0.1%
531.3		12.5%	2.5	0.3	0.9	0.1	0.1%
531.9		12.5%	2.5	0.3	0.9	0.1	0.1%
532.5		10.9%	2.5	0.3	0.9	0.1	0.0%
533.2		12.7%	2.4	0.3	0.9	0.1	0.2%
533.8		12.6%	2.5	0.3	0.9	0.1	0.1%
534.4		12.6%	2.5	0.3	0.9	0.1	0.1%
535.0		12.5%	2.5	0.3	0.9	0.1	0.2%
535.6		12.7%	2.4	0.3	0.9	0.1	0.2%
536.2		12.4%	2.5	0.3	0.9	0.1	0.1%
536.9		12.5%	2.5	0.3	0.9	0.1	0.1%
537.5		12.6%	2.5	0.3	0.9	0.1	0.1%
538.1		12.6%	2.5	0.3	0.9	0.1	0.2%
538.7		12.6%	2.5	0.3	1.0	0.1	0.1%
539.3		12.6%	2.4	0.3	0.9	0.1	0.1%
539.9		12.6%	2.5	0.3	0.9	0.1	0.1%
540.5		12.6%	2.5	0.3	0.9	0.1	0.1%
541.2		12.5%	2.4	0.3	1.0	0.1	0.1%
541.8		12.6%	2.4	0.3	1.0	0.1	0.1%
542.4		12.4%	2.4	0.3	1.0	0.1	0.1%
543.0		12.5%	2.4	0.3	1.0	0.1	0.1%
543.6		12.3%	2.4	0.3	0.9	0.1	0.2%

Time-on-stream (h)	T (°C)	X_{CO}	Molar Flow (mmol/min)				$C_{Balance}$
			H_2	CO	CO_2	Ar	
544.9	375	12.7%	2.5	0.3	0.9	0.1	0.1%
545.5		12.8%	2.4	0.3	0.9	0.1	0.2%
546.7		12.8%	2.4	0.3	1.0	0.1	0.1%
547.3		13.8%	2.4	0.3	0.9	0.1	0.3%
548.0		13.7%	2.4	0.3	0.9	0.1	0.3%
548.6		12.7%	2.4	0.3	0.9	0.1	0.1%
549.2		12.2%	2.4	0.3	1.0	0.1	0.0%
549.8		11.1%	2.4	0.3	1.0	0.1	0.0%

Experiment 18-20 – Catalyst X, Feed 2

Space Velocity – 5,000 h^{-1}

Time-on-stream (h)	T (°C)	X_{CO}	Molar Flow (mmol/min)				$C_{Balance}$
			H_2	CO	CO_2	Ar	
50.9	200	17.5%	1.3	0.4	0.3	0.1	-0.6%
51.5		17.3%	1.3	0.4	0.3	0.1	-0.5%
52.1		16.8%	1.3	0.4	0.3	0.1	-0.4%
52.7		17.9%	1.2	0.4	0.3	0.1	0.0%
53.3		16.7%	1.3	0.4	0.3	0.1	-0.4%
53.9		17.6%	1.3	0.4	0.3	0.1	-0.2%
54.5		17.0%	1.3	0.4	0.3	0.1	-0.3%
55.2		17.4%	1.2	0.4	0.3	0.1	0.0%
55.8		16.2%	1.3	0.4	0.3	0.1	-0.3%
56.4		17.0%	1.2	0.4	0.3	0.1	0.0%
57.0		16.0%	1.3	0.4	0.3	0.1	-0.2%
57.6		15.9%	1.3	0.4	0.3	0.1	-0.2%
58.2		16.1%	1.3	0.4	0.3	0.1	-0.2%
58.9		16.2%	1.3	0.4	0.3	0.1	-0.2%
59.5		17.1%	1.2	0.4	0.3	0.1	0.1%
60.1		16.7%	1.3	0.4	0.3	0.1	-0.2%
60.7		17.0%	1.3	0.4	0.3	0.1	-0.2%
61.3		17.1%	1.3	0.4	0.3	0.1	-0.2%
61.9		16.9%	1.3	0.4	0.3	0.1	-0.2%
62.5		17.0%	1.3	0.4	0.3	0.1	-0.2%
63.2		16.9%	1.3	0.4	0.3	0.1	-0.2%
63.8		17.1%	1.3	0.4	0.3	0.1	-0.2%
64.4		16.9%	1.3	0.4	0.3	0.1	-0.2%
65.0		17.0%	1.3	0.4	0.3	0.1	-0.2%
65.6		17.0%	1.3	0.4	0.3	0.1	-0.2%
66.2		17.0%	1.3	0.4	0.3	0.1	-0.2%
66.8		17.0%	1.3	0.4	0.3	0.1	-0.2%
67.5		17.0%	1.3	0.4	0.3	0.1	-0.2%
68.1		17.0%	1.3	0.4	0.3	0.1	-0.2%

Time-on-stream (h)	T (°C)	X_{CO}	Molar Flow (mmol/min)				$C_{Balance}$
			H_2	CO	CO_2	Ar	
68.7	200	16.9%	1.3	0.4	0.3	0.1	-0.2%
69.3		16.8%	1.3	0.4	0.3	0.1	-0.2%
69.9		16.8%	1.3	0.4	0.3	0.1	-0.2%
70.5		16.5%	1.3	0.4	0.3	0.1	-0.2%
71.1		16.7%	1.3	0.4	0.3	0.1	-0.2%
71.8		18.1%	1.2	0.4	0.3	0.1	0.2%
72.4		17.5%	1.3	0.4	0.3	0.1	-0.2%
73.0		17.0%	1.3	0.4	0.3	0.1	-0.2%
75.5	225	35.3%	1.3	0.3	0.4	0.1	-0.4%
76.1		36.7%	1.3	0.3	0.4	0.1	-0.3%
76.7		37.7%	1.3	0.3	0.4	0.1	-0.1%
77.3		37.8%	1.3	0.3	0.4	0.1	-0.3%
77.9		37.1%	1.3	0.3	0.4	0.1	-0.3%
78.5		36.5%	1.3	0.3	0.4	0.1	-0.4%
79.2		36.8%	1.3	0.3	0.4	0.1	-0.3%
79.8		36.7%	1.3	0.3	0.4	0.1	-0.4%
80.4		36.9%	1.3	0.3	0.4	0.1	-0.4%
81.0		37.9%	1.3	0.3	0.4	0.1	-0.2%
81.6		37.3%	1.3	0.3	0.4	0.1	-0.5%
82.2		36.3%	1.3	0.3	0.4	0.1	-0.5%
82.9		36.3%	1.3	0.3	0.4	0.1	-0.5%
83.5		37.5%	1.3	0.3	0.4	0.1	-0.2%
84.1		36.9%	1.3	0.3	0.4	0.1	-0.5%
84.7		37.8%	1.3	0.3	0.4	0.1	-0.2%
85.3		37.9%	1.3	0.3	0.4	0.1	-0.2%
85.9		37.9%	1.3	0.3	0.4	0.1	-0.1%
86.6		37.1%	1.3	0.3	0.4	0.1	-0.4%
87.2		36.9%	1.3	0.3	0.4	0.1	-0.4%
87.8		37.1%	1.3	0.3	0.4	0.1	-0.2%
88.4		36.9%	1.3	0.3	0.4	0.1	-0.2%
89.0		36.9%	1.3	0.3	0.4	0.1	-0.2%
89.7		37.1%	1.3	0.3	0.4	0.1	-0.2%
90.3		36.5%	1.3	0.3	0.4	0.1	-0.5%
90.9		37.3%	1.3	0.3	0.4	0.1	-0.2%
91.5		37.4%	1.3	0.3	0.4	0.1	-0.2%
92.1		36.4%	1.3	0.3	0.4	0.1	-0.4%
92.7		36.1%	1.3	0.3	0.4	0.1	-0.5%
93.4		36.8%	1.3	0.3	0.4	0.1	-0.2%
94.0		37.0%	1.3	0.3	0.4	0.1	-0.1%
94.6		36.2%	1.3	0.3	0.4	0.1	-0.5%
95.2		36.8%	1.3	0.3	0.4	0.1	-0.4%
95.8		36.4%	1.3	0.3	0.4	0.1	-0.5%
96.4		36.5%	1.3	0.3	0.4	0.1	-0.5%

Time-on-stream (h)	T (°C)	X_{CO}	Molar Flow (mmol/min)				$C_{Balance}$
			H_2	CO	CO_2	Ar	
97.1	225	37.3%	1.3	0.3	0.4	0.1	-0.2%
97.7		37.0%	1.3	0.3	0.4	0.1	-0.5%
98.3		38.1%	1.3	0.3	0.4	0.1	-0.1%
98.9		37.3%	1.3	0.3	0.4	0.1	-0.5%
99.5		37.3%	1.3	0.3	0.4	0.1	-0.2%
100.1		38.0%	1.3	0.3	0.4	0.1	-0.6%
100.8		40.1%	1.3	0.3	0.4	0.1	-0.3%
101.4		39.1%	1.3	0.3	0.4	0.1	-0.5%
102.0		40.1%	1.3	0.3	0.4	0.1	-0.2%
102.6		39.7%	1.3	0.3	0.4	0.1	-0.4%
103.2		40.0%	1.3	0.3	0.4	0.1	-0.2%
103.8		37.6%	1.3	0.3	0.4	0.1	-0.5%
104.4		37.3%	1.3	0.3	0.4	0.1	-0.5%
105.1		37.2%	1.3	0.3	0.4	0.1	-0.5%
105.7		36.9%	1.3	0.3	0.4	0.1	-0.4%
106.3		36.6%	1.3	0.3	0.4	0.1	-0.4%
106.9		37.9%	1.3	0.3	0.4	0.1	-0.6%
107.5		37.7%	1.3	0.3	0.4	0.1	-0.5%
108.1		37.7%	1.3	0.3	0.4	0.1	-0.4%
108.8		38.1%	1.3	0.3	0.4	0.1	-0.5%
109.4		37.9%	1.3	0.3	0.4	0.1	-0.5%
110.0		37.9%	1.3	0.3	0.4	0.1	-0.5%
110.6		38.0%	1.3	0.3	0.4	0.1	-0.5%
111.2		38.5%	1.3	0.3	0.4	0.1	-0.5%
111.8		37.9%	1.3	0.3	0.4	0.1	-0.5%
112.4		38.8%	1.3	0.3	0.4	0.1	-0.2%
113.1		39.4%	1.3	0.3	0.4	0.1	-0.2%
113.7		38.2%	1.3	0.3	0.4	0.1	-0.5%
114.3		38.4%	1.3	0.3	0.4	0.1	-0.4%
114.9		38.5%	1.3	0.3	0.4	0.1	-0.5%
115.5		37.8%	1.3	0.3	0.4	0.1	-0.5%
116.1		38.2%	1.3	0.3	0.4	0.1	-0.2%
116.8		37.7%	1.3	0.3	0.4	0.1	-0.5%
117.4		37.8%	1.3	0.3	0.4	0.1	-0.5%
118.0		38.0%	1.3	0.3	0.4	0.1	-0.4%
118.6		37.7%	1.3	0.3	0.4	0.1	-0.6%
119.2		37.8%	1.3	0.3	0.4	0.1	-0.5%
119.8		38.1%	1.3	0.3	0.4	0.1	-0.5%
120.4		37.9%	1.3	0.3	0.4	0.1	-0.5%
121.1		41.8%	1.2	0.3	0.4	0.1	1.1%
121.7		37.8%	1.3	0.3	0.4	0.1	-0.4%
122.3		37.4%	1.3	0.3	0.4	0.1	-0.5%
122.9		37.4%	1.3	0.3	0.4	0.1	-0.5%

Time-on-stream (h)	T (°C)	X_{CO}	Molar Flow (mmol/min)				$C_{Balance}$
			H_2	CO	CO_2	Ar	
123.5	225	38.2%	1.3	0.3	0.4	0.1	-0.5%
124.3		37.6%	1.3	0.3	0.4	0.1	-0.6%
124.9		38.3%	1.3	0.3	0.4	0.1	-0.4%
125.5		37.7%	1.3	0.3	0.4	0.1	-0.5%
126.1		37.4%	1.3	0.3	0.4	0.1	-0.5%
126.8		37.4%	1.3	0.3	0.4	0.1	-0.5%
127.4		37.5%	1.3	0.3	0.4	0.1	-0.5%
128.0		37.1%	1.3	0.3	0.4	0.1	-0.5%
128.6		37.5%	1.3	0.3	0.4	0.1	-0.5%
129.2		37.6%	1.3	0.3	0.4	0.1	-0.5%
129.8		41.0%	1.3	0.3	0.4	0.1	-0.6%
130.5		41.1%	1.3	0.3	0.4	0.1	-0.6%
131.1		37.5%	1.3	0.3	0.4	0.1	-0.5%
131.7		37.1%	1.3	0.3	0.4	0.1	-0.5%
132.3		37.6%	1.3	0.3	0.4	0.1	-0.5%
132.9		37.6%	1.3	0.3	0.4	0.1	-0.5%
133.5		37.8%	1.3	0.3	0.4	0.1	-0.5%
134.2		38.0%	1.3	0.3	0.4	0.1	-0.6%
134.8		38.0%	1.3	0.3	0.4	0.1	-0.5%
135.4		38.3%	1.3	0.3	0.4	0.1	-0.4%
136.0		45.3%	1.2	0.2	0.3	0.1	2.2%
136.6		38.0%	1.3	0.3	0.4	0.1	-0.5%
137.2		37.9%	1.3	0.3	0.4	0.1	-0.5%
137.8		38.1%	1.3	0.3	0.4	0.1	-0.5%
138.5		38.2%	1.3	0.3	0.4	0.1	-0.5%
139.1		38.3%	1.3	0.3	0.4	0.1	-0.6%
139.7		37.7%	1.3	0.3	0.4	0.1	-0.5%
140.3		37.7%	1.3	0.3	0.4	0.1	-0.5%
140.9		38.2%	1.3	0.3	0.4	0.1	-0.5%
141.5		37.5%	1.3	0.3	0.4	0.1	-0.5%
142.2		38.1%	1.3	0.3	0.4	0.1	-0.5%
142.8		37.8%	1.3	0.3	0.4	0.1	-0.5%
143.4		38.6%	1.3	0.3	0.4	0.1	-0.3%
144.0		37.6%	1.3	0.3	0.4	0.1	-0.1%
144.6		36.4%	1.3	0.3	0.4	0.1	-0.5%
145.2		37.2%	1.3	0.3	0.4	0.1	-0.1%
148.1	250	69.7%	1.3	0.1	0.5	0.1	-0.2%
148.7		68.9%	1.3	0.1	0.5	0.1	-0.2%
149.3		69.2%	1.3	0.1	0.5	0.1	-0.2%
150.0		70.5%	1.3	0.1	0.5	0.1	-0.2%
150.6		72.7%	1.4	0.1	0.5	0.1	-0.7%
151.2		74.6%	1.3	0.1	0.5	0.1	-0.3%
151.8		73.3%	1.4	0.1	0.5	0.1	-0.8%

Time-on-stream (h)	T (°C)	X_{CO}	Molar Flow (mmol/min)				$C_{Balance}$
			H_2	CO	CO_2	Ar	
152.4	250	72.9%	1.4	0.1	0.6	0.1	-1.0%
153.0		73.7%	1.3	0.1	0.5	0.1	-0.3%
153.6		71.5%	1.3	0.1	0.5	0.1	-0.3%
154.3		71.2%	1.4	0.1	0.5	0.1	-0.7%
154.9		71.5%	1.4	0.1	0.5	0.1	-1.0%
155.5		71.8%	1.4	0.1	0.5	0.1	-0.7%
156.1		72.1%	1.4	0.1	0.5	0.1	-0.8%
156.7		73.2%	1.3	0.1	0.5	0.1	-0.4%
157.3		72.5%	1.4	0.1	0.6	0.1	-1.1%
157.9		72.6%	1.4	0.1	0.5	0.1	-0.8%
158.5		73.9%	1.3	0.1	0.5	0.1	-0.4%
159.2		73.7%	1.3	0.1	0.5	0.1	-0.4%
159.8		73.6%	1.3	0.1	0.5	0.1	-0.4%
160.4		73.3%	1.3	0.1	0.5	0.1	-0.4%
161.0		72.4%	1.4	0.1	0.6	0.1	-1.1%
161.6		72.3%	1.4	0.1	0.6	0.1	-1.0%
162.2		72.7%	1.4	0.1	0.5	0.1	-0.8%
162.8		73.1%	1.4	0.1	0.5	0.1	-0.8%
163.4		72.4%	1.4	0.1	0.5	0.1	-0.8%
164.1		72.4%	1.4	0.1	0.5	0.1	-0.8%
164.7		71.5%	1.4	0.1	0.6	0.1	-1.1%
165.3		72.6%	1.4	0.1	0.5	0.1	-0.8%
165.9		72.0%	1.4	0.1	0.5	0.1	-0.9%
166.5		72.1%	1.4	0.1	0.5	0.1	-0.9%
167.1		72.4%	1.4	0.1	0.5	0.1	-0.9%
167.7		75.0%	1.4	0.1	0.6	0.1	-0.9%
168.4		75.1%	1.4	0.1	0.5	0.1	-0.3%
169.0		72.0%	1.4	0.1	0.5	0.1	-0.7%
224.9	275	93.0%	1.4	0.0	0.6	0.1	-0.7%
225.6		92.8%	1.4	0.0	0.6	0.1	-0.6%
226.2		92.6%	1.4	0.0	0.6	0.1	-0.8%
226.8		92.8%	1.4	0.0	0.6	0.1	-0.6%
227.4		93.4%	1.4	0.0	0.6	0.1	-0.7%
228.0		93.6%	1.4	0.0	0.6	0.1	-0.8%
228.6		93.6%	1.4	0.0	0.6	0.1	-0.6%
229.2		93.3%	1.4	0.0	0.6	0.1	-0.7%
229.9		93.4%	1.4	0.0	0.6	0.1	-0.8%
230.5		92.0%	1.4	0.0	0.6	0.1	-0.7%
231.1		92.6%	1.4	0.0	0.6	0.1	-0.8%
231.7		93.0%	1.4	0.0	0.6	0.1	-0.7%
232.3		93.1%	1.4	0.0	0.6	0.1	-0.7%
232.9		93.1%	1.4	0.0	0.6	0.1	-0.7%
233.6		93.2%	1.4	0.0	0.6	0.1	-0.7%

Time-on-stream (h)	T (°C)	X_{CO}	Molar Flow (mmol/min)				$C_{Balance}$
			H_2	CO	CO_2	Ar	
234.2	275	93.1%	1.4	0.0	0.6	0.1	-0.7%
234.8		92.9%	1.4	0.0	0.6	0.1	-0.7%
235.4		93.1%	1.4	0.0	0.6	0.1	-0.7%
236.0		92.8%	1.4	0.0	0.6	0.1	-0.7%
236.6		92.9%	1.4	0.0	0.6	0.1	-0.5%
237.3		92.5%	1.4	0.0	0.6	0.1	-0.8%
237.9		92.5%	1.4	0.0	0.6	0.1	-0.7%
238.5		92.8%	1.4	0.0	0.6	0.1	-0.7%
239.1		93.2%	1.4	0.0	0.6	0.1	-0.7%
239.7		91.9%	1.4	0.0	0.6	0.1	-0.8%
240.3		91.8%	1.4	0.0	0.6	0.1	-0.7%
240.9		92.5%	1.4	0.0	0.6	0.1	-0.7%
241.6		92.5%	1.4	0.0	0.7	0.1	-1.4%
242.2		92.6%	1.4	0.0	0.6	0.1	-0.7%
242.8		93.3%	1.4	0.0	0.6	0.1	-0.7%
243.4		92.9%	1.4	0.0	0.6	0.1	-0.7%
244.0		92.1%	1.4	0.0	0.6	0.1	-0.6%
244.6		91.8%	1.4	0.0	0.6	0.1	-0.7%
245.3		92.3%	1.4	0.0	0.6	0.1	-0.7%
245.9		87.9%	1.4	0.1	0.6	0.1	-0.6%
246.5		95.0%	1.4	0.0	0.6	0.1	-0.7%
247.1		0.0%	1.4	0.2	0.6	0.1	-4.8%
247.7		92.3%	1.4	0.0	0.7	0.1	-1.4%
248.3		92.3%	1.4	0.0	0.6	0.1	-0.7%
249.0		92.0%	1.4	0.0	0.6	0.1	-0.8%
249.6		96.6%	1.4	0.0	0.7	0.1	-0.8%
250.2		92.7%	1.4	0.0	0.6	0.1	-0.7%
250.8		92.7%	1.4	0.0	0.6	0.1	-0.8%
251.4		92.4%	1.4	0.0	0.6	0.1	-0.8%
252.1		93.4%	1.4	0.0	0.6	0.1	-0.8%
252.7		93.1%	1.4	0.0	0.6	0.1	-0.7%
253.3		93.8%	1.4	0.0	0.6	0.1	-0.8%
253.9		93.7%	1.4	0.0	0.6	0.1	-0.8%
254.5		93.7%	1.4	0.0	0.6	0.1	-0.8%
255.1		93.5%	1.4	0.0	0.6	0.1	-0.8%
255.8		93.2%	1.4	0.0	0.7	0.1	-1.4%
256.4		93.4%	1.4	0.0	0.6	0.1	-0.8%
257.0		92.5%	1.4	0.0	0.7	0.1	-1.4%
257.6		92.5%	1.4	0.0	0.6	0.1	-0.8%
258.2		92.6%	1.4	0.0	0.6	0.1	-0.8%
258.8		92.3%	1.4	0.0	0.6	0.1	-0.8%
259.5		92.7%	1.4	0.0	0.6	0.1	-1.2%
260.1		92.9%	1.4	0.0	0.6	0.1	-0.8%
260.7		96.0%	1.4	0.0	0.7	0.1	-0.8%

Time-on-stream (h)	T (°C)	X_{CO}	Molar Flow (mmol/min)				$C_{Balance}$
			H_2	CO	CO_2	Ar	
261.3	275	92.6%	1.4	0.0	0.7	0.1	-1.3%
261.9		93.0%	1.4	0.0	0.6	0.1	-0.8%
262.6		92.9%	1.4	0.0	0.6	0.1	-0.9%
263.2		93.3%	1.4	0.0	0.6	0.1	-0.8%
263.8		93.1%	1.4	0.0	0.6	0.1	-0.8%
264.4		92.9%	1.4	0.0	0.6	0.1	-0.9%
265.0		93.0%	1.4	0.0	0.6	0.1	-0.8%
265.8		92.7%	1.4	0.0	0.7	0.1	-1.4%
266.4		93.0%	1.4	0.0	0.6	0.1	-0.9%
267.0		93.3%	1.4	0.0	0.6	0.1	-0.7%
267.6		92.9%	1.4	0.0	0.7	0.1	-1.2%
268.2		93.6%	1.4	0.0	0.6	0.1	-0.8%

Space Velocity – 10,000 h^{-1}

Time-on-stream (h)	T (°C)	X_{CO}	Molar Flow (mmol/min)				$C_{Balance}$
			H_2	CO	CO_2	Ar	
50.7	200	5.3%	2.5	0.9	0.4	0.2	-0.1%
51.3		6.4%	2.4	0.9	0.4	0.2	0.2%
51.9		6.1%	2.4	0.9	0.4	0.2	0.1%
52.5		5.5%	2.4	0.9	0.4	0.2	0.0%
53.2		6.4%	2.4	0.9	0.4	0.2	0.2%
53.8		5.3%	2.5	0.9	0.4	0.2	0.0%
54.4		5.6%	2.5	0.9	0.4	0.2	0.0%
55.0		5.5%	2.5	0.9	0.4	0.2	0.0%
55.6		5.3%	2.5	0.9	0.4	0.2	0.0%
56.2		5.3%	2.5	0.9	0.4	0.2	0.0%
56.9		5.3%	2.5	0.9	0.4	0.2	0.0%
57.5		5.3%	2.5	0.9	0.4	0.2	0.0%
58.1		5.3%	2.5	0.9	0.4	0.2	0.0%
58.7		5.3%	2.5	0.9	0.4	0.2	0.0%
59.3		5.2%	2.5	0.9	0.4	0.2	0.0%
59.9		5.4%	2.5	0.9	0.4	0.2	0.0%
60.5		5.5%	2.5	0.9	0.4	0.2	0.0%
61.2		5.5%	2.5	0.9	0.4	0.2	0.0%
61.8		5.5%	2.5	0.9	0.4	0.2	0.0%
62.4		5.5%	2.5	0.9	0.4	0.2	0.0%
63.0		5.5%	2.5	0.9	0.4	0.2	0.0%
63.6		5.6%	2.5	0.9	0.4	0.2	0.0%
64.2		5.5%	2.5	0.9	0.4	0.2	0.0%
64.8		5.5%	2.5	0.9	0.4	0.2	0.0%
65.5		5.5%	2.5	0.9	0.4	0.2	0.0%
66.1		5.5%	2.5	0.9	0.4	0.2	0.0%
66.7		5.6%	2.5	0.9	0.4	0.2	0.0%

Time-on-stream (h)	T (°C)	X_{CO}	Molar Flow (mmol/min)				$C_{Balance}$
			H_2	CO	CO_2	Ar	
67.3	200	5.6%	2.5	0.9	0.4	0.2	0.0%
67.9		5.6%	2.5	0.9	0.4	0.2	0.0%
68.5		5.5%	2.5	0.9	0.4	0.2	0.0%
69.2		5.5%	2.5	0.9	0.4	0.2	0.0%
69.8		5.5%	2.5	0.9	0.4	0.2	0.0%
70.4		5.2%	2.5	0.9	0.4	0.2	0.0%
71.0		5.5%	2.5	0.9	0.4	0.2	0.0%
71.6		6.0%	2.5	0.9	0.4	0.2	0.1%
72.2		5.6%	2.5	0.9	0.4	0.2	0.0%
72.8		5.5%	2.5	0.9	0.4	0.2	0.0%
73.5		5.5%	2.5	0.9	0.4	0.2	0.0%
75.3	225	11.7%	2.5	0.8	0.5	0.2	-0.1%
75.9		11.8%	2.5	0.8	0.5	0.2	-0.1%
76.5		12.2%	2.5	0.8	0.5	0.2	0.0%
77.2		13.9%	2.5	0.8	0.5	0.2	0.1%
77.8		11.9%	2.5	0.8	0.5	0.2	-0.1%
78.4		13.1%	2.5	0.8	0.5	0.2	0.2%
79.0		11.7%	2.5	0.8	0.5	0.2	-0.1%
79.6		12.1%	2.5	0.8	0.5	0.2	-0.1%
80.2		12.8%	2.5	0.8	0.5	0.2	-0.1%
80.9		12.8%	2.5	0.8	0.5	0.2	-0.1%
81.5		12.5%	2.5	0.8	0.5	0.2	-0.1%
82.1		11.9%	2.5	0.8	0.5	0.2	-0.1%
82.7		12.0%	2.5	0.8	0.5	0.2	-0.1%
83.3		12.2%	2.5	0.8	0.5	0.2	-0.1%
83.9		13.4%	2.5	0.8	0.5	0.2	0.2%
84.6		12.2%	2.5	0.8	0.5	0.2	-0.1%
85.2		12.3%	2.5	0.8	0.5	0.2	-0.1%
85.8		12.3%	2.5	0.8	0.5	0.2	-0.1%
86.4		12.1%	2.5	0.8	0.5	0.2	-0.1%
87.0		12.1%	2.5	0.8	0.5	0.2	-0.1%
87.6		12.3%	2.5	0.8	0.5	0.2	-0.1%
88.3		13.4%	2.5	0.8	0.5	0.2	0.2%
88.9		12.2%	2.5	0.8	0.5	0.2	-0.1%
89.5		12.2%	2.5	0.8	0.5	0.2	-0.1%
90.1		12.2%	2.5	0.8	0.5	0.2	-0.1%
90.7		12.2%	2.5	0.8	0.5	0.2	-0.1%
91.4		12.1%	2.5	0.8	0.5	0.2	-0.1%
92.0		12.0%	2.5	0.8	0.5	0.2	-0.1%
92.6		12.1%	2.5	0.8	0.5	0.2	-0.1%
93.2		12.1%	2.5	0.8	0.5	0.2	-0.1%
93.8		12.0%	2.5	0.8	0.5	0.2	-0.1%
94.4		12.1%	2.5	0.8	0.5	0.2	-0.1%
95.1		12.3%	2.5	0.8	0.5	0.2	-0.1%

Time-on-stream (h)	T (°C)	X_{CO}	Molar Flow (mmol/min)				$C_{Balance}$
			H_2	CO	CO_2	Ar	
95.7	225	12.1%	2.5	0.8	0.5	0.2	-0.1%
96.3		11.8%	2.5	0.8	0.5	0.2	-0.1%
96.9		11.9%	2.5	0.8	0.5	0.2	-0.1%
97.5		12.0%	2.5	0.8	0.5	0.2	-0.1%
98.1		12.2%	2.5	0.8	0.5	0.2	-0.1%
98.8		14.2%	2.5	0.8	0.5	0.2	-0.1%
99.4		13.0%	2.5	0.8	0.5	0.2	-0.1%
100.0		12.9%	2.5	0.8	0.5	0.2	-0.1%
100.6		13.5%	2.5	0.8	0.5	0.2	-0.1%
101.2		13.4%	2.5	0.8	0.5	0.2	-0.1%
101.8		13.4%	2.5	0.8	0.5	0.2	-0.1%
102.4		12.0%	2.5	0.8	0.5	0.2	-0.1%
103.1		12.5%	2.5	0.8	0.5	0.2	-0.1%
103.7		12.4%	2.5	0.8	0.5	0.2	-0.1%
104.3		14.1%	2.5	0.8	0.5	0.2	-0.1%
104.9		13.9%	2.5	0.8	0.5	0.2	-0.1%
105.5		13.5%	2.5	0.8	0.5	0.2	-0.1%
106.1		13.4%	2.5	0.8	0.5	0.2	-0.1%
106.8		13.2%	2.5	0.8	0.5	0.2	-0.1%
107.4		12.8%	2.5	0.8	0.5	0.2	-0.1%
108.0		13.0%	2.5	0.8	0.5	0.2	-0.1%
108.6		12.9%	2.5	0.8	0.5	0.2	-0.1%
109.2		12.7%	2.5	0.8	0.5	0.2	-0.1%
109.8		13.1%	2.5	0.8	0.5	0.2	-0.1%
110.4		13.1%	2.5	0.8	0.5	0.2	-0.1%
111.1		12.9%	2.5	0.8	0.5	0.2	-0.1%
111.7		13.0%	2.5	0.8	0.5	0.2	-0.1%
112.3		13.2%	2.5	0.8	0.5	0.2	-0.1%
112.9		12.8%	2.5	0.8	0.5	0.2	-0.1%
113.5		13.1%	2.5	0.8	0.5	0.2	-0.1%
114.1		13.1%	2.5	0.8	0.5	0.2	-0.1%
114.8		13.0%	2.5	0.8	0.5	0.2	-0.1%
115.4		12.9%	2.5	0.8	0.5	0.2	-0.1%
116.0		13.1%	2.5	0.8	0.5	0.2	-0.1%
116.6		13.0%	2.5	0.8	0.5	0.2	-0.1%
117.2		12.9%	2.5	0.8	0.5	0.2	-0.1%
117.8		12.7%	2.5	0.8	0.5	0.2	-0.1%
118.4		13.0%	2.5	0.8	0.5	0.2	-0.1%
119.1		13.0%	2.5	0.8	0.5	0.2	-0.1%
119.7		13.0%	2.5	0.8	0.5	0.2	-0.1%
120.3		12.8%	2.5	0.8	0.5	0.2	-0.1%
121.5		13.0%	2.5	1.0	0.5	0.2	-0.1%
122.1		12.5%	2.5	0.8	0.5	0.2	-0.1%
122.7		12.8%	2.5	0.8	0.5	0.2	-0.1%
123.4		12.8%	2.5	0.8	0.5	0.2	-0.1%

Time-on-stream (h)	T (°C)	X_{CO}	Molar Flow (mmol/min)				$C_{Balance}$
			H_2	CO	CO_2	Ar	
124.1	225	12.8%	2.5	0.8	0.5	0.2	-0.1%
124.8		12.5%	2.5	0.8	0.5	0.2	-0.1%
125.4		12.4%	2.5	0.8	0.5	0.2	-0.1%
126.0		12.7%	2.5	0.8	0.5	0.2	-0.1%
126.6		13.0%	2.5	0.8	0.5	0.2	-0.1%
127.2		12.6%	2.5	0.8	0.5	0.2	-0.1%
127.8		13.2%	2.5	0.8	0.5	0.2	-0.1%
128.5		13.0%	2.5	0.8	0.5	0.2	-0.1%
129.1		13.2%	2.5	0.8	0.5	0.2	-0.1%
129.7		13.3%	2.5	0.8	0.5	0.2	-0.1%
130.3		13.4%	2.5	0.8	0.5	0.2	-0.1%
130.9		13.5%	2.5	0.8	0.5	0.2	-0.1%
131.5		13.5%	2.5	0.8	0.5	0.2	-0.1%
132.2		13.6%	2.5	0.8	0.5	0.2	-0.1%
132.8		13.3%	2.5	0.8	0.5	0.2	-0.1%
133.4		11.1%	2.5	0.8	0.5	0.2	-0.1%
134.0		11.0%	2.5	0.8	0.5	0.2	-0.1%
134.6		11.0%	2.5	0.8	0.5	0.2	-0.1%
135.2		13.4%	2.5	0.8	0.5	0.2	-0.1%
135.8		13.9%	2.5	0.8	0.5	0.2	0.0%
136.5		13.5%	2.5	0.8	0.5	0.2	-0.1%
137.1		13.5%	2.5	0.8	0.5	0.2	-0.1%
137.7		13.4%	2.5	0.8	0.5	0.2	-0.1%
138.3		13.5%	2.5	0.8	0.5	0.2	-0.1%
138.9		13.7%	2.5	0.8	0.5	0.2	-0.1%
139.5		13.7%	2.5	0.8	0.5	0.2	-0.1%
140.2		13.7%	2.5	0.8	0.5	0.2	-0.1%
140.8		12.7%	2.5	0.8	0.5	0.2	0.0%
141.4		12.1%	2.5	0.8	0.5	0.2	-0.1%
142.0		12.9%	2.5	0.8	0.5	0.2	-0.1%
142.6		14.0%	2.5	0.8	0.5	0.2	0.2%
143.2		12.8%	2.5	0.8	0.5	0.2	-0.1%
143.9		11.6%	2.5	0.8	0.5	0.2	-0.1%
144.5		11.1%	2.5	0.8	0.5	0.2	-0.1%
145.1		15.2%	2.5	0.8	0.5	0.2	0.1%
148.6	250	32.5%	2.5	0.6	0.7	0.2	0.1%
149.2		34.0%	2.5	0.6	0.7	0.2	0.5%
149.8		31.2%	2.6	0.6	0.7	0.2	-0.3%
150.4		33.1%	2.6	0.6	0.7	0.2	-0.4%
151.0		32.9%	2.6	0.6	0.7	0.2	-0.3%
151.6		30.6%	2.6	0.6	0.7	0.2	-0.4%
152.3		30.3%	2.6	0.6	0.7	0.2	-0.4%
152.9		30.7%	2.6	0.6	0.7	0.2	-0.3%

Time-on-stream (h)	T (°C)	X_{CO}	Molar Flow (mmol/min)				$C_{Balance}$
			H_2	CO	CO_2	Ar	
153.5	250	31.1%	2.6	0.6	0.7	0.2	-0.4%
154.1		32.3%	2.5	0.6	0.7	0.2	-0.1%
154.7		31.6%	2.6	0.6	0.7	0.2	-0.4%
155.3		32.8%	2.6	0.6	0.7	0.2	-0.4%
155.9		33.2%	2.6	0.6	0.7	0.2	-0.5%
156.6		33.3%	2.6	0.6	0.7	0.2	-0.4%
157.2		33.2%	2.6	0.6	0.7	0.2	-0.4%
157.8		32.9%	2.6	0.6	0.7	0.2	-0.4%
158.4		32.8%	2.6	0.6	0.7	0.2	-0.4%
159.0		32.8%	2.6	0.6	0.7	0.2	-0.4%
159.6		32.8%	2.6	0.6	0.7	0.2	-0.4%
160.2		33.1%	2.6	0.6	0.7	0.2	-0.4%
160.8		32.1%	2.6	0.6	0.7	0.2	-0.4%
161.5		32.2%	2.6	0.6	0.7	0.2	-0.4%
162.1		32.0%	2.6	0.6	0.7	0.2	-0.4%
162.7		32.1%	2.6	0.6	0.7	0.2	-0.4%
163.3		31.9%	2.6	0.6	0.7	0.2	-0.4%
163.9		32.0%	2.6	0.6	0.7	0.2	-0.4%
164.5		31.7%	2.6	0.6	0.7	0.2	-0.4%
165.1		31.9%	2.6	0.6	0.7	0.2	-0.4%
165.7		31.7%	2.6	0.6	0.7	0.2	-0.4%
166.4		31.8%	2.6	0.6	0.7	0.2	-0.4%
167.0		31.6%	2.6	0.6	0.7	0.2	-0.4%
167.6		32.6%	2.6	0.6	0.7	0.2	-0.4%
168.2		32.6%	2.6	0.6	0.7	0.2	-0.4%
168.8		32.4%	2.6	0.6	0.7	0.2	-0.4%
169.4		31.6%	2.6	0.6	0.7	0.2	-0.4%
226.0	275	63.4%	2.6	0.3	1.0	0.2	-0.2%
226.6		63.2%	2.6	0.3	1.0	0.2	-0.1%
227.2		62.5%	2.6	0.3	1.0	0.2	-0.1%
227.9		62.9%	2.7	0.3	1.0	0.2	-0.2%
228.5		63.3%	2.7	0.3	1.0	0.2	-0.2%
229.1		62.9%	2.6	0.3	1.0	0.2	-0.1%
229.7		63.1%	2.6	0.3	1.0	0.2	-0.1%
230.3		62.8%	2.6	0.3	1.0	0.2	-0.1%
230.9		62.5%	2.6	0.3	1.0	0.2	-0.2%
232.2		62.6%	2.7	0.3	1.1	0.2	-0.2%
232.8		61.9%	2.6	0.3	1.0	0.2	-0.7%
233.4		62.5%	2.7	0.3	1.0	0.2	-0.1%
234.0		61.0%	2.6	0.3	1.0	0.2	-0.9%
234.6		62.3%	2.7	0.4	1.0	0.2	-0.2%
235.3		61.8%	2.7	0.3	1.0	0.2	-0.1%
235.9		62.2%	2.7	0.3	1.0	0.2	-0.2%

Time-on-stream (h)	T (°C)	X_{CO}	Molar Flow (mmol/min)				$C_{Balance}$
			H_2	CO	CO_2	Ar	
236.5	275	61.9%	2.7	0.3	1.0	0.2	-0.2%
237.1		60.7%	2.7	0.3	1.0	0.2	-0.2%
237.7		63.2%	2.6	0.4	0.9	0.2	-0.2%
238.3		62.6%	2.7	0.3	1.0	0.2	-0.2%
238.9		62.2%	2.7	0.3	1.0	0.2	-0.2%
239.6		58.4%	2.7	0.3	1.0	0.2	-0.2%
240.8		58.0%	2.7	0.4	0.9	0.2	-0.7%
242.0		58.7%	2.7	0.3	1.0	0.2	-0.1%
242.6		63.0%	2.7	0.4	1.0	0.2	-0.4%
243.3		62.7%	2.8	0.3	1.1	0.2	-0.1%
243.9		61.1%	2.6	0.4	0.9	0.2	0.0%
244.5		59.4%	2.7	0.3	1.0	0.2	-0.1%
245.1		59.3%	2.7	0.3	1.0	0.2	-0.8%
245.7		62.0%	2.6	0.4	0.9	0.2	-0.1%
246.3		65.4%	2.6	0.4	0.9	0.2	0.0%
247.0		67.5%	2.7	0.4	1.0	0.2	-0.2%
247.6		64.2%	2.6	0.3	1.0	0.2	-0.2%
248.2		64.7%	2.6	0.3	1.0	0.2	-0.2%
248.8		64.0%	2.7	0.3	1.0	0.2	-0.2%
249.4		63.3%	2.7	0.3	1.0	0.2	-0.2%
250.0		63.7%	2.7	0.3	1.0	0.2	-0.2%
250.7		64.5%	2.7	0.3	1.0	0.2	-0.2%
251.3		65.0%	2.7	0.3	1.0	0.2	-0.2%
251.9		64.5%	2.7	0.3	1.0	0.2	-0.2%
252.5		64.0%	2.7	0.3	1.0	0.2	-0.2%
253.1		63.7%	2.7	0.3	1.0	0.2	-0.3%
253.8		63.7%	2.7	0.3	1.0	0.2	-0.2%
254.4		63.7%	2.7	0.3	1.0	0.2	-0.9%
255.0		63.9%	2.7	0.3	1.0	0.2	-0.3%
255.6		63.1%	2.7	0.3	1.0	0.2	-0.3%
256.2		64.1%	2.7	0.3	1.0	0.2	-0.2%
256.8		64.1%	2.7	0.3	1.0	0.2	-0.2%
257.5		63.8%	2.7	0.3	1.0	0.2	-0.3%
258.1		63.1%	2.7	0.3	1.0	0.2	-0.7%
258.7		63.9%	2.7	0.3	1.0	0.2	-0.3%
259.3		64.0%	2.7	0.3	1.0	0.2	-0.3%
259.9		63.4%	2.7	0.3	1.0	0.2	-0.3%
260.5		62.8%	2.7	0.3	1.0	0.2	-0.9%
261.2		66.6%	2.7	0.3	1.0	0.2	-0.3%
263.0		63.5%	2.7	0.3	1.0	0.2	-0.2%
263.6		63.5%	2.7	0.3	1.0	0.2	-0.7%
264.2		63.5%	2.7	0.3	1.0	0.2	-0.3%
264.9		63.0%	2.7	0.3	1.0	0.2	-0.8%
265.6		63.4%	2.7	0.3	1.0	0.2	-0.9%

Time-on-stream (h)	T (°C)	X_{CO}	Molar Flow (mmol/min)				$C_{Balance}$
			H_2	CO	CO_2	Ar	
266.3	275	63.9%	2.7	0.3	1.0	0.2	-0.3%
483.7	300	78.7%	2.7	0.2	1.1	0.2	-0.5%
484.3		77.1%	2.7	0.2	1.1	0.2	-0.6%
484.9		79.4%	2.7	0.2	1.1	0.2	-0.5%
485.5		77.9%	2.7	0.2	1.1	0.2	-0.5%
486.2		78.6%	2.7	0.2	1.1	0.2	-0.6%
486.8		77.6%	2.7	0.2	1.1	0.2	-0.6%
487.4		77.5%	2.7	0.2	1.1	0.2	-0.5%
488.0		77.9%	2.7	0.2	1.1	0.2	-0.5%
488.6		78.2%	2.7	0.2	1.1	0.2	-0.6%
489.8		76.5%	2.7	0.3	1.0	0.2	-0.8%
491.1		77.8%	2.8	0.2	1.1	0.2	-0.5%
491.7		78.9%	2.8	0.2	1.2	0.2	-0.6%
492.3		79.6%	2.7	0.2	1.1	0.2	-0.6%
492.9		79.4%	2.7	0.2	1.1	0.2	-0.6%
163.2	350	87.1%	4.3	0.1	1.2	0.2	0.6%
163.8		87.0%	4.4	0.1	1.2	0.2	0.6%
164.4		86.0%	4.4	0.2	1.2	0.2	0.6%
165.0		86.5%	4.4	0.2	1.2	0.2	0.5%
165.6		85.9%	4.4	0.2	1.1	0.2	0.6%
166.2		85.5%	4.4	0.1	1.2	0.2	0.6%
166.9		85.2%	4.4	0.2	1.2	0.2	0.4%
167.5		84.1%	4.4	0.2	1.1	0.2	0.5%
168.1		85.0%	4.4	0.2	1.1	0.2	0.5%
168.7		85.9%	4.4	0.2	1.2	0.2	0.5%
169.3		86.1%	4.4	0.2	1.2	0.2	0.5%
169.9		86.2%	4.4	0.2	1.2	0.2	0.5%
170.5		86.1%	4.4	0.2	1.2	0.2	0.5%
171.2		86.2%	4.4	0.2	1.2	0.2	0.5%
171.8		85.8%	4.4	0.2	1.2	0.2	0.5%
172.4		86.3%	4.4	0.2	1.2	0.2	0.6%
173.0		86.2%	4.4	0.2	1.2	0.2	0.6%
173.6		86.2%	4.4	0.2	1.2	0.2	0.5%
174.2		86.1%	4.4	0.2	1.2	0.2	0.5%
174.8		86.1%	4.4	0.2	1.2	0.2	0.5%
175.5		86.2%	4.4	0.2	1.2	0.2	0.6%
176.1		86.0%	4.4	0.2	1.2	0.2	0.5%
176.7		85.9%	4.4	0.2	1.2	0.2	0.5%
177.3		85.8%	4.4	0.2	1.2	0.2	0.5%
177.9		88.0%	4.4	0.1	1.2	0.2	0.6%
178.6		88.8%	4.4	0.1	1.2	0.2	0.6%
179.2		85.3%	4.4	0.2	1.2	0.2	0.5%
179.8		86.3%	4.4	0.2	1.2	0.2	0.5%

Time-on-stream (h)	T (°C)	X_{CO}	Molar Flow (mmol/min)				$C_{Balance}$
			H_2	CO	CO_2	Ar	
180.4		86.4%	4.3	0.2	1.2	0.2	0.6%
181.0		84.2%	4.3	0.2	1.1	0.2	0.6%
181.6		84.2%	4.3	0.2	1.1	0.2	0.6%
182.3		83.1%	4.4	0.2	1.1	0.2	0.4%
182.9		84.3%	4.4	0.2	1.1	0.2	0.7%
183.5		88.0%	4.4	0.1	1.2	0.2	0.7%
184.1		85.4%	4.4	0.2	1.2	0.2	0.7%
184.7		85.5%	4.4	0.2	1.1	0.2	0.7%
185.3		85.7%	4.4	0.2	1.1	0.2	0.7%
186.0		85.6%	4.4	0.2	1.1	0.2	0.7%
186.6		85.5%	4.4	0.2	1.1	0.2	0.7%
187.2		85.5%	4.4	0.2	1.1	0.2	0.7%
187.8		85.4%	4.4	0.2	1.1	0.2	0.7%
188.4		85.4%	4.4	0.2	1.1	0.2	0.7%
189.1		86.2%	4.4	0.2	1.2	0.2	0.7%
189.7		85.9%	4.4	0.2	1.2	0.2	0.7%
190.3		85.4%	4.4	0.2	1.2	0.2	0.6%
190.9		83.1%	4.4	0.2	1.1	0.2	0.6%
191.5		86.4%	4.4	0.1	1.2	0.2	0.7%
192.1		85.5%	4.4	0.2	1.1	0.2	0.6%
192.8		86.1%	4.4	0.2	1.2	0.2	0.7%
193.4	350	86.3%	4.4	0.1	1.2	0.2	0.7%
194.0		85.4%	4.4	0.2	1.1	0.2	0.6%
194.6		84.6%	4.4	0.2	1.1	0.2	0.6%
195.2		82.6%	4.4	0.2	1.1	0.2	0.6%
195.8		88.1%	4.4	0.1	1.2	0.2	0.7%
196.5		85.8%	4.4	0.2	1.2	0.2	0.6%
197.1		85.6%	4.4	0.2	1.1	0.2	0.7%
197.7		85.5%	4.4	0.2	1.1	0.2	0.6%
198.3		85.6%	4.4	0.2	1.2	0.2	0.7%
198.9		85.4%	4.4	0.2	1.1	0.2	0.7%
199.6		85.4%	4.4	0.2	1.1	0.2	0.7%
200.2		85.3%	4.4	0.2	1.1	0.2	0.6%
200.8		85.3%	4.4	0.2	1.1	0.2	0.6%
201.4		85.5%	4.4	0.2	1.1	0.2	0.7%
202.0		85.5%	4.4	0.2	1.2	0.2	0.6%
202.7		85.7%	4.4	0.2	1.1	0.2	0.7%
203.3		85.5%	4.4	0.2	1.1	0.2	0.7%
203.9		85.8%	4.4	0.2	1.2	0.2	0.6%
204.5		85.8%	4.5	0.2	1.2	0.2	0.4%
205.1		85.4%	4.4	0.2	1.1	0.2	0.7%
205.8		84.6%	4.4	0.2	1.1	0.2	0.7%
206.4		86.4%	4.4	0.2	1.1	0.2	0.8%
207.0		86.5%	4.4	0.1	1.2	0.2	0.7%

Space Velocity – 20,000 h^{-1}

Time-on-stream (h)	T (°C)	X_{CO}	Molar Flow (mmol/min)				$C_{Balance}$
			H_2	CO	CO_2	Ar	
51.0	200	4.1%	2.4	0.9	0.4	0.2	0.1%
51.6		4.2%	2.4	0.9	0.4	0.2	0.2%
52.2		3.0%	2.4	0.9	0.4	0.2	-0.1%
52.9		3.2%	2.4	0.9	0.4	0.2	0.0%
53.5		3.2%	2.4	0.9	0.4	0.2	0.0%
54.1		3.3%	2.4	0.9	0.4	0.2	0.0%
54.7		3.1%	2.4	0.9	0.4	0.2	0.0%
55.3		3.2%	2.4	0.9	0.4	0.2	0.0%
55.9		3.0%	2.5	0.9	0.4	0.2	0.0%
56.5		3.0%	2.5	0.9	0.4	0.2	0.0%
57.2		3.1%	2.5	0.9	0.4	0.2	0.0%
57.8		3.1%	2.5	0.9	0.4	0.2	0.0%
58.4		3.1%	2.5	0.9	0.4	0.2	0.0%
59.0		3.0%	2.5	0.9	0.4	0.2	0.0%
59.6		3.0%	2.5	0.9	0.4	0.2	0.0%
60.2		3.1%	2.5	0.9	0.4	0.2	0.0%
60.9		3.1%	2.4	0.9	0.4	0.2	0.0%
61.5		3.2%	2.5	0.9	0.4	0.2	0.0%
62.1		3.2%	2.5	0.9	0.4	0.2	0.0%
62.7		3.2%	2.5	0.9	0.4	0.2	0.0%
63.3		3.3%	2.5	0.9	0.4	0.2	0.0%
63.9		3.2%	2.5	0.9	0.4	0.2	0.0%
64.5		3.2%	2.5	0.9	0.4	0.2	0.0%
65.2		3.1%	2.5	0.9	0.4	0.2	0.0%
65.8		3.2%	2.5	0.9	0.4	0.2	0.0%
66.4		3.3%	2.5	0.9	0.4	0.2	0.0%
67.0		3.2%	2.5	0.9	0.4	0.2	0.0%
67.6		3.2%	2.5	0.9	0.4	0.2	0.0%
68.2		3.2%	2.4	0.9	0.4	0.2	0.0%
68.8		3.1%	2.5	0.9	0.4	0.2	0.0%
69.5		3.2%	2.5	0.9	0.4	0.2	0.0%
70.1		3.2%	2.5	0.9	0.4	0.2	0.0%
70.7		3.2%	2.5	0.9	0.4	0.2	0.0%
71.3		3.1%	2.5	0.9	0.4	0.2	0.0%
71.9		3.2%	2.5	0.9	0.4	0.2	0.0%
72.5		3.4%	2.5	0.9	0.4	0.2	0.0%
73.2		3.2%	2.5	0.9	0.4	0.2	0.0%
75.6	225	7.1%	2.5	0.8	0.9	0.2	0.0%
76.2		6.8%	2.5	0.8	0.9	0.2	0.0%
76.8		7.5%	2.5	0.8	0.9	0.2	0.0%
77.5		7.4%	2.5	0.8	0.9	0.2	-0.1%
78.1		7.3%	2.5	0.8	0.9	0.2	0.0%

Time-on-stream (h)	T (°C)	X_{CO}	Molar Flow (mmol/min)				$C_{Balance}$
			H_2	CO	CO_2	Ar	
78.7		7.2%	2.5	0.8	0.9	0.2	0.0%
79.3		7.3%	2.5	0.8	0.9	0.2	0.0%
79.9		7.2%	2.5	0.8	0.9	0.2	-0.1%
80.6		7.2%	2.5	0.8	0.9	0.2	-0.1%
81.2		7.4%	2.5	0.8	0.9	0.2	0.0%
81.8		7.1%	2.5	0.8	0.9	0.2	-0.1%
82.4		7.1%	2.5	0.8	0.9	0.2	0.0%
83.0		8.2%	2.4	0.8	0.9	0.2	0.2%
83.6		7.1%	2.5	0.8	0.9	0.2	0.0%
84.2		7.3%	2.5	0.8	0.9	0.2	0.0%
84.9		7.2%	2.5	0.8	0.9	0.2	0.0%
85.5		7.1%	2.5	0.8	0.9	0.2	0.0%
86.1		7.2%	2.5	0.8	0.9	0.2	0.0%
86.7		7.2%	2.5	0.8	0.9	0.2	0.0%
87.3		7.1%	2.5	0.8	0.9	0.2	0.0%
88.0		7.2%	2.5	0.8	0.9	0.2	0.0%
88.6		7.2%	2.5	0.8	1.0	0.2	0.0%
89.2		7.1%	2.5	0.8	1.0	0.2	-0.1%
89.8		7.1%	2.5	0.8	0.9	0.2	-0.1%
90.4		7.4%	2.5	0.8	0.9	0.2	-0.1%
91.0		7.1%	2.5	0.8	1.0	0.2	-0.1%
91.7	225	7.1%	2.5	0.8	0.9	0.2	-0.1%
92.3		7.1%	2.5	0.8	1.0	0.2	-0.1%
92.9		7.0%	2.5	0.8	0.9	0.2	-0.1%
93.5		7.2%	2.5	0.8	0.9	0.2	0.0%
94.1		7.0%	2.5	0.8	0.9	0.2	0.0%
94.7		7.2%	2.5	0.8	0.9	0.2	-0.1%
95.4		7.2%	2.5	0.8	0.5	0.2	0.0%
96.0		7.1%	2.5	0.8	0.4	0.2	-0.1%
96.6		7.2%	2.5	0.8	0.4	0.2	-0.1%
97.2		7.2%	2.5	0.8	0.4	0.2	0.0%
97.8		7.3%	2.5	0.8	0.4	0.2	0.0%
98.4		6.8%	2.5	0.8	0.4	0.2	0.0%
99.1		7.1%	2.5	0.8	0.4	0.2	0.0%
99.7		8.1%	2.5	0.8	0.4	0.2	-0.1%
100.3		7.7%	2.5	0.8	0.4	0.2	0.0%
100.9		7.5%	2.5	0.8	0.4	0.2	-0.1%
101.5		7.5%	2.5	0.8	0.4	0.2	-0.1%
102.1		7.5%	2.5	0.8	0.4	0.2	-0.1%
102.8		7.6%	2.5	0.8	0.4	0.2	0.0%
103.4		7.6%	2.5	0.8	0.4	0.2	0.0%
104.0		7.6%	2.5	0.8	0.4	0.2	0.0%
104.6		7.6%	2.5	0.8	0.4	0.2	0.0%
105.2		7.5%	2.5	0.8	0.4	0.2	0.0%
105.8		7.3%	2.5	0.8	0.4	0.2	0.0%

Time-on-stream (h)	T (°C)	X_{CO}	Molar Flow (mmol/min)				$C_{Balance}$
			H_2	CO	CO_2	Ar	
106.4	225	7.2%	2.5	0.8	0.4	0.2	0.0%
107.1		7.2%	2.5	0.8	0.4	0.2	0.0%
107.7		7.4%	2.5	0.8	0.4	0.2	0.0%
108.3		7.6%	2.5	0.8	0.4	0.2	0.0%
108.9		7.5%	2.5	0.8	0.4	0.2	0.0%
109.5		7.4%	2.5	0.8	0.4	0.2	0.0%
110.1		7.3%	2.5	0.8	0.4	0.2	0.0%
110.7		7.4%	2.5	0.8	0.4	0.2	0.0%
111.4		7.2%	2.5	0.8	0.4	0.2	-0.1%
112.0		7.4%	2.5	0.8	0.4	0.2	0.0%
112.6		7.3%	2.5	0.8	0.4	0.2	-0.1%
113.2		7.2%	2.5	0.8	0.4	0.2	-0.1%
113.8		7.7%	2.5	0.8	0.4	0.2	0.0%
114.4		7.7%	2.5	0.8	0.4	0.2	0.0%
115.1		7.5%	2.5	0.8	0.4	0.2	0.0%
115.7		7.4%	2.5	0.8	0.4	0.2	0.0%
116.3		7.4%	2.5	0.8	0.4	0.2	-0.1%
116.9		7.4%	2.5	0.8	0.4	0.2	0.0%
117.5		7.3%	2.5	0.8	0.4	0.2	0.0%
118.1		7.3%	2.5	0.8	0.4	0.2	0.0%
118.8		7.5%	2.5	0.8	0.4	0.2	0.0%
119.4		7.4%	2.5	0.8	0.4	0.2	-0.1%
120.0		8.6%	2.4	0.8	0.4	0.2	0.2%
120.6		7.3%	2.5	0.8	0.4	0.2	-0.1%
121.2		7.4%	2.5	0.8	0.5	0.2	-0.1%
121.8		7.3%	2.5	0.8	0.4	0.2	-0.1%
122.4		7.4%	2.5	0.8	0.5	0.2	-0.1%
123.1		7.5%	2.5	0.8	0.5	0.2	-0.1%
123.7		7.3%	2.5	0.8	0.5	0.2	-0.1%
124.4		7.4%	2.5	0.8	0.5	0.2	-0.1%
125.1		7.4%	2.5	0.8	0.5	0.2	-0.1%
125.7		7.2%	2.5	0.8	0.5	0.2	-0.1%
126.3		7.3%	2.5	0.8	0.5	0.2	-0.1%
126.9		7.4%	2.5	0.8	0.5	0.2	0.0%
127.5		7.3%	2.5	0.8	0.5	0.2	-0.1%
128.1		7.4%	2.5	0.8	0.5	0.2	0.0%
128.8		7.4%	2.5	0.8	0.4	0.2	-0.1%
129.4		7.4%	2.5	0.8	0.5	0.2	0.0%
130.0		7.4%	2.5	0.8	0.5	0.2	-0.1%
130.6		7.4%	2.5	0.8	0.5	0.2	0.0%
131.2		7.4%	2.5	0.8	0.5	0.2	-0.1%
131.8		7.4%	2.5	0.8	0.5	0.2	0.0%
132.5		7.5%	2.5	0.8	0.5	0.2	0.0%
133.1		7.5%	2.5	0.8	0.5	0.2	0.0%

Time-on-stream (h)	T (°C)	X_{CO}	Molar Flow (mmol/min)				$C_{Balance}$
			H_2	CO	CO_2	Ar	
133.7	225	7.4%	2.5	0.8	0.5	0.2	0.0%
134.3		7.3%	2.5	0.8	0.5	0.2	-0.1%
134.9		7.3%	2.5	0.8	0.5	0.2	0.0%
135.5		7.3%	2.5	0.8	0.5	0.2	-0.1%
136.1		7.4%	2.5	0.8	0.5	0.2	0.0%
136.8		7.3%	2.5	0.8	0.5	0.2	-0.1%
137.4		7.4%	2.5	0.8	0.5	0.2	0.0%
138.0		7.3%	2.5	0.8	0.5	0.2	-0.1%
138.6		7.4%	2.5	0.8	0.5	0.2	0.0%
139.2		7.3%	2.5	0.8	0.5	0.2	-0.1%
139.8		7.3%	2.5	0.8	0.5	0.2	0.0%
140.5		7.3%	2.5	0.8	0.5	0.2	0.0%
141.1		7.2%	2.5	0.8	0.5	0.2	-0.1%
141.7		7.2%	2.5	0.8	0.5	0.2	-0.1%
142.3		7.1%	2.5	0.8	0.5	0.2	0.0%
142.9		8.2%	2.5	0.8	0.5	0.2	-0.1%
143.5		7.1%	2.5	0.8	0.5	0.2	-0.1%
144.2		7.2%	2.5	0.8	0.4	0.2	0.0%
144.8		7.3%	2.5	0.8	0.5	0.2	0.0%
145.4		7.2%	2.5	0.8	0.5	0.2	0.0%
148.9	250	18.9%	2.5	0.7	0.5	0.2	0.1%
149.5		18.6%	2.5	0.7	0.5	0.2	-0.2%
150.1		19.5%	2.5	0.7	0.5	0.2	0.1%
150.7		19.1%	2.5	0.7	0.5	0.2	-0.2%
151.3		18.9%	2.5	0.7	0.5	0.2	-0.3%
152.0		18.7%	2.5	0.7	0.5	0.2	-0.3%
152.6		18.7%	2.5	0.7	0.5	0.2	-0.2%
153.2		19.0%	2.5	0.7	0.5	0.2	-0.2%
153.8		18.8%	2.5	0.7	0.5	0.2	-0.2%
154.4		18.7%	2.5	0.7	0.5	0.2	-0.3%
155.0		18.9%	2.5	0.7	0.5	0.2	-0.3%
155.6		19.9%	2.5	0.7	0.5	0.2	0.0%
156.2		18.8%	2.5	0.7	0.5	0.2	-0.3%
156.9		18.9%	2.5	0.7	0.5	0.2	-0.2%
157.5		18.9%	2.5	0.7	0.5	0.2	-0.2%
158.1		19.0%	2.5	0.7	0.5	0.2	-0.2%
158.7		19.1%	2.5	0.7	0.5	0.2	-0.3%
159.3		19.1%	2.5	0.7	0.5	0.2	-0.2%
159.9		19.0%	2.5	0.7	0.5	0.2	-0.2%
160.5		19.0%	2.5	0.7	0.5	0.2	-0.2%
161.2		19.1%	2.5	0.7	0.5	0.2	-0.2%
161.8		19.2%	2.5	0.7	0.5	0.2	-0.2%
162.4		19.0%	2.5	0.7	0.5	0.2	-0.2%
163.0		19.1%	2.5	0.7	0.5	0.2	-0.2%

Time-on-stream (h)	T (°C)	X_{CO}	Molar Flow (mmol/min)				$C_{Balance}$
			H_2	CO	CO_2	Ar	
163.6	250	19.0%	2.5	0.7	0.5	0.2	-0.3%
164.2		18.9%	2.5	0.7	0.5	0.2	-0.3%
164.8		19.0%	2.5	0.7	0.5	0.2	-0.3%
165.4		19.2%	2.5	0.7	0.5	0.2	-0.3%
166.1		18.9%	2.5	0.7	0.5	0.2	-0.2%
166.7		19.2%	2.5	0.7	0.5	0.2	-0.3%
167.3		19.8%	2.5	0.7	0.5	0.2	-0.1%
167.9		22.1%	2.4	0.7	0.5	0.2	0.7%
168.5		19.0%	2.5	0.7	0.5	0.2	-0.2%
169.1		19.3%	2.5	0.7	0.5	0.2	-0.2%
225.7	275	40.8%	2.5	0.5	0.6	0.2	0.2%
226.3		42.0%	2.6	0.5	0.6	0.2	0.1%
226.9		40.7%	2.6	0.5	0.6	0.2	-0.4%
227.6		40.1%	2.6	0.5	0.6	0.2	-0.5%
228.2		41.7%	2.6	0.5	0.6	0.2	0.1%
228.8		42.0%	2.5	0.5	0.6	0.2	0.2%
229.4		41.8%	2.6	0.5	0.6	0.2	0.2%
230.0		41.9%	2.5	0.5	0.6	0.2	0.2%
230.6		41.2%	2.5	0.5	0.6	0.2	0.2%
231.3		39.8%	2.6	0.5	0.6	0.2	-0.4%
231.9		39.4%	2.6	0.6	0.6	0.2	-0.5%
232.5		41.4%	2.5	0.5	0.6	0.2	0.2%
233.1		41.4%	2.6	0.5	0.6	0.2	0.1%
233.7		39.8%	2.6	0.5	0.6	0.2	-0.4%
234.3		39.5%	2.6	0.6	0.6	0.2	-0.5%
234.9		41.3%	2.5	0.5	0.6	0.2	0.2%
235.6		41.1%	2.6	0.5	0.6	0.2	0.2%
236.2		38.9%	2.6	0.6	0.6	0.2	-0.5%
236.8		39.2%	2.6	0.6	0.6	0.2	-0.5%
237.4		40.1%	2.6	0.5	0.6	0.2	0.1%
238.0		40.0%	2.6	0.5	0.6	0.2	0.1%
238.6		39.4%	2.6	0.6	0.6	0.2	-0.4%
239.3		39.6%	2.6	0.5	0.6	0.2	-0.3%
239.9		39.8%	2.5	0.5	0.6	0.2	0.3%
240.5		39.2%	2.6	0.6	0.6	0.2	-0.4%
241.1		39.1%	2.6	0.6	0.6	0.2	-0.3%
241.7		38.3%	2.6	0.6	0.6	0.2	-0.3%
242.3		39.4%	2.6	0.6	0.6	0.2	-0.4%
242.9		39.3%	2.6	0.6	0.6	0.2	-0.4%
243.6		38.9%	2.6	0.6	0.6	0.2	-0.2%
244.2		37.8%	2.6	0.6	0.6	0.2	-0.3%
244.8		37.4%	2.6	0.6	0.6	0.2	-0.3%
245.4		38.9%	2.6	0.6	0.6	0.2	0.0%
246.0		40.1%	2.6	0.5	0.6	0.2	-0.6%

Time-on-stream (h)	T (°C)	X_{CO}	Molar Flow (mmol/min)				$C_{Balance}$
			H_2	CO	CO_2	Ar	
246.7	275	43.0%	2.6	0.5	0.6	0.2	0.1%
247.3		40.6%	2.6	0.5	0.6	0.2	-0.4%
247.9		42.2%	2.6	0.5	0.6	0.2	0.1%
248.5		40.7%	2.6	0.5	0.6	0.2	-0.5%
249.1		40.9%	2.6	0.5	0.6	0.2	-0.4%
249.7		40.8%	2.6	0.5	0.6	0.2	-0.4%
250.4		42.3%	2.6	0.5	0.6	0.2	0.1%
251.0		42.8%	2.6	0.5	0.6	0.2	0.1%
251.6		41.4%	2.6	0.5	0.6	0.2	-0.4%
252.2		41.3%	2.6	0.5	0.6	0.2	0.1%
252.8		41.6%	2.6	0.5	0.6	0.2	0.1%
253.4		41.4%	2.6	0.5	0.6	0.2	0.0%
254.1		41.4%	2.6	0.5	0.6	0.2	0.1%
254.7		0.0%	2.6	0.5	0.6	0.2	-0.5%
255.3		39.8%	2.6	0.5	0.6	0.2	-0.4%
255.9		39.9%	2.6	0.5	0.6	0.2	-0.4%
256.5		40.2%	2.6	0.5	0.6	0.2	-0.4%
257.1		39.5%	2.6	0.6	0.6	0.2	-0.4%
257.8		39.4%	2.6	0.6	0.6	0.2	-0.4%
258.4		40.7%	2.6	0.5	0.6	0.2	0.0%
259.0		39.7%	2.6	0.5	0.6	0.2	-0.5%
259.6		40.1%	2.6	0.5	0.6	0.2	-0.5%
260.2		40.2%	2.6	0.5	0.6	0.2	-0.3%
260.9		41.0%	2.6	0.5	0.0	0.2	0.1%
261.5		42.4%	2.6	0.5	0.6	0.2	0.1%
262.1		41.3%	2.6	0.5	0.6	0.2	-0.5%
262.7		42.0%	2.6	0.5	0.6	0.2	0.0%
263.3		41.9%	2.6	0.5	0.6	0.2	0.0%
263.9		40.9%	2.6	0.5	0.7	0.2	-0.3%
264.6		40.7%	2.6	0.5	0.7	0.2	-0.3%
265.2		41.6%	2.6	0.5	0.7	0.2	0.1%
265.9		40.0%	2.6	0.5	0.7	0.2	-0.3%
482.2	300	52.6%	2.6	0.4	0.7	0.2	-0.2%
482.8		53.9%	2.6	0.4	0.7	0.2	-0.2%
483.4		52.5%	2.7	0.4	0.6	0.2	-0.8%
484.0		54.2%	2.6	0.4	0.7	0.2	-0.2%
484.6		53.9%	2.6	0.4	0.7	0.2	-0.2%
485.2		54.3%	2.6	0.4	0.6	0.2	-0.1%
485.8		54.3%	2.6	0.4	0.7	0.2	-0.2%
486.5		53.0%	2.7	0.4	0.7	0.2	-0.6%
487.1		54.1%	2.6	0.4	0.7	0.2	-0.1%
487.7		54.2%	2.6	0.4	0.7	0.2	-0.1%
488.3		53.8%	2.6	0.4	0.7	0.2	-0.2%
488.9		53.3%	2.6	0.4	0.7	0.2	-0.1%

Time-on-stream (h)	T (°C)	X_{CO}	Molar Flow (mmol/min)				$C_{Balance}$
			H_2	CO	CO_2	Ar	
489.5	300	53.3%	2.6	0.4	0.7	0.2	-0.1%
490.1		53.1%	2.6	0.4	0.7	0.2	-0.1%
490.8		52.4%	2.6	0.4	0.7	0.2	-0.1%
491.4		54.1%	2.6	0.4	0.7	0.2	-0.1%